Mechanical Prestressing of Electrical Insulation

A thesis submitted to the University of Manchester for the degree of Doctor of Philosophy in the Faculty of Science

by

Graham J Malkin BEng (Hons)

THE UNIVERSITY
of MANCHESTER

Department of Electrical Engineering
School of Engineering

June 2000

ProQuest LLC.
789 East Eisenhower Parkway
P.O. Box 1346
Ann Arbor, MI 48106 – 1346

CONTENTS

List of Figures

CHAPTER

List of Tables

ABSTRACT

In recent years there has been a growing body of evidence that the mechanical characteristics of insulating resins have a direct influence on the degradation of electrical insulation by treeing. Researchers at the University of Manchester's Division of Electrical Engineering have been at the forefront of this research into the mechanical aspects of treeing. These researchers have demonstrated that tensile stress accelerates tree growth and compressive stress retards it. This research project proposed to produce resin samples with an in-built resistance to treeing by the establishment of a controlled region of compressive stress. This has been achieved by the inclusion of fibres under tension during the curing process, in a manner not dissimilar to that used in the prestressing of concrete.

There were several prerequisites to the attainment of pre-stress. Firstly, fibre yarns were examined with a view to selecting one that was suitable to act as a pre-stressing member. The next step entailed the choice of a resin that would be conducive to pre-stressing. This process involved the establishment of criteria for pre-stress. Finally, having determined the appropriate level of pre-loading, methods of applying the load were investigated.

It was essential to produce test samples that required no machining or polishing, thereby avoiding the risk of alien stresses adversely affecting results. Unlike previous work into the mechanical aspects of treeing, which has been inconclusive, this work endeavoured to clarify the nature of the internal stresses and to quantify them. Internal stress levels were monitored using a non-destructive test method and the identically prepared, stress monitored samples were subsequently used to perform tensile and electrical tree tests. In order to isolate the benefits of pre-stressing, three distinct sample types were produced for testing. The attainment of pre-stress has not only produced a retardation in tree growth but also increased the mechanical strength of the insulation. Moreover the aging process, due to water absorption, further enhanced the effects of pre-stressing.

DECLARATION

No portion of the work referred to in the thesis has been submitted in support of an application for another degree or qualification of this or any other university or other institute of learning.

Graham J. Malkin

The following notes on copyright and the ownership of intellectual property rights:

(1) Copyright in text of this thesis rests with the Author. Copies (by any process) either in full, or of extracts, may be made **only** in accordance with the instructions given by the Author and lodged in the John Rylands University Library of Manchester. Details may be obtained from the Librarian. This page must form part of any such copies made. Further copies (by any process) of copies made in accordance with such instructions may not be made without the permission (in writing) of the Author.

(2) The ownership of any intellectual property rights which may be described in this thesis is vested in the University of Manchester, subject to any prior agreement to the contrary, and may not be made available for use by third parties without the written permission of the University, which will prescribe the terms and conditions of any such agreement.

Further information on the conditions under which disclosures and exploitation may take place is available from the Head of the Department of Electrical Engineering.

DEDICATION

This thesis is dedicated to the memory of Arnold Lockett a dearly missed friend and mentor. Arnold's insight and wisdom, support and encouragement gave me the courage to leave an established career and embark on another of even greater challenges and rewards.

THE AUTHOR

The author worked in the motor industry for 14 years, initially as an apprentice auto electrician and then successfully running his own business. In September 1993, as a mature student, he embarked on an Electronic and Electrical Engineering degree course at the University of Manchester. In July 1996 the author graduated from the Faculty of Science and Engineering with an upper second class Bachelor of Engineering Honours degree.

Upon graduation the author joined the Electrical Energy Systems Research Group at the University of Manchester as a full time Research Engineer. The author's role was to manage the three year fixed term project, whilst undertaking the technical research presented in this Ph.D thesis. The project was funded by the Engineering and Physical Sciences Research Council (EPSRC).

Shortly after finishing the contract at the University the author joined ALSTOM Electrical Machines Limited at Rugby as an Insulation Engineer in the Technical Development Department. The author's role includes research and development into improving and developing new insulation systems for medium and high voltage machines (Motors & Generators).

ACKNOWLEDGEMENTS

I would like to express my gratitude to my supervisor Dr Brian R Varlow and to Professor David W Auckland for their guidance and encouragement throughout this project. The technician, Mr Bob Bain, provided valuable suggestions and assistance in the development of the project, for which I am most grateful.

I am indebted to Professor R. J. Young of Manchester Materials Science Centre, for his willingness to devote time and resources to the project. My discussions with Professor Young have been particularly productive and the use of his Raman Spectrometer has been invaluable.

This project was made possible by the financial support of the Engineering and Physical Research Council (EPSRC) and the Member's funded Research Programme at ERA Technology Ltd, for which I am most grateful. My thanks also go to Mr. John Billing (ERA Technology Ltd) and Mr. Doug Warne (REMaCS) for their advice and guidance.

In addition the help, support and suggestions from colleagues and staff, both past and present, at the University of Manchester, UMIST and the Manchester Materials Science Centre has been greatly appreciated.

Finally, the author would like to thank Debra for her patience, support and encouragement throughout the course of this work.

CHAPTER 1

Introduction

1.0 General Background

Polymeric materials are now widely used in the manufacture of electrical insulation because they have a high electrical strength, coupled with a combination of mechanical and thermal properties, that lend themselves well to economical manufacturing processes. However to date the full potential of these insulating materials has not fully been exploited. This is due to the degradation phenomena collectively known as *treeing*, which occurs in polymeric insulation over a period of time in service. Of particular significance is *electrical treeing*, whereby localised partial discharge activity produces an array of narrow gas-filled tubules which propagate through the insulation leading to breakdown. On cross-sectional examination this random array of narrow tubules resembles a dentrite or tree structure.

The electrical treeing process itself can be divided into three stages:-

(i) Initiation - The time from voltage application to the first appearance of a tree channel.

(ii) Propagation – The time from initiation to the complete bridging of the electrode gap.

(iii) Breakdown - This is the time to failure, which can be:
a. The time from initiation to breakdown or
b. The time from voltage application to breakdown, this will be referred to as the Overall Breakdown time.

The stages of electrical tree growth are shown in the photographs in **Figure (1.1)**. These frames are from an electrical tree test performed during the course of this project. This particular experiment was the **P**lain resin sample containing a **T**ungsten needle, batch number **01** **N**eedle number **4** (Photo set **PT01N4**), the time duration results can be seen in *Appendix 8*.

Figure (1.1) The Stages of Electrical Tree Growth

(i) Initiation (ii) Propagation (iii) Breakdown

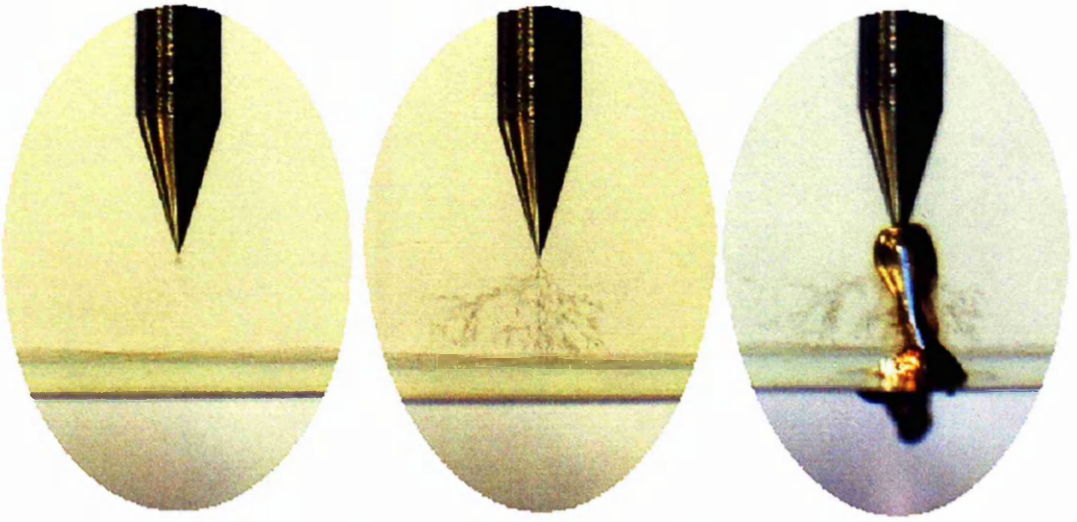

NOTE: All needles used in this project are 1mm in diameter.

Electrical trees originate at points of high divergent electrical stress and tree growth proceeds sporadically from this point. Tree type and growth depends on a combination of applied electrical, thermal, environmental and mechanical stress conditions. A review of the initiation mechanisms of electrical trees is given in a recent paper by Shimizu *et al* [1].

The retardation of this degradation process has prompted extensive investigations by the Electrical Energy Systems Research Group at the University of Manchester. This resulted in Auckland and Varlow [2] evolving a mechanical theory for electrical treeing, showing that the growth of trees is related to fracture mechanics. Auckland and Varlow [3,4] established a correlation between the mechanical characteristics of insulating resins and electrical tree growth within those resins. It was demonstrated by Billing *et al* [5] and later by Arbab *et al* [6], that the internal mechanical stresses in insulating resins affect the electrical strength, namely that tensile stress accelerates, and compressive stress inhibits tree growth. This has been confirmed by many other sources including Champion *et al* [7]. In order to retard the degradation process this research project intends to utilise the mechanical effects by inducing compressive stresses into the insulating resins, as announced by Varlow [8].

1.1 Objectives of this Research Project

The main objectives of this research project are:

- To increase the lifetime of electrical insulation, by improving the resistance of composite insulation to the growth of electrical trees.
- To utilise the inherent mechanical properties of composite materials, by inducing compressive stresses into composite insulation.
- To cast high performance fibre yarns (HPFY) that have been tensioned (hence pre-stressed) within a resin matrix

The theoretical result of this tensioning operation will be the production of a self-balancing system of internal stresses, tensile stresses in the fibre yarn and compressive stresses in the resin matrix. This is similar to the mechanism employed in the prestressing of concrete, as discussed by Collins *et al* [9], leading to improved treeing resistance in composite insulation.

1.2 Sample Configurations

In order to show the full potential of mechanically prestressing electrical insulation it was essential to investigate three distinct sample configurations:

1. ***PLAIN*** resin samples,
   to observe the characteristics of the resin matrix in isolation.

2. ***PRE-TENSIONED*** samples,
   to observe the effects of embedding yarn in the resin matrix.

3. ***PRE-STRESSED*** samples,
   to observe the effects of pre-stressing the fibres in yarn embedded samples.

1.3 EPSRC Contract

The research into the *Mechanical Pre-stressing of Electrical Insulation* has been funded by a Standard Research Grant from the Engineering and Physical Research Council (EPSRC). The work carried out was in keeping with the terms and conditions of the grant contract and was subject to quarterly project review meetings with an independent specialist from ERA Technology Ltd. These meetings monitored the progress of the project and allowed for the discussion of future work.

The duration of the contract was for three years, from 1-7-96 to the 30-6-99. Daily notebooks were kept in accordance with the guidelines on laboratory notebooks, as set out by the BTG plc [10]. Annual reports were submitted and the research had to be completed by the end of the contract. The effective use of time and an appreciation of costs have played a critical role in the project's development. The need to complete the project within the three-year period had to be balanced against the need to develop a cost-effective process for potential commercial exploitation.

Beneficiaries of this research in the electrical engineering industry will be those involved with the manufacture of transformers, switchgear and rotating machinery made using polymeric resin insulation. Enhanced treeing resistance due to pre-stressing will also lead to a reduction in size and weight of the insulation, resulting in improved thermal properties and most importantly reduced costs.

1.4 Survey of the Thesis

To achieve the objectives it has been necessary to perform detailed investigations. These are presented in the following chapters.

A literature review in *Chapter 2* examines the development of the mechanical theory relating to electrical degradation and breakdown in polymers.

The introduction to polymers in *Chapter 3* identifies and characterises the fundamental properties of organic polymers and yarns. A selection criteria for high performance yarn leads to the acquisition of a range of suitable yarns to act as potential pre-stressing members.

The analysis of the shortlisted high performance yarns in *Chapter 4* provides the starting point for the project. The process of yarn analysis allows for practical experience of handling and using the yarns. By establishing the working parameters of the yarn samples, this work permits the selection of the most suitable yarn for the attainment of pre-stress.

A detailed review of aramid fibres is carried out in *Chapter 5*. It explores the development, chemistry and physics of these extraordinary organic polymer fibres. In particular the significance of the *'bond angle'* and its effect on the molecular vibrations is examined.

Non-destructive Raman Spectroscopy is introduced in *Chapter 6* and the benefits of using such a technique to analyse the stresses at the fibre/resin interface are examined. Raman analysis provides a high level of understanding about the internal state of the resin matrix. This understanding led directly to significant changes in sample design and the choice of encapsulating resin, which resulted in the production of pre-stressed samples.

The selection of insulating resins in *Chapter 7* was initially dependent on previous work in this area. Important considerations were suitable physical and electrical properties, dimensional stability, good adhesion and optical clarity. Later, due to the improved level of understanding provided by Raman analysis, criteria were developed for pre-stress. As a result of these developments an alternative resin was selected and pre-stress was attained.

Compromises over initial sample design and the continual development of the sample configuration in *Chapter 8* demonstrate the flexibility of the systematic approach applied to this project. Three main sample types have all been developed using the same metal die, thus allowing comparability. The use of high quality moulds made

from silicone rubber ensured the production of reproducible quality samples that needed no machining or polishing.

The mechanical tensile testing process is examined in *Chapter 9*. It describes the development of sample geometry in relation to the end-pieces and to the bonding agent. The Chapter goes on to explain the statistical testing carried out to compare plain samples to yarn embedded samples.

The electrical tree testing presented in *Chapter 10* is in keeping with previous work relating to sample size, test equipment and test conditions. The statistical testing carried out on Plain, Pre-tensioned and Pre-stressed samples is examined. In particular, the chapter highlights the effect of pre-stressing on the propagation time. The Chapter goes on to investigate the effects of water absorption on the treeing process.

Taking each Chapter in turn conclusions are drawn from the work carried out and discussed in *Chapter 11.*

In the final Chapter, *Chapter 12,* the author comments on the possible future development of work on *'Mechanical Prestressing of Electrical Insulation'*. This Chapter concludes that the research presented in this thesis provides a clear starting point for extensive future work. The author also outlines potential future directions for this research and puts forward ideas for its practical development.

CHAPTER 2

Literature Review

2.0 Background

It is not the purpose of this investigation to explore the numerous proposed mechanisms for tree initiation, but to focus on the mechanical aspects of treeing and utilise the inherent mechanical properties of the insulation materials to retard the treeing process. This is not to say that electrical treeing is exclusively a mechanical phenomenon. Clearly it is an electrically generated phenomenon: no volts – no trees. Nevertheless, one cannot ignore the varied and numerous evidence of the mechanical influence, which suggest an aspect of tree propagation similar to fracture mechanics as applied to mechanical crack propagation.

Over the last 80 years a considerable amount of research has been undertaken into the degradation and breakdown of electrical insulating materials, with respect to the treeing phenomenon. Notwithstanding, to date no defining theory has been developed. There have been numerous reviews examining treeing processes. This was evident in Volume 9 of the IEE materials and devices series written by Dissado and Fothergill [11], published in 1992, which had no less than 939 references on the subject. Among the most authoritative reviews of the subject are those of Bahder *et al* [12], Eichorn [13], Ieda [14] and McMahon [15]. Although these reviews vary in detail, the underlying view is the same, namely that trees are initiated at sites of high divergent electrical stress, producing the narrow initiatory channel. Further growth takes place and they develop to form a tree-like structure in a random manner, as observed by Bolton *et al* [16], eventually the tree bridges the insulation. The branches of the tree broaden with time to a point where they are unable to sustain discharge activity and then breakdown occurs. This view of the process, which has remained unchanged since the 1950s, is based on the original electronic process proposals of Mason *et al* [17,18] and later others such as Shibuya *et al* [19,20]. In later years a mechanical aspect was introduced. For example, Zeller *et al* [21] modified the theory by proposing that initiation and growth involve fracture mechanisms induced by electrostatic forces.

2.1 The Mechanical Approach

Although the established theories of tree initiation and growth characterise electronic, thermal, environmental and mechanical breakdown processes, it is only more recent work that has placed greater emphasis on the mechanical influence on breakdown. An example of this exclusion is the review by O'Dwyer [22], published 1973, where the mechanical aspect is not considered in the main section on breakdown. This is despite the findings of Stark and Garton [23] in 1955 and again in 1969 Yamada [24], both of which postulated that Maxwell stresses had caused a mechanical breakdown process to occur. Interest was growing and in 1972, whilst examining the induction period to initiate a tree, Ieda *et al* [25] concluded that a tree initiates as a result of mechanical fatigue due to Maxwell stresses. This conclusion was also supported in 1974 by Noto *et al* [26] as an important factor in pre-treeing degradation of solid dielectrics. However, these authors provided no real evidence and no details about the mechanism involved.

A practical approach to the observation of mechanical effects on tree growth was taken in 1974 by Billing *et al* [5], whereby electrodes were offset and the samples were bent. This meant that the polymer adjacent to the high-voltage electrode was subject to a tensile stress while the earth electrode was under a compressive stress. The results showed the formation of a tree in the electrically weak direction perpendicular to the direction of the applied tensile stress. Investigations in 1979 by Densley *et al* [27] reported a time to breakdown reduction in cross-linked polyethylene (XLPE) cable samples when the mechanical strain was increased. This was also shown by Ildstad *et al* [28] in 1992. Ongoing work at the University of Manchester into the treeing breakdown mechanism supported the mechanical approach as a primary cause of breakdown, see Auckland *et al* [29]. Nonetheless, if the importance of the mechanical aspects of treeing were to be appreciated and accepted then the mechanical effect would have to be isolated and examined

2.2 Isolating the Mechanical Effect

Experiments carried out by Arbab *et al* [30,31] proved that mechanical effects were pre-dominant in the initiatory process. A sensitive balance beam was used to measure

the electrostatic forces in the samples for an applied voltage of $7kV_{rms}$. An instrument was made which simulated these forces electromagnetically, so that the samples would be exposed to equivalent Maxwell forces without simultaneous exposure to high voltage. In this way electrostatic and mechanical effects were separated. One set of samples, was then tested by applying a potential of $7kV_{rms}$ up to tree initiation and an average time for tree initiation obtained. An identical set of samples was exposed to mechanical vibrations equal in magnitude to those induced electrostatically within the previous set for the same average initiation time. Photographic records showed that the nature and extent of the degradation caused was the same for all the samples.

It could be seen that treeing followed the formation of cracks emanating from the needle/resin interface. These cracks, once developed, provided a source of discharge activity necessary to induce tree growth. The cracks resulted from brittle fracture caused by cyclical electrostatic forces and did not involve the electronic processes. Further work by Auckland *et al* [32] confirmed that the internal strain present in resin insulation is influenced by vibrational electrostatic forces.

2.3 The Effects of Bending Stresses

The effects of bending stresses on tree growth in polymeric insulation was clearly demonstrated by Arbab *et al* [6] when bending a sample of material containing treeing needles, shown in **Figure (2.1)**. The lower part of the sample was placed in tension whilst the upper part was in compression. Observation of electrical tree growth in such a system showed an acceleration of the tree growth in the tensile region and a deceleration in the compressive part. This is directly akin to the propagation of mechanical cracks, and the rules of fracture mechanics appear to apply.

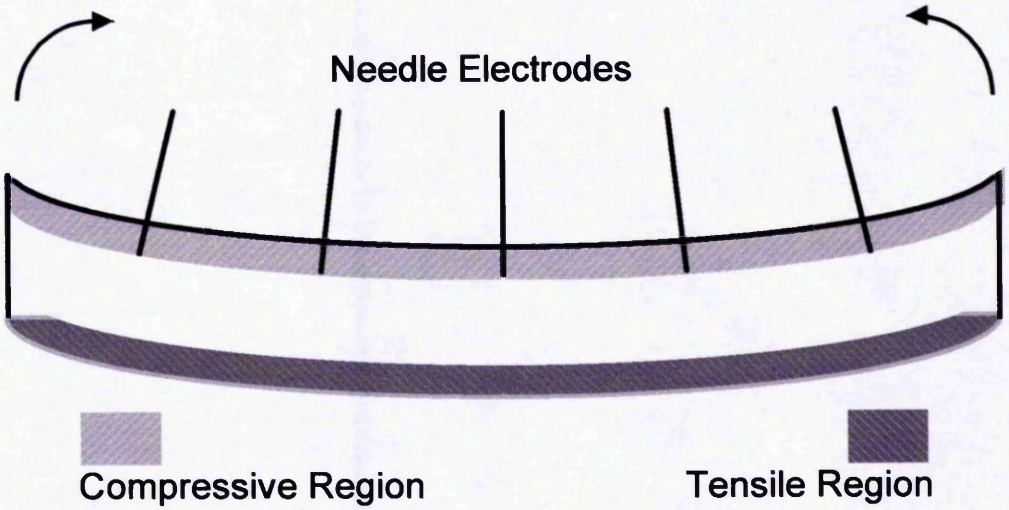

Figure (2.1) Bending Stresses

2.3.1 Photoelastic Effects

Arbab built his own circular polariscope to observe the photoelastic effects of the internal stresses on the samples in his experiments. Photoelastic techniques have also been used by Champion *et al* [7,33,34] and David *et al* [35,36,37] to determine the effects of internal stresses on electrical tree growth, their findings supported the mechanical approach. In particular Champion *et al* [38] concluded '*that increasing compressive stress suppresses tree initiation and increasing tensile stress enhances it*', thus confirming the findings of Arbab.

2.3.2 Theoretical Analysis

The theoretical analysis of the mechanical aspects of tree growth began with Zeller *et al* [21,38] who attributed the growth of filamentary cracks to electrostatic forces; a process that was termed '*electrofracture*'. This theoretical approach has been developed subsequently by Hitika *et al* [39] and Fothergill [40].

2.4 Plasticisation

When the mechanical properties of an electrical insulating material are directly degraded, e.g. by the introduction of a plasticising agent, a correlation can be found between the changes in the resulting mechanical properties and those in the initiation

and growth of electrical trees, as shown in Auckland *et al* [2]. Thus a decrease in the tensile strength, modulus of elasticity and fracture toughness, as a result of plasticisation, is mirrored in the decreasing resistance of the material to electrical tree propagation.

2.5 Internal Barriers

In Auckland *et al* [41] the effects of the presence of internal barriers on the mechanical aspect of treeing was examined. The manufacturing process involved laying down one layer of resin then, after curing, the addition of a barrier material and subsequent second resin layer. This process generates mechanical stress in the barrier region. The key factor in determining this stress is the quality of the mechanical bond between the barrier material and the resin matrix.

To investigate this barrier phenomenon a range of barrier materials, including particulate aluminium oxide, PET and PTFE films, glass sheet and glass fibre, were cast mid-way between pin plane electrodes with a 2mm inter-electrode separation. It was observed that, when the work of adhesion between the barrier and the surrounding resin was low, the growing tree channels caused local debonding as they impinged on the barrier. In the case of a high work of adhesion this did not occur. The occurrence or otherwise of debonding determined the nature of the subsequent tree development. In the case where a very weak bond (low work of adhesion) existed between the barrier and the matrix, there was a tendency for breakdown to occur along the barrier/resin interface. If a material had a high melting point, e.g. PTFE, breakdown occurred by going around the edge of the barrier. Conversely if the barrier material had a low melting point, the developing activity in the incident channel could cause localised thermal degradation, puncture the barrier and breakdown. When the work of adhesion was very high no debonding occurred. This was illustrated when glass and aluminium oxide barriers were tested.

When the progress of a tree was monitored for different barrier materials, the barrier itself determined the total treeing time (defined as the time from voltage application to complete tree formation), furthermore the tree channel appeared to anticipate the barrier, approaching at different rates for different barrier materials. It is worthy of

note that the presence of a physical internal barrier is not of itself essential to produce the retardation effect. Samples without an internal barrier, but cast in two stages, showed a six-fold increase in the treeing resistance, compared with samples with the same spacing cast in a single operation, where resistance is measured as the time for a tree to propagate across the inter-electrode spacing. This also demonstrates that the phenomenon is not permittivity driven, as proposed by Williams and Dissado [42], as no materials of dissimilar permittivity are used in this instance.

The suggested cause of the apparent retardation of the tree channels as they approach the barrier is the compressive stress in the region of the barrier arising from the manufacturing process. The quality of the adhesive bond between the resin matrix and the various barrier materials determines the degree of compressive stress in the barrier region and therefore the resultant retardation in tree growth. Specimens in which the barrier/resin adhesive bond has been deliberately reduced by a coating of oil exhibit rapid tree growth unimpaired by any compressive stress, as demonstrated by Auckland *et al* [43].

2.6 Water Trees

Although the primary purpose of this thesis relates to electrical treeing, it is worth noting that a mechanical aspect of water tree growth has been recorded by Auckland *et al* [44]. The degradation in the mechanical properties of polyester resin as a result of its plasticisation has an effect on the growth of water trees. Using the water needle method, water tree initiation times and growth rates were determined for a range of samples with different degrees of plasticisation. The polymer was in contact with 0.1 M NaCl solution and a 50Hz a.c. voltage was applied to each specimen. It was found that the initiation time for water trees decreased (and growth rate increased) with increasing plasticiser content. A correlation was found between the initiation time and the tensile strength, both of which decreased due to plasticisation, based on the assumption that the initiation occurs when the osmotic pressure in the cavity at the water needle tip exceeds the mechanical strength of the material. The increase in propagation rate correlates well with the decrease in mechanical strength as plasticiser is added.

2.7 Temperature Effects

When considering the effects of temperature on electrical treeing, from a mechanical point of view, there are several ways in which its influence may be observed. In homogeneous resin samples the tensile strength and modulus of elasticity all show a pronounced decrease in value as the temperature is increased. The resistance of the material to crack propagation becomes lower with the application of heat. Similarly, the treeing resistance falls as temperature exceeds the glass transition temperature (Tg). The effect of elevated temperatures on barriered specimens is complex. The effect of temperature may show itself in the decrease in the mechanical strength of the barrier material or the resin matrix or by the reduction on the bond strength between the two components, which has been seen to be a controlling factor in the development of internal stress.

Polyester specimens containing barriers such as PET and Polyimide films, glass cloths and micapaper have been tested for bond strength, barrier strength and tree lifetime from room temperature to 100°C, as seen in Auckland *et al* [45]. Here the "bond strength" is the tensile stress required to produce fracture between the barrier and the resin. The "barrier strength" is the tensile strength of the barrier material itself and the "tree lifetime" is the number of cycles of 50Hz alternating voltage, at 25kV, required to produce breakdown by treeing across the full inter-electrode spacing of 2mm. For all of these barrier materials the bond and barrier strengths decreased dramatically with increasing temperature, with a corresponding effect on the tree lifetime. As a general rule, tree propagation through polyester resin was relatively rapid, the great proportion of the treeing time taking place in the vicinity of the barrier.

There may also be an additional factor. The significant reduction in the treeing time at elevated temperatures may be attributed to a decrease in compressive stress at the barrier/resin interface. Such a reduction in stress as the temperature is increased was observed in the samples tested using a polariscope, which employs photo-elastic interferometry.

2.8 Summary

A diverse range of previous work on the subject of electrical treeing was identified. Nevertheless, it was not the intention of this project to become involved in the wider debate regarding the treeing phenomenon. Apart from a brief overview of previous work therefore, Chapter 2 has largely confined itself to a more detailed review of the work relating to the mechanical approach to tree propagation and, in particular, to an examination of previous work where the mechanical effects have been isolated. Of particular significance in this Chapter was the review of previous work undertaken in relation to internal barriers.

As a result of this accumulation of data demonstrating strong mechanical influences on the development of electrical trees in polymeric insulation, it was considered possible to produce an increased treeing resistance in polymeric materials. This has significant implications for utilising a controlled region of compressive stress in the retardation of tree propagation. The effects of internal mechanical stress appear to play a pivotal role and may be used to advantage in the production of *mechanically pre-stressed* electrical insulation. Moreover, this pre-stressed material should have an enhanced mechanical strength, which is of great importance where the electrical insulation also acts as a structural member or where insulation thickness limits the operating temperature of the equipment. In the following chapters of this thesis the development of the concept of pre-stress is examined.

CHAPTER 3

Polymers & Yarns

3.0 Polymers

This project involves the use of various synthetic polymer materials such as yarns in *Chapter 4*, resins as described in *Chapter 7* and silicone rubbers, which are examined in *Chapter 8*. In order to appreciate their contribution to this investigation, this chapter briefly identifies and characterises the fundamental properties of polymers. It introduces the terminology and explains the background to the processes used to produce them.

Polymers are very large molecules which contain a multiple repetition of groups of atoms (repeat units) and are made up by the successive linking of one or more types of molecule. These small molecules are known as *monomers* (single part), which when joined together become polymers (many parts). The way in which polymers are built up from component monomers influences their properties. Polymers can be classified into two types :

1. Long-chain polymers
2. Network polymers

3.1 Long-chain Polymers

As the name suggests the monomers are linked to a neighbouring molecule, allowing a long-chain polymer to be formed. The chemical process of joining monomers together is known as *polymerisation*. Over the years the words polymer and plastic have become interchangeable yet they have different meanings. A polymer is a large molecule whereas a plastic is a product consisting of a blend of polymers with a diversity of materials added for specific purposes, for instance pigments for colour or plasticisers to make the product softer or easier to mould. The development of such numerous types of synthetic polymeric materials is based on the fact that different

kinds of molecule produce different properties in the bulk material. The intention is to produce polymers for specific functions, or improvements in existing materials.

3.2 Network Polymers

A network polymer can form a material that is composed of a continuous three dimensional molecule, the whole of which is bound together by primary bonds. Therefore network polymeric materials have very different properties from those made from long-chain molecules. Their structure is not so easily disrupted by heat or mechanical forces. Networks can be formed in two ways :

1. The linking of long chains by atoms or small molecules. The atom or molecule forms a *cross-link* between chains by forming a covalent bond with each. Cross-links occur by addition polymerisation and so no by-products are produced e.g. the forming of polyester and epoxy resins.
2. The successive condensation polymerisation reactions with the emission of by-products.

3.3 Polymerisation

Polymerisation is the process which results in the formation of large molecules (macromolecules), that consist of repeated structural units as in polymers. These structural units (mers) are aided by the reacting monomers but are not necessarily identical to them; this depends on what type of reaction is taking place. There are two main types of reaction :

1. Addition polymerisation also known as chain-growth polymerisation.
2. Condensation polymerisation also known as step-growth polymerisation.

3.3.1 Addition Polymerisation

Addition polymerisation refers to a process where the resulting polymer is produced by mers identical to the reacting monomers. The polymer chain is built up by adding the monomer units to one another using one of the bonds in the double carbon bond **C=C**, or any monomer with a double bond between the carbon atom. Characteristics of addition polymerisations are that they have extremely rapid rates, achieved at relatively

low temperatures and the polymer produced is the sole product of this type of reaction. The kinetics are indicative of those seen in chain reactions.

3.3.2 Condensation Polymerisation

Condensation polymerisation is a process whereby the polymer is formed by the reaction of monomers, each step in the successive process resulting in the elimination of some by-product, usually water. Here the composition of the polymer and reacting monomers are different and the polymer structure depends on the monomer components. The kinetics are indicative of simple condensation.

3.4 The Characteristics of Polymers

Having considered the principles of polymers and established the ways in which they are formed, it is necessary to consider some of the characteristics which determine the way in which they are used.

3.4.1 Thermoplastics

A thermoplastic is a material that melts upon heating and is capable of being moulded. Upon warming thermoplastics become soft and can be formed into the desired shape they then become rigid upon cooling, but soften again on reheating. They consist of long-chain polymers coupled with various other molecules to modify their properties. A long-chain polymer is held together by weak secondary bonds between neighbouring molecules, therefore they can be made to slide over one another easily by increasing the temperature. The weak bonds between molecules influence the characteristics of a thermoplastic.

3.4.2 Thermosetting Polymers - Thermosets

Thermosetting polymers are materials which, when fully cured (polymerised), become a continuous network polymer in which no sliding between molecules can take place. This is because the whole structure is one large molecule in which all the atoms are linked by primary covalent bonds. The application of heat speeds up polymerisation and creates a permanent *set* of the polymer, hence **thermoset**.

A thermoset, once fully cured, sets irreversibly and is inclined to be brittle and hard; it does not soften on reheating but will char, burn or disintegrate. All necessary shaping must therefore be undertaken prior to curing since an uncured thermoset is still a thermoplastic, consisting of long-chain molecules that have not yet been joined together. After moulding the full polymer network can be initiated by starting the cross-linking process. This is a useful feature because the monomer which creates the cross-links can be kept separate until needed. Hence the two-pack systems, in which one pack contains pre-produced long-chain polymers and the other contains hardener that produces the cross-links.

3.4.3 Elastomers

Elastomers are cross-linked rubbery polymers which exhibit elastic properties. They are materials which can be stretched to several times their original length without breaking and which, on release of the applied stress, returns to their original length. That is to say deformation in an elastomer is reversible. This is due to their molecular structure in which the network is of low cross-link density. Therefore when the polymer chains become extended upon deformation they are prevented from permanent flow by the cross-links, and driven by entropy, spring back to their original positions on the removal of stress. The word rubber is often used in the place of elastomer. However natural rubbers are rubbery polymers which are not cross-linked.

3.4.4 Polymer Structure

Polymers clearly illustrate the relationship between the ways in which the properties of a material are determined by their internal structure. These can be classified at three different levels :

1. Atom type and how they are held together in the molecule.
2. Shape and size of the molecules.
3. The arrangement of the molecules relative to one another.

To appreciate the internal structure it is essential to examine crystalline and amorphous solids. A solid is said to be crystalline when the atoms or molecules in that solid form a regular three-dimensional array. This arrangement of the atoms or molecules is when they are in their most stable positions, crystallinity therefore is the normal condition of

solids. It is based on the regular internal structure and not the external appearance. Whereas when a solid has an arrangement of atoms or molecules which have no regular order over any appreciable distance it is called an amorphous solid.

Polymers contain varying proportions of crystalline and amorphous regions, therefore the degree of crystallinity has the greatest influence on the properties of a polymer. For instance crystalline materials have a definite melting point whereas amorphous materials change gradually from a solid to a liquid over a range of temperature just like glasses. The lower limit of this range is known as the *glass transition temperature* **(Tg)**. At this temperature the thermal energy available is small in comparison to the forces holding the molecules together. Beneath this temperature, virtually no molecular change is possible. An amorphous polymer below Tg is hard and brittle, and above Tg it is soft and rubber-like. Some thermoplastics classed as crystalline also have a Tg because they contain amorphous regions.

The Tg of a polymer is therefore an important consideration in the use of the polymer. By adding other chemicals to the long-chain polymers, it is possible to lower the Tg. These additives are called plasticisers and merge between the molecules of individual polymers thus weakening the inter-molecular bonds. They separate the long-chains and allow for easier movement relative to one another and produce rubber-like properties giving improved flow at lower temperatures.

The extent of crystallinity within the internal structure of a long-chain polymer (thermoplastic) is significant in determining its properties. This is due to the molecules being so very closely packed together in the crystalline region compared with the amorphous region, therefore the spaces between molecules are smaller and so the binding forces are stronger. As a result of this generally a crystalline polymer has a higher strength and rigidity than the equivalent amorphous polymer.

Network polymers (generally thermosets) are amorphous and, as they consist of one continuous molecule, they experience glass transition in a more gradual way than do thermoplastics. Their hardness, rigidity and mechanical strength is determined by the spacing between the cross-links along the molecule, therefore, the more frequent the cross-links, the more rigid the material.

3.5 Fibres and Yarns

Significant progress was made in the development of thermoplastic polymers when it was established that, by drawing the polymer out into a fibre or filament (a fibre, that which is long in relation to its thickness and is fine and flexible), the crystallinity is increased. Stretching or drawing of the polymer aligns many of the molecules in the direction of the pull. A thread made up of a group of fibres is referred to as a yarn. The continued improvements in fibre manufacture and the development of extrusion processes has led to the development of highly crystalline filaments with superior qualities. These have become known as high performance fibre yarns.

3.6 High Performance Fibre Yarns

Man-made organic high performance fibre yarns (HPFY) have been developed to combine low density, high strength and high stiffness to varying degrees. The selection of suitable fibre yarns to act as pre-stressing members was based on the properties given in **Table (3.1)**.

Table (3.1) Yarn Selection Criteria

(i)	COST	It must be commercially viable.
(ii)	LIGHTWEIGHT	It is not desirable to make insulating structures any heavier than they currently are.
(iii) (iv) (v)	HIGH TENSILE STRENGTH HIGH TENSILE MODULUS LOW ELONGATION TO BREAK	These three properties are closely related to mechanical strength.
(vi)	GOOD THERMAL STABILITY	Not only under varying operating conditions but, more importantly, at high temperatures experienced during manufacture. It is important that none of the properties of the material are undermined or lost.
(vii)	LOW THERMAL SHRINKAGE	Too much shrinkage could lead to de-bonding and accelerate breakdown.
(viii)	GOOD ADHESION	A high degree of adhesive bonding between yarn and resin matrix is essential to induce the tensile strain in the yarn into compressive strain in the resin.
(ix)	GOOD PROCESSABILITY	It must be possible to work easily with the materials when manufacturing, again to minimise costs.

3.7 The Selected Yarns

Using the list of properties as a guide, four fibre yarns were initially selected as potentially suitable for this project. These were Nylon, Kevlar, Twaron and Dyneema.

3.7.1 NYLON (High Tenacity)

At the threshold of the high performance multi filament fibre yarn category is **NYLON 6.6**, a polyamide based on hexamethylene diamine and adiplic acid. Nylon 6.6 forms particularly strong interchain hydrogen bonds, giving a stronger, more crystalline polymer which does not soften or melt until very high temperatures. As a consequence it has a higher tenacity and modulus and exhibits less shrinkage and creep than standard Nylon 6. The numerals 6.6 distinguishes the number of carbon atoms lying between successive amide groups in the chain. Thus Nylon 6.6 is produced from two monomers and has the structure shown in **Figure (3.1)**.

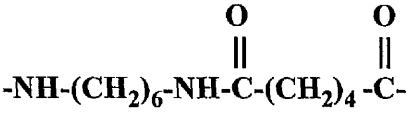

Figure (3.1) Nylon 6.6 (poly-hexamethylene adipamide) [46]

It has alternate sequences of six amide groups then six carbon atoms between the nitrogen atoms. A nylon with two numbers indicates that it contains dibasic acid and diamine moieties, the first number relates to the diamine and the second to the diacid used in the reaction.

Nylon 6.6 is produced by a form of linear condensation polymerisation known as melt polymerisation. Firstly hexamethylene diamine and adipic acid are reacted together at a low temperature to form nylon 6.6 salt (hexamethylene diammonium adipate) which is then purified by recrystallisation. This salt is then slowly heated up to about 280°C under pressure (1.7 MPa), to cause melt polymerisation; it is then kept at this temperature whilst removing the water (by-product) in the form of steam whilst maintaining the pressure. The pressure is reduced to atmospheric for one hour, then the polymer is extruded by oxygen-free nitrogen on to a water-cooled casting wheel.

Employing melt polymerisation by *salt dehydration,* gives the advantage of the use of pure salt which guarantees exact 1:1 stoichiometry (the determination of exact proportions of elements to make pure chemical compounds).

The sample type :-

6.6 (T-728) a high tenacity heat stabilised and fatigue resistant yarn with good adhesion properties (**Sample No.1**), cost approximately £3 per kilo.

3.7.2 DYNEEMA

'Dyneema' is a registered trademark of DSM (Dutch State Mines) and is manufactured by the High Performance Fibers Division in the Netherlands. Dyneema is based on polyethylene with an ultra high molecular weight (UHMWPE), formed by a process known as gel-spinning, which involves creating a dry gel from theta-solvents. In standard polyethylene the molecules are not orientated and can easily be torn apart. The gel-spinning process involves dissolving the molecules in a solvent which is then spun through a spinneret. Whilst in the solution, the molecules, which in the solid state form clusters (chain folds), become disentangled and remain so after the solution is cooled to give filaments. As the fibre is hot stretched and drawn some 72 times, the chains crystallise and orient along the fibre axis and thus a very high level of macromolecular orientation is achieved. It is possible for the fibre to be drawn conventionally, however it is impossible to eliminate the chain folded crystals originally present. As shown in **Figure (3.2[a])**, eliminating these chain folded crystals in **Figure (3.3[b])** gives Dyneema its very high strength. Dyneema is also made under licence by Allied-Signal in America under the name SPECTRA® and is identical.

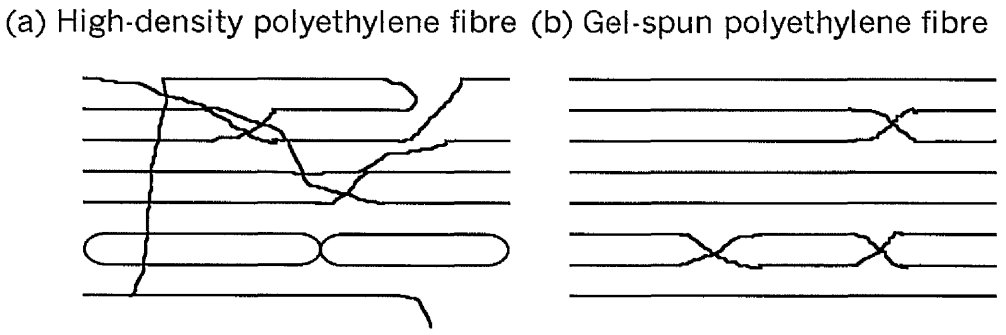

Figure (3.2) Chain Fold Elimination in DYNEEMA [47]

The sample types are :-

SK65 used where a high performance is required and maximum weight savings are to be achieved (**Sample No.2**), cost approximately £30 per kilo.

SK66 has a higher strength than SK65 (**Sample No.3**).

3.7.3 KEVLAR

'Kevlar' is a registered trademark of the Du Pont Company and is manufactured by the Advanced Fibre Systems Division. Kevlar is an aramid fibre. The term *'aramid'* is defined by the U.S. Federal Trade Commission as the generic term for *'a manufactured fiber in which the fiber-forming substance is a long chain synthetic polyamide in which at least 85% of the amide linkages are attached directly to two aromatic rings'*[48], as shown below in **Figure (3.3)**.

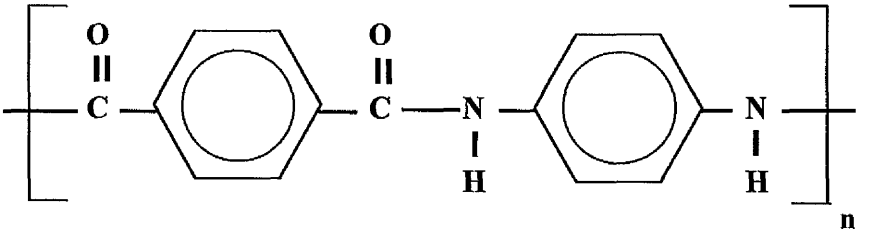

Figure (3.3) Aramid Fibre Chemical Structure [49]

This draws a distinction between aramids and polyamides for example NYLON where the main polymer chain contains mostly aliphatic and cycloaliphatic units.

Kevlar aramid fibres are skin core systems produced from a liquid crystalline polymer, that is where the molecular chains are already aligned along the flow direction. The fibre is spun from a sulphuric acid solution of the polymer, which results in a further alignment of the molecules. The spinning process resembles extrusion, the polymer is forced under pressure through a perforated plate known as a spinneret. The sulphuric acid (solvent) is removed by a Dry-jet wet spinning process whereby the spun filaments are washed, neutralised and finally dried. Once the solvent has been removed, the

resulting fibre has a more uniform alignment than could be obtained by drawing. This results in superior mechanical properties.

The sample types :-

29 the standard high performance fibre yarn (**Sample No.4**), cost approximately £17 per kilo.

119 He (High elongation) this gives 20% higher elongation than Kevlar 29 for improved fatigue resistance and dimensional stability (**Sample No.5**).

129 Ht (High tenacity) this gives up to 20% increased tenacity over Kevlar 29 for improved strength (**Sample No.6**).

29/10 a 10 year old sample for comparison with fresh Kevlar 29 (**Sample No.7**).

49/8 an 8 year old sample, has a higher modulus and lower elongation than 29 (**Sample No.8**).

3.7.4 TWARON

'Twaron' is a registered trademark of the Akzo-Nobel Company and is manufactured in the Netherlands. Twaron is also an aramid fibre virtually identical to Kevlar having the same polymer and solution. However they are made using different spinning processes. This affects both the modulus and the strength. Aramid fibres, as already mentioned, are skin core systems spun from a solution of sulphuric acid. To get rid of the acid an on-line washing process is used and this affects the skin depth.

To obtain a very fast removal of the acid from the inside to the outside, it is displaced by water going from the outside to the inside. This means the outside is washed faster. It is the outside skin that affects the Modulus of the filament, which for Twaron measures approximately 1-2 μm thick. The inside affects the strength of the filament, which for Twaron measures approximately 10 μm. It is the spinning and washing processes that separate Twaron from Kevlar and is most noticeable in the values quoted for tensile modulus Twaron 1000 at 70GPa and Kevlar 29 at 60GPa.

The sample type :-

1000 provides a direct comparison to Kevlar 29 **(Sample No.9)**, cost approximately £12 per kilo.

3.8 Enhanced Adhesion Yarns

Surface treatments are possible to enhance the adhesion of the yarns producing high bond strengths at interfaces. These fall into three main categories :

1. Chemically Treated
2. Corona Treated
3. Plasma Treated

3.8.1. Chemically Treated Yarn

The simplest method is a chemical pretreatment, involving dipping the yarn in a solution to give it an adhesive coating. In large scale manufacture this can be achieved at a relatively small increase in production costs.

3.8.2. Corona Treated Yarn

Corona treated yarn has undergone a form of electrical discharge treatment hence the term corona discharge treatment. The yarn is subject to a short duration (approximately a few seconds) high intensity discharge in air at atmospheric pressure and ambient temperature. This gives the yarn an oxide coating that etches the surface enhancing the adhesive characteristics of the yarn.

The yarn is passed over an earthed metal bar which is covered with an insulating material (the *dielectric sleeve*). A second bar a few millimetres above the yarn is a metal electrode to which high voltage is supplied. The applied voltage increases until it exceeds the value for the electrical breakdown of the air gap, so the air is ionised and it becomes a plasma. The discharge looks like a random series of faint sparks (streamers) over a blue-purple glow. Discrete intense sparks can also be seen coming from localised regions of the electrode, therefore 'corona' is not an exact description for this discharge process.

In the UV-visible region the ionised air consists of electrons, ions, excited neutrons and photons. This is enough to break C-C and C-H bonds to form radicals which by oxidation chemistry produce a variety of oxides on the surface. The extent of surface change is related to the exposure time, discharge power, discharge gap and the cleanliness of the operating conditions. This process can be achieved for a reasonable cost and therefore a small increase in the selling price of the yarn.

3.8.3. Plasma Treated Yarn

Plasma treated yarn refers to yarn that has had electrical discharge treatment at low-pressure requiring vacuum equipment. This process is also known as glow discharge treatment. The process involves a high frequency discharge at vacuum or very low pressure for time periods of 30 seconds and above, this makes it less intense and so more difficult to produce a constant repeatable surface treatment. The controlled atmosphere allows the use of a wide range of gases depending upon the type of oxidisation required. Therefore a selective reaction of specific groups is possible. A better surface penetration of internal fibres is achieved giving greater adhesion. This is certainly a more versatile process although it is very costly due to the specialised conditions needed which roughly doubles the cost of the yarn. Essentially there are three different forms of treatment possible depending on the gas used to generate the plasma and the plasma parameters, a fact which makes it much more interesting from a scientific point of view:

The first form uses *noble* gas plasmas (helium, neon, argon, etc)and was previously referred to as *casing*. The main effect is surface cross-linking and the elimination of potentially weak boundary layers. Moreover it also leads to the generation of a barrier layer to additive diffusion.

The second type of treatment uses the *reactive* gas plasmas (oxygen, nitrogen, sulphur, etc). Here the main effect is the introduction of functional groups containing the elements present in the gas molecules. Both of the first two methods will lead to etching and surface texturing after prolonged exposure.

The third method makes use of polymerisable gas plasmas capable of depositing a film on to the yarn. A highly cross-linked polymer is laid down on the yarn. It is possible by using mixed gases to build up graded interface structures. This method gives considerable control over surface properties but is not currently commercially viable.

3.9 High Adhesion Yarns

At the time of yarn selection two high adhesion yarns suitable for this project were commercially available.

3.9.1 Twaron 1001 (Sample No.10)

Twaron 1001 has an epoxy coating and is a chemically treated version of Twaron 1000. Bundles of one thousand filaments (Twaron 1000) are immersed in an emulsion of the epoxy mix. They are then heated very quickly (approximately 5-10 seconds) at a temperature of over 200°C. This cures the epoxy on to the Twaron giving an average depth of a few nanometres. This adds about £7 per kilo to the cost of Twaron 1000 (total cost £19 per kilo).

3.9.2 Dyneema SK65C (Sample No.11)

Dyneema SK65C is a corona pretreated version of Dyneema SK65 hence the prefix C. The corona treatment improves its surface energy by more than 50%. This adds about £10 per kilo to the cost of Dyneema SK65C (total cost £40 per kilo).

3.10 Yarn Industry Convention

It should be noted that yarn is sold in quantites denoted by weight. The weight of yarn can be expressed in terms of its length by using its linear density (the mass per unit length) value, unit known as the tex. The tex value is equal to the mass of a 1000m length of yarn expressed in grams e.g. Sample No.10 Twaron 1001, tex value 168 means for every 168g of yarn purchased there is 1000m in length. However for convienience the manufacturers quote the unit of decitex (**dtex**) which is the mass of a

10 000m length of yarn expressed in grams. Therefore a 2kg package gives a length of 11 900m.

$$\textbf{length} = \frac{\textbf{weight (g)}}{\textbf{dtex}} \textbf{ x 10 000} \qquad \textbf{(3-1)}$$

$$\textbf{length} = \frac{\textbf{2000}}{\textbf{1680}} \textbf{ x 10 000}$$

$$\textbf{length = 1.19 x 10 000}$$

$$\textbf{length = 11 900m}$$

The tex value is calculated from linear density tests, see *Chapter 4 section 4.4*, and is an important parameter when performing mechanical tests on the yarn, see *Chapter 4 section 4.2*. The tex value is then used when calculating the tensile strength for the yarn, known as its Tenacity. The Tenacity value allows a direct strength comparison to be made with other yarns, as it takes into account the fact that the yarns have different densities.

3.11 Summary

The foregoing Chapter was concerned with identifying and characterising the fundamental properties of polymers. This led to the determination of criteria for selection of, and eventual choice of suitable High Performance Fibre Yarns for this project.

Having given a general background to fibre yarns the Chapter introduced the yarn industry terminology and gave an overview of the processes used to produce the various yarns. Enhanced adhesion yarns were also examined and the commercial availability of such yarns was investigated. Samples of the most suitable HPFY were then acquired and profiles obtained from the manufacturer's data for each yarn Sample. These are contained in *Appendix 1.*. Yarn analysis carried out in *Chapter 4* establishes the practical data for the yarn samples obtained.

Chapter 4

Yarn Analysis

4.0 Yarn Analysis

Having procured a total of 11 different samples of HPFY it was necessary to establish the working parameters of the yarn samples and to select the most suitable HPFY for the attainment of pre-stress. During initial investigations researchers in the field of textile fibres had cautioned against relying on manufacturers given data, which they described as optimistic. The process of yarn analysis allows for practical experience of handling and using the yarns. Starting with mechanical testing of the yarns, it became clear that although the yarns are very strong in tension the filaments of the yarns are very easily damaged and the wearing of rubber gloves became obligatory. All yarns were supplied on supported packages eg cones, bobbins, tubes or spools. A package being a length of yarn in a form suitable for use, handing, storing, etc.

4.1 High Performance Fibre Yarn Samples

Table (4.1) The Initial List of HPFY for Analysis :

Sample No.	Yarn	Type of package
1.	Nylon 6.6	bobbin
2.	Dyneema SK65	bobbin
3.	Dyneema SK66	bobbin
4.	Kevlar 29	small tube
5.	Kevlar 119	small tube
6.	Kevlar 129	small tube
7.	Kevlar 29/10 years old	cone
8.	Kevlar K49/8 years old	cone
9.	Twaron 1000	spool
10.	Twaron 1001	spool
11.	Dyneema SK65C	bobbin

For full sample details see **Appendix 1.**

The yarns were withdrawn overend from the packages during testing, in the standard manner.

4.2 Mechanical Testing of Yarn

The mechanical testing of samples of HPFY was carried out in accordance with the BSi Standards :

[50] BS EN 20139 : 1992
Textiles
'Standard Atmospheres for Conditioning and Testing'.

[51] BS EN ISO 2062 : 1995
Textiles - Yarns from packages.
'Determination of Single-end Breaking Force and Elongation at Break'.

4.2.1 Conditioning and Testing Atmosphere

Tensile testing of yarns was carried out in a *standard temperate atmosphere* with a constant relative humidity and a constant temperature.

4.2.1.1 Relative Humidity (rh)

Relative humidity is the ratio of the actual pressure of the water vapour in the atmosphere to the saturation vapour pressure at the same temperature and is expressed as a percentage. The standard relative humidity for testing is **rh 65%** constant.

4.2.1.2 Temperature

The standard temperature for testing is a constant **20°C**.

4.2.1.3 Conditioning Time

With reference to BS EN ISO 2062 section 7.3, the samples were brought to moisture equilibrium under the conditioning atmosphere. For tightly wound packages a minimum of 48 hours is recommended and all the samples were conditioned for at least this length of time.

4.2.2 Sampling Scheme

For statistical analysis a minimum of 20 valid specimen results were needed; that is to say the number of specimens tested minus the number of specimens discarded should equal at least 20.

4.2.2.1 Discarded Specimens

With reference to BS EN ISO 2062 section 8.1.10 it was necessary to discard the results of the tests where *slippage occurs* and to discard results of *jaw breaks* where breaks occur within 5mm of the jaws.

4.2.3 Testing Arrangements

Research not only highlighted the need for a standard temperate atmosphere but also revealed a requirement for special pneumatic grips for yarn testing. Enquires were made at the University and it was established that UMIST has a Textile Technology Laboratory (B47) equipped for the testing of HPFY. Negotiations were undertaken with the Laboratory Technician Miss J. Walton and it was agreed that during periods when the laboratory was vacant, free use of the facilities could be granted. This meant however that there were considerable delays while waiting for vacant laboratory periods. The standard temperate atmosphere laboratory consisted of a sealed lab housed within a larger workroom. An Instron 1122 tensile testing machine was housed within the lab.

4.2.4 Test Method

In accordance with BS EN ISO 2062 the test method used was Method A, manual (section 8.2). The specimens were taken directly from the conditioned package. Following the procedures 8.1.1 to 8.1.11 the test specimens were inserted manually into the clamps for the tests to be performed.

A 500mm gauge length (sample length) was used and therefore a constant rate of specimen extension of 100% per minute meant a 500mm/min rate of displacement (crosshead speed). Under section 4 the basic principle was that a specimen of yarn was extended until ruptured by the mechanical device and the breaking force and elongation at break were recorded. A standard pretension of 0.5 cN/tex ±0.1 cN/tex (section 8.1.7) for the conditioned specimens was applied to keep the yarn in alignment before the testing, pretension values listed in **Table (4.2)**.

Table (4.2) Pretension Values :

Sample Number	Yarn	tex	Pretension
1.	Nylon 6.6	140	70g
2.	Dyneema SK65	176	88g
3.	Dyneema SK66	44	22g
4.	Kevlar 29	167	83.5g
5.	Kevlar 119	167	83.5g
6.	Kevlar 129	167	83.5g
7.	Kevlar 29/10 yrs old	167	83.5g
8.	Kevlar 49/8 yrs old	158	79g
9.	Twaron 1000	168	84g
10.	Twaron 1001	168	84g
11.	Dyneema SK65C	176	88g

The yarn was wrapped around pneumatic grips with bollard jaws, starting from the top grip which was then closed, thus ensuring the yarn was kept straight, then wrapped around the bottom grip. This would close automatically as soon as the pretension was applied and the test began instantaneously. The results were recorded directly onto graph paper. Each result was numbered as the tests proceeded. Before each set of tests the following information was recorded e.g.

Sample number	**10**
Name of Yarn	**Twaron 1001**
tex	**168**
dtex	**1680**
Pretension	**84g**
Full Scale Deflection (maximum load)	**50kg**
Crosshead Speed (rate of displacement)	**500mm/min**
Chart Speed (rate of graph displacement)	**1000mm/min**
Sample length (gauge length)	**500mm**
date of the tests.	**29-01-97**

4.2.5 Calculations

Using Sample No.10 – Twaron 1001 as an example the first step was to calculate the mean maximum deflection and the mean chart distance from the results obtained in the tests recorded on the graphs.

Estimation of the mean

$$\bar{x} = \frac{1}{n}\sum_{i=1}^{n} x_i \quad (i = 1,2,3.....n) \qquad (4\text{-}1)$$

Maximum Deflection = (9.8 N = 1kg) read directly from the scaled graph.

(mean deflection) = **251 N – (26kg)**

Sample Extension (mm) = $\frac{\text{Crosshead Speed}}{\text{Chart Speed}} \times \text{Chart Distance}$ (4-2)

(mean chart distance) = $\frac{500 \times \mathbf{25.68}}{1000}$

= **12.84mm**

% Elongation = $\frac{\text{Sample Extension}}{\text{Sample length}} \times 100$ (4-3)

= $\frac{12.84 \times 100}{500}$

= **2.6%**

Breaking Tenacity (cN/tex) = $\frac{\text{mean breaking force}}{\text{tex}}$ (4-4)

= $\frac{25\ 132\ \text{cN}}{168\ \text{tex}}$

= **150cN/tex**

4.2.6 Results

Table (4.3) HPFY Tensile Test Results

Manufacturer's Yarn data.
Yarn test results.

Sample No.	mean breaking force N - (kg)	% Elongation	Breaking Tenacity cN/tex
1. Nylon 6.6	120 - (12 kg) **109 - (11 kg)**	19% **14%**	86 **78**
2. Dyneema SK65	484 - (49 kg) **380 - (39 kg)**	3.6% **3.2%**	310 **216**
3. Dyneema SK66	145 - (15 kg) **119 - (12 kg)**	3.7% **3.2%**	330 **270**
4. Kevlar 29	342 - (35 kg) **250 - (26 kg)**	3.6% **2.6%**	205 **150**
5. Kevlar 119	342 - (35 kg) **288 - (30 kg)**	4.5% **3.4%**	205 **173**
6. Kevlar 129	393 - (40 kg) **280 - (29 kg)**	3.6% **2.4%**	235 **167**
7. Kevlar 29/10	342 - (35 kg) **204 - (21 kg)**	3.6% **2.5%**	205 **122**
8. Kevlar 49/8	324 - (33 kg) **208 - (21 kg)**	1.9% **1.6%**	205 **132**
9. Twaron 1000	331 - (34 kg) **248 - (25 kg)**	3.6% **2.3%**	197 **147**
10. Twaron 1001	331 - (34 kg) **251 - (26 kg)**	3.6% **2.6%**	197 **150**
11. Dyneema SK65C	484 - (49 kg) **399 - (41 kg)**	3.6% **3.2%**	310 **227**

NOTE:

All HPFY Tensile Test Results based on a minimum of 20 valid specimen results

4.2.7 Observations

4.2.7.1 Sample Breakdown

Two types of breakdown were observed as follows:

Type 1 denotes a breakdown whereby all filaments break simultaneously at the same point, emitting substantial noise.

Type 2 denotes a breakdown involving fracturing where the filaments of the yarn break at different points.

Sample No.1. Nylon 6.6.
Breakdown Type 1.

Sample No.2. Dyneema SK65 and Sample No.11. Dyneema SK65C.
Breakdown Types 1 and 2 were observed.
Slippage was also a major problem because Dyneema has a low coefficient of friction.

Sample No.3. Dyneema SK66
Breakdown Type 1.

Sample No.4. Kevlar 29, Sample No.5. Kevlar 119 and Sample No.6. Kevlar 129.
Kevlar 129 with high loads experienced Breakdown Type 1.
The remaining samples experienced Breakdown Type 2.

Sample No.7. Kevlar 29/10 and Sample No.8. 49/8.
Samples displayed Breakdown Type 2, but at lower loads than the new yarns.

Sample No.9. Twaron 1000 and Sample No.10. Twaron 1001.
Breakdown Type 2.

4.2.7.2 Results Analysis

All the results are, as expected, lower than the manufacturer's given data. Nevertheless, they are all in proportion relative to each other. The only anomaly is the mean breaking force of Sample No.5. Kevlar 119 He (High elongation) which is greater than Sample No.6. Kevlar 129 Ht (High tenacity), where it should be the opposite. It is speculated that Sample No.6. is older than Sample No.5. and the aging process has affected the result. A subsequent retesting of the two yarns confirmed the first results.

4.3 Elevated Temperature Testing

It was envisaged that the yarn could be tested at elevated temperatures to observe the effect of heat on the molecular backbone of the yarn. However high temperature pneumatic grips have been unobtainable. The option of heating the yarn whilst in the grips was rejected by the pneumatic grip manufacturers due to the significant possibility of damage to the rubber seals. Pneumatic grips have a maximum working temperature of 35°C. A more practical option was to heat treat the yarns and test at ambient as before. This will at least show the effects of heat cycling on the yarns. It is worth noting that during the manufacture of yarn embedded samples the tensioning of the yarn takes place at room temperature and is not altered during the resin curing process.

4.3.1 Heat Treatment Rack

The simplest and least expensive method was to construct a rack so that sufficient lengths of yarn could be wound on to it for heat treatment. The rack complete with heat treated yarn, could be transported for conditioning and testing could be carried out straight from the rack. It was decided to modify one of the existing Oven Trays, by adding rods to the ends of the tray. This gave 700mm straight lengths of heat treated yarn for testing, the rack is shown in **Figure (4.1)**.

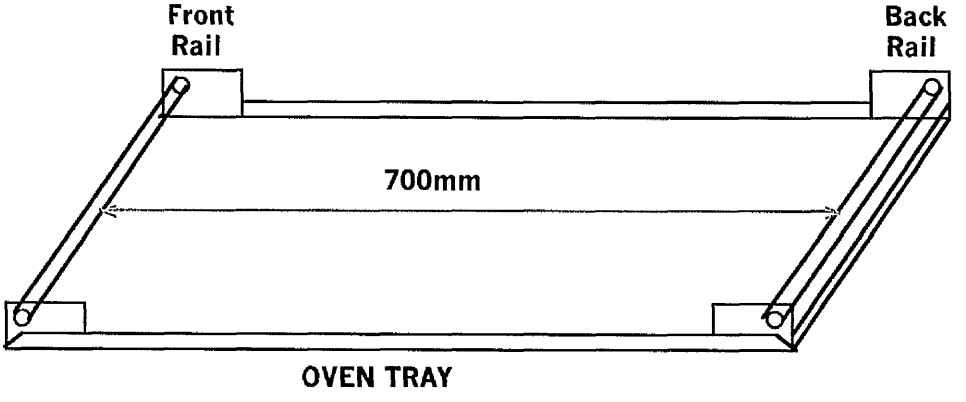

Figure (4.1) Oven tray with rails.

Heat treatment took the form of the yarn undergoing the cure cycle followed by the postcure cycle for the epoxy resin CT1200. The cure cycle reaching 135°C for 14

hours and the postcure reaching 150°C for 8 hours. Dyneema cannot be taken above 120°C therefore different settings were needed if CT 1200, was still to be used. After consulting with Dr. John Champion at the London Guildhall University, a cure cycle of 120°C for 14 hours (allowed to cool to RT), followed by a postcure cycle of 120°C for 24 hours was used. Epoxy samples cured and postcured at this temperature attain a crosslinking of 95% as compared to the manufacturers' recommended settings, and so will still allow the Dyneema samples to be compared with the others.

4.3.2 Tray preparation

Using a free standing paper towel dispenser for mounting the bobbins of yarn, it was possible to wind the yarn onto the rails of the tray. Rubber gloves were worn to ensure the cleanliness of the yarn and also to avoid damage to individual filaments of yarn. One end of the yarn was simply tied to a rail, while the other end of the yarn was attached to pretensioning weights to keep the yarn level on the tray. A pretension of 0.5 cN/tex was used as recommended for tensile testing. Experimentation showed that for ease of wrapping and handling no more than six lengths of yarn between the tie-off and weights was possible. To allow for discarded results, 24 lengths of each yarn were wrapped on to the tray. When ready the tray was placed into the oven and the cure cycle commenced immediately.

4.3.3 Conditioning and Testing

After the postcure the tray was delivered to UMIST's Textile Technology Laboratory for conditioning, in this case only 4 hours was needed because the yarn had been removed from the spool. Testing was then carried out following the same procedures as before; the yarn was simply cut from the tray and tested.

4.3.4 Heat Treated Yarn Results

Table (4.4) Heat Treated HPFY Tensile Test Results

Untreated yarn results.
Heat treated yarn results.

Sample No.	mean breaking force N - (kg)	% Elongation	Breaking Tenacity cN/tex
1. Nylon 6.6	109 - (11 kg) **100 - (10 kg)**	14 % **15%**	78 **72**
2. Dyneema SK65	380 - (39 kg) **250 - (26 kg)**	3.2% **2.1%**	216 **142**
3. Dyneema SK66	119 - (12 kg) **53 - (05 kg)**	3.2% **1.8%**	270 **120**
4. Kevlar 29	250 - (26 kg) **215 - (22 kg)**	2.6% **2.1%**	150 **129**
5. Kevlar 119	288 - (30 kg) **259 - (26 kg)**	3.4% **3.0%**	173 **155**
6. Kevlar 129	280 - (29 kg) **254 - (26 Kg)**	2.4% **2.4%**	167 **152**
7. Kevlar 29/10	204 - (21 kg) **187 - (19 kg)**	2.5% **2.2%**	122 **112**
8. Kevlar 49/8	208 - (21 kg) **199 - (20 kg)**	1.6% **1.7%**	132 **126**
9. Twaron 1000	248 - (25 kg) **226 - (23 kg)**	2.3% **2.1%**	147 **134**
10. Twaron 1001	251 - (26 kg) **231 - (24 kg)**	2.6% **2.3%**	150 **138**
11. Dyneema SK65C	399 - (41 kg) **265 - (27 kg)**	3.2% **1.9%**	227 **150**

4.3.5 Observations

The table clearly shows that, despite manufacturer's assurances, all the yarns exhibited strength losses. The most notable being Dyneema, Sample No. 3., which lost over 50% of its strength and Samples No. 2. & 11., which lost about 33% of their strength. This was despite the fact that, because of its low Tg, the Dyneema Samples had only been heat treated to 120°C, whereas all the others had been heat treated to 150°C. These results were used to set the limits for yarn loading during embedded yarn sample manufacture. Therefore it was necessary to re-test Dyneema samples however only heat treating them to 80°C for 3 hours, simulating the postcure cycle of polyester Resin C. This in an attempt to utilise the effects of higher loads in the pre-stressing of polyester at least.

4.3.5.1 Re-testing Dyneema

It was decided to re-test only Samples No. 2. & 11. due to their high loading potential, shown in **Table (4.5)**.

Table (4.5) Dyneema Tensile Tests Results.

Off-the-spool yarn results (Stored at Ambient Temperature).
Heat treated yarn results (3hrs @ 80°C).
Heat treated yarn results (14hrs @ 120°C cooled to RT + 24hrs @ 120°C).

Sample No.	mean breaking force N (kg)	% Elongation	Breaking Tenacity cN/tex
2. Dyneema SK65	380 - (39 kg)	3.2%	216
	330 - (34 kg)	*2.6%*	*188*
	250 - (26 kg)	**2.1%**	**142**
11. Dyneema SK65C	399 - (41 kg)	3.2%	227
	386 - (39 kg)	*2.5%*	*219*
	265 - (27 kg)	**1.9%**	**150**

Clearly by only heating Dyneema to 80°C and not taking it so close to its Tg, it exhibits better heat resistant qualities. Therefore the lower the cure/postcure

temperature of the resin the greater the loading can be applied to the HPFY hence the greater the pre-stress can be obtained.

4.4 Linear Density

It was necessary to check other measurable parameters of the yarns. The most fundamental of these is linear density of the yarns, which relates to the tex of the yarn. This provides the means of comparison with other yarns.

The linear density of the samples was measured in accordance with the BSi Standards:

[52]] BS EN 20139 : 1992
Textiles
'Standard Atmospheres for Conditioning and Testing'.

[53] BS 2010 : 1963 (replaced by BS EN ISO 2060 : 1995)
'Method for Determination of the Linear Density of Yarns from Packages'.

[54] BS EN ISO 2060 : 1995
Textiles - Yarn from packages
'Determination of linear density (mass per unit length) by the skein method'.

The linear density is calculated from the length and mass of suitable specimens in accordance with the conditions as noted in **Option 1:** mass of conditioned yarn at equilibrium with the standard atmosphere for testing.

4.4.1 Testing Arrangements

Within the Textile Technology Laboratory there is a linear density wrap-reel. The reel is motor driven and has a perimeter of 1 metre.

4.4.2 Test Method

The yarn is threaded through eyelets and tied onto the wrap-reel, the reel has a pre-tension of 0.5 ± 0.1 cN/tex. A turn gauge allows the reel to be set to wind off a preset amount of yarn usually multiples of 1000. Lengths of yarn were drawn from the package over-end (the manner in which it would normally be drawn in processing) on to the wrap-reel. When the required length had been removed from the package the reel stops, allowing the test specimen to be cut from the reel at the tie-on position.

After removing the specimen from the reel the yarn was weighed on a balance, inside a closed chamber.

One specimen was reeled from each package, the amount taken depending on the size of the package. A total of 50 turns (50 metres) from large packages and 25 turns (25 metres) from small packages. The minimum required by the BSi standard is 10 metres for yarns having a linear density of more than 100 tex (1000 dtex).

4.4.3 Calculations

To calculate the linear density $\mathbf{Tt_c}$, expressed in tex, from the mass and length of a conditioned specimen the equation used is:

$$\mathbf{Tt_c} = \frac{\mathbf{m_c \times 10^3}}{\mathbf{L}} \qquad (4\text{-}5)$$

eg **Sample No.10**

$$= \frac{4.325 \times 10^3}{25}$$

$$= 173 \text{ tex}$$

$$\mathbf{dtex} = \mathbf{10 \times Tt_c(tex)} \qquad (4\text{-}6)$$

$$= 1730 \text{dtex}$$

where

m_c	is the mass, in grams, of the conditioned test specimen.	**4.325g**
L	is the length, in metres, of the conditioned test specimen.	**25m**

4.4.4 Results

Table (4.6) Linear Density Values.

Sample dtex

Sample No.	Manufacturer's Data dtex	**TEST RESULTS dtex**	Length of sample m
1. Nylon 6.6	1400	**1434**	50m
2.Dyneema 65	1760	**1706**	50m
3.Dyneema 66	440	**436**	50m
4. Kevlar 29	1670	**1742**	25m
5. Kevlar 119	1670	**1715**	25m
6. Kevlar 129	1670	**1716**	25m
7. Kevlar 29/10	1670	**1480**	50m
8. Kevlar 49	1580	**1353**	50m
9. Twaron 1000	1680	**1714**	25m
10. Twaron 1001	1680	**1730**	25m
11. Dyneema 65C	1760	**1796**	50m

4.4.5 Observations

All the fresh samples are close to the manufacturers' given values whereas a significant reduction took place in the two older yarn samples. This indicated that some form of degradation had taken place over the years.

4.5 Adherence Capacity

The ability to sustain a high loading is only one consideration. Moreover, in order for the transfer of stress to take place, the adherence capacity of the HPFY is crucial. Good adhesion at the fibre/resin interface is essential. Indications from Kabir [55] were that for good adhesion the yarn should have a similar or higher value of surface energy than the resin encapsulating it.

A high measure of adhesive bonding between the yarn and the resin matrix is vital if the transfer of stress is to take place. If high bond strength is not achieved, the tensile stress in the yarn will not translate into compression in the resin matrix but will instead result in debonding at the interface. Instead of retarding the breakdown it will accelerate the process. The greater the interfacial bond strength, the greater the transfer of stress through the interface.

4.6 Surface Energy

The surface energy of a material is a measure of its ability to bond to other materials. Polymers are renowned for having low values of surface energy ranging from 20 to 100 mJ/m^2 (1 $mJ/m^2 \approx 1$ dyne/cm). An investigation into the surface energies of the yarn samples will determine the most suitable yarns for use in the polyester and epoxy resins being used. To determine the surface energy of a solid, in this case a single polymer fibre, it is necessary to examine its polar and dispersive characteristics. These are easily determined by a series of contact angle measurements using a variety of probe liquids with different surface tensions and polarities.

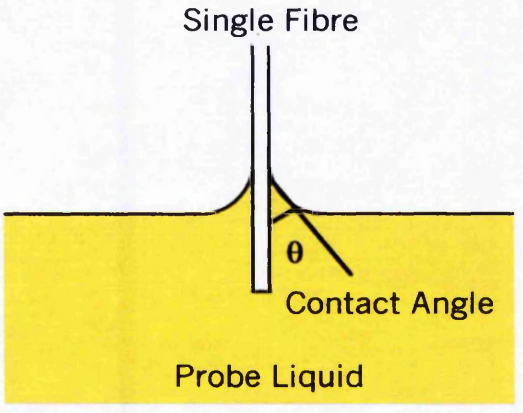

Figure (4.2) The Contact Angle θ.

To measure the tangent found at the three phase solid/liquid/vapour interface the contact angle θ as shown in **Figure (4.2)** was obtained. While the fibre was held in place by a microbalance, the probe liquid housed in a glass beaker, moved at a constant rate to scrutinise the surface of the fibre to produce a unique contact angle hysteresis curve. Then by applying the Wilhelmy plate technique [56], the dynamic contact angle was calculated from the wetting force recorded by the balance, the surface tension of the probe liquid and the wetted perimeter of the fibre using **equation (4-9)** (section 4.6.4). Surface energy calculations are then made using groups of contact angle measurements.

4.6.1 Surface Energy Measurements

Enquiries were made to establish that the British Textile Technology Group (BTTG) based in Didsbury, Manchester have a CAHN Dynamic Contact Angle Analyser (DCA 322) which could be used on a daily basis (the cost of such equipment is in excess of £50,000).

The DCA 322 System uses the Wilhelmy plate technique and comprised of a Stand Assembly coupled to a computer and printer. An electromicrobalance is housed in the top of the Stand Assembly and an O-ring arm hangs down into the testing chamber.

From the O-ring hangs a balance loop (Inline sample stirrup) with a weighing pan for calibration. At the base of the chamber is a controllable Slow Stage Platform on which the probe liquid beaker sits. It is the pre-settable time stage platform that moves slowly up to meet the fibre. The fibre is attached to a flexible support wire that hooks on to the bottom of the balance loop directly above the platform. A flexible support wire must be used in order to protect the sensitive microbalance from shock damage as it meets the liquid. The computer software monitors both advancing and receding contact angles, the stage positions and the microbalance force readings. Calculations are made from the resulting hysteresis between the stage positions (mm) relating to the linear region of the advancing/receding curve.

4.6.2 Conditioning

Lengths of yarn were taken directly from the packages and no cleaning of the yarn was undertaken. One and a half metre lengths of each sample of yarn were delivered to BTTG for conditioning overnight. The conditioning and testing were carried out in humidity and temperature controlled room. A relative humidity (rh.) of 40 % and a temperature of 20°C for the conditioning and testing atmosphere is maintained throughout.

4.6.3 Sampling Scheme

Single filaments of fibre 10mm long were cut using a scalpel from the conditioned yarn samples. The filaments were mounted onto flexible support wires (copper wire tinned) using Bostik SuperGlue. This operation had to be carried out using a Binocular Headband and then checked under a microscope to ensure that only a single filament was present.

4.6.4 Theoretical Considerations.

The Basic Equations

$$F = \frac{ST \times P \times \cos\theta}{g} \quad (4\text{-}7)$$

$$P = \frac{F \times g}{ST \times \cos\theta} \quad (4\text{-}8)$$

$$\cos\theta = \frac{F \times g}{ST \times P} \quad (4\text{-}9)$$

Where :

F = the sample force at zero immersion depth as determined by the microbalance (mg).

P = Perimeter of the sample at the interface (cm).

ST = Surface Tension of the Probe Liquid.

Cos θ = Cosine of the Contact Angle.

g = Acceleration due to gravity, default is 0.980665.

4.6.5 Perimeter Calculations.

The first unknown is the perimeter (circumference) of the fibre. If the fibre filament was perfectly round then the **circumference = πd** where d is the diameter of the filament and could be calculated from the manufacturer's data. Alternatively by dividing the Linear Density (g/m) by the Volume Density (g/m^3) to obtain the area (m^2) and so from the area obtain the radius (m) which is half the diameter. In reality the filament is far from round (the manufacturers refer to them as off-round) and must be determined by a perimeter test because the diameter value effects the perimeter value which in turn effects the surface energy calculations.

4.6.6 Perimeter Tests

The DCA 322 is able to measure the wetted perimeter. This can only be achieved by selecting a probe liquid that completely wets the fibre to ensure that a Zero Contact

Angle (ZCA) is obtained. Hexane is the low surface tension liquid (18.4 dynes/cm) usually used for perimeter measurements. The use of a low surface tension liquid will ensure complete wetting of the solid and thus satisfy the conditions for ZCA.

Complete wetting results in no hysteresis curve being produced so the software simply takes the force reading from the microbalace during the stage position when the advancing and retarding curves merge. Using **equation (4-8)** the perimeter value is obtained as g = 0.980665, ST is already set by the probe liquid at 18.4 dynes/cm and the Cosine 0° = 1. The results were displayed on the computer screen as shown in **Table (4.7)** and include a value for the diameter.

Table (4.7) Computer Screen Display - Perimeter Test Result for S4 (Sample 4 Kevlar 29) in HEX1 (Hexane).

PERIMETER
(output)

File Name	:	S4HEX1		
			FORCE	
Initial position	:	3 mm	---	
Final position	:	6 mm	Average	0.07553 mg
			Max	0.09700 mg
Surface Tension	:	18.4 dynes/cm	Min	0.07200 mg
Perimeter	:	0.042726 mm	Std Dev	0.00394 mg
Diameter	:	0.013600 mm	Variance	0.00002 mg

4.6.7 Perimeter Test Results

The surface energy calculations showing the variation between the diameter and perimeter values obtained from :

(i) Manufacturer's Data giving an average value for the diameter, perimeter = πd.
(ii) DCA Perimeter Tests, the actual measured sample diameter.
(iii) Density Calculations,

Linear Density/Volume Density = Area

where

Area = πr^2
Diameter = $2r$
Perimeter = πd

Table (4.8) Perimeter Test Results

(Diameter) – Perimeter

Sample No.	Manufacturer's Data μm	**Perimeter Tests μm**	Density Calculations μm
1. Nylon 6.6	(27) - 84.82	**(30.09) - 94.51**	(27.29) - 85.73
2. Dyneema SK65	(12) - 37.70	**(15.54) - 48.83**	(12.18) - 38.26
3. Dyneema SK66	(12) - 37.70	**(13.82) - 43.43**	(12.18) - 38.26
4. Kevlar 29	(12) - 37.70	**(13.60) - 42.73**	(12.15) - 38.17
5. Kevlar 119	(12) - 37.70	**(12.33) - 38.74**	(12.15) - 38.17
6. Kevlar 129	(12) - 37.70	**(14.44) - 45.37**	(12.15) - 38.17
7. Kevlar 29/10	(12) - 37.70	**(12.94) - 40.64**	(12.15) - 38.17
8. Kevlar K49	(12) - 37.70	**(12.88) - 40.48**	(11.78) - 37.01
9. Twaron 1000	(12) - 37.70	**(12.71) - 39.93**	(12.19) - 38.30
10. Twaron 1001	(12) - 37.70	**(13.09) - 41.12**	(12.19) - 38.30
11. Dyneema SK65C	(12) - 37.70	**(14.14) - 44.43**	(12.18) - 38.26

NOTE:

Perimeter Test Results are based on a minimum of 2 fibres.

4.6.8 Observations

All of the samples were thicker than the manufacturers' quoted data. When approached about these figures each manufacturer stated that theirs were average values for the fibres. Furthermore, because of the manufacturing process the fibres were not uniform and values would vary, but agreed that the measured wetted perimeter values obtained were the most accurate for our samples of yarn and could be relied upon for further calculations.

4.6.9 Solid Surface Energy Modules

The DCA 322 has three Surface Energy Modules available

(i) Zisman Plot.
(ii) Geometric Mean Multi-Liquid Method.
(iii) Harmonic / Geometric 2-Liquids Method.

For the purpose of yarn tests Modules (ii) and (iii) are used.

(ii) Geometric Mean Multi-Liquid Method.

The Geometric Mean Multi-Liquid method used by the DCA 322 is adapted from the method developed by Kaeble [57]. The original geometric mean equation for surface energy calculations comes from Good *et al* [58] and Fowkes [59]. A summary of the surface energy equations and theory used in the DCA 322 software are contained in the CAHN Application Note entitled "Solid Surface Energy Analysis Yesterday and Today", Domingue [60]. A minimum of 2 and a maximum of 8 different probe liquids are required for the algorithm used in this module.

(iii) Harmonic / Geometric 2-Liquid Method.

The harmonic mean method used is adapted from the equation developed by Wu [61]. The geometric mean equation for surface energy calculations is adapted from Kaeble [57], Good *et al* [58] and Fowkes [59]. For a full summary again see CAHN Application Note Domingue [60]. There are two sets of values for the probe liquid surface tension components, one set based on the harmonic mean the other from the geometeric mean and these were taken from [57], [59], [61] and Dahal [62]. Only 2 probe liquids are required for these calculations. The harmonic data will contain two solutions one which is real and one which is not. When compared with the geometric data, the real solution will be similar. On the other hand the unreal solution may be different as it may contain negative numbers.

A general rule is to choose a balanced combination of polar and non-polar probe liquids for surface energy tests. However the surface tension of the probe liquid must be high enough to avoid complete wetting (ZCA). For example, water is a highly polar liquid and methylene iodide is a highly dispersive liquid both with high surface tensions. They are often used as a pair for these tests. The best results are obtained when the advancing contact angle for the probe liquid is greater than 20 degrees and less than 160 degrees because the cosine function varies little between 0-20° and 160-180°.

4.6.10 Probe Liquids

A total of five probe liquids were used during the course of the tests. They are listed below in **Table (4.9)** showing their respective values of total surface tension and a breakdown of their polar and dispersive contents.

Table (4.9) Breakdown of Probe Liquid Surface Tension Values (dynes/cm)

	GEOMETRIC		HARMONIC		
Probe Liquid	Dispersive	Polar	Dispersive	Polar	**TOTAL**
Water	22.50	50.30	22.10	50.70	**72.80**
Tricresylphosphate	39.20	01.70	39.80	01.10	**40.90**
Methyleneiodide	48.50	02.30	44.10	06.70	**50.80**
Glycerol	37.00	26.40	40.60	22.80	**63.40**
Formamide	39.50	18.70	36.00	22.20	**58.20**

The value of surface energy is determined by the nature of the interparticle bond and relates to the dipoles of atoms and molecules. Polar forces have a net dipole moment, but with dispersion forces (or London Forces) the dipole moments are instantaneous and not permanent. Nonetheless, these dispersion interactions are important to adhesion, a factor in the strengths of bonds and play a major role in the surface phenomena of contact angles.

4.6.11 Surface Energy Results

The **Table (4.10)** below shows the manufacturers' quoted values for Surface Energy and the values obtained for our Samples using at least four liquids for the Geometric Mean Method.

Table (4.10) Surface Energy Test Results

Sample No.	Manufacturer's Data	**TEST RESULTS**
	mJ/m^2	**mJ/m^2**
1. Nylon 6.6	40.7	**37.47**
2.Dyneema SK65	32	**33.44**
3.Dyneema SK66	32	**29.52**
4. Kevlar 29	33	**31.46**
5. Kevlar 119	33	**31.33**
6. Kevlar 129	33	**32.85**
7. Kevlar 29/10	33	**35.38**
8. KEVLAR 49	33	**38.87**
9. Twaron 1000	35	**36.65**
10. Twaron 1001	45	**42.46**
11. Dyneema 65C	49	**47.75**

4.6.12 Observations

On the whole the results are in line with the manufacturer's data. The tests did highlight certain key points in that the fibres are not of a uniform shape and that the spin finish increases the wetted perimeter. Also a patchy distribution of the spin finish was evident when testing Twaron 1001, lower values of surface energy were recorded than for Twaron 1000 where in theory the epoxy coating should have increased the surface energy. However inhomogeneties in the distribution of the spin finish as found by Mahy *et al* [63] and De Lange *et al* [64] for Twaron 1001 would account for the spread of results. Eventually the value obtained was the average of three separate tests.

4.7 The Choice of Yarn

Previous work on the effect of barriers within solid insulation by Kabir [55] gave the Surface energy values for the initial chosen resins :

Polyester resin (Resin C), surface energy 41 mJ/m^2

Epoxy resin (CT1200), surface energy 43 mJ/m^2

From the surface energy tests carried out there were three off-the-shelf yarns with higher values of surface energy:

Sample No. 1. Nylon 6.6

Sample No. 10. Twaron 1001

Sample No. 11. Dyneema SK65C

Nylon 6.6 is not suitable for Raman Analysis and so was discarded. It was therefore decided to proceed using high adhesion yarns along with their basic counterparts for comparison (Twaron 1001 with 1000 and Dyneema SK65C with SK65). The manufacture of multiple yarn samples also revealed problems with yarns that were not chemically treated. In threading the yarns through the silicone tubes and moulds the yarn filaments became electrostatically charged. This had the effect of splaying the yarn and making it very difficult to work with. An elecrostatic gun was purchased but proved ineffective. In the interests of time and cost effective development, therefore the project has concentrated on the use of Twaron 1001 the epoxy coated HPFY. At a later stage, samples containing Twaron 1000 could be produced for comparison purposes, time permitting.

4.8 Additional Yarn

Production of multiple yarn samples necessitated the acquisition of additional Twaron yarn. Akzo-Nobel supplied a further two large bobbins of Twaron (see **Appendix 1**):

i.) Sample No. 9.2 - Twaron 1000 (2kg - bobbin)

ii.) Sample No. 10.2 - Twaron 1001 (2kg - bobbin)

The packages were subject to mechanical testing in accordance with the BSi Standards used on the other samples. They were brought to moisture equilibrium under the conditioning atmosphere for at least 48 hours and then tested. **Table (4.11)** lists the results of the mechanical testing and shows the results of the tests for Sample 9 & 10 for comparison.

Table (4.11) Twaron Comparison Table 1.
Off-the-spool yarn results (Stored at Ambient Temperature)

Original Samples No. 9 & 10
Additional Samples No. 9.2 & 10.2

Sample No.	mean breaking force N (kg)	% Elongation	Breaking Tenacity cN/tex
9. Twaron	248 - (25kg)	2.3%	147
1000	229 - (23kg)	2.7%	136
10. Twaron	251 - (26kg)	2.6%	150
1001	207 - (21kg)	2.5%	123

The second batch of Twaron samples (Samples No. 9.2 & 10.2) exhibit a reduction in strength. It was speculated that this was due to aging (degradation) of the packages. On contacting the manufacturer it was revealed that the second batch of samples were produced 12 months ago, and had then been kept in storage, whereas the first batch had been spun to order and delivered immediately. It was therefore recommended that the outer layers of the packages be removed and then to test the inner layers. Surface degradation occurs because aramid fibres are sensitive to prolonged exposure to ultra-violet (UV) light. Degradation is limited to the outer layers of the packages because aramids have a *self-screening* property.

To avoid wasting the outer layers of the packages, it was decided to transfer some of the yarns on to smaller packages. This could then be used for experimentation and applications where only light loads were used, such as pre-tensioned samples. Enquires were made in the Textile Technology Department at UMIST. UMIST has a wrapping machine suitable for HPFY. On the 9-10-98 approximately 500g of yarn was transferred from each of the main second batch bobbins to small cones. These cones are referred to as:

i.) **Sample No. 9.2.2 - Twaron 1000**

ii.) **Sample No. 10.2.2 - Twaron 1001**

The extra identification number denotes that they are the second package, thus the original bobbins now gain an extra identification number to denote that they are package one, eg. Sample No. 9.2., becomes Sample No. 9.2.1. and so on.

Samples No. 9.2.1 & 10.2.1 were returned for mechanical testing as before. The results of these tests can be seen in **Table (4.12)** along with the results from Samples No.9 & 10. This time the results are in conjunction with the original findings made in the first year.

Table (4.12) Twaron Comparison Table 2.
Off-the-spool yarn results (Stored at Ambient Temperature)

Original Samples No.9 & 10
Additional Samples No. 9.2 & 10.2
Inner Sample No. 9.2.1 & 10.2.1

Sample No.	mean breaking force N (kg)	% Elongation	Breaking Tenacity cN/tex
9. Twaron 1000	248 - (25kg)	2.3%	147
	229 - (23kg)	*2.7%*	*136*
	276 - (28kg)	2.7%	165
10. Twaron 1001	251 - (26kg)	2.6%	150
	207 - (21kg)	*2.5%*	*123*
	253 - (26kg)	2.5%	151

4.9 Pre-stressed Sample Production

Loading of the yarn during pre-stressed sample production has revealed further limitations of the yarns. Sudden shock loads such as the dropping of a weight on to the weight hanger can cause premature failure of the yarn especially at high loads. Loading the yarn within 20% of its mean breaking force causes failure of the yarn after a short time period eg 10-15 minutes. The loading limit for Twaron 1001 would appear to be 20kg as NO samples attempted above this loading have been successful. This indicates that loading is also time dependent ie the yarn exhibits creep. By definition creep is *the continuously increasing defamation of materials over time under steady load* [47], this creep process can, if the material is loaded to excess, lead to the failure of that material.

Finally in an attempt to improve the production process an extra pulley was added to the pre-stressing rigs to separate the top and bottom yarns. The exposure of the extended lengths of top yarn caused the failure of the yarn after a few minutes or hours. Further research indicated that the yarn filaments contain faults. By exposing a greater area of yarn it increases the prospect of finding fault concentrations, hence yarn failure. Adding the extra pulley has however improved the threading process, as the yarn no longer drags over the rig frame.

4.10 Standard Tolerances

Subsequent enquires with the yarn supplier Goodfellow [65], highlighted the existence of standard tolerances for the supplying of fibre materials. These standard tolerances are given in **Table (4.13)**.

Table (4.13) Standard Tolerances

Fibre Diameter:	±25%
Number of Strands:	±10%
Tex Number:	±10%

An examination of the yarn analysis results showed that the procured yarns are nearly all within the acceptable tolerance ranges, the notable exceptions being the older yarn samples.

4.11 Summary

Having procured the 11 samples of HPFY this Chapter describes the analysis of these samples. For each sample actual working parameters are analysed against manufacturer's given data and each sample was then compared against the others in order to produce a final selection.

A methodical approach was adopted to checking the manufacturer's data given in the text and in **Appendix 1**. This consisted of a number of tests, namely: mechanical testing at room temperature, mechanical testing at elevated temperatures, linear density tests and surface energy measurements. These processes narrowed down the choice of yarn for the project. Moreover they also served to identify some deficiencies in the yarn such as its susceptibility to filament damage. Furthermore, some variations between the manufacturer's given data and actual working parameters were revealed, notably the irregular shape of the yarn filaments, the reduction in the mean breaking force and patchy distribution of surface coatings. Nevertheless the yarns were within the accepted standard tolerances.

Additional supplies of the shortlisted yarns were then obtained. Good practice also suggested checking the mechanical strength of any newly acquired yarn supplies to ensure that the strength was comparable to yarn already used. The process finally resulted in the selection of Sample No.10 the aramid fibre yarn Twaron® 1001 due to its high strength and high surface energy. This process also highlighted the susceptibility of Aramid fibres to UV degradation. Resin sample production revealed further deficiencies, such as the potential failure caused by shock loading and the tendency of the yarn to exhibit creep. A more detailed review of aramid fibres is carried out in *Chapter 5*.

CHAPTER 5

Aramid Fibres

5.0 Aramid Fibres

The aramid fibre known as Kevlar was discovered in 1965 when Stephanie Kwolek, a Du Pont research scientist, synthesised a series of para-oriented aromatic polyamides. Kevlar is based on poly(p-phenylene terephthalamide), PPTA shown in **Figure (5.1)**, one of the para-oriented aromatic polyamides synthesised by Kwolek.

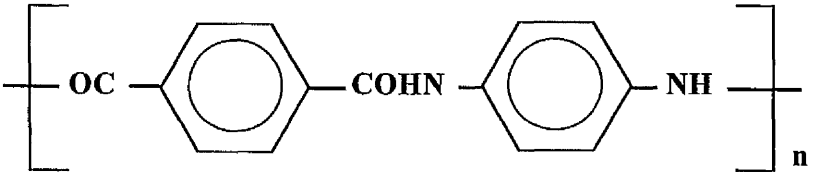

Figure (5.1) Chemical Structure of PPTA [48]

Several more years research were necessary to produce a commercial high-modulus fibre from the linear polymer. It was made possible only when researchers at Du Pont discovered a method of dry-jet, wet spinning the liquid crystal aramid oligomers into aramid fibre. A similar method is used by Akzo-Nobel to produce Twaron aramid fibre. Unlike most polymers, the materials are nearly 100% crystalline and all the chains are aligned along the fibre axis.

Aramid fibre has a highly crystalline, highly ordered structure. This has been confirmed by wide-angle X-ray diffraction. The X-ray patterns show no amorphus halo, indicating high crystallinity as shown in Yang *et al* [66]. X-ray diffraction was also used by Northholt and van Aartsen [67] who proposed the crystal lattice model of PPTA, based on the crystal structure of model compounds.

5.1 Morphological Features

To appreciate the unique combination properties of aramid fibres it is necessary to consider the internal microstructure. As with electrical treeing there are numerous theories, here are three of the most commonly observed morphological features.

5.1.1 Fibrillar Structure

Studies of fracture morphology [68,69,70] enabled investigators to identify the fibrillar structure of Kevlar fibres. The propensity for fibrillation is due to the lack of lateral forces, except for the van der Waals and the hydrogen bond forces between macromolecles. It was shown by Panar et al [68] that the fibrils are oriented along the fibre axis and are about 600nm wide and up to several centimetres long. The proposed model of the fibrillar structure is illustrated in **Figure (5.2)**. It is the highly crystalline, highly ordered fibrils that form the basic load-bearing elements of aramid fibres.

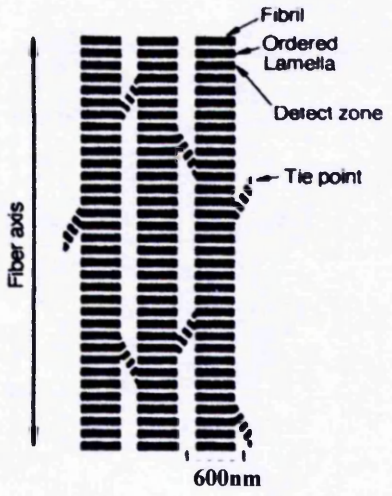

Figure (5.2) Fibrillar Structure of Aramid Fibre [68]

5.1.2 Pleat Structure

A frequently reported structural feature of the Kevlar fibre is the transverse bands observable by optical microscopy [66]. Dobb *et al* [71] suggested that Kevlar fibres consist of a system of H-bonded PPTA sheets regularly pleated along their axes and arranged radially with an angle of 170° between adjacent components of the pleat. They found axial banding at 250 and 500nm periodicities in longitudinal fibre

sections. Based on these observations, they proposed a structural model of radial pleated sheets in Kevlar fibre as shown in **Figure (5.3)**. However, these transverse bands diminish when the aramid fibre is subjected to tension because of the straightening of the pleat structure. The presence of the pleat structure imparts some elasticity to the fibre structure.

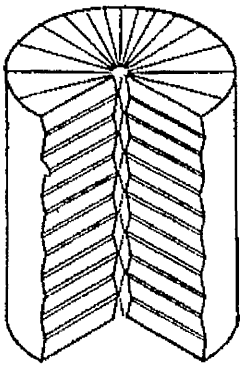

Figure (5.3) Pleat Structure Model of Aramid Fibre [71]

5.1.3 Skin-core structure

The general feature of man-made fibres is a skin-core structure. This is attributed to the difference of friction for skin molecules and core molecules. When molecules pass through the orifice of the spinning nozzle at a constant velocity, skin molecules will suffer higher shear stress than core molecules because skin molecules slide over the surface of the orifice. Panar *et al* [68] postulated that the surface fibrils are uniformly, axially oriented, where as the core fibrils are imperfectly packed and ordered. The proposed simple skin-core model is shown in **Figure (5.4)**. It is the thickness of the skin that affects the Modulus of the fibre and the core that affects its strength. Hence the distinction between the values of Kevlar and Twaron due to their different spinning processes.

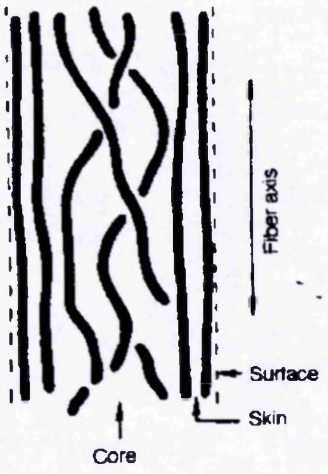

Figure (5.4) Skin-core Structure Model of Aramid Fibre [68]

5.2 Deformation & Fracture Models

So far it can be seen that aramid fibre has a highly ordered crystalline structure, its physical properties, in particular tensile properties, are related to its fine structure. It is the degree of crystalline orientation, crystallite size, and crystallinity of an aramid fibre that significantly affects its physical properties. For this reason it is important to examine a few of the numerous deformation and fracture models in order to understand the tensile fracture and failure modes of the fibres.

5.2.1 Tensile Deformation Model

The mechanical behaviour of an ordinary fibre such as Nylon can be modelled using a two-phase model, which assumes a sandwich structure of crystalline and amorphous domains along the fibre axis. However the morphology of aramid fibres makes this two-phase model unsuitable, because the polymer chains are too rigid to fold, Northolt *et al* [72]. Hence, the polymer chain must be regarded as a rigid rod. Thus, Northholt [73] adopted a one-phase paracrystalline model to explain tensile deformation of the aramid fibre. This crystallite model is schematically shown in **Figure (5.5)**.

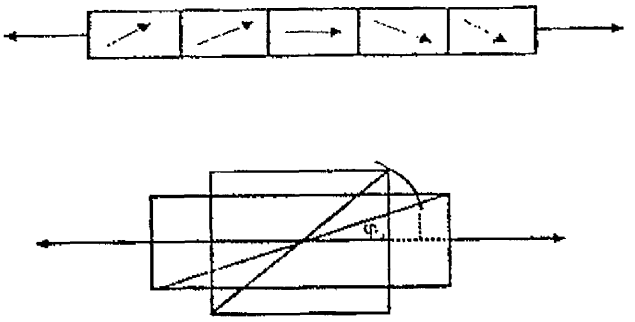

Figure (5.5) Paracrystalline Model of Aramid Fibres [73]

The fibre is considered to be built up of fibrils running parallel to the fibre axis. The fibrils are chains of crystallites arranged end-to-end but the molecular chains have a slight disorientation with respect to the fibre axis. Consequently, a tensile stress applied along the fibre axis causes stretching of the crystallites and a rotation towards the fibre axis due to shear deformation. Therefore the total strain is the sum of both deformation processes, as shown by Northolt [73] and van der Zwaag *et al* [74].

5.2.2 Fracture Model

A fracture model for aramid fibres was put forward by Morgan *et al* [75]. They proposed that 'chain-end' concentration factors affect the deformation and failure process and the strength of aramid fibres. Their model of the chain-end distribution in PPTA fibres is shown in **Figure (5.6)**. The assumption is that the rod-like PPTA macromolecules are aligned parallel to the fibre axis. In the fibre exterior the chain-ends are arranged randomly relative to each other but become progressively more clustered in the fibre interior. This results in periodic transverse weak planes at regular intervals (approximately 200nm) along the fibre axis and the chain ends cluster in the vicinity of these weak planes. The fibre exterior is assumed to be less crystalline than the interior.

The fibre core consists of cylindrical crystallites 60nm in diameter, which have some degree of structural continuity in the fibre direction. A smooth transition in chain-end concentration is envisaged from the fibre exterior to interior resulting in a maximum chain-end concentration at the fibre centre.

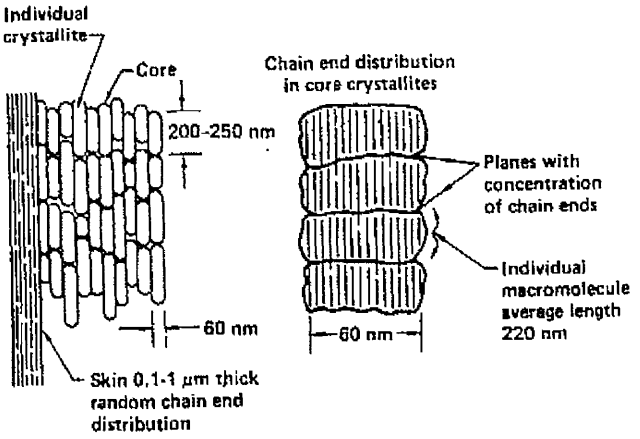

Figure (5.6) Model of the Chain-end Distribution in PPTA Fibres [75]

The chain-end model is consistent with the observed deformation and failure processes of aramid fibres. From the development of the chain-end model Morgan *et al* [75] predicted the propagation of a crack. **Figure (5.7)** illustrates in two dimensions the path of a crack that traverses the macromolecular chain ends of an array of aligned macromolecules with a skin-core distribution of ends. Crack propagation can occur parallel to rods because it requires only the rupture of H-bonds.

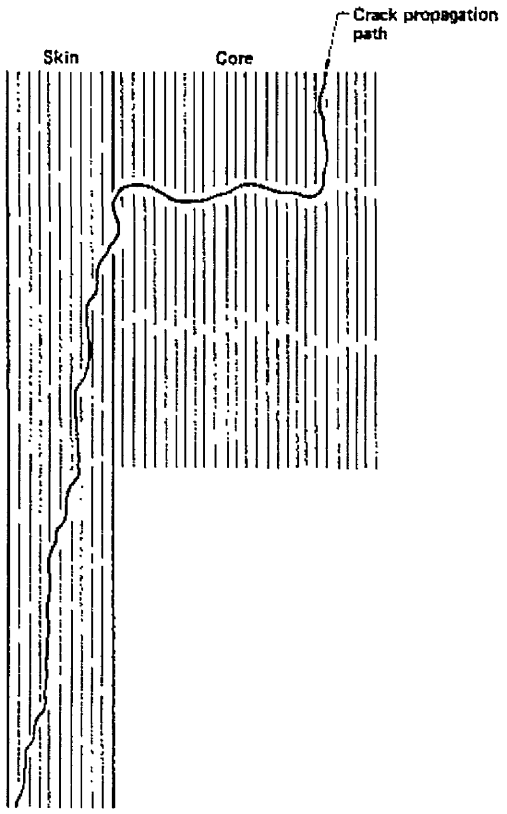

Figure (5.7) Crack Propagation Path in the Skin and Core Region [75]

Figure (5.7) also illustrates that the skin exhibits a more continuous structural integrity in the fibre direction than the core, hence the core will fail more readily on transverse weak internal planes.

5.3 Tensile Fracture and Failure

There are many factors that can affect the type of fibre failure in a tensile break. They included the interaction of neighbouring filaments in the yarn bundle, compressive or flexural fibre stress, the strain rate and the fibre fine structure. It is these factors that change the initiation and propagation of the fibre fracture.

In a tensile break there are three basic types of fibre fracture morphology: (a) point break, (b) fracture break, and (c) kink band break. **Figure (5.8)** shows by microscopy the fracture morphology of aramid fibre in tensile breaks.

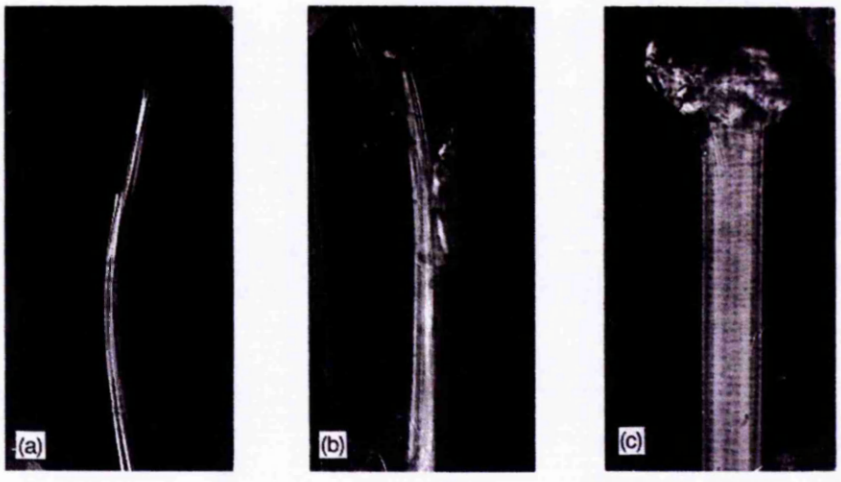

NOTE – Nominal fibre diameter 12μm.

Figure (5.8) Fracture Morphology of Aramid Fibres in Tensile Breaks [66]

Type **(a)** pointed breaks exhibit a gradual tapering of fibre diameter toward the break point and are considered to be the ideal case giving high fibre strength.

Type **(b)** fractured breaks are fibrillated and split at the break. They are the most common form of break and acceptable for most end uses.

Type **(c)** kink band breaks are premature tensile breaks caused by kink band defects. When an aramid fibre is subjected to axial compression it will undergo morphological deformation. The kink band represents a structural discontinuity in the fibre, it tends to depress the strength of the fibre. When a kink band is repeatedly strained, it will lead to a premature failure of the fibre. Kink banding should be avoided because it does not allow the strength of the fibre to be fully exploited.

Therefore to obtain the best results from the use of aramid fibres in composite insulation structures compressive and flexural stresses must be minimised.

5.4 Bond Stretching and the Bond Angle

The standard chemical structure of PPTA is given in **Figure (5.1)**. Unfortunately this does not take into account the 'bond angle' present in the structure of the fibre. **Figure 5.9** illustrates the position of the bond angle in the full chemical structure.

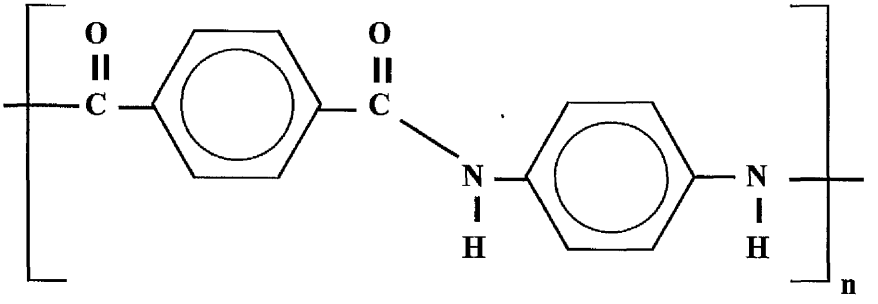

Figure (5.9) Full Chemical Structure of PPTA [76]

The bond angle is the angle made around the carbon atom. It is the bond angle that affects the chain stiffness and controls the modulus of the fibre. If a fibre is put under load the bond angle changes, this is known as *bond stretching*. The bond stretching of the molecular chain also produces changes in the molecular vibrations. The study of these molecular vibrations, which are associated with compression or extension of the molecular chain, indicates the level of stress present in a fibre. These molecular vibrations can be monitored using a form of molecular spectroscopy known as *Raman Spectroscopy*. According to the paracrystalline model put forward by Prasad *et al* [77], the tensile deformation of aramid fibre consists of two components: rotation of crystallites, and the stretching of crystallites. This is important because it was shown by van der Zwaag *et al* [74] that the Raman bandshift is related to the stretching of crystallites only, and independent of the rotation of crystallites. Thus, with Raman spectroscopy, the stretching mode is isolated. This permits the monitoring of the internal stress levels within the resin matrix, as indicated by the molecular vibrations, which was vital to the attainment of pre-stressed insulation.

5.5 Summary

A more detailed review of Aramid fibres has been carried out in this Chapter. It has been demonstrated, through examination of morphological features, that Aramid fibres have a highly ordered crystalline structure. It is this structure that significantly affects its physical properties and these properties in turn directly affect the tensile fracture and failure modes of the fibres. In particular this Chapter has outlined the detrimental effect of kink banding, which leads to premature failure and therefore must be avoided.

The importance of the bond angle and, in particular changes in the bond angle under load, known as bond stretching, has been highlighted. The bond stretching produces changes in molecular vibration, which can be used to monitor the internal stress levels via Raman spectroscopy. The contribution of Raman spectroscopy to the development and success of this research is examined in more detail in *Chapter 6*.

CHAPTER 6

Raman Spectroscopy

6.0 Introduction

It was recognised that the fibre/resin interface has an important influence on the properties of fibre embedded polymer composites. In theory, the epoxy coated aramid fibre yarn Twaron® 1001, the selected yarn, provides a strong and durable fibre/resin interface needed to give good mechanical properties to the resulting composite. A measurement technique that could determine the type of internal stresses generated at the fibre/resin interface and quantify them without destroying the sample, was therefore essential. In the past, the three main test methods commonly used for the analysis of interfacial micromechanics in polymer-based composites were fragmentation, pull-out and microbond tests, see Herro-Franco *et al* [78]. Unfortunately all of these tests result in the destruction of the sample under test and moreover give different results for identically prepared samples. The basic problem is that the tests are all indirect methods of fibre stress or strain measurements, therefore the state of stress in each test will be different. A more direct method of stress analysis is to use Raman spectroscopy.

It has been demonstrated by Young [79,80], using Raman spectroscopy, that the strain-dependent shift of the Raman bands in aramid fibres can be used to measure the point-to-point values of the axial fibre strain along yarn embedded in a resin matrix. This technique permitted the determination of the stress condition of the yarns in all the embedded samples prior to tensile and electrical tree testing, giving an accurate picture of the internal stress characteristics of all the samples tested. This provided a high level of understanding about the internal state of the resin matrix, which was demonstrated by the fact that the samples were not bent, therefore the stresses must be equal and opposite.

6.1 Spectroscopy

Spectroscopy provides significant methods for identifying a material type, determining its structure, and observing its physical properties. It uses the

fundamental principle that atoms in molecules vibrate. Molecules consist of atoms bound together by chemical bonds. These bonds and the angles between them are not completely rigid, thus molecular motions can be observed. These molecular motions consist of translations, rotations and vibrations, but usually a mixture of all three.

Molecules exhibit complex vibrational patterns, but these motions are linear combinations of much simpler fundamental modes of vibration which are usually known as *normal modes*. A mode of vibration in a molecule is a periodic contortion in which the centre of mass of the molecule or its orientation does not change as a result of the vibration and in which all of the atoms pass through their equilibrium position simultaneously, Hendra *et al* [81].

A vibrating molecule may interact with electromagnetic radiation of appropriate frequency in two ways. If the radiation has the same frequency as one of the normal modes it is possible for the molecule to absorb the radiation. This usually takes place in the infrared region of the electromagnetic spectrum. Later, the molecule will lose any energy absorbed by re-radiation. An infrared absorption spectrum of the material is obtained by allowing infrared radiation to pass through the sample and determine what fraction is absorbed at each frequency within a defined range. The second way in which electromagnetic radiation could interact with a molecule is by being scattered, with or without a change in frequency, Bower *et al* [82]. Raman spectroscopy is based on this electromagnetic radiation phenomenon.

Quantum theory indicates that the energy of a molecule is expressed in terms of a series of discrete energy levels. Thus when an electromagnetic field interacts with a molecule, a transfer of energy from the field to the molecule can occur only when Bohr's frequency condition is satisfied, see Ferraro *et al* [83]

$$\Delta E = h\nu_0 = h\frac{c}{\lambda} \qquad (6\text{-}1)$$

Where ΔE is the difference in energy between two quantized states, h is Planck's constant (6.6×10^{-34} Js), c is the velocity of light (3×10^8 m/s), λ is the wavelength of the electromagnetic radiation, and ν_0 is the incident beam frequency.

6.2 The Raman Scattering

In Raman spectroscopy, the sample is irradiated by intense laser beams in the IR-visible region (ν_o). The scattered light is usually observed in the direction perpendicular to the incident beam, as shown in **Figure (6.1).**

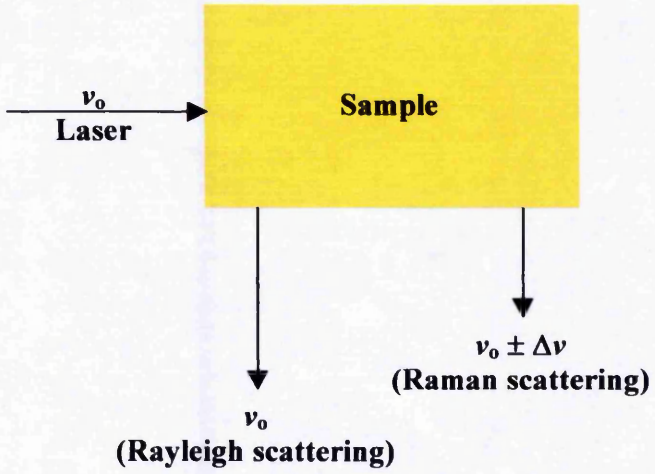

Figure (6.1) Schematic Mechanism of Raman Spectroscopy [83]

The scattered light is made up of two parts: one is called the *Rayleigh scattering*, which is weak and has the same frequency as the incident beam (ν_o). The other is called the *Raman scattering*, which is extremely weak and has frequencies $\nu_o \pm\Delta\nu$, where $\Delta\nu$ is a vibrational frequency of a molecule. The $\nu_o - \Delta\nu$ and $\nu_o + \Delta\nu$ lines are called the *Stokes* and *anti-Stokes* lines respectively. Thus Raman spectroscopy measures the vibrational frequency ($\Delta\nu$) as a shift from the incident beam frequency (ν_o).

Using classical theory the Raman scattering can be explained as follows: the electric field strength E (V/m) of the electromagnetic wave (laser beam) fluctuates with time (t) as shown by Eq. (6-2):

$$E = E_o\cos(2\pi\nu_o t) \qquad (6\text{-}2)$$

where E_o (V/m) is the maximum field strength and ν_o (Hz) is the frequency of the laser. If this light irradiates a diatomic molecule, an electric dipole moment P is induced:

$$P = \alpha E \tag{6-3}$$

On substituting E from Eq. (6-2) into Eq. (6-3) we obtain;

$$P = \alpha E_o \cos(2\pi \nu_o t) \tag{6-4}$$

where α is a proportionality constant and is called *polarizability*. If the molecule is vibrating with a frequency $\Delta\nu$ (Hz), the nuclear displacement q is written

$$q = q_o \cos(2\pi \Delta\nu t) \tag{6-5}$$

where q_o is the maximum distortion. If the distortion is likely to cause an alteration in the polarizability and it is assumed that the variation will be linear and the amplitude of displacement small, the polarizability of the periodically distorting molecule will become

$$\alpha = \alpha_o + \left(\frac{\partial \alpha}{\partial q}\right)_o q + \ldots\ldots\ldots \tag{6-6}$$

where α_o is the polarizability of the molecule in the equilibrium position, and $(\partial\alpha/\partial q)_o$ is the rate of change of α with respect to the change in q, evaluated at the equilibrium position. Hence the variation in polarizability as the molecule vibrates will be in the form:

$$\alpha = \alpha_o + \left(\frac{\partial \alpha}{\partial q}\right)_o q_o \cos(2\pi \Delta\nu t) \tag{6-7}$$

The vibrations mean that the polarizability varies with time. Therefore on substituting α from Eq. (6-7) into Eq. (6-4) we obtain;

$$P = \alpha_o E_o \cos(2\pi \nu_o t) + \left(\frac{\partial \alpha}{\partial q}\right)_o q_o E_o \cos(2\pi \nu_o t)\cos(2\pi \Delta \nu t) \tag{6-8}$$

However, since [84]

$$\cos A \cos B = \frac{1}{2}\,[\,\cos(A + B) + \cos(A - B)\,] \tag{6-9}$$

we can arrange Eq. (6-8) to give,

$$P = \alpha_o E_o \cos(2\pi \nu_o t) + \frac{1}{2}\left(\frac{\partial \alpha}{\partial q}\right)_o q_o E_o \{\,\cos[\,2\pi(\nu_o + \Delta\nu)t\,] + \cos[\,2\pi(\nu_o - \Delta\nu)t\,]\,\} \tag{6-10}$$

The first term in Eq. (6-10) represents an oscillating dipole that radiates light of frequency ν_o (Rayleigh scattering), while the second term corresponds to the Raman scattering of frequency, $\nu_o + \Delta\nu$ (anti-Stokes) and, $\nu_o - \Delta\nu$ (Stokes). If $(\partial\alpha/\partial q)_o$ is zero, the vibration is not Raman-active. Therefore to be Raman-active, the rate of change of polarizability (α) for the vibration must not be zero.

The Raman effect on a fibre subjected to stress is shown schematically in **Figure (6.2)** where a beam of light frequency ν_o is scattered by the material. The majority of the radiation is scattered elastically at the same frequency (the Raleigh scattereing) but a small amount of the radiation is scattered inelastically at a different frequency $\pm\Delta\nu$ (the Raman scattering), Young [76].

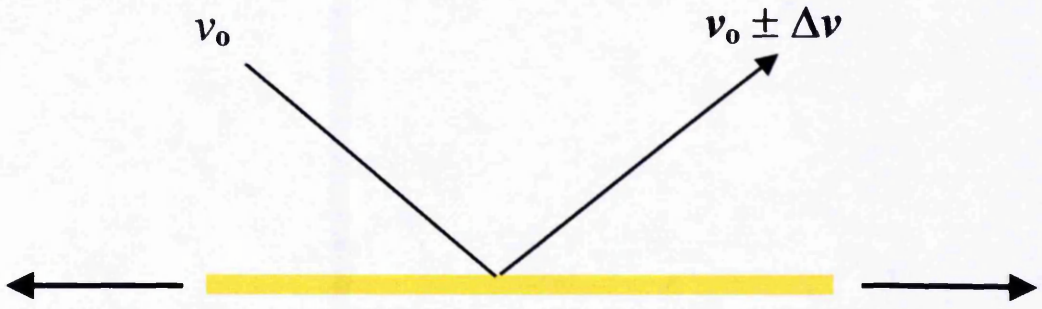

Figure (6.2) Schematic Diagram of the Raman Effect for a Fibre Subjected to Stress [76]

In the past Raman spectroscopy has not been widely used in regular laboratories but confined to use by specialists, using expensive laser spectrometers. Recent progress in instrumentation with lasers has made the equipment less expensive and easier to use. The most significant progress has been made in the cooling systems for lasers, namely becoming air cooled as opposed to water cooled and in the development of highly sensitive photon detectors i.e. charge-coupled device (CCD) cameras. Added to this has been the growth and availability of new polymers that are sensitive to characterisation by Raman Spectroscopy. In particular high performance fibre yarns such as the aramid fibres Kevlar® (Du Pont) and Twaron® (Akzo Nobel) have well defined Raman spectra because of their combination of highly orientated molecular structure and the aromatic nature of their molecular backbones.

6.3 Raman Deformation Studies

It has been demonstrated by Young *et al* [85] that the frequencies or wavenumbers of the Raman bands of many HPFY shift with the application of stress to the fibre. This behaviour is attributed to macroscopic deformation being converted directly into the stressing of the covalent bonds along the polymer backbone and changes in the bond angles. Aromatic polyamides such as Kevlar®, as demonstrated by van der Zwaag *et al* [86], were the first HPFY to display stress- or strain-induced shifts in the position of their Raman bands. Such fibres have well-defined Raman spectrum due to their high levels of molecular alignment and very good physical properties including a high Young's modulus. This means that during deformation, the macroscopic deformation

results in direct stressing of the backbone bonds in the molecules, which can be seen as shifts in the band positions in the spectra.

Subsequent work into the stress- or strain-induced Raman band shifts revealed that this phenomenon could be utilised to observe varying aspects of the structure-property relationships in materials. In particular it could be used to evaluate the interfacial characteristics of polymers and polymer fibre reinforced composites, as shown by Young [79,80]. It was in this respect that Raman analysis offered significant benefits to the development of the project.

A typical Raman spectrum produced from a single filament of aramid fibre (Twaron 1001 shown in **Figure 6.3**) will show at least eight well defined Raman band peaks between 1100 and 1700 cm^{-1}, Young [76]. These Raman band peaks will shift under the application of stress or strain, van der Zwaag *et al* [86].

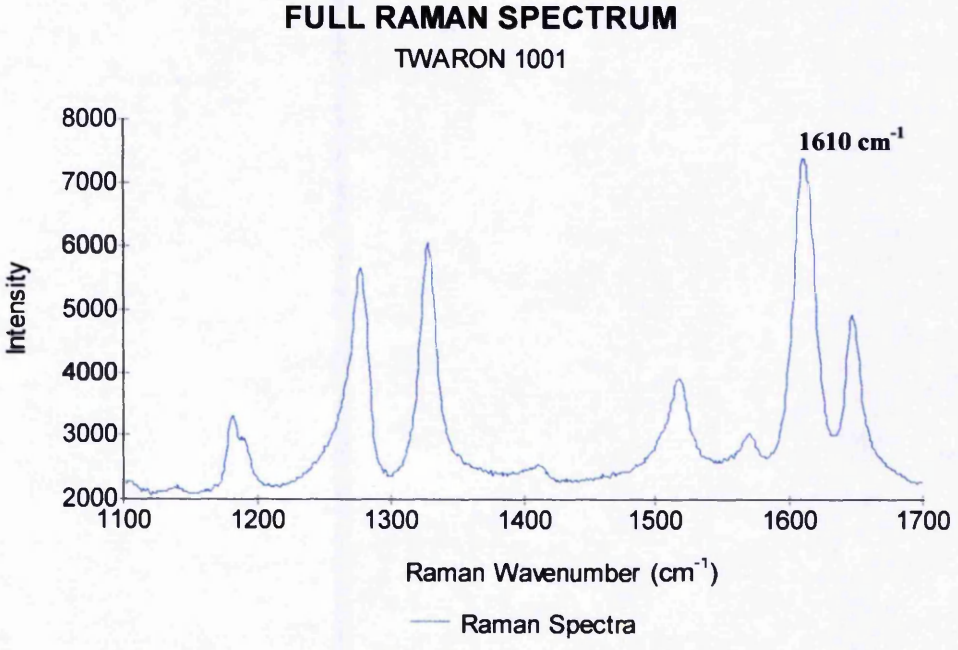

Figure (6.3) A Typical Raman Spectrum from a Single Filament of Twaron 1001

The most critical of these peak band positions is the Raman wavenumber 1610 cm^{-1} which shifts to a lower wavenumber on the application of strain, as demonstrated by Young [76]. This shift to the left (lower wavenumber) shows the fibre is under

tension, as shown in **Figure (6.4)**, whereas a shift to the right (higher wavenumber) shows the fibre under compression, as shown by Andrews *et al* [87].

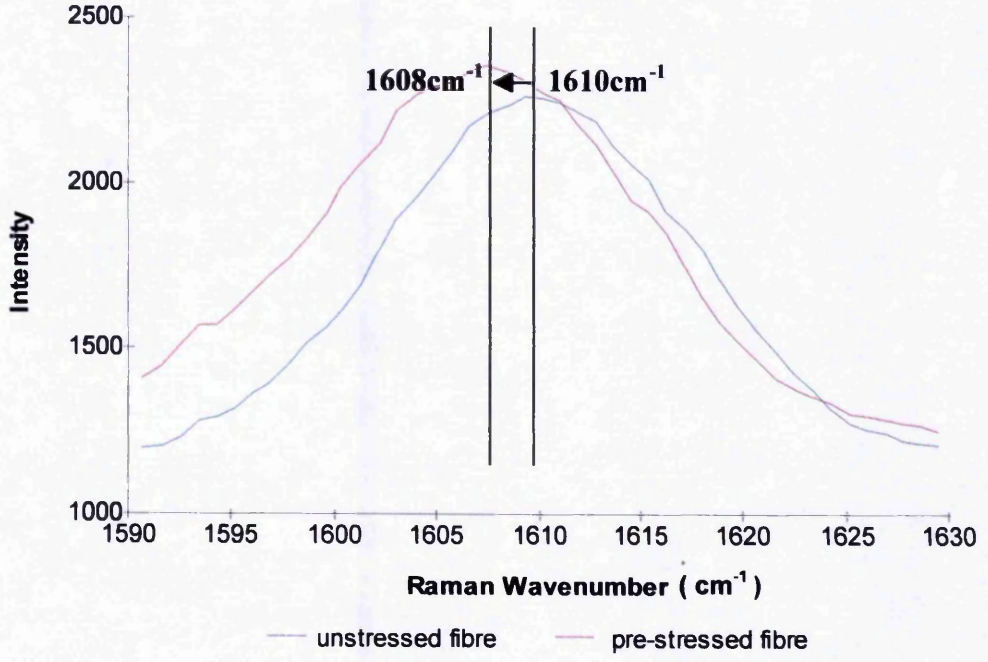

Figure (6.4) The Critical 1610cm^{-1} Peak Under Tensile Stress (Pre-stress) Moving –2.0cm^{-1} Wavenumbers, a Shift to the Left (0.6% strain)

6.4 Manchester Materials Science Centre

The support and assistance provided by Professor R.J. Young and the Manchester Materials Science Centre was invaluable to the development of this project. Initially all sample analysis was carried out by Professor Young's researchers. This started with the analysis of plain samples of polyester Resin C and Araldite® CT1200, to check the levels of fluorescence (Raman interference) inherent in the chosen resins. No significant levels of fluorescence were detected and the production of single yarn embedded samples began. The only prerequisite was that the yarn should be no deeper than 3mm inside the sample face being analysed.

6.4.1 Single Yarn Samples

A selection of single yarn samples, see *Chapter 8* for sample designs, was prepared for Raman analysis and delivered to the Materials Science Centre. Lengths of yarn were left hanging from the ends of the samples to allow analysis of the yarn in air for comparison with the embedded yarn. These initial samples were subject only to their respective resin curing processes. For the lightly loaded samples the pre-tension loads were determined by their tex values in keeping with the yarn analysis carried out in *Chapter 4, section 4.2.4.*

6.4.2 Single Yarn Samples Results

Table (6.1) shows the details of the preliminary Twaron® single yarn samples delivered for Raman analysis. Each resin type lists the number of samples made, the applied loading and the resulting bandshift.

Table (6.1) Preliminary Single Yarn Sample Results

No. of Samples	Yarn Type	Applied Load (g)	Bandshift
Polyester Resin C cured at room temperature for 24 hours.			
1	Twaron	0.5 x tex (84g)	+ 2.0cm^{-1}
1	Twaron	1.0 x tex (168g)	+ 0.5cm^{-1}
2	Twaron	5kg (5000g)	0.0cm^{-1}
1	Twaron	10kg (10000g)	0.0cm^{-1}
Araldite® CT1200 cured at 135°C for 14 hours			
1	Twaron	0.5 x tex (84g)	+ 1.0cm^{-1}
1	Twaron	1.0 x tex (84g)	+ 0.5cm^{-1}

All samples with a positive bandshifts indicate that the yarn was under compression. It was noted that where the bandshift exceeded +1.0 there were kink bands present in the samples. Excessive shrinkage leads to 'kink-bands' and as, already mentioned in *Chapter 5, section 5.3*, these lead to premature failure of the yarn, as shown by Andrews *et al* [35]. The samples that showed no overall bandshifts were in a state of

equilibrium and showed that a reasonable amount of pre-tension was needed to counteract the compressive tendency (shrinkage) of the resins.

It was also noted that all of the samples were bent. However the bottom faces (the base) of the samples were not all bending in the same way. The samples with a positive bandshift had concave bases, indicating resin shrinkage consistent with the Raman analysis, whereas the samples in equilibrium had convex bases, indicating that stress absorption was occurring, this was attributed to the asymmetrical design of the single yarn samples. Therefore samples had to be produced with symmetrical yarn configurations in order to balance the internal stresses experienced during curing due to differences in the coefficients of linear expansion of the yarns and the encapsulating resin.

6.4.3 Sample Production Modifications

Production of symmetrical samples began by using the polyester Resin C and the bending aspect was eliminated. Nevertheless, the problem of resin shrinkage remained and it was concluded that a low shrinkage resin would have to be used to establish pre-stress in the samples, see *Chapter 7, section 7.3*. For a number of years Professor R.J. Young's researchers have used the cold cure epoxy novalak resin Araldite® 5052, made by Ciba Polymers, in order to overcome the problems caused by resin shrinkage, as used in Young *et al* [88] and Andrews *et al* [89]. The use of Araldite® 5052 resin made the production of yarn embedded Pre-stressed samples possible.

6.5 Sample Analysis

During the course of the second and third years, the Raman testing facilities were made available to the author for sample analysis. The University code of practice requires that any person using a laser should undergo laser safety training and have a laser medical, in order to obtain a Laser Safety Certificate. Professor R.J.Young provided instruction in the use of the Renishaw 1000 Raman System, which uses a Helium Neon Laser Class 3B. In accordance with safety procedures set out in Laser Safety Notes of Guidance [90], a pair of laser safety spectacles were worn at all times

when working with the Raman laser. Initially this equipment was used once a week, unfortunately, demand within the Manchester Materials Science Centre meant that this reduced to once a month.

A special Ultra Long Working Distance (ULWD) lens was purchased which allowed the laser to focus on the embedded yarn. Several different magnification levels were tried but the only suitable magnification was x50. The Olympus Optical Co. Ltd manufactured the ULWD MS Plan x50 lens purchased.

6.5.1 Setting up Procedure

Before carrying out Raman analysis, it is first necessary to set up the computer program, Renishaw WiRE 32, which runs on Windows '95. On screen icons allow access to files to adjust and execute the program. In the *Experimental Setup* files, the system was set to display the 1610cm^{-1} peak with an exposure time of 3 seconds, using a x50 objective lens. Using the *Image Area* file, the *CCD-Area Setup* is used to fine tune the camera to the 1610cm^{-1} peak.

6.5.2 Yarn in Air

The first step in Raman analysis was to find the normal peak position of the yarn. This calibrates the laser to the specific yarn being used and was done by analysing a sample of yarn in air. A length of yarn, taped to a microscope slide, was used for this purpose. The on screen *Video Viewer* shows the view from the CCD camera. Using the CCD camera, the microscope is focused onto one fibre in the yarn cluster. The microscope is then switched off and the laser shutters opened. The *Video Viewer* then displays the scatter from the yarn in the form of *'a glow'*. A spectrum is obtained by clicking on to the *Get Spectrum* icon. After a few seconds a spectrum appears on screen; clicking on the *Fit* icon starts the curve fit routine. The operator works through the routine to obtain the peak value of the spectrum, around 1610cm^{-1}.

6.5.3 Yarn Embedded in Resin

Analysis of yarn embedded samples is more complex. When using the microscope the *Video Viewer* is only able to focus on the surface of the resin sample above the yarn. Therefore with yarn embedded samples the microscope is switched off after focusing on the resin surface. Switching to the laser, the operator adjusts the position

of the lens until the scatter (a glow) appears on screen; a spectrum can then be taken. This is a painstaking procedure and can take up to an hour. However, once the scatter is in focus, i.e. the lens is at the correct height above the embedded yarn, all of the samples can be analysed with small adjustments. This is only made possible by having embedded yarn samples that are of a consistent quality.

Readings taken from the yarn embedded samples are then compared with the yarn in air; a negative waveband shift indicates yarn in tension, a positive shift indicates yarn in compression. As far as possible all yarn embedded samples were analysed to ensure the uniformity of each different type of sample. Key samples e.g. Sample I (the first 20kg Pre-stressed sample) were analysed on a regular basis to monitor the effect of aging on Pre-stressing.

When a sample was being analysed, readings had to be taken using the base of the sample, which was flat and therefore gave a clear path for the laser to focus on the yarn. The top of the sample was unsuitable for Raman analysis because it was curved due to the meniscus, which had formed on the surface at the resin/mould interface during manufacture. A series of readings were taken along the length of the sample and a representative spectrum was saved to a file. This procedure was carried out on each of the fibre bundles embedded in the base of the sample, this was done to check the uniformity of the stress distribution. In a symmetrical (Quad) sample the side on which the identification character was etched was called the front and the yarn bundles were denoted front yarn and back yarn accordingly.

6.6 Araldite® 5052 Quad Sample Results

The Raman bandshifts resulting from the tensile loading of the embedded fibres are shown in **Table (6.2)**. These results are for samples that have experienced the standard cure cycle conditions i.e. cured for one day at RT followed by a postcure for 6 days at RT. The results for one week old quad samples show bandshifts for a range of applied loads. These range from 2.25kg (Pre-tensioned) samples through to 20kg (Pre-stressed) samples. There is a systematic decrease in the wavenumber of the 1610 cm^{-1} peak in the Raman spectrum of the Twaron 1001 fibres, indicating that the

tensile strain increases, as the loading is increased. It should be noted that a bandshift of $0.2cm^{-1}$ is not significant and can be due to statistical error. For a standard cured sample a difference of no more than $0.2cm^{-1}$ bandshift was recorded between the front and back yarns.

Table (6.2) Negative Raman Bandshifts in One Week Old Quad Samples

	Load applied to fibres	Raman bandshifts
Pre-tensioned	**2.25kg**	**$0.0 \pm 0.1\ cm^{-1}$**
	5kg	**$-0.5 \pm 0.1\ cm^{-1}$**
	10kg	**$-1.0 \pm 0.1\ cm^{-1}$**
	15kg	**$-1.5 \pm 0.2\ cm^{-1}$**
Pre-stressed	**20kg**	**$-2.0 \pm 0.2\ cm^{-1}$**

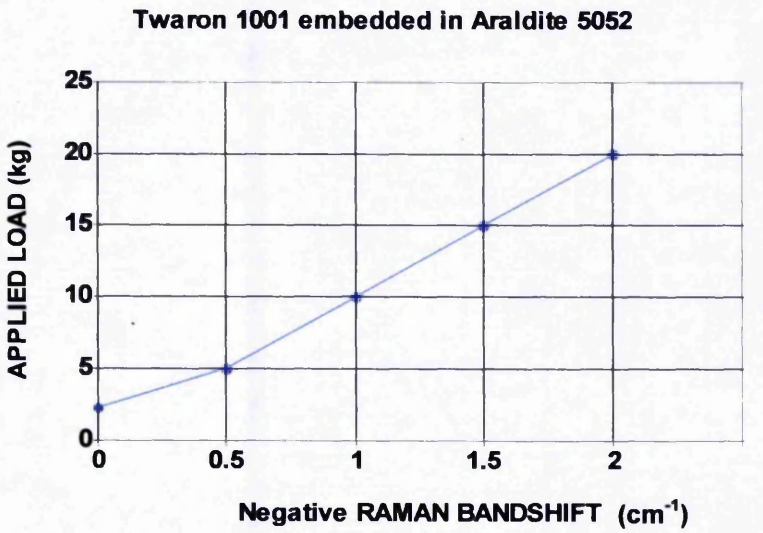

Figure (6.5) Negative Raman Bandshifts in One Week Old Quad Samples

The graph of the results in **Figure (6.5)** shows a linear relationship between the Raman bandshift and the applied load, but this only occurs after the strain in the yarn has exceeded the strain in the resin, see *Chapter 7 section 7.3*. A zero bandshift indicates a state of equilibrium within the sample ie the strain in the resin (shrinkage) is equivalent to the strain in the yarn (pre-tension). Whereas, if the strain in the resin exceeds the strain in the yarn, i.e. excessive shrinkage in the resin, a positive bandshift

is recorded and the yarn is in compression, as shown in **Table (6.3).** The results recorded in **Table (6.3)** are for samples that experienced different cure and postcure conditions or a lower load than those in **Table (6.2).** It should be noted that no kink bands were evident in any of the samples

Table (6.3) Positive Raman Bandshifts in One Week Old Quad Samples

Cure/postcure procedures		Load Applied	Raman Bandshift
Case A	**NO RT CURE**		
	10hrs @ 50°C	**2kg**	**+0.5cm^{-1}**
Case B	**NO RT CURE**		
	8hrs @ 80°C	**2kg**	**+0.6cm^{-1}**
Case C	**1d @ RT +**		
	2hrs @ 80°C	**2kg**	**+0.2cm^{-1}**
Case D	**1d @ RT +**		
	6d @ RT	**2kg**	**0.0cm^{-1}**

The 2kg loaded samples (Cases A-D) clearly show the thermal effects of elevated temperature postcure on resin shrinkage. This is highlighted in the samples which were postcured without curing them first (Cases A & B), producing samples with higher levels of shrinkage. It is the effect of the temperature drop from the postcure level to the final temperature i.e. RT, that has the biggest effect on the resin shrinkage. Applying a staged cure/postcure procedure reduces the thermal effect on resin shrinkage (as seen with Case C). By eliminating the temperature drop i.e. RT cure and postcure (Case D), and applying the correct load (to give the equivalent percentage strain in the yarn to percentage strain in the resin) the shrinkage can be overcome to reach a state of equilibrium i.e. zero bandshift.

It became apparent that even if the yarn is encapsulated within the resin and cured at room temperature the shrinkage of the resin causes a loss of tension in the yarn. The

size of the pre-stressing rigs prevented the analysis of the yarn under tension. The development of the more compact heavy duty stress bed, on the other hand, provided the opportunity to analyse the yarn under tension. The author had hoped to perform Raman analysis on the yarn in the stress bed prior to encapsulation by the resin. To perform Raman analysis of the yarn in the stress bed, it would be necessary to remove the microscope platform from the Raman microscope. The stress bed would have to be mounted on a set of interconnected hydraulic bench jacks (available from Mechanical Engineering Department) in order to provide the vertical movement necessary for alignment. This would be a delicate operation, as any shock vibration would cause misalignment of the laser. Ideally, this analysis would best be performed prior to the servicing of the Raman microscope to ensure that no misalignment had occurred. Unfortunately the time limits for this project did not permit this analysis.

6.7 Stress/Strain Calibration

In order to quantify the Raman bandshift values, a stress/strain calibration was performed. A single fibre was bonded lengthways across the middle of a card frame with an aperture measuring 50mm x 10mm. It was left to cure for 48 hours. The card sample was then glued (with Superglue®) onto two brackets of a calibration platform. A load cell with a digital readout was connected to the fixed mounting bracket. A micrometer controlled the sliding bracket. Initial readings were taken from both the micrometer and load cell along with a Raman spectrum. The micrometer was then adjusted by 0.02mm; a load cell reading was taken followed by a Raman spectrum. This continued until the fibre was broken; the data was then used to plot graphs of stress and strain with respect to the bandshift movement of the peak band position $1610cm^{-1}$.

The effect of bandshift movement on the Raman spectrum for Twaron® 1001 is shown in **Figure (6.6).** This shows the position of the peak Raman band for a single fibre of Twaron® 1001 plotted as a function of **(a)** fibre strain and **(b)** fibre stress. The rate of band shift per unit strain $d\Delta\nu/de = S$ for the Twaron fibre in **Figure (6.6) (a)** is -3.4cm^{-1}/ % strain. Therefore in the 20kg Pre-stressed sample:

$$\textbf{Fibre strain} = \frac{\textbf{Raman wavenumber shift (cm}^{-1}\textbf{)}}{\textbf{Strain calibration factor (cm}^{-1}\textbf{/\%)}} \qquad (6\text{-}11)$$

$$\textbf{Fibre strain} = \frac{-2.0}{-3.4}$$

$$\textbf{Fibre strain} = 0.6\%$$

hence **Fibre Strain** for samples with lower values of pre-stress are

-1.5/-3.4 = 0.44%

-1.0/-3.4 = 0.29%

-0.5/-3.4 = 0.15%

-0.2/-3.4 = 0.06%

-0.1/-3.4 = 0.03%

Figure (6.6) (a) Strain Calibration Graph

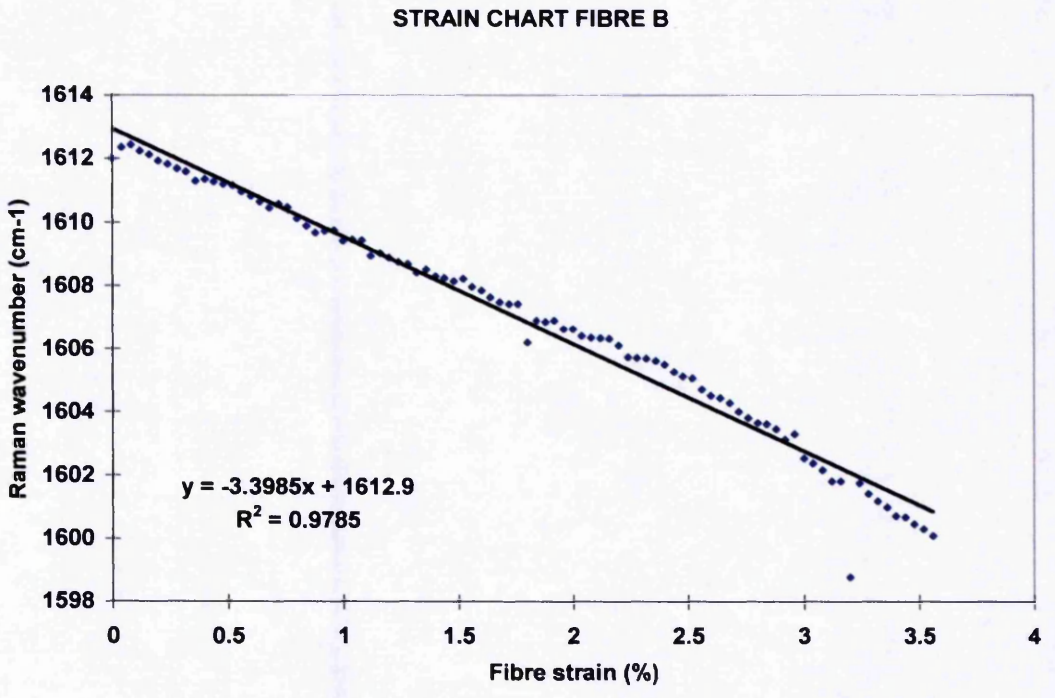

Figure (6.6) (b) Stress Calibration Graph

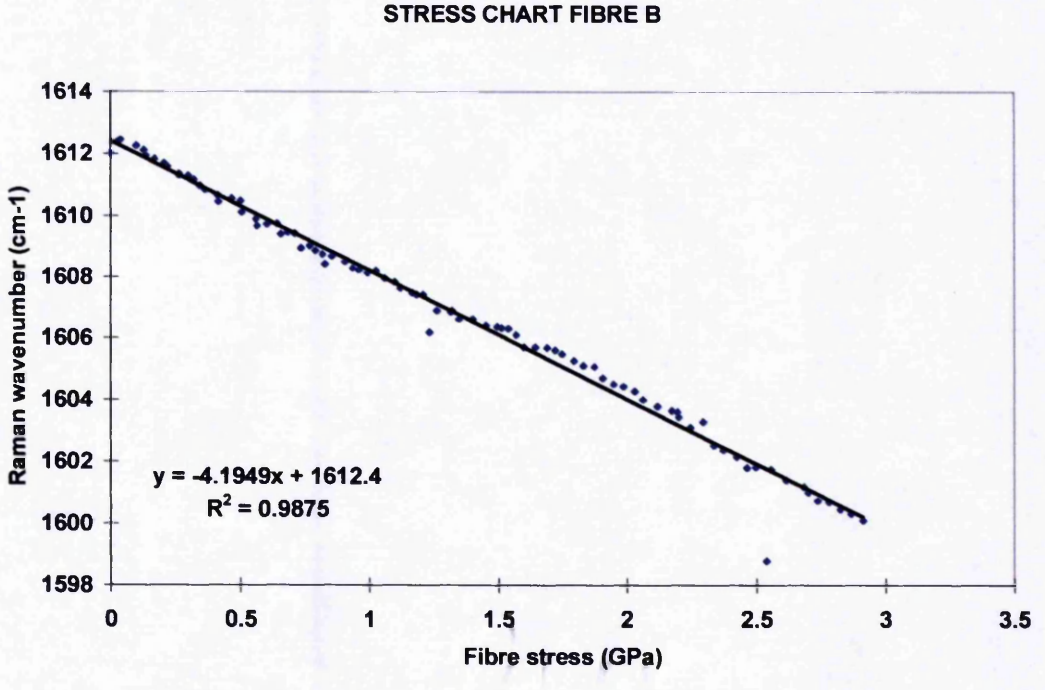

It was found by Young *et al* [85] that the rate of band shift, *S*, is proportional to the Young's modulus of aramid fibres. Consequently the rate of band shift per unit stress is constant at about -4cm^{-1}/GPa for all aramid fibres, Young *et al* [76]. In **Figure (6.6) (b)** the rate of bandshift per unit stress is -4.2cm^{-1}/GPa. Hence in the 20kg Pre-stressed sample:

$$\textbf{Fibre stress} = \frac{\textbf{Raman wavenumber shift (cm}^{-1}\textbf{)}}{\textbf{Bandshift per unit stress (cm}^{-1}\textbf{/GPa)}}$$

$$\textbf{Fibre stress} = \frac{-2.0}{-4.2}$$

Fibre stress = 0.5GPa (500MPa)

hence **Fibre Stress** for samples with lower values of pre-stress are

-1.5/-4.2 = 0.36GPa (360MPa)

-1.0/-4.2 = 0.24GPa (240MPa)

-0.5/-4.2 = 0.12GPa (120MPa)

-0.2/-4.2 = 0.05GPa (50MPa)

-0.1/-4.2 = 0.02GPa (20MPa)

6.8 Internal Stress Evaluation

To calculate how much compressive stress was present in the resin matrix, it was necessary to consider the equations used to calculate thermal expansivities. In particular to examine Axial Residual Stress in a continuous fibre embedded in a resin matrix that shrinks, Hull *et al* [91].

Taking the ***force balance*** equation

$$(1-f)\,\sigma_m + f\,\sigma_f = 0 \qquad (6\text{-}12)$$

*The **force balance** is simply a requirement that, since there is no applied stress, the two internal stresses must counterbalance each other when they are converted to forces (multiplied by the relative sectional areas).* [91]

where

σ_m	= stress in matrix	
σ_f	= stress in yarn	(500MPa)
f	= cross sectional area of yarn (1000 fibres)	($\pi r^2 \times 1000 = 0.113mm^2$)
		($r = 6\mu m$)
$1-f$	= cross sectional area of matrix	($24 \times 10 = 240mm^2$)

then

$$-\sigma_m = \sigma_f \times \frac{f}{(1-f)} \qquad \textbf{(per yarn bundle)} \qquad (6\text{-}13)$$

gives

$$-\sigma_m = 500 \times \frac{0.113}{240}$$

$$-\sigma_m = 0.235MPa \qquad \textbf{(per yarn bundle)}$$

Therefore a $-2.0cm^{-1}$ Raman bandshift in a Quad sample (4 yarn bundles) gives a cross sectional compressive stress of approximately **1MPa**. This compressive stress must be uniform, since there is no evidence of bending in the quad samples. It follows therefore that increasing the number of fibre bundles embedded in the matrix will increase the extent of compressive stress.

6.9 The Effect of Aging on Quad Samples

This level of Raman bandshift was maintained for about 8 to 10 weeks before there was any noticeable level of bandshift. At first the variation in the level of the bandshift in the samples was attributed to experimental error. However an increase in the treeing time of 9-month-old samples (*Chapter 10, section 10.7*) initiated a re-examination of the Raman results. Closer inspection of the results revealed that a bandshift movement, indicating increased tension in the fibres, was occurring in all the quad sample types. The aging of the samples produced an increase in the levels of pre-stress to a point where pre-tensioned samples were now giving pre-stress readings, as shown in **Table (6.4)** and **Figure (6.7)**.

Table (6.4) The Effect of Aging

Sample Type		**Raman Bandshift Readings (cm^{-1})**		
		Age of Samples		
Cure Cycle	Applied Load	4 weeks (1 month)	39 weeks (9 months)	60 weeks
1d @ RT + 6d @ RT				
	2kg	**0.0**	**-0.2**	**-0.3**
	2.25kg	**0.0**	**-0.7**	
	5kg	**-0.5**	**-1.0**	**-1.3**
	10kg	**-1.0**	**-1.3**	**-1.4**
	15kg	**-1.5**	**-2.0**	**-2.1**
	20kg	**-2.0**	**-2.3**	**-2.7**

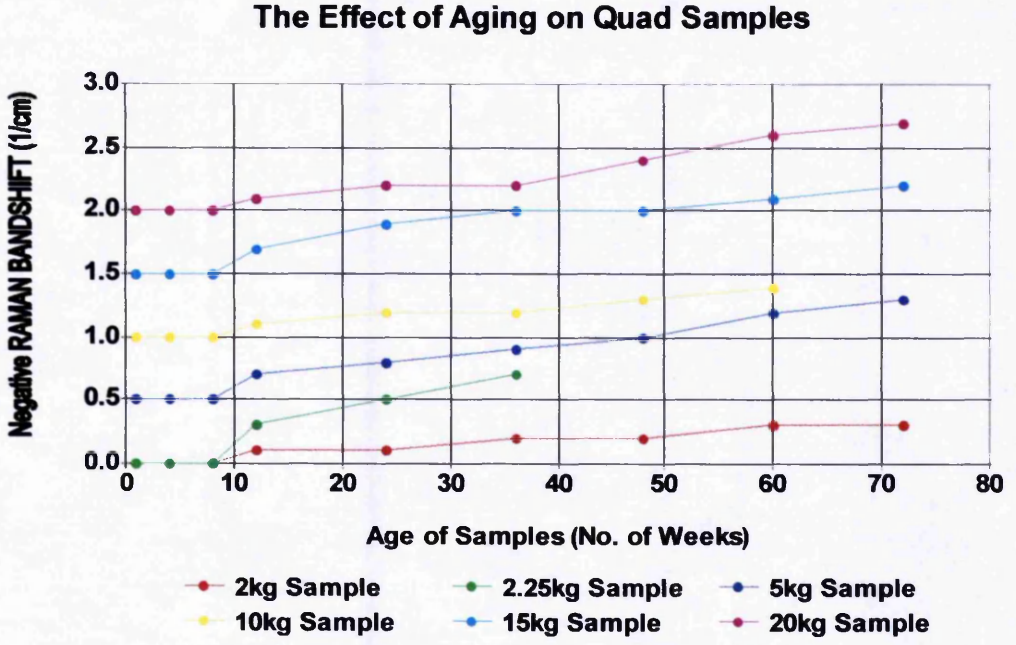

Figure (6.7) The Effect of Aging on Quad Samples Containing Twaron 1001

It was speculated that the cause of this increased tension in the fibres was due to water absorption. Consultations with Professor R.J. Young confirmed that water absorption would have this effect as demonstrated by Cervenka *et al* [92]. Cervenka had shown that *'if the level of the thermodynamic interaction between a polymer and a penetrant is high (in the case of highly hygroscopic epoxy matrices with respect to water), the presence of a penetrant will cause polymer swelling, this exerting non-mechanical stresses in the fibre, i.e. in the x-direction.'* This was examined in greater depth by Cervenka's co-author Bannister in his Ph.D [93] in which he examined the micromechanical and hydrothermal behaviour of fibre(Twaron)/resin(5052) composites. Experimental confirmation of water absorption can be found in *Chapter 7, section 7.6.2.*

6.10 The Effect of Elevated Postcure

It has already been seen in **Table (6.3)** that elevated temperature postcure on quad samples with a 2kg loading produces resin shrinkage, causing crushing of the yarn. A later batch of Pre-tensioned (2.25kg) samples was produced and subjected to the 8 hours at 80°C postcure cycle. Again the yarn was in compression with a Raman bandshift of $+0.3cm^{-1}$, as shown in **Table (6.5)**. In an attempt to obtain equilibrium the load was doubled to 4.5kg resulting in a Raman bandshift of $+0.2cm^{-1}$. Therefore a much greater load was needed than could be handled by the Pre-tension platforms to counteract the effect of elevated temperature postcure. This would not be possible until the development of the Heavy Duty Stress Bed had been completed at the end of the project.

Table (6.5) The Raman Results of the Elevated Temperature Postcure of Pre-tensioned and Pre-stressed Samples.

		Raman Bandshifts	
Cure Cycle	**Applied Load**	**Front Yarn**	**Back Yarn**
1d @ RT + 8hrs @ 80°C			
	2.25kg	**$+0.3cm^{-1}$**	**$+0.3cm^{-1}$**
	4.5kg	**$+0.2cm^{-1}$**	**$+0.3cm^{-1}$**
1d @ RT + 4hrs @ 100°C			
(Sample Z)	**2.25kg**	**$+0.5cm^{-1}$**	**$+0.5cm^{-1}$**
(Sample Y)	**20kg (17kg)**	**$-1.2cm^{-1}$**	**$-1.6cm^{-1}$**

In the final month of the project the first pre-stressed sample at an elevated temperature was produced. Sample Y (PC 03-06-99) was cured for one day at RT, followed by a postcure at 100°C for four hours before finally cooling down at a rate of 10°C/hour. Initially it was loaded to 20kg per yarn layer (total 40kg) but during the cure cycle this dropped to 14kg per layer, see *Chapter 8 section 8.12.5*. A Raman analysis was performed after one week and confirmed the presence of pre-stress,

although the pre-stress was not uniformly distributed between the front and back yarns. In a standard RT cured 20kg pre-stressed sample a difference of no more than $0.2cm^{-1}$ bandshift was recorded between the front and back yarns, in Sample Y the difference was at least $0.4cm^{-1}$. Furthermore the sum total of the pre-stress bandshifts ($-1.2cm^{-1}$ front, and $-1.6cm^{-1}$ back) $-2.8cm^{-1}$ signified the equivalent of a room temperature pre-stress load level of 28kg (14kg per layer) which is less than the recorded load applied before the postcure.

For comparison purposes a pre-tensioned sample (sample Z) was produced and subjected to the same cure/postcure conditions. Raman analysis recorded readings of $+0.5cm^{-1}$ bandshifts for both front and back yarns. This confirmed that, to obtain equilibrium in elevated temperature postcured samples, a considerable amount of pre-stress would be needed to overcome the increased thermal shrinkage. The results of the elevated temperature postcure of pre-tensioned and pre-stressed samples is shown at the bottom of **Table (6.5)**.

6.11 Ensuring Comparable Raman Readings

During the course of Raman analysis it became evident that several key factors can have an adverse impact on the Raman bandshift readings, when comparing a yarn sample in air (on a microscope slide) with yarn embedded in a resin matrix. These are as follows:

1.) If the Raman laser is out of alignment it may not be possible to obtain a reading.

2.) The age of the yarn on the microscope slide, due to a.) UV light on the exposed yarn and b.) water absorption by the epoxy coating, will alter the differential.

3.) The age of the yarn embedded sample, due to water absorption in the resin matrix, will increase the differential

It was found that, using a fresh RT postcured 20kg pre-stressed sample (less than 8 weeks old) as a benchmark, in conjunction with yarn taken from the same section of yarn (therefore comparing like with like), resulted in a consistent Raman bandshift reading of $-2cm^{-1}$ ($\pm 0.2cm^{-1}$). This eliminates these adverse effects and ensures reliable results for comparison with the older samples.

6.12 Summary

At this point in the project it was necessary to find a technique for measuring the internal stresses in the samples. It had originally been envisaged that the internal state of the resin matrix would be analysed using the department's circular polariscope. However, it was stated by Taha [94] that the polariscope only indicates the presence of strain and cannot measure it or quantify it as being tensile or compressive. The polariscope therefore presents a two dimensional image from a three dimensional sample, ignoring the integration effects of the sample thickness, thereby making it inaccurate as outlined by Cooper [95]. Other traditional test methods were known to destroy the samples and hence were also unsuitable.

By contrast Raman Spectroscopy is a reliable and accurate method of measuring axial fibre strain in HPFY embedded in a resin matrix. The background to and operation of Raman spectroscopy has been described in detail in this Chapter. Firstly the theoretical calculations which form the basis of Raman Spectroscopy were set out. The groundbreaking work of Professor R J Young was outlined, in particular the significance of the 1610cm^{-1} Raman waveband and its strain dependent shift in relation to aramid fibres (Twaron).

The collaboration and assistance provided by Professor Young and his research team is also noted in this Chapter. Initially the support took the form of technical information for the production of samples and analysis of the samples provided by the author. Later in the project, training and guidance was provided to the author on use of the Raman laser equipment. The Chapter goes on to describe the significant impact of Raman Spectroscopy on the progress of the project.

The Raman laser set up procedures are given for both the yarn in air and the yarn embedded in a resin matrix. This forms the basis of the comparison process. The analysis of the yarn embedded in the resin matrices was helped considerably by the consistent quality of the samples. Raman analysis of one week old RT postcured samples demonstrated a linear relationship between the applied load and the negative Raman bandshift (yarn in tension) in pre-stressed samples. On the other hand, RT

postcured pre-tensioned samples of the same age showed no bandshift at all (yarn in equilibrium). Furthermore, pre-tensioned samples that had been postcured at elevated temperatures exhibited a positive Raman bandshift (yarn in compression) due to increased resin shrinkage.

The Chapter outlined the stress/strain calibration procedure carried out on the Twaron 1001 fibres. The results of this were used to evaluate the internal stress levels present in the resin matrix of the pre-stressed samples. This was calculated using the force balance equation for axial radial stress in a continuous fibre embedded in a resin matrix that shrinks. The resulting compressive stress must be uniform since there was no evidence of bending in the quad samples.

The effects of aging became evident during the course of the work described in this Chapter. Aging was indicated by increased levels of pre-stress found in the quad samples. This was attributed to the effect of water absorption swelling the resin matrix.

The construction of a heavy duty stress bed enabled the production of elevated temperature postcured pre-stressed samples. Raman analysis showed that pre-stress was retained but at a reduced level.

Finally, this Chapter identified several factors that adversely affect Raman readings. It went on to outline the procedures followed to ensure that reliable and comparable readings were obtained.

Raman analysis has provided a high level of understanding about the internal state of the resin matrix. This understanding has led directly to significant changes in the choice of resin, examined in *Chapter 7* and sample design, to be examined in *Chapter 8*. It is these changes that have resulted in the successful production of pre-stressed samples.

CHAPTER 7

Resins

7.0 Resin

In the past the term resin was generally used to describe any synthetic polymeric material. Today the precise meaning refers to a thermosetting polymer prior to curing ie. epoxy. A clear polymer in a pure state, a resin to which no other substance has been added, was necessary for the purposes of this project. The latter is known as a homogeneous resin. Homogeneous refers to a one phase system in which the chemical composition and physical state of any tangible portion is the same as any other portion. In the interests of comparability with previous work carried out at the University of Manchester, as in Cooper [95], it was initially decided to use the homogeneous resins, polyester Resin C by Scott Bader and the epoxy resin Araldite® CT1200 by Ciba Polymers.

7.1 Polyester

Polymers which are characterised by an ester functional group **(-CO-O-)** in the repeat units of their main chains are known as polyesters.

7.1.1 Resin C

Resin C is supplied in liquid form and is an unsaturated polyester resin. This means that under the right conditions it is capable of being cured from a liquid to a solid state. Resin C consists of a solution of polyester in a monomer which is a small molecule with a high chemical reactivity, in this case styrene. It is the styrene which enables the resin to cure from a liquid to a solid state by crosslinking the molecular chains of the polyester, without the formation of any by-products. This means it can be moulded without the use of pressure, hence the terms contact or low pressure resin.

The inclusion of styrene in the solution requires only the presence of a catalyst and accelerator to create the right conditions for the styrene to crosslink the polymer chains

to form a highly complex three-dimensional network. Once this process has taken place, the polyester resin is said to be cured, giving a chemically resistant hard solid. The crosslinking or curing process is known as polymerisation and is a non-reversible chemical reaction. An accelerator is built into Resin C in the form of a trace level of Cobalt; this is the minimum required for curing and enables the excellent initial colour of the resin to be preserved. This also makes it possible for the curing process to take place without the use of heat. Clear casting Resin C is a two pack system comprising the pre-accelerated resin and a catalyst 'M' (Methyl Ethyl Ketone Peroxide - MEKP). Catalyst 'M' gives good stability and the best results were found using 1.5% by weight proportion of catalyst (adding 1.5g of catalyst to 100g of resin) for this size of sample. This is midway between the minimum and maximum ratios recommended by the manufacturer [96,97].

The curing process commences by adding the catalyst to the resin solution. Decomposition of the catalyst into free radicals by the accelerator at room temperature provides a rapid RT cure. Once the catalyst is neutralised, the crosslinking reaction takes place. Cure takes place in three phases, starting with *gel time*: this is a period of approximately 20 minutes from the addition of the catalyst to the setting of the resin into a soft gel. This is followed by the *hardening time* between the setting of the resin and the stage where the resin is hard enough to allow the sample to be released from the mould. This takes approximately 24 hours. Finally, *maturing time* is the time taken for the sample to acquire its full hardness and a complete cure is achieved by postcuring. For the postcure cycle the oven is set to rise to a temperature of 80°C and maintained for 3 hours before falling at a rate of 10°C per hour until the oven reaches room temperature. This staged temperature postcure improves the heat resistance and decreases the water absorption of the samples. Postcuring also hardens the surface, overcoming the problem caused by oxygen suppressing the free radical reactions between the styrene and the unsaturated polyester at the mould/sample interface, which inhibits the curing process and produces a sticky sample surface after the initial cure.

In Resin C manufacturer states that the exothermic heat of curing is developed over a longer period of time than with other resins. This reduces thermal effects and permits the manufacture of larger castings which is adventageous to this application. Added to

this, the ease of handling, a rapid RT cure, good physical and electrical properties, dimensional stability and good optical clarity of Resin C made it a satisfactory initial choice.

7.1.2 Sample Manufacture

Resin C and catalyst 'M' were weighed and mixed thoroughly in a plastic beaker at room temperature. The resulting mixture was then degassed in a vacuum oven to remove entrapped air bubbles. The mixture was poured into each mould, gently moving lengthwise up and down the mould until full and then degassed again. Finally a sheet of Melinex® (polyethylene terephthalate - PET) was smoothed over the top of the mould to exclude air during hardening. The samples were then left to cure for twenty-four hours. Once enough samples had been produced for testing, all of the samples were postcured together and numbered before being left to age ready for testing. In order to give comparability to the results obtained for plain and yarn samples, it was necessary for all tests to be carried out using samples of the same age as shown by Champion *et al* [34]. The Resin C samples produced are listed in **Appendices 2 & 3**.

7.2 Epoxy

Polymers derived from epichlorhydrin and bisphenol-A are epoxy resins. They are characterised by the possession of more than one of the 3-membered epoxide group shown in **Figure (7.1)**.

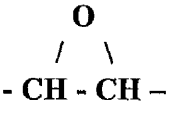

Figure (7.1) The Epoxide Group

The highly strained 3-membered epoxide ring is reactive to many substances, especially those with proton donors. These reactions permit chain extension and/or crosslinking without the elimination of small molecules, so they occur by a rearrangement polymerisation type of reaction. Consequently these materials display lower shrinkage than other types of thermosetting plastics such as polyester. Curing takes place between the resin and a hardener under the application of heat.

7.2.1 Araldite® CT1200

Araldite® CT1200 is supplied as a solid amber bisphenol-A epoxy resin and is used with Hardener HT901, a white flake phthalic anhydride. The mix ratio of CT1200 to HT 901 for unfilled resin is 100:30 parts by weight and is mixed at 140°C [98,99]. After casting the resin is cured at 135°C for 14 hours and then cooled at 10°C per hour until the oven reaches room temperature. For the postcure cycle the oven is heated up at 20°C per hour until it reaches 150°C and maintained for 8 hours. A slow cooling takes place at 3°C per hour until it reaches room temperature. This staged temperature postcure completes the chemical reactions and reduces the residual internal mechanical stresses within the resin to a minimum, Champion *et al* [33,34]. The end of the postcure cycle marks the start of the physical aging (structural relaxation) process for the samples. Subsequent postcures can be performed to restart this physical aging process, since this is reversible and reproducible behaviour. CT1200 was initially chosen for its mechanical and electrical strength, chemical and corrosion resistance, thermal properties and, most importantly, good adhesion, especially to high performance fibres.

7.2.2 Sample Manufacture

The CT1200 is weighed out into a sealable glass vessel and melted in an oven that has been preheated to 140°C. In a second glass vessel, the HT 901 is weighed and melted at 140°C; melting the hardener improves the cross-linking process. When both are fully melted, the HT 901 is mixed into the CT1200. The mixing process involves placing the sealable glass vessel containing the CT1200 onto a hot plate magnetic stirrer, set at 150°C. Then the HT 901 is discharged into the CT1200 and stirred for 3 minutes. After stirring, the mixture is degassed to 14mbar for 10 minutes (any less than 14mbar would cause the loss of the anhydride). The resin is then cast and a further degassing takes place before being returned into the oven to cure at 135°C for 14 hours. Once again, when enough samples were produced all of the samples were postcured together and numbered; before being left to age ready for testing. The age of the sample is expressed from the end of the postcure cycle as shown by Champion *et al* [34,100]. A list of the epoxy CT1200 samples produced is shown in **Appendix 2.**

7.3 The Criteria for Pre-stress

The initial production of single yarn embedded samples, see *Chapter 8*, was divided into two distinct forms:

1. Lightly loaded or **Pre-tensioned** to give no internal stresses (equilibrium).
2. Highly loaded or **Pre-stressed** to place the resin matrix in compression.

Results from Raman analysis (see *Chapter 6*) showed that in samples with a low pre-tension, the resin places the yarn under compression. A reasonable amount of pre-tensioning load would therefore be needed to counteract this compressive tendency, which is due to the thermal shrinkage of the resin during the curing process. In the highly loaded samples a state of equilibrium existed due to the resin absorbing the stress. This is attributed to the asymmetrical design of the initial samples. It was therefore necessary to produce symmetrical samples to counteract this effect and so allow the stresses to take effect on the resin matrix.

The development of the symmetrical samples eliminated the problem of stress absorption by balancing the forces within the sample during curing. Pre-tensioned samples were now being produced in a state of equilibrium as required, nevertheless, the problem of resin (thermal) shrinkage remained in the pre-stressed samples. This resin shrinkage produced a state of equilibrium which meant that the desired compressive forces were not present.

The problem of resin shrinkage led to a re-examination of the choice of resins. To obtain pre-stress it was concluded that the strain in the yarn must exceed the strain in the resin (shrinkage). The most critical factors were the effects of the coefficients of linear expansion and temperature fall following the cure/postcure cycles. Discussions with Ciba Polymers revealed that the only way to decrease the coefficient of linear expansion in the resins initially chosen for this project would be to minimise shrinkage by incorporating a filler, as indicated in Ciba [98]. This was not a practical alternative at this stage, since it would make the samples opaque, thereby preventing observation of the treeing process.

In basic terms if ***X%*** is the strain in the resin matrix and ***Y%*** the strain in the yarn then for the **RESIN**

[101] $$X\% = (\Delta L/L) \times 100 \quad (7\text{-}1)$$

where

ΔL = **change in length** (negative value = resin shrinkage)

L = original length

from [102] $$\Delta L = \alpha \times L \times \Delta T \quad (7\text{-}2)$$

where

α = **coefficient of linear expansion**

ΔT = **change in temperature**

(temperature falls from postcure to ambient therefore negative)

and for the **YARN**

[101] $$Y\% = (\Delta l / lo) \times 100 \quad (7\text{-}3)$$

$Y\%$ = failure strain of the yarn or elongation at break

where

Δl = **change in length**

lo = original length

Note. Maximum strain occurs just before the yarn breaks.

Therefore to obtain Prestress

$$X\% < Y\% \quad (7\text{-}4)$$

if however

$$X\% \approx Y\% \quad (7\text{-}5)$$

then a state of equilibrium will exist.

Twaron® 1001, with an elongation at break of 2.6% at ambient, reducing to 2.3% after 150°C heat treatment, was the chosen yarn for embedding. Although Araldite®

CT1200 (65 x 10^{-6}/°C) has a lower coefficient of linear expansion than Resin C (100 x 10^{-6}/°C), its greater postcure temperature means they both have an ***X%*** of over 1%. When a graph is plotted of Breaking Force (kg) against Elongation (%) in Twaron 1001, see **Figure (7.2),** it can be seen that in order to obtain pre-stress the yarn would have to be loaded to its maximum for pre-stressing of the resin to occur. If, however, a cold cure resin were used this would all but eliminate **ΔT** bringing ***X%*** down to less than 1% and so enable pre-stress to be obtained at more reasonable loads.

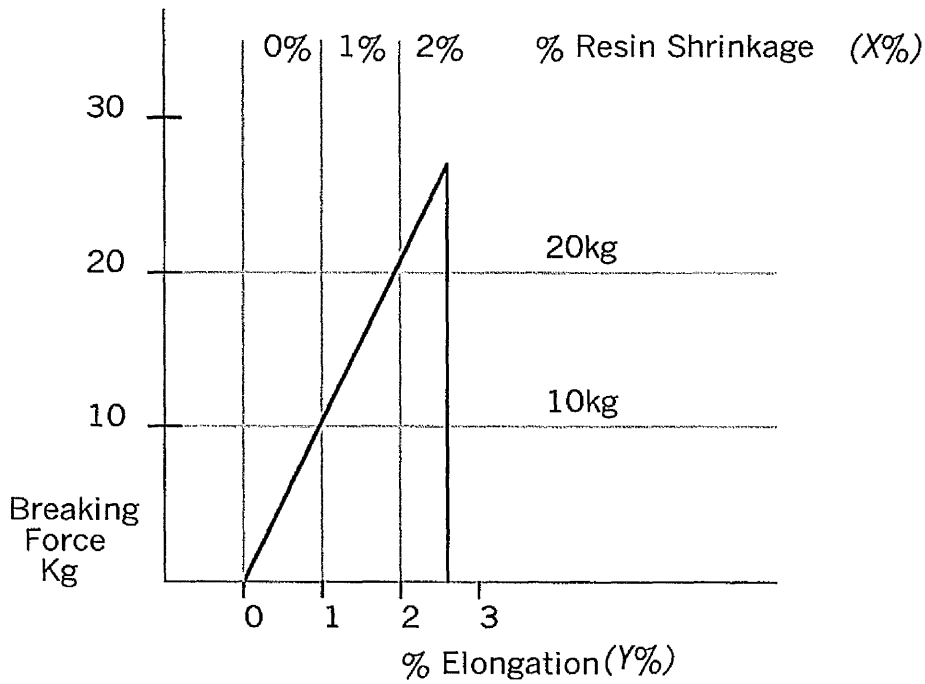

Figure (7.2) Graph of Breaking Force (kg) against Elongation (%) in Twaron 1001

7.4 Epoxy Novalak Resin

For a number of years Professor R.J. Young at the Manchester Materials Science Centre has used the cold cure epoxy novalak resin Araldite® 5052 (α = 97 x 10^{-6}/°C), made by Ciba Polymers to overcome the problems caused by resin (thermal) shrinkage. Novalaks are resins that have been epoxidized by reacting phenols with formaldehyde followed by glycidylization with epichlorohydrin.

7.4.1 Araldite® 5052

The Araldite epoxy novalak matrix system 5052 consists of an epoxy resin Araldite® LY 5052 and an amine Hardener HY 5052. This two-part, cold-curing epoxy resin has a mix ratio of (LY 5052) 100:38 (HY 5052) parts by weight; both produced by Ciba Polymers [103,104]. The low viscosity components allow for easy mixing at room temperature (RT) and a thorough impregnation of reinforcement fibres such as aramid. It can be cured at RT or elevated temperatures, depending on the required properties of the product as shown in **Table (7.1)**.

Table (7.1) Temperature Effects on the Properties of the Cured System [104]

Glass Transition Temperature (Tg)

Cure/Postcure Cycle	Tg (°C)	Tensile Strength (MPa)
1 day @ RT + 1 day @ RT	52 - 55	
1 day @ RT + 7 days @ RT	62 - 66	49 - 71
1 day @ RT + 10 hours @ 40°C	70 - 76	
1 day @ RT + 20 hours @ 40°C	74 - 80	
1 day @ RT + 10 hours @ 50°C	80 - 85	
1 day @ RT + 15 hours @ 50°C	82 - 88	82 - 86
1 day @ RT + 10 hours @ 60°C	94 - 104	
1 day @ RT + 15 hours @ 60°C	96 - 106	
1 day @ RT + 2 hours @ 80°C	108 - 114	
1 day @ RT + 8 hours @ 80°C	114 - 122	84 - 86
1 day @ RT + 1 hour @ 90°C	108 - 118	
1 day @ RT + 4 hour @ 90°C	116 - 126	
1 day @ RT + 1 hour @ 100°C	118 - 130	
1 day @ RT + 4 hours @ 100°C	124 - 136	

7.4.2 Sample Manufacture

The resin contains a 60-70 % concentration of epoxy phenol novolak and 34-42 % of butane-diol diglycidyl ether, a low molecular weight reactive dilutant. The hardener is

a mixture of polyamines, primarily 35-45 % isophorone diamine, 50-60 % 2,2 '-dimethyl-4,4 'methylenebis (cyclohexylamine) and with a small amount 1-5 % of 2,4,6 - tris (dimethylaminomethyl) phenol. These are thoroughly mixed at room temperature, degassed and poured directly into the moulds. Every sample was subjected to a 1 day cure at room temperature before any postcure was completed. The use of 5052 resin has made the production of yarn embedded pre-stressed samples possible, although they have a low Tg value. A list of preliminary yarn embedded Quad samples can be seen in **Appendix 4**, Pre-stressed samples are expressed in **Bold**.

7.5 Operating Temperature

Initially all samples were postcured at RT giving them a Tg of between 62-66°C. It is known from *Chapter 3* that below the Tg very few molecular changes take place in the resin matrix, but as the Tg is approached changes occur. The Tg limits the operating temperature of the resin, also experienced by Auckland *et al* [105]. Thus if pre-stressed samples are exposed to the Tg, pre-stress will be lost. This was confirmed by heat treating pre-stressed samples: Sample V at 40°C which retained its pre-stress and Sample M at 80°C which lost its pre-stress. The samples used were sections of pre-stressed samples remaining from tensile testing. The sections were Raman tested after tensile testing and again after heat treatment.

A temperature of 40°C is clearly not a practical operating limit for electrical insulation. Therefore it would be necessary either to produce pre-stressed samples at elevated temperatures under load or to examine the possibility of raising the Tg by gradually heat-cycling the samples eg. postcuring at 40°C then 60°C then 80°C. Before pre-stressed samples could be produced at elevated temperatures a 'Stress Bed', which would fit into an oven, would be required. In the meantime a suitable heat-cycling programme was implemented (see section 7.7). After heat-cycling samples it was considered prudent to check the Tg of the samples being produced and compare them with the manufacturer's data.

7.6 Examination of 5052

A range of 5052 samples and double end-pieces (*see page 163 for description*) was produced, cured for 1 day at room temperature and postcured over a range of temperatures, specifically to examine the Tg and water absorption characteristics of Araldite 5052. The samples produced are detailed in **Table (7.2)**.

Table (7.2) Samples Produced for Tg and Water Absorption Tests

All samples cured for 1 day at room temperature.

Sample dimensions: **210mm x 24mm x 10mm**
End-piece dimensions: **90mm x 25mm x 3mm**

Batch No.	Sample No.	Postcure Cycle	Test Type
1.			
sample	1.	RT	Water
end-piece	1A		Tg
end-piece	1B		Water
sample	2	20hrs @ 40°C	Water
end-piece	2A		Tg
end-piece	2B		Water
sample	3	15hrs @ 60°C	Water
end-piece	3A		Tg
end-piece	3B		Water
sample	4	8hrs @ 80°C	Water
end-piece	4A		Tg
end-piece	4B		Water
2.			
sample	5	4hrs @ 100°C	Water
end-piece	5A		Tg
end-piece	5B		Water
sample	6	RT	Water
end-piece	6A		Water
end-piece	6B		Water
end-piece	6C		Water
sample	7	6d @ RT	Water
end-piece	7A		Water
end-piece	7B		Water
end-piece	7C		Water
sample	8	6d @ RT	Water
end-piece	8A		Water
end-piece	8B		Water

7.6.1 Tg Tests

Starting with the Tg tests one specimen (a double end-piece) from each postcure temperature was given to Mr. J. Billing for DSC (differential scanning calorimetry) testing at ERA Technology Ltd, Leatherhead, Surrey. The results of the DSC tests can be seen below in **Table (7.3)**, for comparison Tg tests previously carried out on samples V and M after their heat treatment are included in the final column.

Table (7.3) Tg Test Results

Cure/Postcure Cycle	Tg (°C)	(Heat treated)
1 day @ RT + 7 days @ RT	65°C	
1 day @ RT + 20 hours @ 40°C	65°C	69°C – (V)
1 day @ RT + 15 hours @ 60°C	83°C	
1 day @ RT + 8 hours @ 80°C	95°C	93°C – (M)
1 day @ RT + 4 hours @ 100°C	113°C	

Differential scanning calorimetry is a type of thermal analysis similar to differential thermal analysis (DTA). It is used for the detection and measurement of changes in state and heats of reaction, in solids and melts. The sample under investigation is tested side by side and simultaneously with a thermally inert material and the difference between them noted. This difference becomes very marked when one of the two samples passes through a transition temperature with evolution or absorption of heat whereas the other does not. This is seen as a step change on a DSC plot.

During the first run of the DSC tests the samples were heated to a temperature of 200°C this completes the curing process. A second run of the test showed that the Tg had increased to 126°C. When the results were compared to the manufacturer's data, given in **Table (7.1)** it can be seen that they are as stated for RT postcured samples but lower for the rest. The Tg for RT and 40°C samples are the same and may explain why pre-stress is retained in Sample V re-heated to 40°C. A heat-cycling experiment

was carried out to see when pre-stress was lost in RT postcured samples, see section 7.7.

The Tg results were discussed with Ciba Polymers who recommeneded comparing the percentage cure obtained with the percentage cure expected from their data. The formula for calculating the percentage cure was given by Ciba Polymers as:

$$\% \text{ Cure} = \frac{Tg_{sample}}{Tg_{max}} \times 100 \qquad (7\text{-}6)$$

Therefore the percentage cure for manufacturer's data and the samples produced is shown for comparison in **Table (7.4)**.

Table (7.4) The Percentage Cure Results

From Manufacturer's Data (Tg_{max} = 136°C)

Postcure Cycle	**Tg**	**% Cure**
6days @ RT	62°C	46%
20hrs @ 40°C	74°C	54%
15hrs @ 60°C	96°C	71%
8hrs @ 80°C	114°C	84%
4hrs @ 100°C	124°C	91%

From DSC Tests of the Samples Produced (Tg_{max} = 126°C)

Postcure Cycle	**Tg**	**% Cure**
6days @ RT	65°C	52%
20hrs @ 40°C	65°C	52%
15hrs @ 60°C	83°C	66%
8hrs @ 80°C	95°C	76%
4hrs @ 100°C	113°C	90%

Tg comparison shown in **Figure (7.3) (a)**

% Cure comparison shown in **Figure (7.3) (b)**

Figure (7.3) (a) Tg Comparison

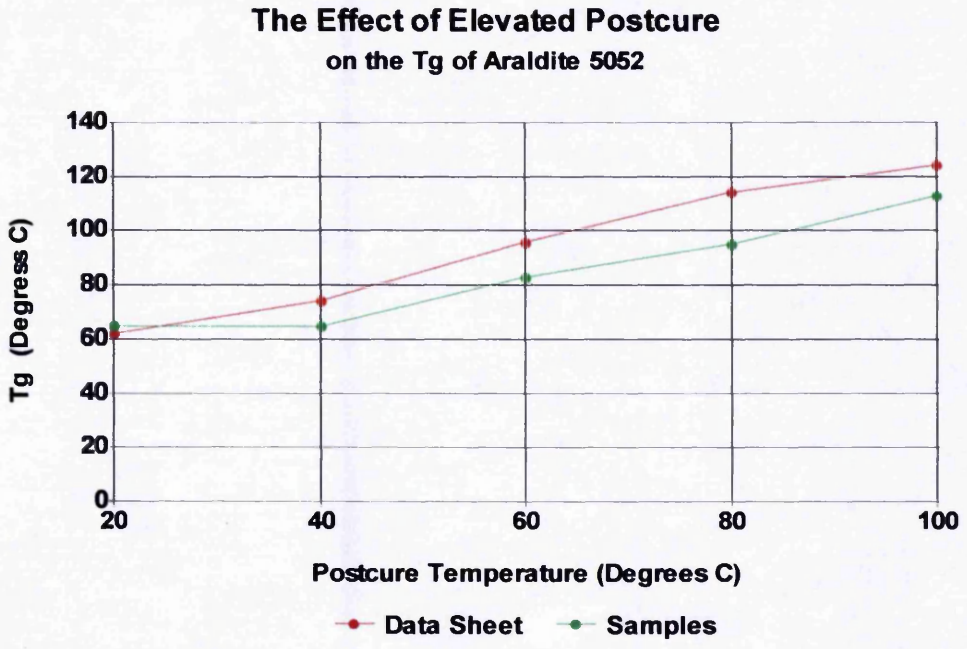

Figure (7.3) (b) % Cure Comparison

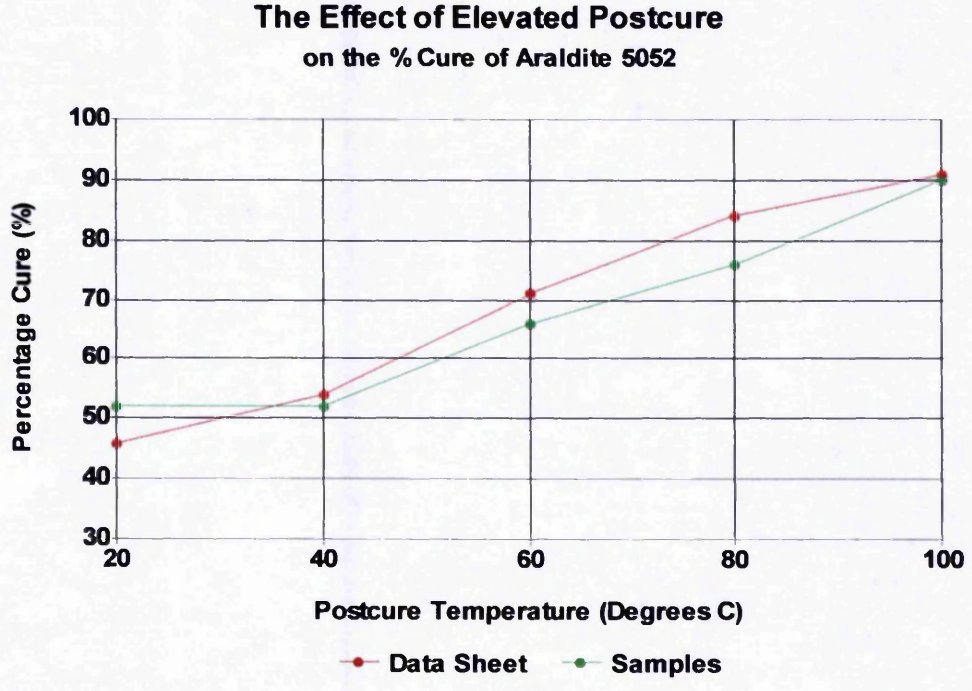

It can be seen from the results that the overall percentage cure obtained for the samples produced is in line with the manufacturers estimates for a given postcure cycle.

7.6.2 Water Absorption Evaluation

The remaining specimens were used for a water absorption evaluation, which was carried out on site in laboratory G.29. Upon demoulding the specimens were weighed and measured, and the temperature and relative humidity of the room recorded. For a period of 6 months the majority of the samples were left to age in the ambient conditions of G.29 and a few were immersed in water (providing 100% relative humidity). A list of the specimens is shown in **Table (7.5)** indicating their testing environment. Once a week the temperature and relative humidity were recorded and the specimens were weighed and measured. Dimensions are given in **Table (7.2)**.

Table (7.5) Water Absorption Evaluation Environments

Batch No.	Specimen No.	Postcure Cycle	Testing Environment
1.			
sample	1.	RT	Ambient
end-piece	1B		Ambient
sample	2	20hrs @ 40°C	Ambient
end-piece	2B		Ambient
sample	3	15hrs @ 60°C	Ambient
end-piece	3B		Ambient
sample	4	8hrs @ 80°C	Ambient
end-piece	4B		Ambient
2.			
sample	5	4hrs @ 100°C	Ambient
end-piece	5B		Ambient
sample	6	RT	In Water
end-piece	6A		In Water
end-piece	6B		In Water
end-piece	6C		In Water
sample	7	6d @ RT	In Water
end-piece	7A		In Water
end-piece	7B		In Water
end-piece	7C		In Water
sample	8	6d @ RT	Ambient
end-piece	8A		Ambient
end-piece	8B		Ambient

7.6.2.1 Water Absorption Results

Indications from the manufacturer were that the specimens would absorb moisture for the first month and then the matrix would stabilise. This was not supported by the results from the Raman analysis, which suggested a continuous uptake of moisture, see *Chapter 6 section 6.9* showing a continual steady increase in pre-stress.

The results of the Water Absorption Evaluation were consistent with the Raman analysis findings and the specimens showed a continuous uptake of moisture over the 6-month period. Overall, the increase in weight of those samples immersed in water (equivalent to 100% relative humidity) was 33% greater than the weight gain of those samples left in the ambient atmosphere (average relative humidity of 37% in the room). These results are supported by the findings of Champion *et al* [106] who found that the moisture uptake of the sample is be similar to the relative humidity of the environment (the sample will try to reach equilibrium with its environment). No increase in dimensions were recorded. The effects of water absorption on Electrical Treeing are examined in *Chapter 10, section 10.7.*

7.7 Heat-cycling of Pre-stressed Samples

A heat-cycling experiment was performed on sections of two pre-stressed samples. These were produced from the same batch of resin (PS 2.1 and PS 2.2) which had been previously tensile tested. Each sample underwent Raman analysis and was cut into five sections, numbered 1 to 5. Sections 2,3 and 4 were subjected to various combinations of heat-cycling at 40°C, 50°C and 60°C, as indicated under **Heat-cycle** in **Table (7.6)**. The sections were then subjected to a further Raman analysis. If pre-stress was retained at these levels then the samples could be exposed to higher temperatures. The results of the Raman analysis are shown in **Table (7.6)**.

Table (7.6) Heat-cycling Raman Results

Sample PS 2.1 PC 11-11-98

Section Number	**Heat-cycle**	**Raman Shift**
1	None	-2.0 cm^{-1}
2	10hrs @ 60°C	+0.3 cm^{-1}
3	10hrs @ 50°C + 10hrs @ 60°C	+0.2 cm^{-1}
4	10hrs @ 50°C	-0.5 cm^{-1}
5	None	-2.0 cm^{-1}

Sample PS 2.2 PC 11-11-98

Section Number	**Heat-cycle**	**Raman Shift**
1	None	-1.8 cm^{-1}
2	10hrs @ 40°C	-1.8 cm^{-1}
3	10hrs @ 40°C + 10hrs @ 50°C	+0.1 cm^{-1}
4	10hrs @ 40°C + 10hrs @ 50°C + 10hrs @ 60°C +	+0.3 cm^{-1}
5	None	-1.8 cm^{-1}

Pre-stress was again retained at a 40°C, only partially retained at a 50°C, and lost completely at a 60°C. In heat-cycled samples pre-stress was lost and the yarn was placed in compression. This shows that the operating temperature is governed by the Tg of the resin because, in order to retain pre-stress, the temperature of the insulating resin must be kept below the Tg. Pre-stressed resin samples postcured at room temperature therefore have a safe operating temperature of 40°C, which is below the Tg of the resin. This is not a sufficiently high operating temperature for resin insulation. The Tg itself can only be raised by elevated temperature postcure.

Consequently, if the Tg is to be raised and a workable operating temperature achieved for practical applications, the pre-stressed insulation must be manufactured at elevated temperatures with the yarn under load.

7.8 Summary

The selection of resins described in the foregoing Chapter was initially in keeping with previous work in this area. The background and usage for the resins is discussed and the manufacture of plain and single yarn embedded samples is outlined.

As already stated in *Chapter 6* the results of Raman Spectroscopy identified problems relating to sample design and resin shrinkage. The introduction of symmetrical yarn samples eliminated the effect of sample bending, yet the effects of resin shrinkage remained. Consequently it was necessary to develop the criteria for pre-stress as highlighted in this Chapter. It was identified that, to obtain pre-stress, the strain in the yarn must exceed the strain in the resin (shrinkage). It was further identified that the most critical factors affecting this were the effects of coefficients of linear expansion and the temperature fall following the cure/postcure cycles. From the equations given it can be seen that the temperature fall has by far the most significant impact on the shrinkage. It was therefore decided to use the cold cure resin Araldite® 5052, as used by the Materials Science Centre.

The Chapter goes on to examine the Araldite epoxy novalak matrix system 5052 and its use. Preliminary tests showed that, because of its low Tg, (around 65°C), RT postcured samples had a safe operating temperature of only 40°C. A range of samples was manufactured at different postcure temperatures, some of which were used for determining the different levels of Tg. The remainder was used to determine the extent of water absorption in order to confirm the results of the Raman analysis of older samples (as noted in *Chapter 6*). These results were compared to manufacturer's data.

A operating temperature of 40°C is too low for electrical insulation. Therefore it became necessary to examine methods by which the Tg could be raised. The

unsuccessful attempts at heat cycling the RT postcured samples were described in this Chapter.

In order to manufacture pre-stressed samples at elevated temperatures it was necessary to design and build a Heavy Duty Stress Bed. This was only made possible toward the end of the research contract due to the experience gained in sample design during the project. *Chapter 8* examines the development of Sample Design, resulting in the production of a pre-stressed sample with a realistic Tg.

CHAPTER 8

Sample Design

8.0 Factors of Sample Design

From the beginning of this research a systematic modular approach to sample design was adopted, as outlined by Pahl and Beitz [107] and Cross [108]. This allowed changes to be made to the sample configuration without the need to start afresh. This flexibility has been necessary since the form of the sample was initially a compromise between the requirements of tensile testing and those of electrical tree testing. In the beginning the number of yarns needed to obtain pre-stress was unknown. Nonetheless, it was apparent that there was a need for comparability between different types of test sample, adequate space for the inclusion of more yarns and, most importantly, a reproducible quality sample that needed no machining or polishing. Any machining or polishing would introduce alien stresses into the samples and so invalidate the results. The requirements of Raman analysis would determine the positioning of the yarns within the samples. A further consideration was the size of the oven available for sample manufacture, as this would have to accommodate the sample mould mounted in some form of yarn stress bed.

Three main areas of investigation were identified for the assessment of the Mechanical Pre-stressing of Electrical Insulation:

(1) Electrical Tree Testing in order to observe the time to breakdown and thus show the increased resistance to treeing offered by mechanically pre-stressed insulation.

(2) Tensile Testing to demonstrate the effect of the inclusion of high performance fibre yarns on the mechanical strength of the insulation sample and its potential to reduce insulation thickness.

(3) Raman analysis to monitor the internal stresses of the yarn and to observe its effect on both the electrical treeing and tensile strength of the samples.

8.1 Sample Design Constraints

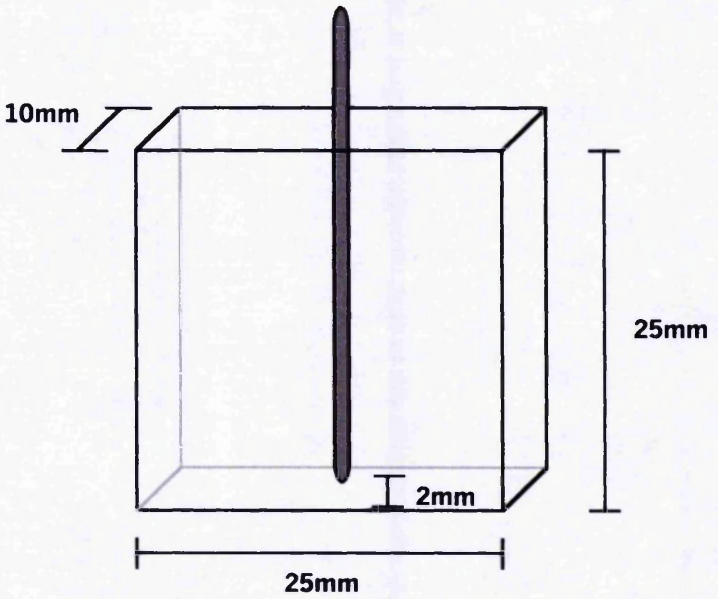

Figure (8.1) Electrical Treeing Sample.

Electrical tree testing required test samples measuring 25mm x 25mm x 10mm as used by Arbab & Auckland [2,12] with a distance from pin tip to base of 2mm, shown in **Figure (8.1)**.

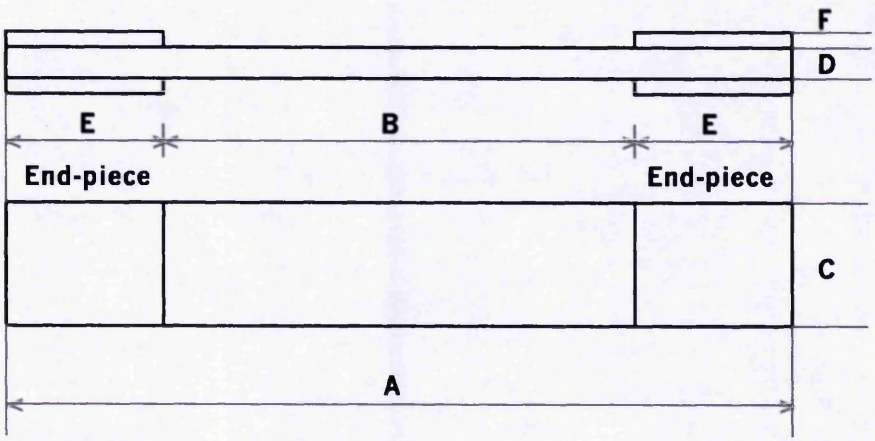

Figure (8.2) Tensile Testing Sample.

The size of tensile testing samples is set out in BS 2782 : Part 3 : Method 320E, for full dimensions see *Chapter 9*. It requires samples measuring A, 200mm (min.) x C, 25mm x D, 10mm (max) with end-pieces E, 45mm x C, 25mm x F, 3mm (min.) at a distance of B, 110mm (min.) apart, shown in **Figure (8.2)**.

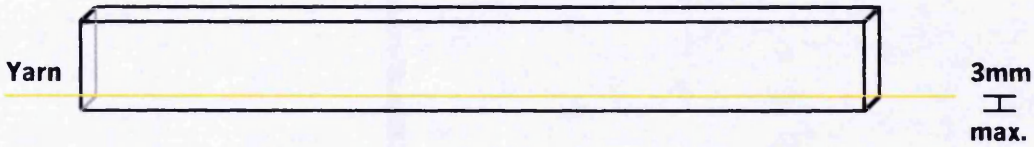

Figure (8.3) Raman Spectroscopy Analysis.

Raman Spectroscopy requires the high performance fibre yarn to be no more than 3mm from the surface under analysis, shown in **Figure (8.3)**.

Added to this is the size of the oven available for sample manufacture. The top shelf measures 700mm x 450mm x 200mm and bottom shelf 700mm x 370mm x 150mm. This would have to accommodate a yarn stress bed.

8.2 Yarn Stress Bed & Standard Sample Size

By far the simplest method of applying stress to the yarn when cast into the resin matrix, is by attaching weights to one end of the yarn and securing the other end. Whilst this method was sufficient at very small pre-tensioning loads, where the yarn can be secured by crushing it in a vice like action, this method would weaken the yarn at higher loads causing it to break. Taking into account the theory behind prestressed concrete some form of stress bed needed to be developed. A stress bed would give far greater control over the tensioning process during manufacture, cure and postcure of the resins. The design of Yarn Stress Bed 1 is shown in **Figure (8.4)**.

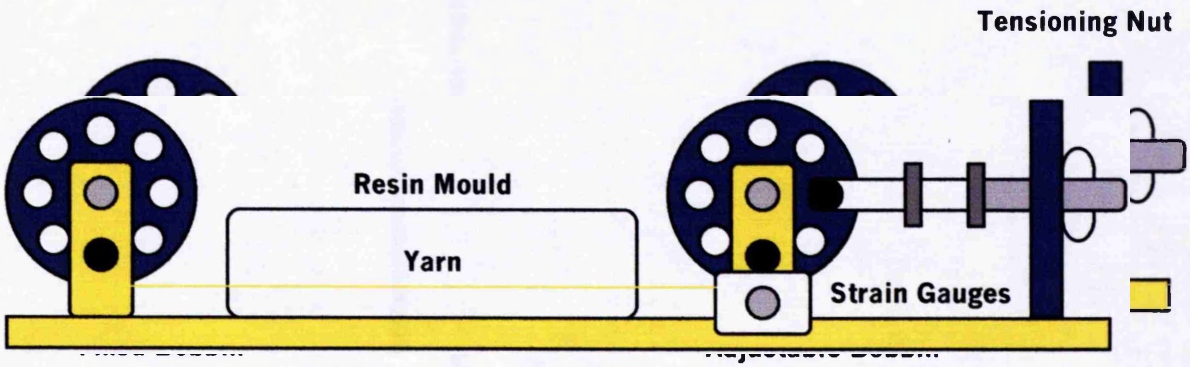

Figure (8.4) Yarn Stress Bed 1.

The basic pulley arrangement with strain gauges and tensioner in **Figure (8.4)** permitted the determination of sizing parameters for a sample mould. A standard mould in **Figure (8.5)** measuring 250mm x 47mm x 50mm allowed for the production of a standard sample measuring 210mm x 24mm x 10mm shown in **Figure (8.6)**.

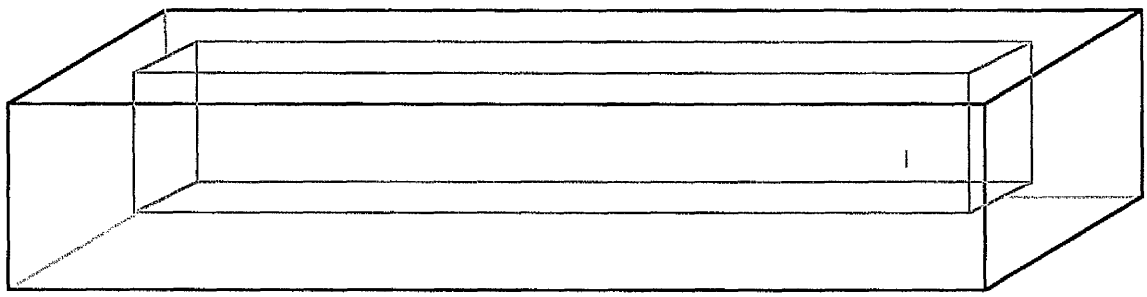

Figure (8.5) Standard Mould.

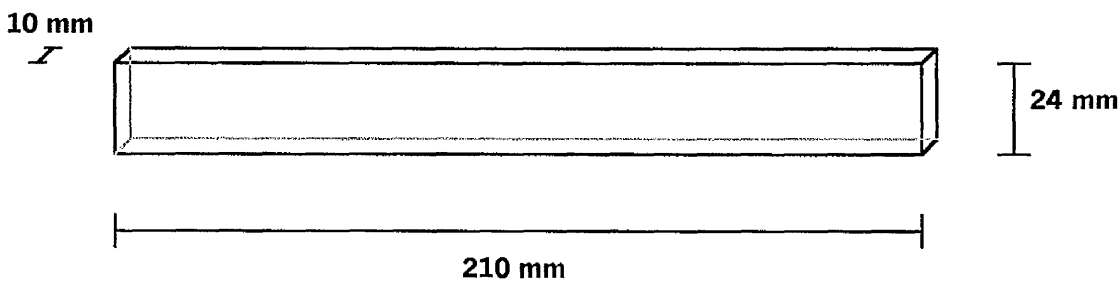

Figure (8.6) Standard Sample.

Further development of the stress bed was made possible by the purchasing of a metal modelling kit by Meccano®. This permitted multiple prototyping, as in **Figure (8.7)** which shows the Yarn Stress Bed 2 which had a sliding bobbin that runs on a track. It was found on building Stress Bed 1 that the height of the yarn altered as the stress was altered. Consequently in Stress Bed 2 the height of the yarn was fixed parallel to the base of the bed so that only stress changes took place. It was determined that future development would involve the manufacture of a full size stress bed for use in the oven at elevated temperatures.

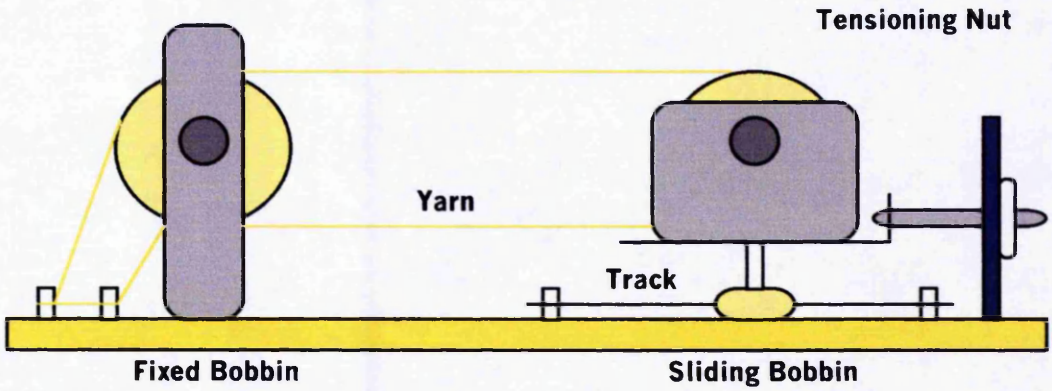

Figure (8.7) Yarn Stress Bed 2.

8.3 Mould Selection.

Any form of machining or machine polishing would introduce alien stresses into the samples and affect any results. Therefore the highest quality of finish possible was required for the sample in order for it to be used directly from the mould. Initially moulds were made from existing stocks of Silastic® 3120 RTV Rubber [109], which is a red, medium viscosity silicone rubber that has a high strength and is claimed to have excellent heat stability. It is a general purpose condensation cure mouldmaking rubber which is used with a RTV Catalyst BC which cures in 24 hours. A graduated postcure is then applied to the mould where the temperature is increased by 25°C per hour. A final bake for four hours at a temperature of 50°C above the maximum operating temperature of the mould (50°C + 135°C = 185°C) is recommended. The manufacturer Dow Corning advised that the maximum constant operating temperature was 200°C, therefore at 135°C (the cure temperature of CT1200) it was well within its limit.

After only two or three samples had been made in each mould, depolymerisation began to take place and the moulds collapsed. Inspection of the moulds revealed nothing to suggest contamination during either mould or sample production. An independent mouldmaker was consulted who instantly pointed out that 200°C was a maximum flash temperature and the actual maximum constant operating temperature is 120°C, after which point depolymerisation takes place. This exaggeration on the part of the manufacturer cost the project a considerable number of weeks. Nevertheless it led to

the discovery of high performance addition cure silicone rubbers that can be used for high temperature casting applications ie. epoxy resins. To avoid cross contamination, translucent Silastic® T-1 moulds were used for polyester production and the green Silastic® S moulds for epoxy production.

For the manufacture of high quality polyester samples, the use of Silastic® T-1 base/curing agent [110] proved most effective. Its translucent appearance allowed visual inspection of the sample under manufacture inside the mould. This was a remarkably useful property particularly when making yarn samples and pin samples to ensure alignment. Silastic® T-1 has a very low shrinkage (Linear shrinkage % < 0.05) and good dimensional stability, ensuring consistently good quality, identical samples. T-1 has outstanding release properties along with a medium-high hardness (35 Shore A) and is flexible and very tough, thus easy to work with. Most importantly, not only did it cure at room temperature but, if required, the cure could also be heat accelerated, hence curing in 2 hours at 45°C permitting more efficient use of time. Initially no postcure was carried out and moulds were used straight from cure.

High quality epoxy samples were manufactured using Silastic® S base/curing agent [111], a green high strength silicone mouldmaking rubber. It has a low viscosity allowing easy mixing and degassing, giving a fast thick section cure at room temperature. Again this rubber had a very low shrinkage (Linear shrinkage % < 0.1) good dimensional stability providing consistant quality samples, together with very high tear resistance and elasticity with a medium hardness (25 Shore A). It could be cured at room temperature but could be heat accelerated so that at 45°C it would cure in 2 hours.

As the research progressed it was found that the lifetime of both types of mould were extended by initially postcuring the moulds in the same way as Silastic® 3120 RTV. Further lifetime enhancements could be obtained by regular recovery cure heat treatments. This drives off solvents absorbed by the rubber moulds. The absorption causes a ballooning effect in the mould. The recovery cure took place after three castings and involved heating the empty mould to 100°C for 3 hours.

With the large scale production of Araldite® 5052 samples a further problem became evident. At the sample interface the moulds began to discolour and harden. The consequences of this were twofold; firstly the faces of the sample had an 'orange peel' effect instead of being smooth and the samples were thicker at the top than the bottom. Eventually the sample/mould interface began to bond to the sample resulting in the destruction of the mould. A chemical reaction had taken place. The suppliers were consulted and two other types of silastics were obtained J and E.

The two additional cure silicone rubbers were a light green Silastic® J and a white Silastic® E. The Silastic® J was a much harder silicone rubber and was very difficult to work with once the sample had cured. After only a couple of castings the interface was very hard and discoloured. The Silastic® E moulds were not so hard and were much easier to work with. However they too absorbed reactants causing the interface to harden, bonding to the samples resulting in the loss of the mould. It was therefore decided to revert to the use of the more flexible Silastic® S and closely monitor the mould condition replacing them when necessary. The use of a demoulding agent was considered but this would have resulted in contamination of the yarn leading to debonding of the sample. The use of a silicone-based mould release agent is recommended by Dow Corning whereas the work of Hepburn *et al* [112] has shown that these demoulding agents result in contamination of the exposed surface layers. In the case of resin samples this leads to premature failure.

8.4 The Cast/Former

The design for the case of the former was adaptable. This permitted the production of different types of moulds for the proposed inclusion of yarn in resin samples. The basic structure of the former is comprised of a base with a metal die and the two longest sides and is shown in **Figure (8.8).** Once assembled, the basic former did not need to be altered. All changes to the mould design took place by the use of interchangeable end-sections which allowed for the inclusion of a single yarn or multiple yarn configurations, illustrated in **Figure (8.9).**

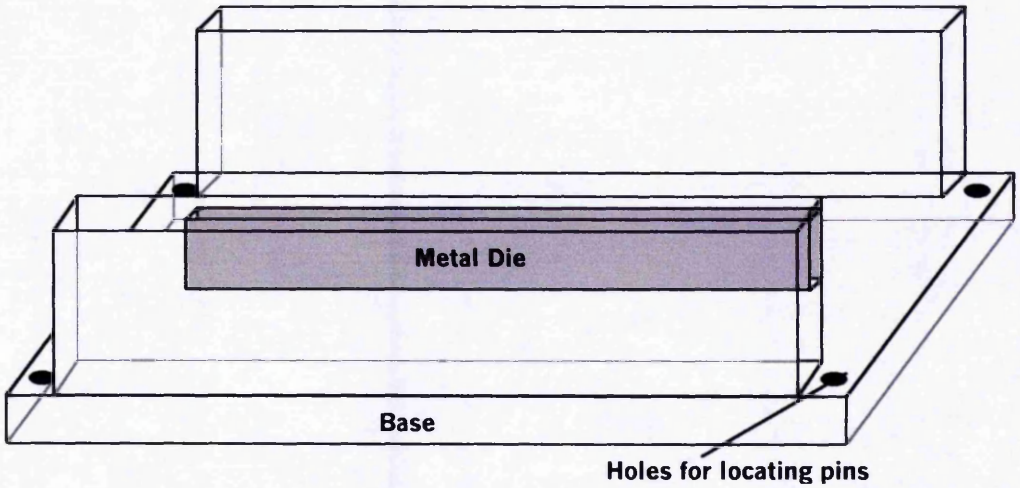

Figure (8.8) Basic Structure of the Former.

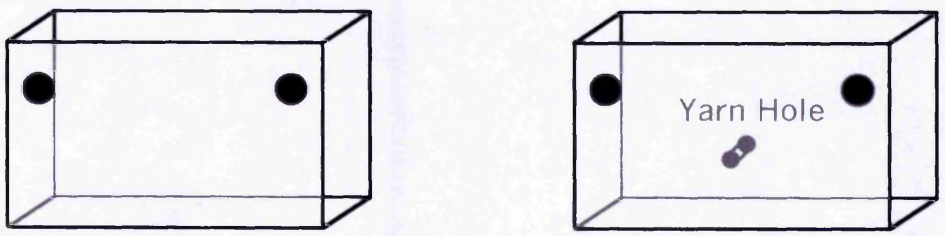

Figure (8.9) Interchangeable End-sections.

8.5 Yarn Moulds

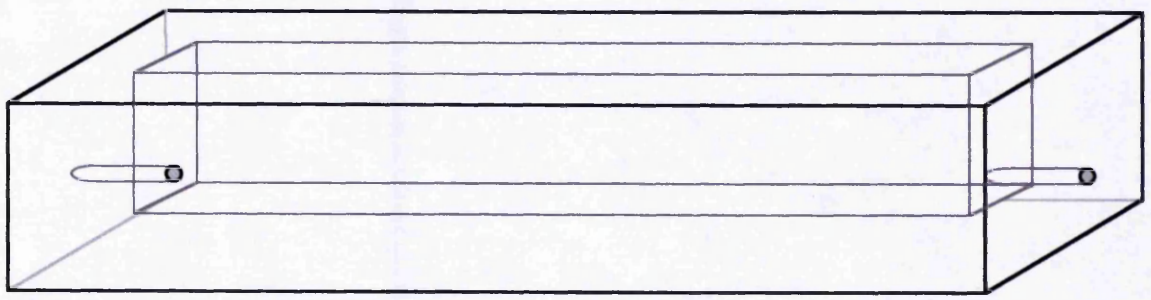

Figure (8.10) Single Yarn Mould.

When the former was constructed with the single yarn end-sections, yarn apertures were created by inserting rods, 3mm in diameter, into the holes in each end-section, these rods butted up to the metal die. Silicone rubber was then poured into the mould and left to cure after degassing. Once the cure cycle was complete, the rods were

removed, followed by the end-sections and the single yarn mould was released ready for sample production, a single yarn mould is shown in **Figure (8.10)**. A 3mm diameter hole was needed to accommodate the protective tubing in which the yarn was threaded for insertion into the mould. This silicone rubber tubing in **Figure (8.11)** provided an inexpensive disposable method of sealing the mould and yarn during sample manufacture. It also helped to protect the mould from damage that could occur at high loadings from the yarn cutting into the mould, thus extending the longevity of the moulds. The tubing can be used up to 200°C.

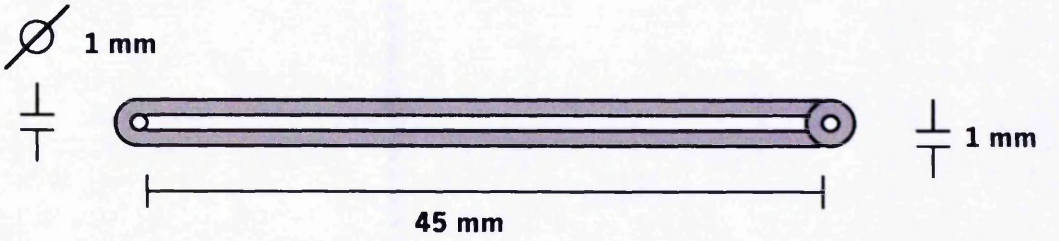

Figure (8.11) Protective Silicone Rubber Tubing.

After the yarn sample has been loaded, silicone grease was applied to the exposed end of the tubing to ensure a resin tight seal around the yarn. The grease used was M 490 silicone grease manufactured by Ambersil Limited. This grease can be used at high temperatures such as those experienced during the postcure of epoxy samples.

8.6 Single Yarn Samples

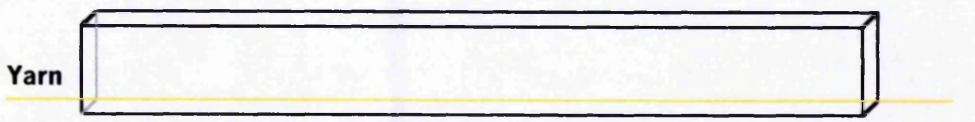

Figure (8.12) Single Yarn Sample.

In **Figure (8.12)** a single yarn under a low pre-tension was encapsulated into the resin sample. Slight pre-tension is applied to prevent the yarn rippling inside the resin during manufacture. Initially in order to allow direct comparisons between different types of yarn cast into the resins, the pre-tension was defined as the result of multiplying a constant by the tex value, similar to tensile testing of yarns, to give a value in grams.

Example.

$$C \times tex = Pretension \quad (8\text{-}1)$$

C was an arbitrary constant chosen for the preliminary experiments.

Pretension for Dyneema SK65 $2 \times 176 = 352$ grams

Pretension for Twaron 1001 $2 \times 168 = 336$ grams

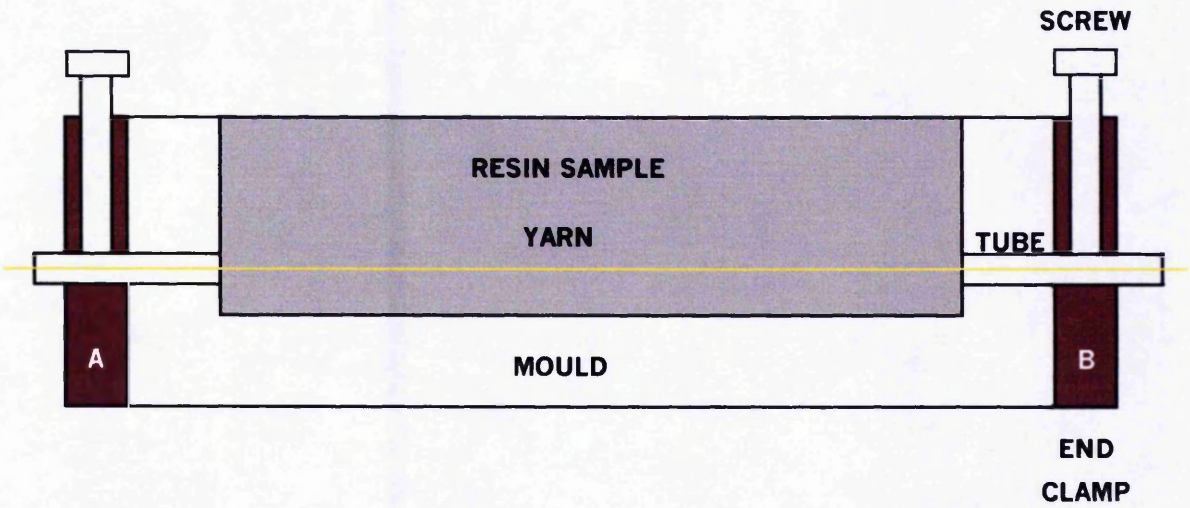

Figure (8.13) Complete Single Yarn Sample Assembly

In **Figure (8.13)** the complete assembly for single yarn sample production is shown. Initially single yarn samples were produced by using screwed end-clamps that butted-up against the ends of the rubber moulds. Weights to the value of the pre-tension for the particular yarn being used were hung from end A of the yarn. The other end, B, had already been secured by the end-clamp screw. Once the pre-tension weights had stabilised the end-clamp A was fastened allowing the removal of the weights, making the manufacturing process less cumbersome. Resin was poured directly into the mould over the yarn. After degassing the complete assembly is left on a level metal plate to cure. Once completed, the end-clamps were removed and the sample was demoulded ready for Raman anaysis.

By the end of the first year only plain and single yarn samples had been produced for testing. The results of the Raman analysis of the single yarn samples revealed two major problems that were preventing the attainement pre-stress and causing the

samples to bend. The first problem was related to yarn sample configuration, causing stress absorption, due to the asymmetric sample design. The second problem was due to resin shrinkage, which at this stage was believed to be caused by the under loading of the yarn. However this later proved to be a thermal problem which was eliminated by the use of a cold cure resin (Araldite® 5052).

8.7 Symmetrical Yarn Samples

The conclusive findings of Raman analysis on single yarn embedded samples led to the development of symmetrical yarn sample configurations to eliminate sample bending. The obvious progression was to produce a symmetrical two yarn or **double sample** as shown in **Figure (8.14)**, using a mould made from the former, constructed with new double end-sections. Problems then arose in the manufacture of pin samples regarding the position of the needles in relation to the position of the top yarn, which was directly above the bottom yarn. Although not practical for electrical tree testing, double moulds were made for the comparison of tensile test samples. In order to accommodate the pin samples it was necessary to produce a symmetrical four yarn or quad sample.

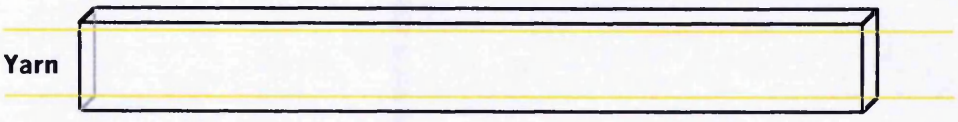

Figure (8.14) Double Sample

The modular approach to sample design enabled the production of symmetrical moulds with the minimum of modification to the mould production process. A pair of end-sections was produced with four locating holes for use with the basic structure of the former. A quad end-section is shown below in **Figure (8.15)**.

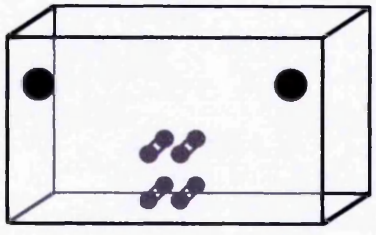

Figure (8.15) One Quad End-section

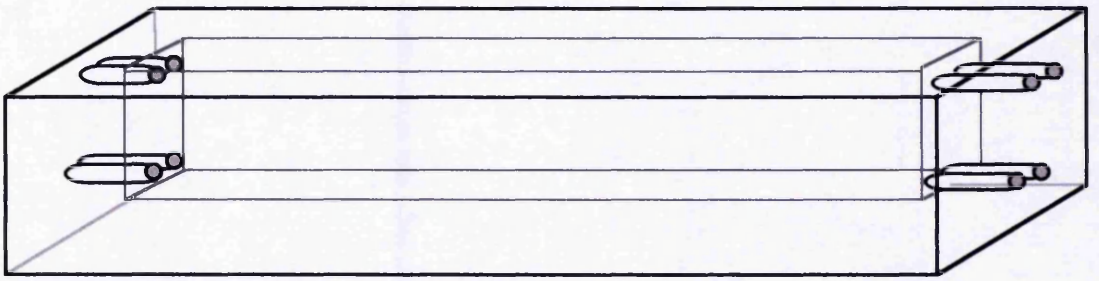

Figure (8.16) A Quad Mould

Quad mould production began immediately, a quad mould is shown in **Figure (8.16)**. This was followed by the production of quad samples and the elimination of sample bending.

Figure (8.17) Quad Sample

A **quad sample** is shown in **Figure (8.17)**. This permitted the needles to be positioned in the middle of the sample in between both top and bottom layers of yarn as in **Figure (8.18)**.

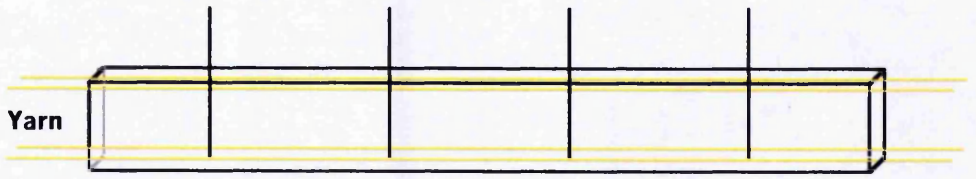

Figure (8.18) Quad Pin Sample

Quad sample production was divided into two distinct categories: Pre-tensioned samples (section 8.10) and Pre-stressed samples (section 8.11). Developments in sample design nevertheless had an impact on both types of production. To give traceability to the production processes each set of assemblies have retained their own set of moulds. These moulds have all been produced from the original cast.

Having established a suitable sample design for plain and yarn embedded samples, the production process, in particular mould maintenance and renewal, needed to be monitored. The development of Pre-tensioned and Pre-stressed assemblies involved further adjustments and modifications. One modification was the provision for pin sample production.

8.8 Needle Gantry Positioning Frame

The purpose of the needle gantry, see *Chapter 10, section 10.3*, is to provide a means for controlling the height of the treeing needles in resin samples. Therefore it was necessary to develop a needle gantry positioning frame to ensure that the needles were centrally aligned in the samples. This development was crucial for the yarn embedded samples where the needles had to sit in the middle of the space between the yarns.

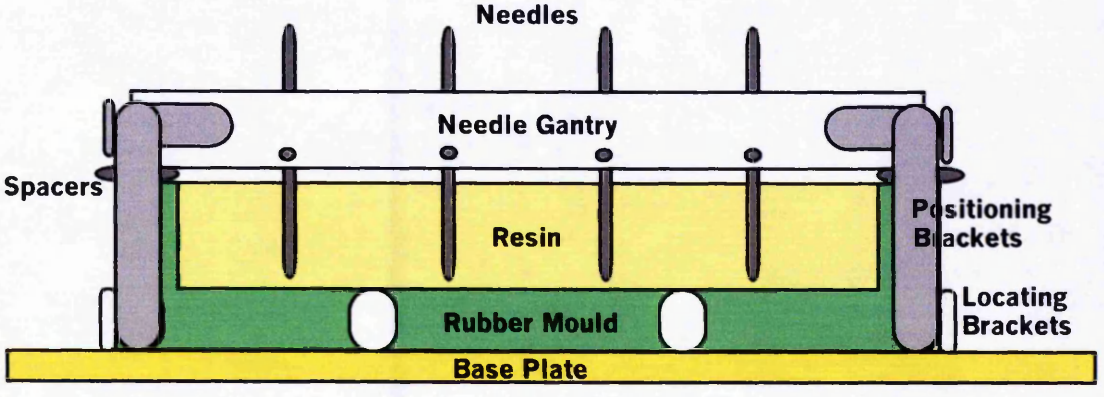

Figure (8.19) Needle Gantry Positioning Frame

The needle gantry positioning frame for Plain pin samples used the Meccano® Base Plate as a platform, as shown in **Figure (8.19)**. Locating brackets are fastened to the Base Plate holding the standard size rubber mould in position. Needle gantry positioning brackets (shaded in grey) were fastened to the mould locating brackets at each end of the mould. Spacers (dark grey) fit between the needle gantry and the rubber mould to provide an air gap for the curing resin.

Four needle gantry positioning frames were built for Plain pin sample production. Each frame had its own numbered needle gantry and mould. Production assemblies for

yarn embedded samples also use the Meccano® Base Plate with locating brackets. Therefore to produce yarn embedded pin samples, the needle gantry positioning brackets were added to the existing locating brackets at each end of the mould.

8.9 Sample Clarity

Silastic rubbers give high quality surface reproduction hence the surface finish on the machined metal die was reproduced on the resin samples. When producing polyester pin samples optical clarity had not been a problem but epoxy samples are not as clear. Preliminary pin samples of Araldite® epoxy 5052 produced for electrical tree testing were difficult to photograph due to the surface finish of the samples. One of the pin samples was polished to give the optical clarity needed for photography. Unfortunately considerable heat was generated in the process. The polishing of pre-stressed samples could affect the value of the residual pre-stress therefore the metal die was polished instead. New moulds were produced and the resulting samples were not only easier to photograph but also facilitated Raman analysis.

8.10 Pre-tensioned

Samples are pre-tensioned in order to provide a straight and uniform yarn outline for the Raman Laser. Results from the Raman analysis of samples had previously indicated that a reasonable amount of pre-tension was needed to counteract the thermal shrinkage of the resin. Initially pre-tensioned loads applied to the samples were related to the tex value of the HPFY being encapsulated. Therefore the HPFYs were loaded by the same load factor for comparison, however now that larger loads were required, it was more relevant to use the same weights. A pre-tensioned sample had a loading of no more than 2.5kg - approximately 10% of its heat treated mean breaking force.

8.10.1 Pre-tensioning Samples

The production of pre-tensioned Quad samples began with the use of a double screwed end-clamp arrangement at both ends of the mould. This arrangement was awkward for

one person to assemble and so one set of end-clamps was replaced with a bobbin as shown in **Figure (8.20)**.

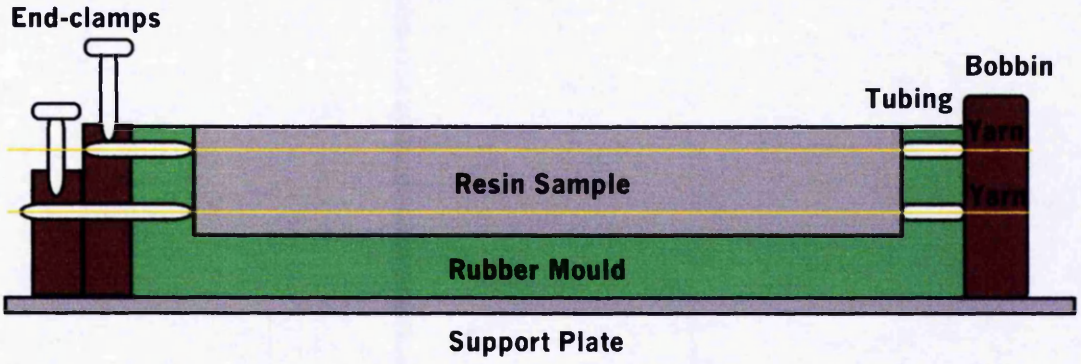

Figure (8.20) End-clamp and Bobbin Arrangement.

The yarn was simply threaded through the end clamp, down one side of the mould, taken around the bobbin and then threaded through the other side of the mould and out again through the end-clamp. Starting with the bottom yarn then the top yarn, resin was poured into the mould. Weights were applied to the yarn ends before all four yarns were clamped. Notice that the resin was poured into the mould before the weights were applied, this allowed for resin penetration of the yarn filaments and therefore gave greater fibre/resin adhesion.

Problems with the mould bending under load were experienced and metal bars were placed on top of the mould during curing to counteract this. An assembly was therefore required which would permit the mould to be free standing and therefore not subject to any of the stressing forces. At this time Meccano® was being used to develop Pre-stress Assembly prototypes for the high loads needed for pre-stressing. From the original idea for a Pre-stressed Assembly, see **section 8.11.1 Figure (8.23)**, a Pre-tensioned Platform was built.

8.10.2 Pre-tensioned Platform.

The **Pre-tensioned Platform** shown in **Figure (8.21)** consisted of a base plate on which was mounted an end-clamp, mould locating brackets and a removable roller. The end-clamp no longer acted as a clamp but as a guide upon which to rest the yarn on during loading and curing. Mould locating brackets allowed the moulds to sit in a

central position on the platform. A removable roller replaced the fixed bobbin in the earlier construction as this made it easier to thread the platform prior to pouring in the resin. Threading was as previously, the yarn passing around the front spindle, namely the spindle on which the roller sits. After threading, the roller was replaced and fastened to the two rear support spindles. Again the weights were attached after the resin had been poured in, although now the weights were left in place during the cure and postcure process.

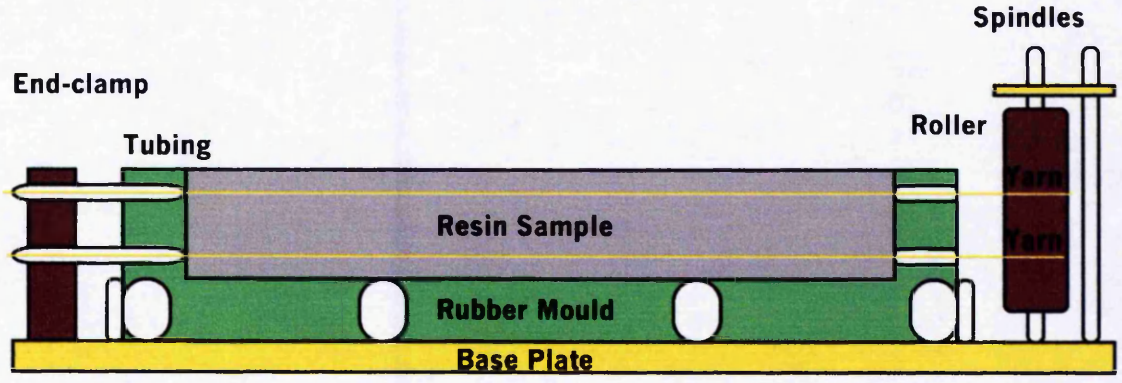

Figure (8.21) Pre-tensioned Platform

A total of four numbered Pre-tensioned Platforms were built; each platform had its own mould and set of weights to give traceability to the production process. The Platforms were numbered from one to four and a colour coding system was used for the weights :-

Platform Number	Colour Coding
1	Gold
2	Silver
3	Red
4	Blue

Each Platform had two 2.25kg (5lb) weights, the top weights were denoted by a white spot on their weight marking.

8.10.3 Pin Samples

To accommodate the production of pin samples, needle gantry positioning brackets were simply added to the mould locating brackets at each end of the mould. Once

again the advantage of using a modular approach to the design process gave flexibility to production. This modular approach has been aided by the use of Meccano®. It has proved to be an effective and time saving modelling tool, used in conjunction with in-house manufactured end-clamps and bobbin/rollers to produce Pre-tensioned pin samples. Meccano® had the added advantage of being heat resistant and was used for elevated postcuring of samples.

8.11 Pre-stressed

By the end of the first year two prototype yarn stress beds had been modelled using Meccano®, neither of which were suitable for sample production. The need for symmetrical samples required further modifications to **Yarn Stress Bed 2**, shown in **Figure (8.7)**.

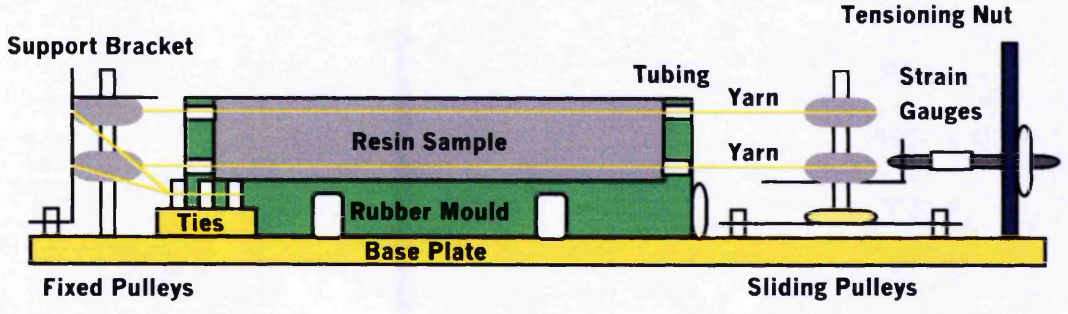

Figure (8.22) Yarn Stress Bed 3.

These modifications involved replacing the vertical bobbins with double horizontal pulley arrangements: **Yarn Stress Bed 3** is shown in **Figure (8.22)**. As in Bed 2 the height of the yarn is fixed parallel to the base of the bed, to ensure no changes other than stress changes take place when the tensioning nut is tightened. Strain gauges incorporated into the tensioning rod control and monitor the applied force. A working model was built, although this did not include strain gauges. Two strain gauges could be mounted on a plate which would fit into the tensioning assembly; these would be coupled to a strain gauge amplifier and display.

A Digital Strain Gauge Monitor Series SGA 800 was purchased from Graham & White Instruments Limited, Herfordshire. The SGA 800 provided dummy gauges to

complete the Wheatstone Bridge which were used in conjunction with its high stability low noise strain gauge amplifier type SGA 202, and digital liquid crystal display. The latter is housed in a portable case and can be used direct from the mains or with its internal rechargeable batteries, thus eliminating mains interference. The SGA 800 also has a Zero function to allow for recalibration for the individual stress beds as each pair of strain gauges is unique.

Whilst the Stress Bed strain gauge components were being sourced, attention was turned to the development of a Weighted Stress Bed. At this point there was no clear indication of the size of the applied load needed in order to obtain pre-stress. Since pairs of yarns were now required at the top and bottom of the samples, no crushing of the yarns was necessary to secure it. The yarns could simply be looped at one end and the yarn ends tied to the loading weights. This would provide actual experience of working with the yarn and Meccano® constructions under load.

8.11.1 Pre-stressing Samples

Production of a pre-stressed quad sample was attempted using a prototype stressing assembly, originally referred to as a **Weighted Stress Bed**, which is shown in **Figure (8.23)**. The whole assembly was designed to fit on to the top shelf of the large Heraeus cylindrical oven in the laboratory G.29.

The mould was free standing and fitted into mould locating brackets to ensure correct central alignment. At the front of the assembly two removable end-clamps acted as guides on which to rest the yarn during loading and curing/postcuring of samples. A clamping bracket fitted around the end-clamps and locates on the U bracket holding the end-clamps in position. The U bracket, mould locating brackets and roller assembly were mounted on to the base plate. The base plate was in turn fastened onto a fixing plate made from a larger flat sheet of metal. At the end of the base plate was the roller assembly which consisted of three fixed spindles, one in front and two behind. A removable roller fits on to the front spindle. A removable roller made it easier to thread the yarn prior to pouring in the resin. After threading, the roller was replaced and fastened to the two rear spindles for support. Again the weights were attached after the resin had been poured in. The larger fixing plate acted as a weight

carrier to stop the hanging weights from pulling the assembly off the shelf and was loaded before the weights were attached to the yarn ends.

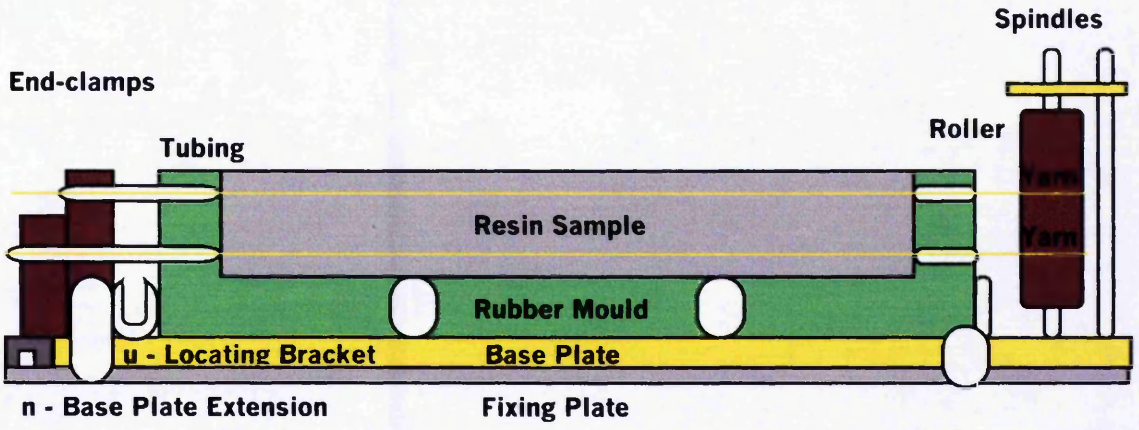

Figure (8.23) Prototype Stressing Assembly (Weighted Stress Bed)

Threading was performed on the bench with the end-clamps located by the clamping bracket and the roller removed. Starting with the bottom yarn, the yarns were simply threaded through the end-clamps, down one side of the mould, taken around the spindle, then back through the other side of the mould and out through the end-clamps. The process was repeated with the top yarn before refitting the roller and pouring in the resin. The whole assembly was then transferred onto the top shelf of the oven before attaching the weights. Curing and postcuring of the sample could then be carried out without disturbing it.

Problems were encountered when loading the fixing plate due to the weight on the oven shelf and in one instance the shelf had to be reinforced to prevent it from collapsing. This was unsatisfactory and furthermore no pre-stress was obtained. As the extent of the size of loading necessary to initiate pre-stress became apparent, it was clear that some form of heavy duty Pre-stressing Rig or Stress Bed was needed. By the end of 1997 this need for high loading had been confirmed by the results of Raman analysis and, as a result of problems with resin shrinkage, a new resin had been acquired which did not require elevated temperature postcure. In the light of these developments, work on the Stress Bed was suspended since, in the basic Meccano® form, the component parts were not strong enough for pre-stressed sample manufacture. For pre-stressing to take place heavy duty versions of the components

would have to be made and considerable time would be needed. Now that elevated postcure was no longer needed, the more expedient option was to develop a heavy duty Pre-stressing Rig.

8.11.2 Pre-stressing Rig

In the first year of the project a metal frame had been used to house the single yarn moulds during weighted sample manufacture. This metal frame formed the bottom half of a tensile test rig that was used by McNicol in his investigations into 'The Electrical Degradation of Polymeric Insulation' [113]. The frame comprised of 4 legs and 4 pairs of angle 'L' steel sections welded together. It was converted into the **Pre-stressing Rig Frame** by adding a metal Fixing Plate, Support Bracket and a pair of Pulley Arms at the top of the frame as shown in **Figure (8.24)**.

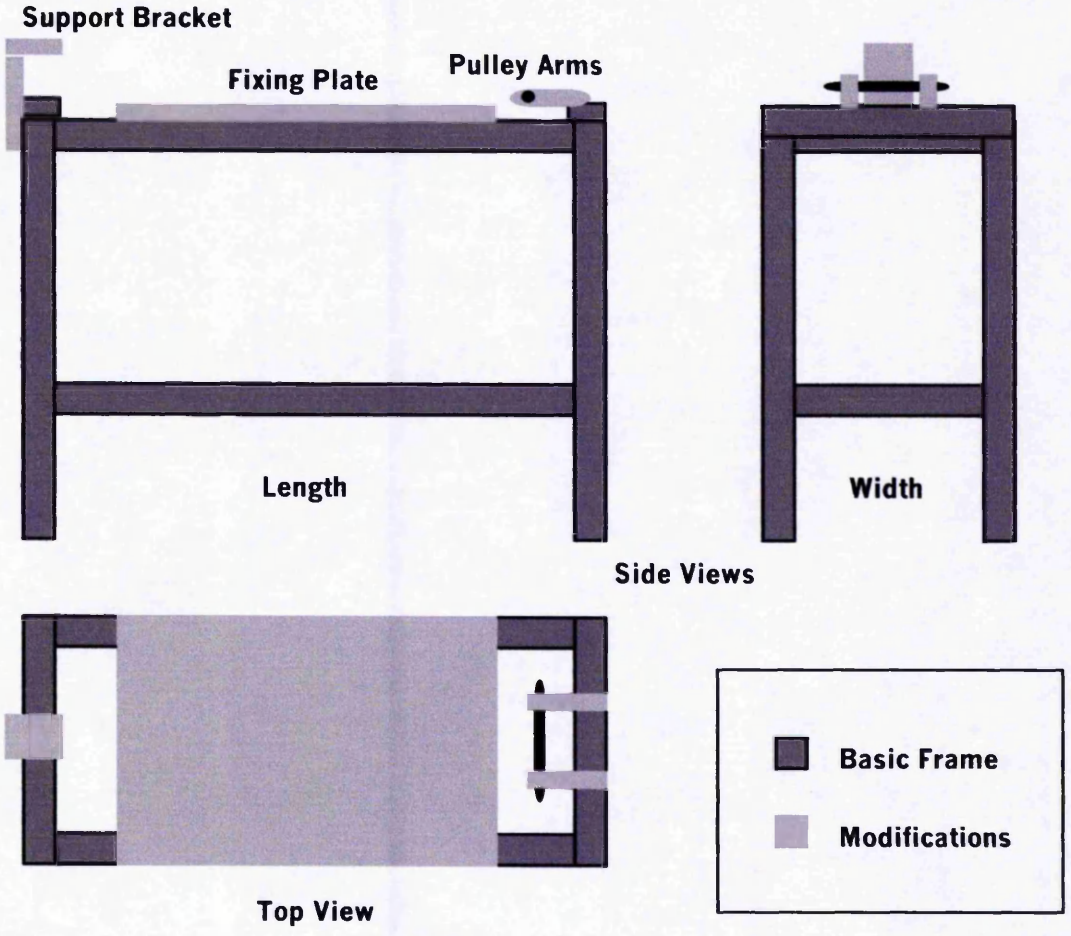

Figure (8.24) Pre-stressing Rig Frame

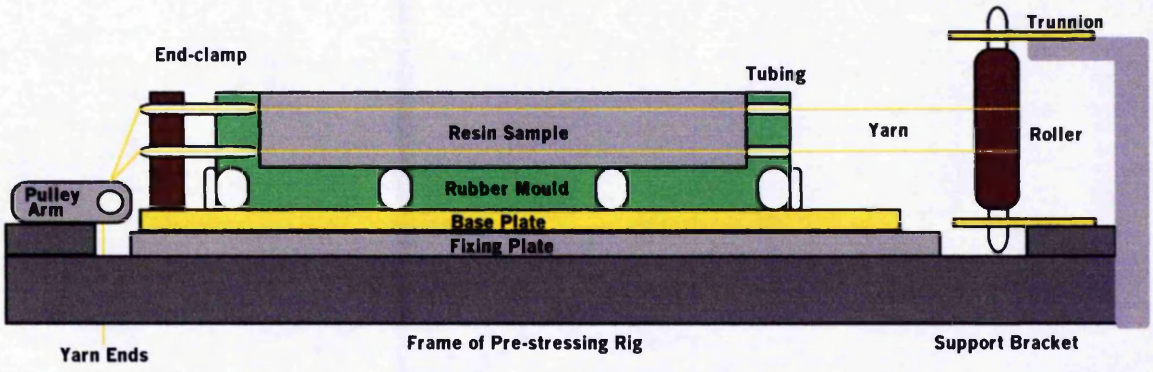

Figure (8.25) Pre-stressing Assembly

Modifications were then made to the Meccano® **Pre-tensioned Platform** shown in **section 8.10.2 Figure (8.21)**, by removing the Roller from the Base Plate and securing it to the Support Bracket. The **Pre-stressing Assembly** which mounts on top of the frame can be seen in **Figure (8.25)**. The HPFY is threaded through the mould around the Roller and tied to the weights off the front pulley. The Rig supports the load by means of the Support Bracket and Pulley Arms.

During threading the Roller is replaced by a spindle. The bottom yarn was threaded up first then the top yarn. Again the load was applied after the mould had been filled with resin to allow better resin impregnation of the yarn. The yarn ends were tied to a 1kg weight hanger and weights were placed on the hanger one at a time starting with the heaviest. For a 20kg loading the weights used are 1 x 9kg + 1 x 5kg + 2 x 2kg + 1 x 1kg (+ 1kg weight hanger = 20kg).

The first successful Pre-stressed sample manufactured using the Pre-stressing Rig was produced on 13-1-98 and postcured by 20-1-98. Raman analysis showed that in Sample I the yarn was in tension because it had a Raman bandshift of -2.0 cm^{-1}.

8.11.3 Pin Samples

To accommodate the production of pin samples, needle gantry positioning frames were added to the mould locating brackets at each end of the mould. A further 3 Pre-

stressing Rigs were produced, each Rig having its own moulds, needle gantry, weight hangers and set of weights. This gave tracebility to the production process. The Rigs were numbered from one to four and a colour coding system was used for the weights:

Rig Number	**Colour Coding**
1.	Gold
2.	Silver
3.	Red
4.	Blue

The top set of weights were denoted by a white spot on their weight markings. The photograph in **Figure (8.26)** shows Pre-stress Rig Frame No.2 during the postcure of a 20kg Pre-stressed tensile sample.

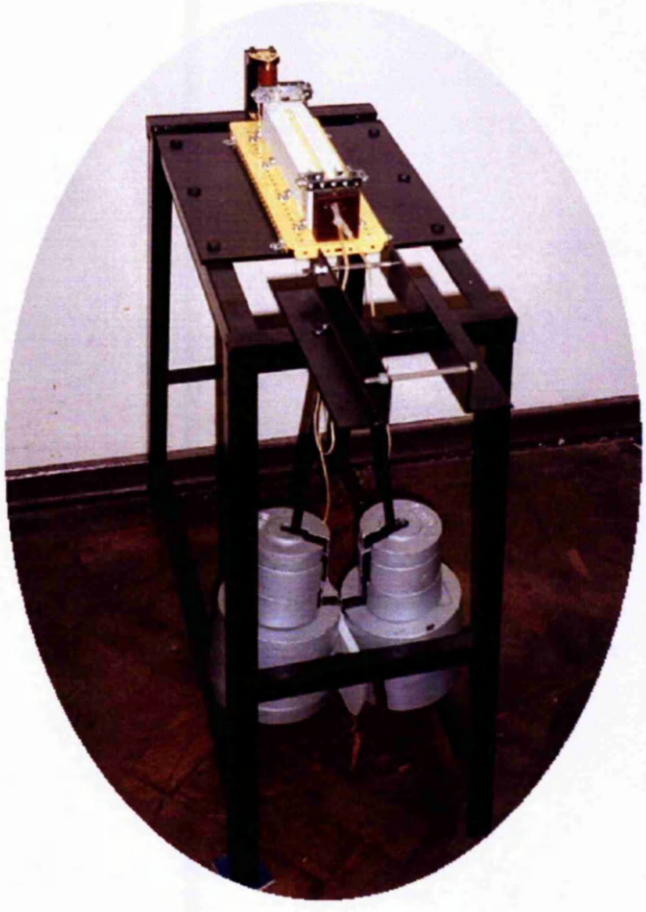

Figure (8.26) Photograph of Pre-stress Rig Frame No.2

8.12 Heavy Duty Stress Bed

The pre-stressing rigs provided the means to manufacture pre-stressed samples with a consistent level of pre-stress. A loading of 20kg gives a pre-stress of $-2.0cm^{-1}$ Raman wavenumber shift, see *Chapter 6*. The electrical tree testing of some of these samples has shown that pre-stressing retards electrical treeing, see *Chapter 9*. However the pre-stressing rigs only allow postcure at room temperature (RT), which means that the samples have a Tg of around 65°C and a safe working temperature of 40°C (see *Chapter 7*), clearly not suitable for practical applications. In order to produce pre-stressed insulation with a realistic safe working temperature, it would be necessary to postcure the samples at elevated temperatures with the yarn under load. A loading of 20kg for each layer of yarn (top and bottom), giving a total loading of 40kg would be needed, clearly beyond the capabilities of the Meccano® Stress Bed 3. The next stage in the development of the project therefore was to design and manufacture a Heavy Duty Stress Bed. The high loading also meant that strain gauges would not be reliable enough and so a load cell would be needed.

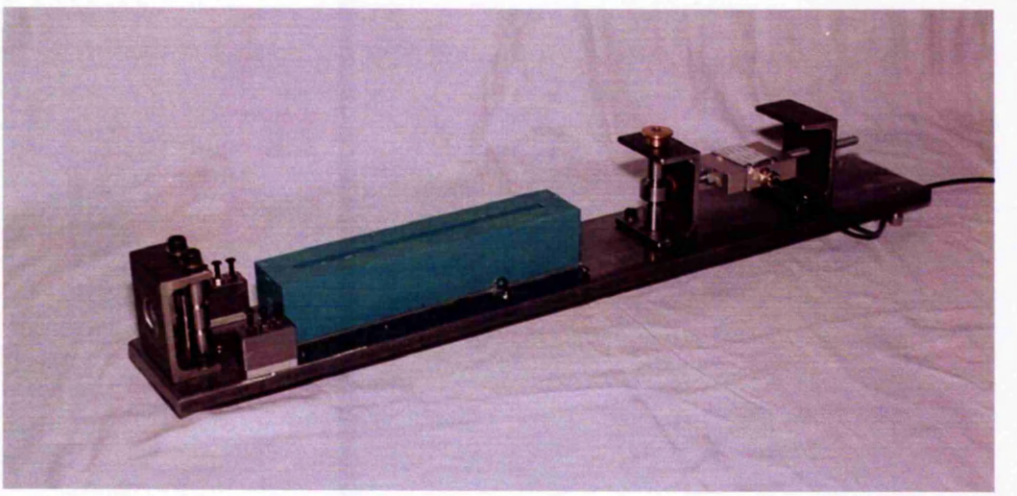

Figure (8.27) Photograph of Heavy Duty Stress Bed No.1

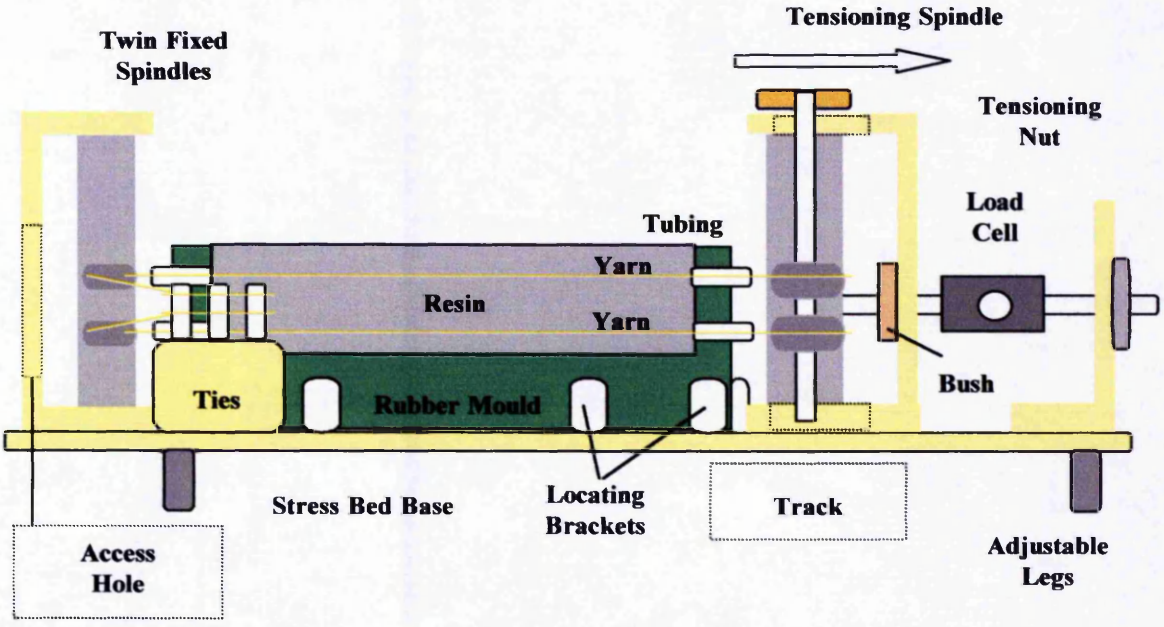

Figure (8.28) Heavy Duty Stress Bed

Using Stress Bed 3 (**Figure (8.22)**) as the starting point for the design it was decided to build the Heavy Duty Stress Bed (HDSB), shown as a photograph in **Figure (8.27)** and schematically in **Figure (8.28)**, in thick gauge steel. The Base of the Stress Bed was made from metal plate 12.5mm deep, 680mm long, and 100mm wide, two stress beds could potentially fit side-by-side on one shelf in the oven (see section 8.1). The top edge of the base was radiused to prevent the yarn from snagging when threading took place. Threaded holes were made in the base to allow for the use of the Meccano® locating brackets to position the rubber mould. This would also permit the use of the needle gantry frames for making pin samples. The rubber mould was positioned between the two fixed spindles (at the back of the stress bed) and the tensioning spindle.

Steel spindles replaced the brass pulleys, these had machined grooves that positioned and aligned the top and bottom yarns. The two fixed spindles were housed in a C-bracket made from three 9.5mm thick pieces of steel welded together for extra strength. Later an access hole was added to permit calibration of the load cell with

weights and this also made it easier to thread the yarn. In front of the fixed spindles on each side of the bed were blocks with three tie points for the yarns.

The tensioning spindle (replacing the sliding pulleys) was also housed in a C-Bracket, but the top and bottom plates had a 40mm track which permitted the spindle to move backwards (when threading) and forwards (when tensioning). A centre dowel could be removed to allow the spindle to be withdrawn to permit the load cell to be fitted. A threaded rod connected the spindle to the load cell. A phosphor-bronze bush fitted into the C-bracket allowed for the smooth operation of the threaded rod. Initially a third C-bracket provided the housing for the tensioning nut, but the top plate served no structural purpose and on later HDSBs was replaced with a simpler L-bracket.

8.12.1 The Load Cell

The load cells had to be made to order as they would have to endure the elevated temperature postcure of the samples. Graham & White Instruments Ltd. built a total of four ET-'S' Load Cells, three 50kg and one 100kg capacity load cells, which could be used up to a temperature of 110°C. The first 50kg Load Cell Serial Number 74656/54653 was calibrated to the Digital Strain Gauge Monitor SGA800 by Graham & White Instruments Ltd. The system was calibrated to give a display of 0-500 units and an output of 0.5V for a 0-50kg-tension load.

8.12.2 Load Cell Calibration

The connections to the load cell are:

Terminal	Colour	Function	SGA800
+ BS	RED	+Bridge Supply	BROWN
+ IP	GREEN	+Signal Input	GREEN
- IP		-Signal Input	
- BS	BLUE	-Bridge Supply	BLUE

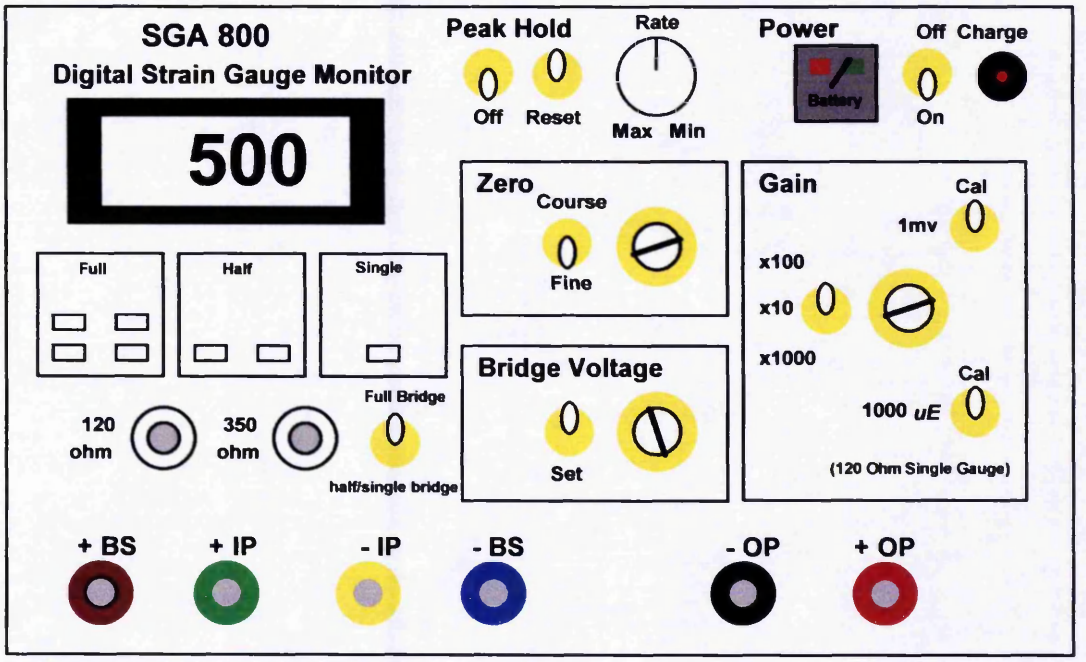

Figure (8.29) Digital Strain Gauge Monitor SGA800 (Front Panel)

The front panel of the Digital Strain Gauge Monitor SGA800 is shown in **Figure (8.29)**. The SGA800 indicator switch settings are:

Full Bridge
Gain x 100
Peak Hold off
Zero fine

With these switch settings and the load cell connected, the Bridge Supply was adjusted to +10V (Display 1000 with Bridge Voltage Set switch held down). The indicator was calibrated by injecting the load cell full scale output (2.000mV x 10V = 20mV) across the input terminals with the load cell connected. With no load on the load cell and 0mV input, the fine Zero was adjusted for a display of zero. With no load on the load cell and 20mV input, the Gain was adjusted for a display of 500. Following calibration, the Bridge Supply and Gain controls were locked. With these calibration settings, the 1mV Cal switch gave a display of 25, and the 1000 Cal switch gave a

display of 368. Adjustment of the Gain or Bridge Supply settings on the indicator will void this calibration.

8.12.3 Stress Bed Calibration

Having calibrated the uncoupled Load Cell with the SGA800 it was then necessary to calibrate the Load Cell coupled to the Stress Bed. To avoid confusion this will be referred to as Stress Bed calibration. A rubber mould was fitted into the HDSB no. 1 and threaded with Twaron 1001. The stress bed was mounted in a vice and the yarn allowed to hang through the access hole. The tensioning pulley was positioned in the middle of the track, a first reading was taken from the indicator to ascertain the effect of the weight of the pulley on the readings, and this offset value was then subtracted from subsequent readings. A 1kg weight hanger was tied to the yarn ends and an indicator reading taken. Weights were then added to the weight hanger 1kg at a time and readings taken until the yarn broke. This became the standard stress bed calibration procedure and was carried out every time the HDSB was used.

The first calibration was carried out using the bottom layer of yarn only, see **Figure (8.30)**; surprisingly the yarn was loaded to 32kg, much higher than the rig loading (20kg) and the tensile test results (26kg). This is attributed to the gradual 1kg loading of the yarn and the fact that the weights were hung directly from the yarn, without having to go through the 90° angle necessary with the Pre-stressing Rigs. A second calibration was carried out using both layers of yarn, see **Figure (8.31)**, where premature failure at 34kg was caused by a knot in the yarn. In each case the indicator gave a reading of 9.8 for every 1kg applied to the weight hanger. To a first approximation the indicator was displaying the load in Newtons.

Figure (8.30) Load Cell Calibration 01 Using The Bottom Layer Only (1kg = 9.8)

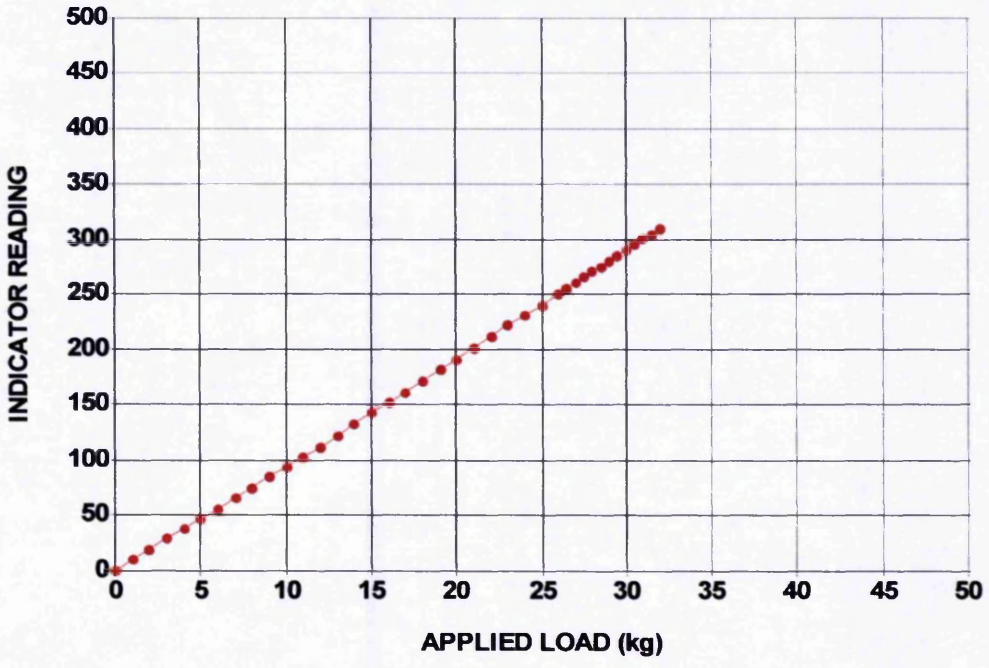

Figure (8.31) Load Cell Calibration 02 Using Both Layers (1kg = 9.8)

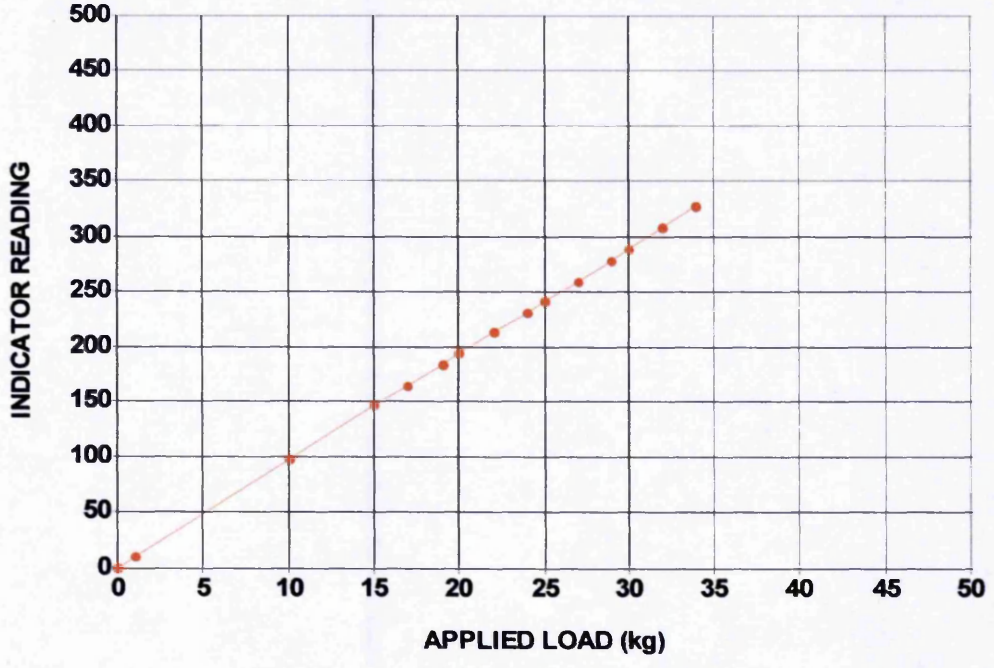

8.12.4 Sample Manufacture

The first step when using the heavy duty stress bed was to connect the load cell to the digital strain gauge monitor and set the tensioning spindle to its minimum position. A reading was taken to determine the effect of the components on the load cell. This offset value was then subtracted from subsequent readings. The rubber mould was then placed into position and eight 30mm lengths of the rubber sealing tube cut from the spool. Starting with the bottom layer the yarn was threaded via the access hole at the end of the stress bed into the mould, then inserting the sealing tubes where necessary. The yarn then threaded around the tensioning spindle and back through the mould. Initially the yarn is taken back out of the access hole to allow for equal lengths of yarn to be cut from the package. The two lengths of yarn went back through the access hole and were taken around their respective fixed spindles. The procedure was repeated for the top layer of yarn.

Having threaded the yarn the resin was mixed and degassed before being poured into the mould. In keeping with earlier yarn embedded samples the resin was allowed to penetrate the yarn before implementing any tensioning operation. Starting with the bottom layer, the two yarn ends were simultaneously wrapped (in a figure of eight) and tied to their respective side tie points. This tying of the left and right yarns must be carried out together in order to stop the yarn from pulling out from one side or the other. The procedure was repeated for the top layer of yarn. With both layers of yarn secured the tensioning operation could begin. Turning the tensioning nut clockwise pulls the tensioning spindle forward and the indicator reading increases. Applying the load in such a direct and controlled way means that it is loaded in a progressive manner. It has already been demonstrated during the Stress Bed Calibration that a more gradual loading of the yarn can lead to much higher loads being obtained and sustained.

8.12.5 Loading the Yarn

For the manufacture of Sample Y, the first elevated temperature postcured pre-stressed sample, it was decided to try and produce an equivalent to the 20kg RT postcured sample. This would mean loading the yarn to 40kg, requiring an indicator reading of 392 (40kg x 9.8), plus the offset which on the first production run was 003

giving a total reading of 395. It was at this point that the effects of stress relaxation in the yarn became apparent. Stress relaxation is defined as *the decrease in stress with time in a viscoelastic material* (a polymer fibre) *held under constant strain* [47]. Using weights on the pre-stress rigs had eliminated the consequence of stress relaxation in the yarn because gravity acting vertically on the load had compensated for this effect. In the case of the stress bed, the yarn is being stretched horizontally between the spindles (under a constant strain), therefore only by applying more external force can there be compensation for any relaxation within the yarn. On loading the yarn to 395 it immediately started to relax and the reading fell. Subsequent adjustment to 405 gave a stable reading of 380. A further increase to 410 stabilised at 395 after 2-3 minutes. The sample was then left to cure for one day and intermittent readings were taken to monitor the effects of the stress relaxation on the indicator reading.

After one hour the reading had fallen to 369, indicating a loading of 366, the equivalent of 37kg (18.5kg per layer). Another reading taken after two hours and the indicator had dropped to 355, indicating a load of 352, the equivalent of 36kg (18kg per layer). The final reading taken after the cure period (24hours) showed a reading of 349, indicating a loading of 346, the equivalent of 35kg (17.5kg per layer). The digital strain gauge monitor was disconnected from the stress bed and the stress bed was transferred into the oven for postcuring. The sample was postcured for 4 hours at 100°C followed by a stepped cooling period of 10°C/hour until it reached RT. Sample Y was then left to age for 1 week before undergoing Raman analysis. In the meantime another stress bed calibration was carried out.

8.12.6 Calibration After Postcure

It was considered prudent to perform another stress bed calibration after the postcuring of Sample Y in order to ascertain the effects of elevated temperatures on the load cell. The third calibration was carried out by loading the two layers of yarn in 1kg increments. The yarn was loaded up to the 50kg capacity of the load cell without any visual or audible signs of problems to the yarn. Furthermore, the indicator reading had fallen to 9.55 for every 1kg applied to the weight hanger. The results can be seen

in **Figure (8.32)**. This would indicate that the load cell should be re-calibrated after use at elevated temperatures.

Figure (8.32) Load Cell Calibration 03 (1kg = 9.55)

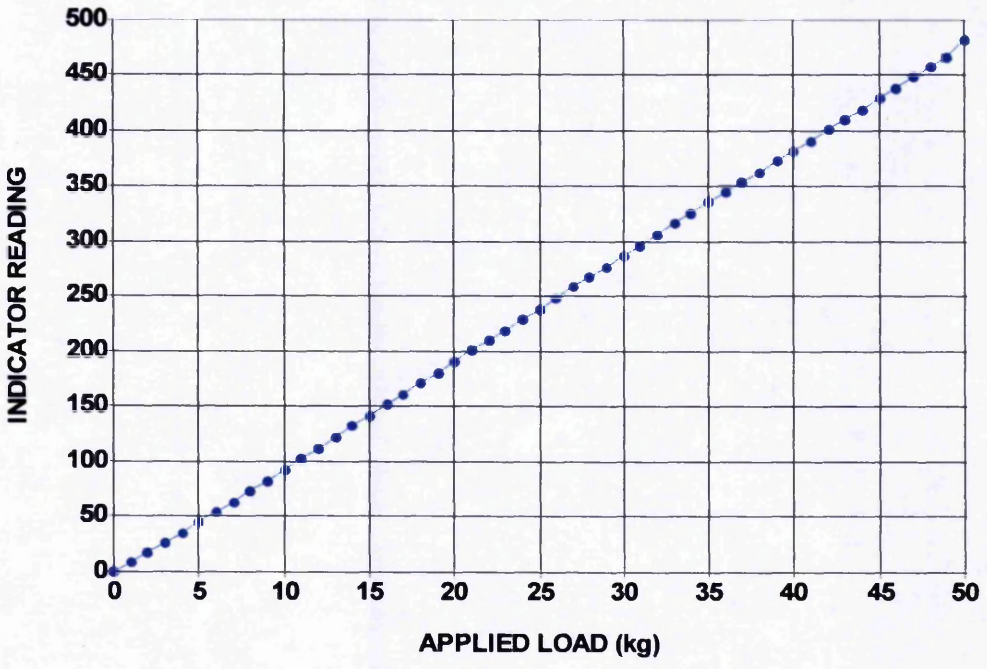

8.12.7 Raman Findings

Raman analysis of Sample Y confirmed the presence of pre-stress although revealed anomalies. In the RT cured pre-stressed samples, the difference in loading between the front and back yarns was no more than a negligible $0.2cm^{-1}$, however in Sample Y there was a difference of $0.4cm^{-1}$, indicating a loading imbalance. Furthermore the sum total of the pre-stress bandshifts ($-1.2cm^{-1}$ front, $-1.6cm^{-1}$ back) $-2.8cm^{-1}$ signified a pre-stress load level of 28kg (14kg per layer). This could suggest either further relaxation in the yarn or a reduction in pre-stress levels due to thermal shrinkage. If this effect is attributable to relaxation, this could be caused either by the inherent characteristics of the yarn, or by the method being used to tie the yarn. Certainly if the tie points were not securing the yarn equally on both sides, this could explain the difference in the Raman bandshift values.

8.13 Summary

The systematic modular approach to sample design described in this Chapter allowed maximum flexibility and changes to the sample configuration with the minimum of disruption to the progress of the research. The work began by identifying the areas of investigation and the limitations this placed on the sample configuration. The end result was a compromise between the requirements of Raman analysis, tensile testing, electrical tree testing and the size of the production apparatus itself.

The modular approach was enhanced by the use of Meccano® as a prototyping tool. An initial Meccano® model of a stress bed that would fit inside the oven determined the required size of the mould, hence the dimensions of the standard sample.

The selection of a high quality moulding material ensured the production of reproducible quality samples that needed no machining or polishing. The moulds were cast from a former that was again built in a modular and flexible style to allow for the production of plain, single yarn and multiple yarn samples.

The manufacture of single yarn samples was abandoned due to the findings of Raman analysis. This led to the production of symmetrical yarn samples which eliminated sample bending. The symmetrical quad sample configuration allowed for the production of pin samples. This Chapter also describes how the central alignment of the treeing needles was achieved using a needle gantry positioning frame.

Quad sample production is detailed. It was split into pre-tensioned and pre-stressed samples, each with their own set of apparatus. The development of the two sample types took place concurrently. The development of the criteria for pre-stress highlighted the need for higher loadings. This necessitated the development of apparatus with freestanding moulds and also identified the need for a heavy duty stress bed. In the short term the use of weights on a pre-stressed rig enabled the production of pre-stressed samples cured at Room Temperature. The manufacture of samples cured at elevated temperatures was only possible upon construction of a heavy duty

stress bed. The heavy duty stress bed gave more control over the pre-stressing process and made it possible to consider the manufacture of samples at higher loadings.

Procedures have been established in *Chapter 8* for the manufacture of plain, pre-tensioned and pre-stressed samples with and without needles at RT and at elevated temperatures. The production of reproducible high quality samples has now been achieved for all sample types. Visual inspection and consistent Raman analysis results have confirmed this. The effect of yarn inclusion on the mechanical strength of the insulation samples and its potential to reduce insulation thickness is examined in *Chapter 9.*

CHAPTER 9

Mechanical Testing

9.0 Mechanical Testing of Resin

The mechanical testing of plain, pre-tensioned and pre-stressed resin samples was carried out to establish the effects and potential benefits of yarn inclusion in the resin matrix. Mechanical testing of resin samples is covered under the general introduction of the BSi Standard [114]:

BS 2782 : Part 0 : 1995

'Methods of Testing Plastics.'

Part 0. Introduction.

In annex B the individual test methods are listed referring to Part 3 Mechanical properties the BSi Standard [115]:

BS 2782 : Part 3 : 1976 (Confirmed 1986)

Part 3. Mechanical properties.

'Methods 320A to 320F. Tensile strength, elongation and elastic modulus.'

These methods describe procedures for determination of the tensile properties of plastic materials, each applicable to a specific type of material. Method 320E refers to the testing of fibre reinforced materials and is shown in **Figure (9.1)**. The principle of the test is the subjection of the test pieces of Method 320E, plastics materials, to a tensile force and the calculation of their mechanical properties. A controlled atmosphere is not necessary and the prevailing ambient atmospheric conditions are adequate under BS 2782, annex A, conditioning procedure E, in the range of 22°C ±3°C.

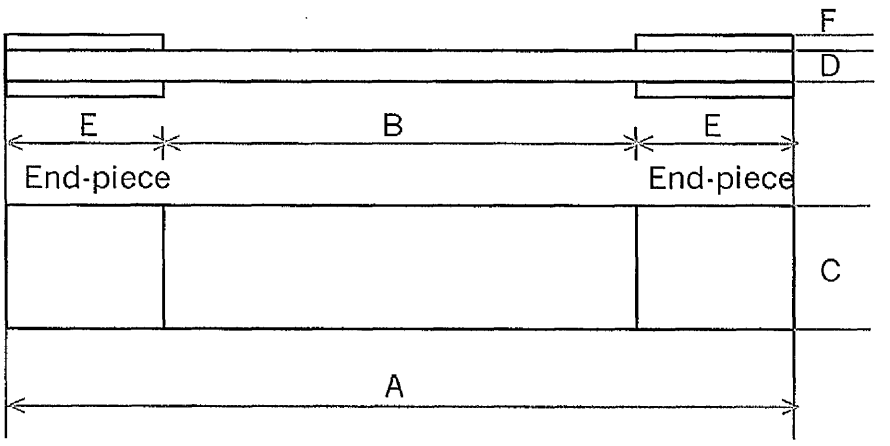

Dimensions are in millimetres (mm).

	BSi specification	**Actual specification**
A Overall length, (minimum)	(200)	**210**
B Length between end-pieces (minimum)	(110)	**120**
C Width for tensile strength determinations	(25)	**24**
D Thickness of mat. under test (min- max)	(1-10)	**10**
E Length of end-pieces (minimum)	(45)	**45**
F Thickness of end-pieces (minimum)	(3)	**3**

Figure (9.1) Method 320E Test Pieces

The mechanical tests were carried out on an Avery-Denision 7116 tensile testing machine with a 100kN load capacity. This machine is located in the Simon Engineering Building, which is part of the Mechanical Engineering Department. The unrestricted use of this equipment was granted as part of the ongoing collaboration between the departments within the School of Engineering at the University of Manchester.

The tensile testing machine is power driven and is capable of maintaining a set rate of grip separation. It has a display for the continuous indication of the force applied to the test piece and records the test autographically up to the maximum force applied. The machine has capstan action self tightening heavy duty wedge grips. This type of

grip increases grip pressure as the force applied to the test piece increases, in an effort to eliminate, as far as possible, slip relative to the grips. Test pieces were mounted in the test machine in axial alignment with the direction of the pull. Once secured in the grips, protective shields were attached to the grip assembly for safety. The tests then commenced and finished when the sample broke. The speed of the tests is determined by the rate of grip separation which was set at 1mm/min.

During the first year batches of polyester samples were manufactured and preliminary tests were carried out to evaluate the sample configuration, in particular the suitability of both the end-pieces and the glue. The first end-pieces were produced from existing moulds and glued together using Loctite® 4210, a single component temperature resistant adhesive. The low number of valid results highlighted the poor quality of the end-pieces and the failure of the glue, but the results indicated that the inclusion of the yarn improved the strength of the samples. A new former was made using metal dies cut from '*ground flat stock*' bars, dimensions 90mm x 25mm x 3mm double the size of an end-piece (hence a **double end-piece**). This was done for ease of manufacture particularly when demoulding such a narrow section of resin. The resulting moulds were made in Silastic® S which yielded quality flat end-pieces requiring a simple saw cut to give two end-pieces. However a suitable bonding agent had to be found before the format of the end-pieces could be concluded.

9.1 Bonding Agent

Section 7.6 Method 320E of BS 2782 Part 3. (Mechanical properties) relates to the selection of a cold setting epoxide adhesive as the bonding agent. It was necessary for the bonding agent to withstand elevated temperatures because the project was aiming to utilise a tensile testing machine with an environmental chamber. GRACE Specialty Polymers in Belgium produce ECCOBOND®, a range of high temperature operating speciality epoxide adhesives [116]. The general purpose adhesive ECCOBOND® 286 is a two part room temperature curing epoxy adhesive, which will bond to a wide variety of materials including polyester and epoxy resins.

ECCOBOND® 286 is supplied as a kit containing two squeeze tubes (Parts A & B) and a mixing stick. Part A is a reaction product of 90-98% epichlorohydrin/Bisphenol A and Part B is a reaction product of 8-10% epichlorohydrin/Bisphenol A with 18-22% 4,7,10-Trioxatridecane-1,13-diamine. It contains no solvent, volatiles or corrosive matter. Equal volumes (1:1 ratio) of each component are squeezed out side by side and then thoroughly blended. The resulting glue has a pot life of 2-3 hours at room temperature and is ready to be applied to the mating surfaces. The proper amount of thixotropy is built-in to assure minimum runout without sacrificing wetting. Only contact pressure is needed and it sets in about 4 hours, with a complete cure in 24 hours. The cure can be accelerated by using elevated temperatures e.g. 1 hour at 60°C. Once fully cured, the glue has a service temperature range from -55°C to +120°C. It is this range of properties and qualities that made Eccobond® ideally suited to the requirements of the project.

9.2 End-piece Geometry

Having obtained a reliable bonding agent, the question of end-piece geometry could now be addressed. The first year tests had identified the problem of premature sample failure due to fracture at and inside the 90° sample/end-piece interface. It was decided to imitate the conventional tensile testing *dog bone* configuration by introducing a gradient to the end-piece in the form of a taper shown in **Figure (9.2)**. The most suitable taper would be determined by the manufacture and testing of a series of samples with varying angles of taper, the results of which can be seen in **Appendix 3**. All of the samples and end-pieces were produced using polyester Resin C cured for one day at room temperature followed by a postcure for 3 hours at 80°C.

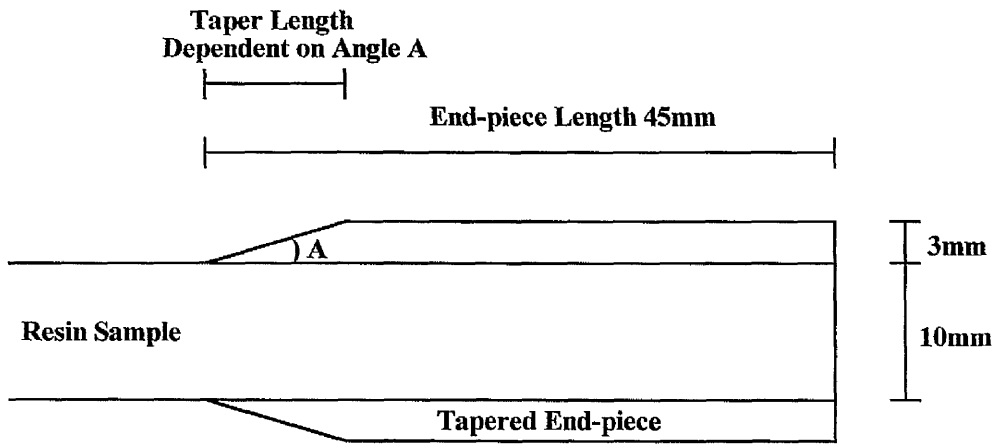

Figure (9.2) End-piece with Taper

To ensure repeatability Central Workshops constructed a jig to enable exact angles to be machined on to the end-pieces. Initially 60°, 45° and 30° tapers were made and tested. The 30° taper showed not only a tendency to fracture in the gauge of the sample but also a marked increase in the load needed to break it. The next stage was a comparison with tapers of around 30°, so tapers of 15°, 20°, 25° and 35° were examined. Again problems with fracture inside the end-piece/sample interface area were recorded. Problems were also seen with taper breakage during machining of tapers less than 30°.

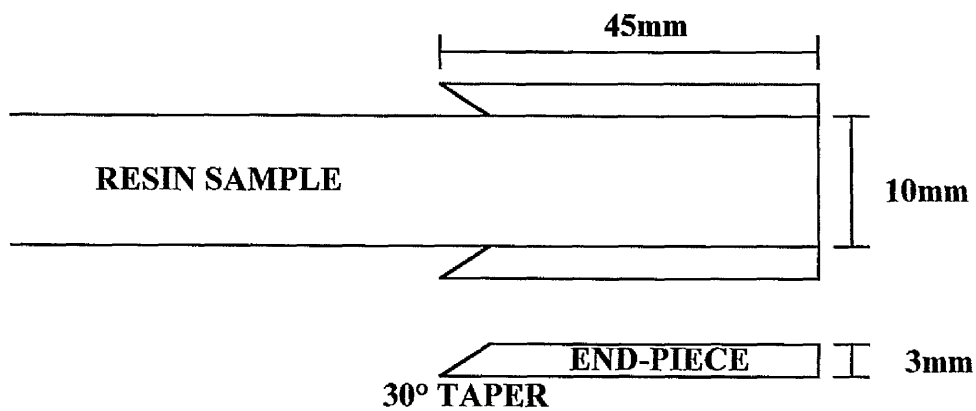

Figure (9.3) Inverting the End-pieces.

Further investigations involved **inverting the end-pieces** as shown in **Figure (9.3)** and the production of **30° tapered lugs** which fitted on to the top and bottom of the samples rather than the sides as shown in **Figure (9.4)**.

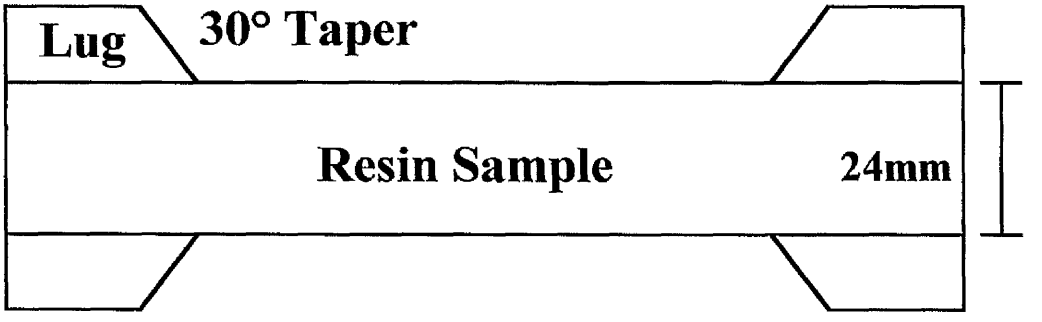

Figure (9.4) 30° Tapered Lugs.

The lugs exhibited fracture inside the end-piece/sample interface area, hence were discarded. Inverted end-piece samples on the other hand showed an increase in the load needed to break them. This configuration was adopted as the *standard geometry* for all of the test samples in this project. Once all tensile testing samples were fitted with inverted 30° tapered end-pieces, attention could be focused on the statistical testing of the resin samples.

9.3 Statistical Testing

During the course of investigations into the mechanical testing of fibre reinforced materials, it became evident that BS 2782 was only a starting point, serving as a guide to general testing criteria. Further research undertaken during the development of the tapered end-pieces revealed a more comprehensive testing standard issued by the American Society for Testing and Materials (ASTM) [117] as used by Naik [118].

ASTM D 3039/D 3039M - 95a
Standard Test Method for
Tensile Properties of Polymer Matrix Composite Materials.

This test method determines the in-plane tensile properties of polymer matrix composite materials reinforced by high modulus fibres. The standard is 12 pages long and covers all aspects of mechanical testing: tensile specimen geometry, the use of tabs (end-pieces), conditioning of samples, test apparatus, sampling, test procedure, failure characterisation and calculations.

9.3.1 Specimen Geometry

Over three pages (a quarter of the standard) are devoted to tensile specimen geometry, beginning with the paragraph:

8.2 ***Geometry****-Design of mechanical test coupons (samples), especially those using end-tabs (end pieces), remains to a large extent an art rather than a science, with no industry concensus on how to approach the engineering of the gripping interface. Each major composite testing laboratory has developed gripping methods for the specific material systems and environments commonly encountered within that laboratory. Comparison of these methods shows them to differ widely, making it extremely difficult to recommend a universally useful approach or set of approaches. Because of this difficulty, definition of the geometry of the test coupon is broken down into the following three levels, which are discussed further in each appropriate section:*

Purpose	*Degree of Geometry Definition*
8.2.1 ***General Requirements***	*Mandatory Shape & Tolerances*
8.2.2 ***Specific Recommendations***	*Non Mandatory Suggested Dimensions*
8.2.3 ***Detailed Examples***	*Non Mandatory Typical Practices*

The standard sets out guidelines and suggests the use of tapered end-tabs to reduce stress concentrations at the test piece/machine grip interface. To determine the most suitable end-tab angle for a specific composite material, a period of trial and error is recommended, as already undergone in this project. It also highlights the fact that a uniform bondline of minimum thickness is needed to reduce stress concentrations at the tab/coupon (end-piece/sample) interface. Uneven or thick bondlines cause premature failure of the coupon (sample).

9.3.2 Failure Characterisation

ASTM D3039, Section 11.9 *Failure Mode,* recommends recording the mode and location of failure of the specimen in accordance with a standard description three-part failure mode code, shown in **Table (9.1)**. The First Character denotes the failure type, the Second Character denotes the failure area and the Third Character denotes the failure location. For example a specimen with the failure code **AGM** indicates an **A**ngled break in the **G**auge area in the **M**iddle of the specimen. The failure mode code provides a standard characterisation system for sample comparison. This has been implemented and all of the results obtained in the second & third years have been analysed in this way.

Table (9.1) Tensile Test Failure Codes

First Character

Failure Type	Code
Angled	A
edge Delamination	D
Grip / tab	G
Lateral	L
Multi-mode	M(xyz)
long Splitting	S
eXplosive	X
Other	O

Second Character

Failure Area	Code
Inside grip/tab	I
At grip/tab	A
<1W from grip/tab	W
Gauge	G
Multiple areas	M
Various	V
Unknown	U

Third Character

Failure Location	Code
Bottom	B
Top	T
Left	L
Right	R
Middle	M
Various	V
Unknown	U

9.3.3 Invalid Results

ASTM D3039 provides a reliable and repeatable system which not only validates results but also invalidates results, providing a system of rejection for the project. These invalid or rejected results have been split into two categories. Firstly **R**eject **T**hickness **(RT)** this applies to the thickness and evenness of the bondline at the tab/coupon interface, a cause of premature failure. Secondly **R**eject **B**reak **(RB)** these are specimens that have failed with failure type **G** (Grip/tab) or whose failure area is **I** (Inside grip/tab) or **A** (At grip/tab) as with BS 2782 failures experienced inside or at the grip/tab interface are discarded.

9.4 Results

The valid results shown in the following sections are based on a standard size specimen fitted with inverted 30° tapered end-pieces tested at 1mm/min. A full set of valid results for Araldite® 5052 samples can be found in **Appendices 6 & 7**. The results were calculated using the following the equations:

Tensile stress [115]

$$\sigma = \frac{F}{A} \tag{9-1}$$

where

σ = maximum tensile stress **(MPa)**

F = maximum breaking force **(N)**

A = mean cross-sectional area (240mm^2) **(mm^2)**

(NOTE: 1N/mm^2 = 1MPa)

The results are displayed showing both their mean values and their median values for comparison.

The (arithmetic) **mean** of a set of observations is the sum of the observations divided by the number of observations [119].

$$\bar{x} = \frac{1}{n}\sum_{i=1}^{n} x_i \quad (i = 1,2,3.....n) \tag{9-2}$$

The ***median*** is the value of the middle item [120].

$$\text{median} = \frac{(n+1)}{2}\text{th item} \tag{9-3}$$

Note, where there is an even number of data the median will be in between two actual values of data, and so the two values are averaged.

9.4.1 Polyester Resin C

Polyester Resin C samples in **Table (9.2)** have had a 1 day cure at room temperature followed by a 3 hour postcure at 80°C.

Table (9.2) Polyester Resin C

PLAIN	**Full Results in Appendix 3**	
Number Tested - 6	Valid Results - **3**	
manufacturer's data [121]	42MPa	10080 N
previous work [122]	26MPa	6240 N
mean	**24MPa**	**5641 N**
median	***24MPa***	***5708 N***

9.4.2 Epoxy Araldite CT1200

Epoxy Araldite CT1200 samples in **Table (9.3)** have had a 14 hour cure at 135°C followed by an 8 hour postcure at 150°C.

Table (9.3) Epoxy Araldite CT1200

PLAIN	**Full Results in Appendix 2**	
Number Tested - 5	Valid Results - **2**	
manufacturer's data [98]	80MPa	19200 N
mean	**73MPa**	**17430 N**
median	***73MPa***	***17430 N***

9.4.3 Epoxy Araldite 5052

Epoxy Araldite 5052 samples in **Tables (9.4) & (9.5)** have had a 1 day cure at room temperature followed by a 6 day postcure at room temperature.

Table (9.4) TESTED AFTER 30 DAYS

Full Results in Appendix 6

PLAIN

Number Tested - 24	Valid Results – **10**	
manufacturer's data [104]	49MPa	11760 N
mean	**34.4MPa**	**8254 N**
median	*34.1MPa*	*8190 N*

PRE-TENSIONED DOUBLES – 2.25kg

Number Tested - 8	Valid Results - **2**	
mean	**37.4MPa**	**8980 N**
median	*37.4MPa*	*8980 N*

PRE-TENSIONED QUADS - 2.25kg

Number Tested - 18	Valid Results - **11**	
mean	**39.4MPa**	**9445 N**
median	*38.1MPa*	*9140 N*

PRE-STRESSED QUADS - 20kg

Number Tested - 14	Valid Results - **9**	
mean	**38.8MPa**	**9315 N**
median	*39.1MPa*	*9380 N*

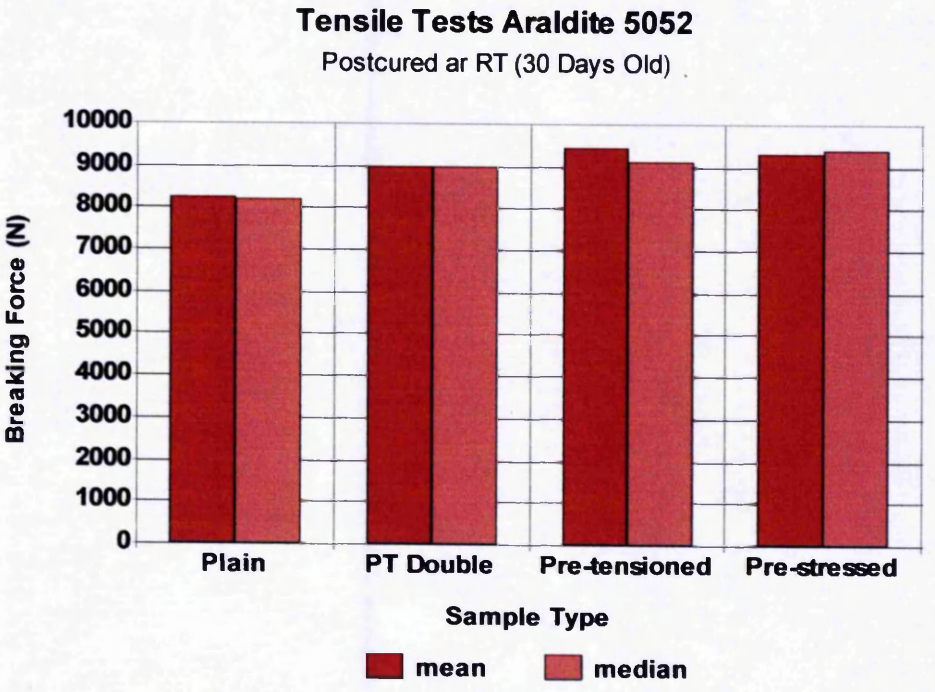

Figure (9.5) Tensile Test Results Samples Postcured at RT (30 Days Old)

Table (9.5) TESTED AFTER 15 WEEKS

Full Results in Appendix 7

PLAIN

Number Tested - 34 Valid Results - **13**

mean	**36.9MPa**	**8860 N**
median	*36.1MPa*	*8660 N*

PRE-TENSIONED QUADS - 2.25kg

Number Tested - 10 Valid Results - **5**

mean	**38.8MPa**	**9300 N**
median	*38.4MPa*	*9220 N*

PRE-STRESSED QUADS - 20kg

Number Tested - 11 Valid Results - **5**

mean	**43.8MPa**	**10500 N**
median	*42.8MPa*	*10260 N*

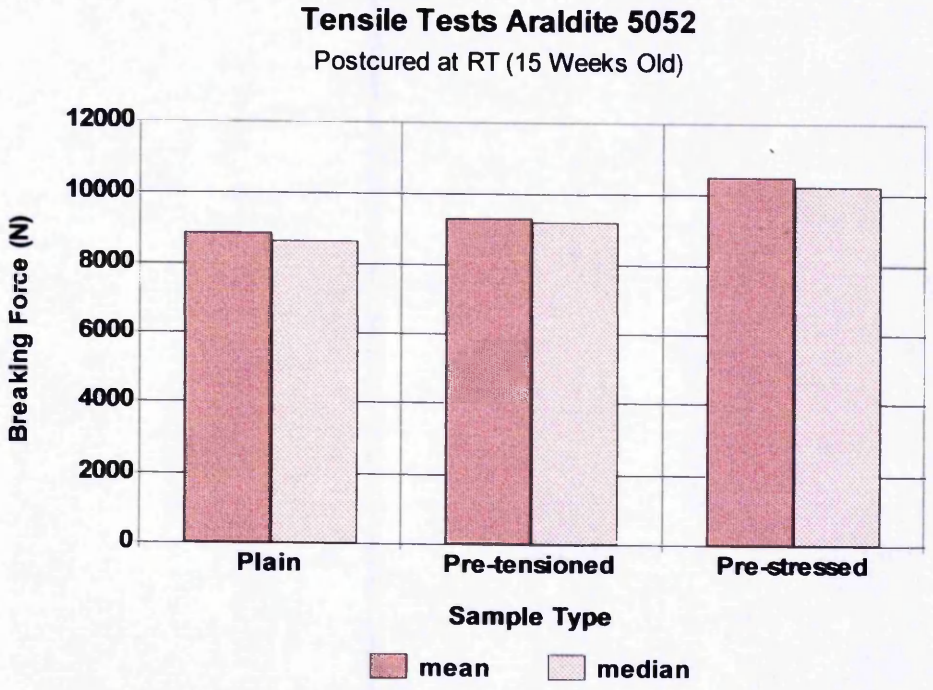

Figure (9.6) Tensile Test Results Samples Postcured at RT (15 Weeks Old)

9.4.3.1 Postcured at Elevated Temperatures

Epoxy Araldite 5052 samples In **Table (9.6)** have had a 1 day cure at room temperature followed by a 8 hour postcure at 80°C.

Table (9.6) Postcured at 80°C

TESTED AFTER 30 DAYS	**Full Results in Appendix 6**		
PLAIN			
Number Tested - 10	Valid Results – **8**		
manufacturer's data [104]		84MPa	20160 N
mean		**60.7MPa**	**14500 N**
median		59.8MPa	14360 N
TESTED AFTER 15 WEEKS	**Full Results in Appendix 7**		
PLAIN			
Number Tested - 24	Valid Results - **7**		
mean		**59MPa**	**14170 N**
median		*59.3MPa*	*14240 N*
PRE-TENSIONED QUADS			
Number Tested - 6	Valid Results - **2**		
mean		**65.3MPa**	**15660 N**
median		*65.3MPa*	*15660 N*

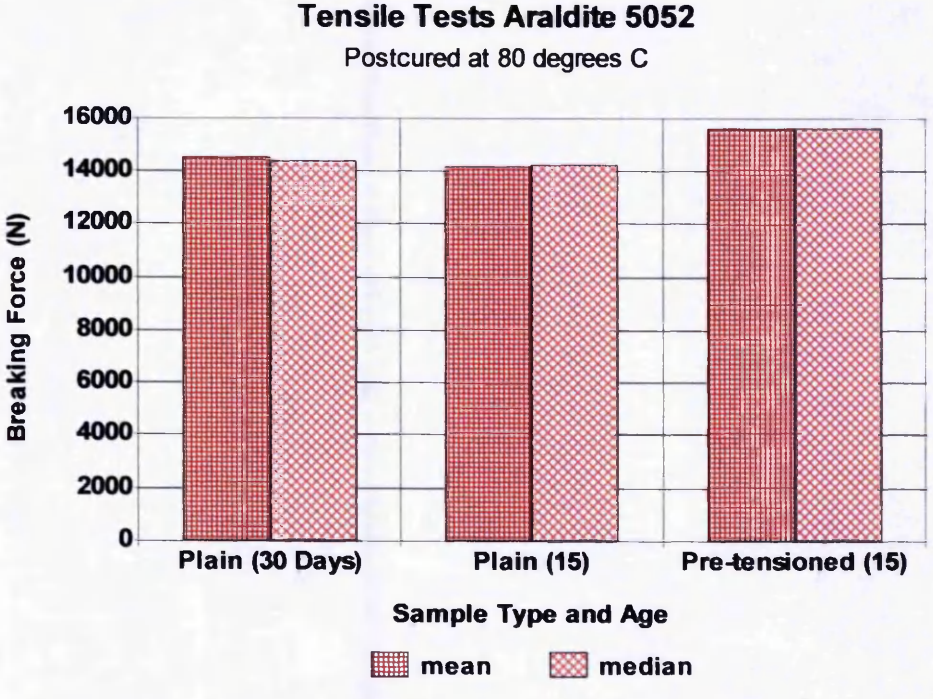

Figure (9.7) Tensile Test Results Samples Postcured at 80°C

9.5 Observations

It must be noted that traditional dog bone samples are widely accepted as being more reliable i.e. fewer rejected samples. Nevertheless, the dog bone sample type was simply not practical for the purposes of this project. The need to test samples taken from the mould with no machining or polishing is essential if the benefits of mechanical pre-stressing are to be isolated and appreciated. Considerable time and effort has been spent obtaining the most suitable geometry for the tensile testing of samples. This standard geometry has been applied to all of the samples tested in the results given. Time has also been spent choosing a suitable bonding agent. The application of the bonding agent has also proved critical and has led to the rejection of thick and uneven samples.

9.5.1 Polyester Resin C - Appendix 3

The results obtained using the standard test sample fitted with tapered end-pieces or tabs are not dissimilar to results obtained by Abderrazzaq [122], who used standard dog bone samples.

9.5.2 Epoxy CT1200 - Appendix 2

Results obtained are not dissimilar to the manufacturer's given data.

9.5.3 Epoxy Araldite® 5052 - Appendix 6 & Appendix 7

From December 1997 on, all production was concentrated on the epoxy Araldite® 5052 resin samples. The use of 5052 allowed the production of Pre-stressed samples without the use of an oven. Results are encouraging and the inclusion of the HPFY alone increases the strength of the resin samples. Of particular note are the results obtained from testing failed Pre-stressed Quad samples, shown in **Table (9.7)**. Here the yarn had failed and hence no load was present during the cure/postcure cycle yet the results are inkeeping with the other Quad samples.

Table (9.7) Failed Pre-stressed Quads

Full Results in Appendix 6

Number Tested - 8	Valid Results - **3**		
mean		**37.9MPa**	**9090 N**
median		*35.9MPa*	*8620 N*

9.5.3.1 Tested After 30 Days

The results show that the inclusion of yarn in a resin sample has more than just an additive effect on the mechanical strength of the sample. Using a Plain sample as a benchmark, the strength of a yarn embedded sample is equivalent to a Plain sample plus the sum of the included yarns, e.g. 8250 N + (250 N x 4 yarn bundles) = 9250 N (Pre-stressed sample 9305 N). Clearly the yarn permits the production of a thinner Pre-stressed Quad (20kg) sample with the equivalent tensile strength of a Plain sample (10mm wide). Conversely, to produce a Plain sample with the equivalent strength of the Pre-stressed Quad (20kg) sample (10mm wide), the Plain sample would have to be 12.8% thicker, e.g. 11.3mm wide, this would in turn make it 12.8% heavier.

9.5.3.2 Tested After 15 Weeks

Samples tested after 15 weeks (105 days) showed less than a 10% increase in strength compared with samples tested after 30 days.

9.5.3.3 Postcured at Elevated Temperatures

Elevated postcured samples almost double in strength. This is due to the improved percentage curing, which is confirmed by the increased glass transition temperature, as shown in ***Chapter 7*** **Table (7.3).**

9.6 Increasing the Number of Fibres

The tensile test composite samples (double or quad) are made using continuous fibres, all parallel to the sample axis, in the resin matrix. When tensile forces are applied to the composite samples, each element in the composite has a share of the applied force. Thus

$$\textbf{Total force = forces on fibres + force on resin matrix} \tag{9-4}$$

However, since stress = force/area then the force on the fibres is equal to the product of the stress σ_f on the fibres and their total cross-sectional area A_f. Likewise, the force

on the matrix is equal to the product of the stress σ_m on the matrix and its cross-sectional area A_m. Hence [123]

$$\textbf{Total force} = \sigma_f A_f + \sigma_m A_m \qquad (9\text{-}4)$$

The equation above is used to obtain the value of the force on the fibres.

Substituting in the mean result for a pre-tensioned quad sample:

$$\textbf{Total force} = 9445 \text{ N}$$

then taking the force on the resin to be the mean result for a plain sample:

$$\sigma_m A_m = 8250 \text{ N}$$

(Note that the area taken up by fibre is negligible compared to the resin.)

gives:

$$9445 \text{ N} = \sigma_f A_f + 8250 \text{ N}$$

therefore (force on fibres)

$$\sigma_f A_f = 1195 \text{ N}$$

where

$A_f = \pi r^2 \times 4000$ (filaments – 4 yarn bundles) $= \pi(6\mu m)^2 \times 4000 = 0.452\mu m^2$

gives

$$\sigma_f = \frac{1195 \text{ N}}{0.452\mu m^2}$$

(Tensile strength of fibres) $\sigma_f = \mathbf{2.65GPa}$

According to [66] $\sigma_f = 2.9GPa$

Hence a double sample should have a total force of

$$\text{Total force} = 2.65GPa \times 0.226\mu m^2 + 8250 \text{ N}$$

$$\text{Total force} = 600 \text{ N} + 8250 \text{ N}$$

$$\textbf{Total force = 8850 N (Test Result = 8980 N)}$$

Total Tensile Strength = 37MPa (Test Result = 37.4MPa)

This is futher supported by the results from the samples postcured at 80°C.

Total force (Pre-tensioned Quad) = Total force (Plain) + 1200N

Total force (Quad) = 14400N + 1200N

= 15600N (Test Result = 15660N)

Total Strength = 65MPa (Test Result = 65.5MPa)

Hence it is speculated that 8 yarn bundles in a sample would give:

	RT postcure	(80°C Postcure)
Total force = 2.65GPa x 905ηm^2	+ 8250 N	(14400 N)
Total force = 2400 N	+ 8250 N	(14400 N)
Total force	**= 10650 N**	**(16800 N)**
Total Tensile Strength	= 44MPa	(70MPa)

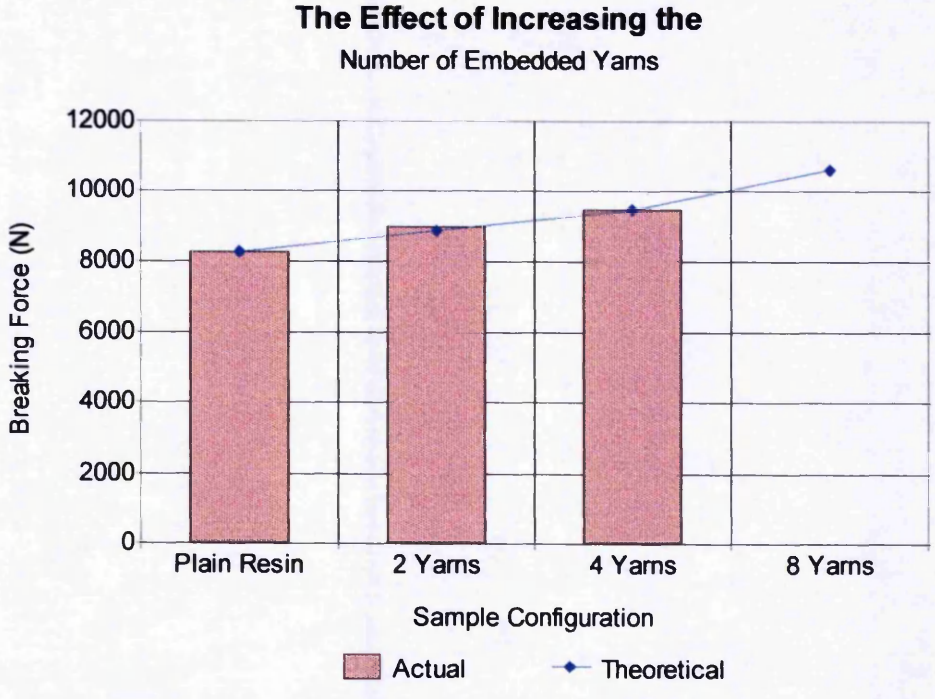

Figure (9.8) The Effect of Increasing the Number of Embedded Yarns

Therefore it is reasonable to conclude that increasing the number of embedded yarn bundles within the resin matrix would increase the tensile strength of the sample. It is expected that this increase would be linear due to the characteristics of the aramid fibres e.g. Twaron 1001, as illustrated in **Figure (9.8)** which shows the actual results compared with theorectical values (RT postcured).

9.7 Summary

Chapter 9 has described the mechanical testing that was carried out to establish the effects and potential benefits of yarn inclusion in the resin matrix. Mechanical testing of resins is covered under the BSi standard BS 2782. The traditional dog bone sample (Method 320C) was not found to be practical for the purposes of this project. Instead Method 320E, which is applicable to the testing of fibre reinforced materials, was identified as a more suitable configuration.

This sample configuration required end-pieces to be fitted to each end of the sample. A suitable cold setting epoxide adhesive was sourced to act as the bonding agent. The standard 90° end-piece geometry was shown to cause premature failure of the samples within the grip area of the test piece. Considerable work was therefore involved in establishing a suitable geometry for the end-pieces and the work is described in this Chapter. It was found that the fitting of 30° inverted tapered end-pieces gave reliable and consistent results, with the samples failing in the gauge length of the test piece. The tapering of end-pieces is outlined in ASTM D3039. This standard makes several stipulations in respect of sample configuration and bondlines in order to reduce stress concentrations at the test piece/machine grip interface.

The ASTM standard referred to in this Chapter also incorporates a failure mode code, which is a characterisation system for the comparison of failed samples. All tensile tested samples in this project were characterised as valid or invalid by means of this code. All tests carried out on Araldite® 5052 standard size samples, fitted with inverted 30° taper end-pieces, were carried out at a rate of 1mm/min. Results from Resin C and Araldite® CT1200 samples prepared in the same manner have shown the

validity of this procedure. Statistical analysis of each category of sample is also provided through the mean and median values.

Results obtained in Chapter 9 show that the inclusion of yarn in the resin matrix increases the tensile strength of the sample. It can also be seen that there is a linear relationship between the increase in tensile strength and the number of yarns embedded in the resin matrix. This makes it possible to reduce the thickness of electrical insulation systems, which potentially gives rise to important benefits, namely lighter structures and improved heat dissipation, enabling equipment to operate at higher loads. Both of these benefits could lead to reduced costs and improved efficiency. These potential benefits, whilst not the main objectives of this research are, nonetheless, significant by products. In *Chapter 10* the capacity for pre-stressed electrical insulation to increase the lifetime of insulation systems is examined. Electrical tree tests are performed on identically prepared samples of the same dimensions of those used for tensile testing.

CHAPTER 10

Electrical Tree Testing

10.0 Electrical Treeing

In this project the purpose of electrical tree testing is to observe the electrical breakdown process in plain and yarn embedded samples, comparing the effects on the lifetime of the samples. Of particular importance is the observation of the effects of the inclusion of HPFY under differing mechanical stresses in the yarn embedded samples.

10.1 Pin-plane Samples

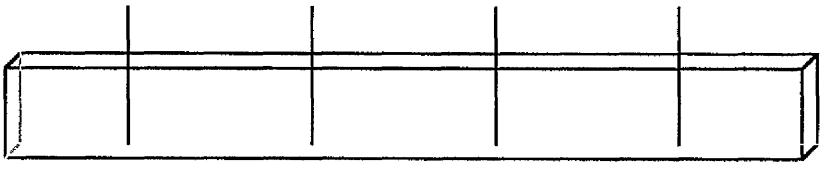

Figure (10.1) Plain Pin Sample Containing Four Needles

A standard size for the test samples was finalised in the first year; this meant that there was sufficient spacing for seven needles to be cast into one Sample at a time. However, as each needle would create a stress field of its own, it was decided to cast in only four needles as in **Figure (10.1)**. In this way each needle block has a space equal to one block between it and the next needle block as in **Figure (10.2)**, essentially creating a stress free zone. This was in keeping with spacing in specimens developed previously by Arbab & Auckland [6,30] for their study of treeing, and consists of pin electrodes in clear resin blocks measuring 25 mm x 25 mm x 10 mm dimensions similar to those given in BSi DD ENV 61072 :1995 [124]. Unlike other specimens developed previously they were ready for use, no polishing or machining takes place as this would introduce alien stresses into the samples, in particular those containing fibre yarns.

This *'ready to use'* property was only made possible due to the high quality samples produced in the addition cure silicone rubber moulds.

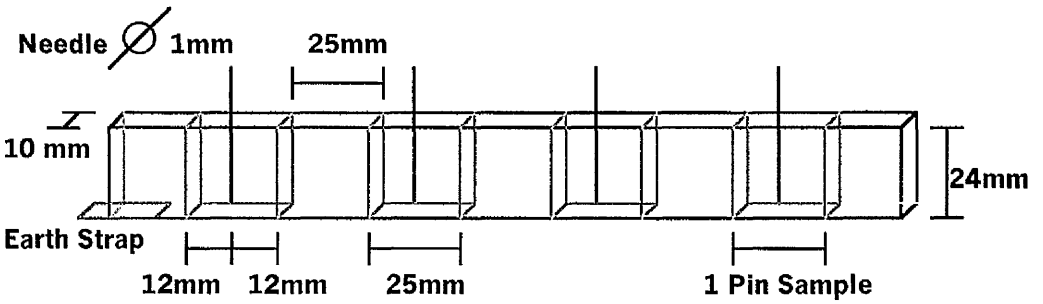

Figure (10.2) Pin Sample Containing Four Needles Shown in Individual Blocks

After postcuring, the yarn embedded pin samples could then undergo analysis by Raman Spectroscopy. Finally, before electrical tree testing could take place, the base of the sample was painted with RS Electrically Conductive Paint [125]. This provided a silver-loaded (56% silver content) coating designed to make a highly conductive path. The paint is used to make electrical connections to non-solderable surfaces such as resin. A metal foil earth strap was attached to the painted base of the pin-sample while it was still wet, turning it into a pin-plane sample. Samples were ready for use in 30 minutes; each pin is tested in turn, starting with the pin at the opposite end of the sample to the earth strap.

10.2 Types of Needle

Three types of needle were used for electrical treeing testing:

1. Hypodermic
2. Ogura
3. Tungsten

10.2.1 Hypodermic

In the past gramophone needles were used because they were readily available and of a standard shape. The radius of curvature of the tip of these needles is large at 25 +/- 0.5 μm. The results produced using these needles were not consistent. The work of

Arbab & Auckland [6,30] promoted the use of medical hypodermic needles cast into resin for treeing investigation. Although hypodermic needles produce results quickly and easily, they are asymmetric and therefore the radius of curvature of the tip cannot be quantified. In addition to this there are problems regarding resin/electrode adhesion, all of which has led to much debate concerning the reliability of hypodermic needles. Nonetheless, hypodermic needles are the least expensive option. First year results highlighted problems with the silicone coating on the hypodermic needles. Acetone alone is not sufficient to remove this coating, therefore another solution was needed to remove the silicone. Penn-White Limited are silicone specialists and produce a safe and totally effective *'digestant'* which completely removes silicone coatings, leaving surface finishes unaffected. The photographs in **Figure (10.3)** show two hypodermic needles (**needle diameters 1mm**):

(a) with the silicone coating, note the shiny surface.

(b) with the silicone coating removed, note the matt surface.

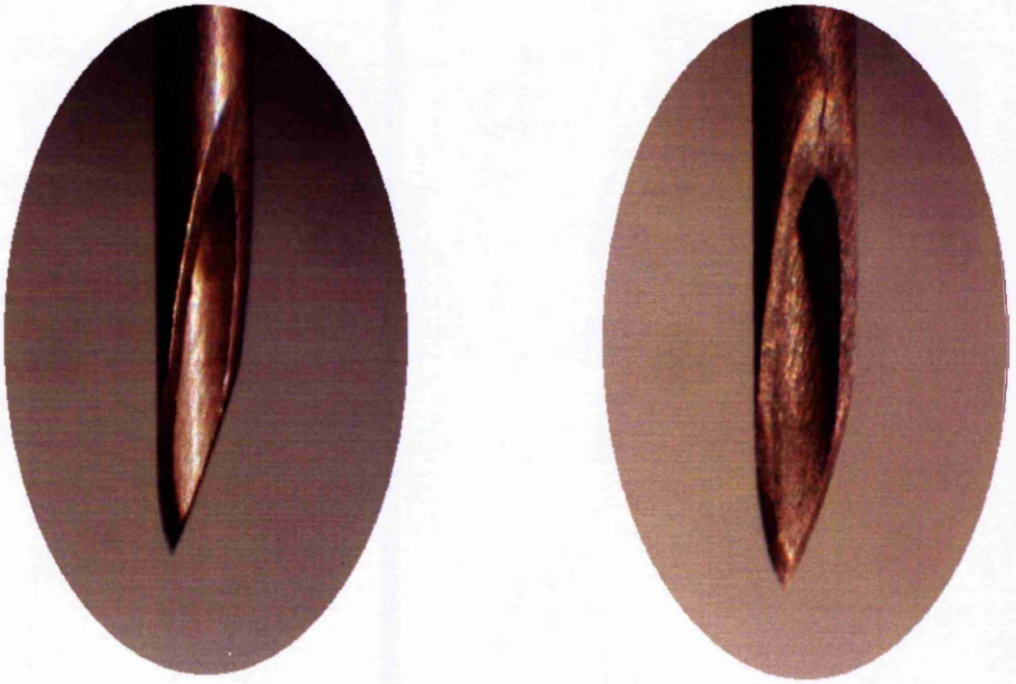

Figure (10.3) Hypodermic Needles

(a) With Silicone Coating **(b) Silicone Coating Removed**

10.2.1.1 Silstrip® NHLO Liquid

Silstrip® NHLO (non-hazardous low-odour) is a dark tan liquid [126], which chemically digests cured and uncured silicone elastomers and polymers, making them solvent rinsable. User-friendly and environmentally benign, the effects of Silstrip® are achieved without the use of flammable, aromatic or halogenated solvents. Silstrip® is specific as it digests silicone only and is suppressed by moisture. Contamination by water or oxygenated solvents affects the ionic state of the Silstrip® solution, preventing its action as a silicone *'digestant'*. Therefore, for the best results, it was vital that the surfaces to be treated were clean and dry. A small glass dish was used to totally immerse the hypodermic needles in the Silstrip® and a lid was fitted to minimise the risk of contamination by airborne moisture. Silstrip® has a low odour, low evaporation, high flash point (of at least 70°C) and it has a minimum rating of hazard classification, see Health and Safety information [127].

From the second year onwards, all the hypodermic needles were left for 72 hours in a bath of Silstrip®. The Silstrip® depolymerises the silicone allowing complete removal of the coating. A gel formed on the surface of the needle, which was wiped clean using acetone. Silstrip® was cleared from the inside of the needle by injecting acetone into the centre using a thinner needle attached to a syringe filled with acetone. To ensure that the needles were being cleaned effectively the Silstrip® solution was renewed at least every two weeks, earlier if the solution became cloudy.

Prior to soaking in a bath of Silstrip® the medical hypodermic needles had their plastic syringe cup, known as a Luer fitting, removed. This was done by melting the cup, using the departments heat gun. Any remaining cup adhesive was then removed using an abrasive sheet. The needle was then placed in one of the needle gantrys, see section 10.3, to ensure that it fitted smoothly into the needle guides. It was important that the needles should slide smoothly in the needle guides because, after the resin has been postcured, the gantry had to be carefully removed from the pin sample to avoid debonding the needles.

10.2.2 Ogura

More reliable results have been obtained from *'treeing needles'* produced in Japan by the Ogura Jewel Company Ltd, as illustrated by Auckland *et al* [128]. These needles are made from 50 mm lengths of 1 mm shank diameter steel (SUS303) wire. The tips are machined in a variety of tip radii (5 μm being the most common), to an accuracy claimed to be 1 μm with a cone angle of 30°, as shown in the photograph in **Figure (10.4)**. These needles have proved to give better adhesion at the resin/electrode interface and consequently produce more consistent results.

Figure (10.4) Ogura Needle

10.2.3 Tungsten

Due to extensive research by the National Grid Company, the development of a superior treeing needle has been achieved by MST (Micro Scientific Techniques). Using their experience gained in the manufacture of diamond record needle tips MST have produced a high quality treeing needle. The needles are manufactured from 38mm lengths of 1mm shank diameter sub-micron particle tungsten carbide wire. The cone angle is first ground, then the electrode undergoes two polishing operations, before a radiusing process generates the tip radius. This is a costly operation as reflected in the price of £8.80 plus VAT per needle. Nevertheless, there is a guaranteed tip radius of 3-5 μm in accuracy at the end of a 30° angle cone, as shown in the photograph in **Figure (10.5)**. Experiments carried out by Champion *et al* [34,100] have demonstrated the reproducibility of results using these needles.

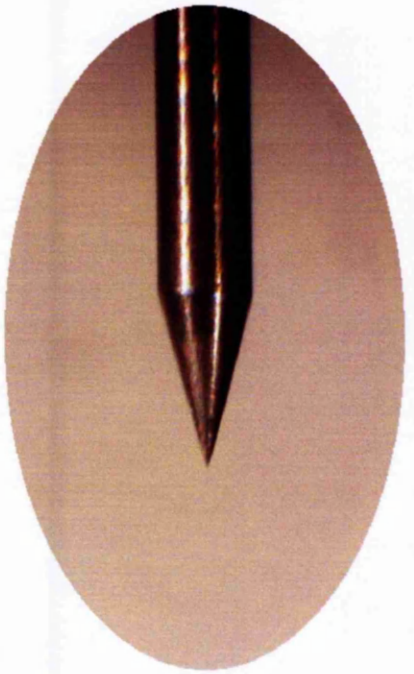

Figure (10.5) Tungsten Needle

To minimise cost all preliminary experimental work has been undertaken using the least expensive hypodermic needles. Once suitable manufacturing methods had been developed, the department's existing stock of Ogura needles was used to obtain further preliminary results. For the statistical results needed to validate research, batches of samples were manufactured using both hypodermic and tungsten needles. These results make a further contribution to the debate over the reliability of data obtained from using hypodermic needles.

10.3 Needle Gantry

To hold the needles in place when casting the resin samples it was necessary to manufacture a needle gantry. Not only does the gantry hold the needles in place during the resin production process but it also allows for accurate needle positioning. The gantry is made of PTFE which does not bond itself to the pin sample. Using the top face of the high quality Silastic moulds as a reference point, the depth of the mould (which is the height of the sample) is 24mm. In the plain resin samples therefore, if the needle length from pin tip to gantry base was set to 22mm, a consistent 2mm gap between pin and plane would result. This could easily be checked with a powerful fibreoptic dentist's tooth light, shining through the translucent Silastic T-1 moulds.

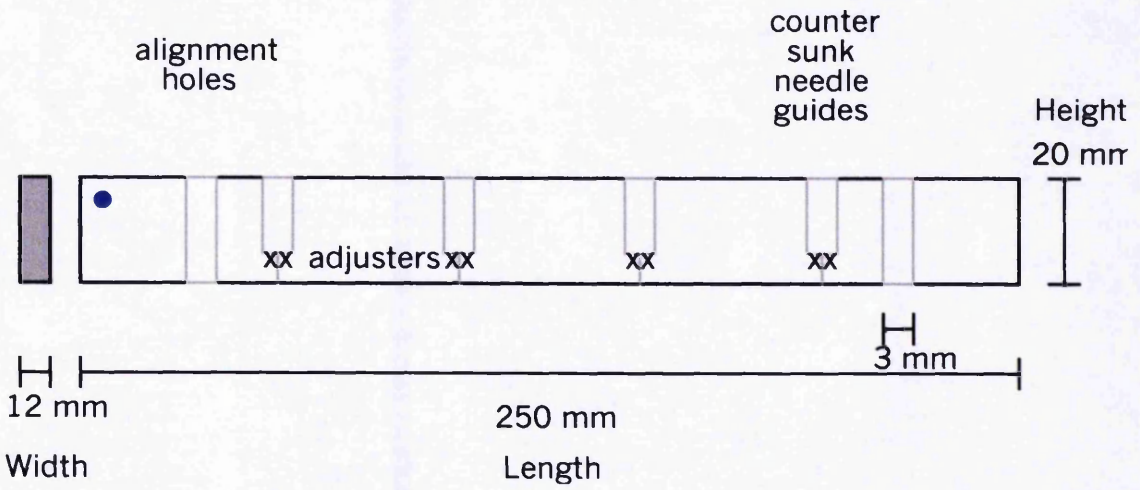

Figure (10.6) Front View of PTFE Needle Gantry

A front view of the needle gantry in **Figure (10.6)** shows the countersunk needle guides with the screw adjusters holding the needles in position. The small blue dot in the top left hand corner denotes the machined straight edge for alignment with the edge of the mould. Alignment holes were added to the gantries for the yarn samples, this enabled the needle tips to be accurately positioned between the yarns with the assistance of the tooth light. It was also found that the inclusion of air gap spacers (1.5mm washers), one at each end of the mould, eliminated the trapping of air bubbles on the top of the samples (needles then set to 23½mm). All of the needles were again cleaned using cotton wool soaked in acetone. The needle was held at the top and drawn across the cotton wool down the needle shaft to the tip, so as not to damage the tip, prior to inserting it into the gantry.

10.3.1 Needle Spacing

The introduction of the needle gantry positioning frames meant that, once a needle gantry had been centrally aligned to a frame, the opaque moulds (Silastic S & E) could be used without any further adjustments. The pin-plane positioning dimensions for Plain samples are illustrated in **Figure (10.7)**, Pre-stressed samples in **Figure (10.8)** and Pre-tensioned samples in **Figure (10.9)**.

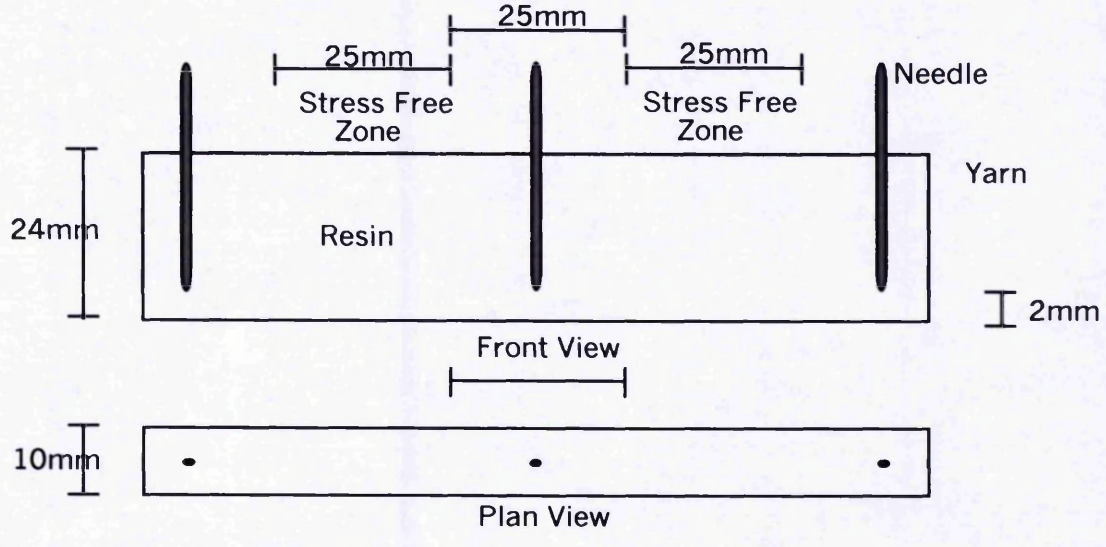

Figure (10.7) Plain Pin Sample Positioning Dimensions

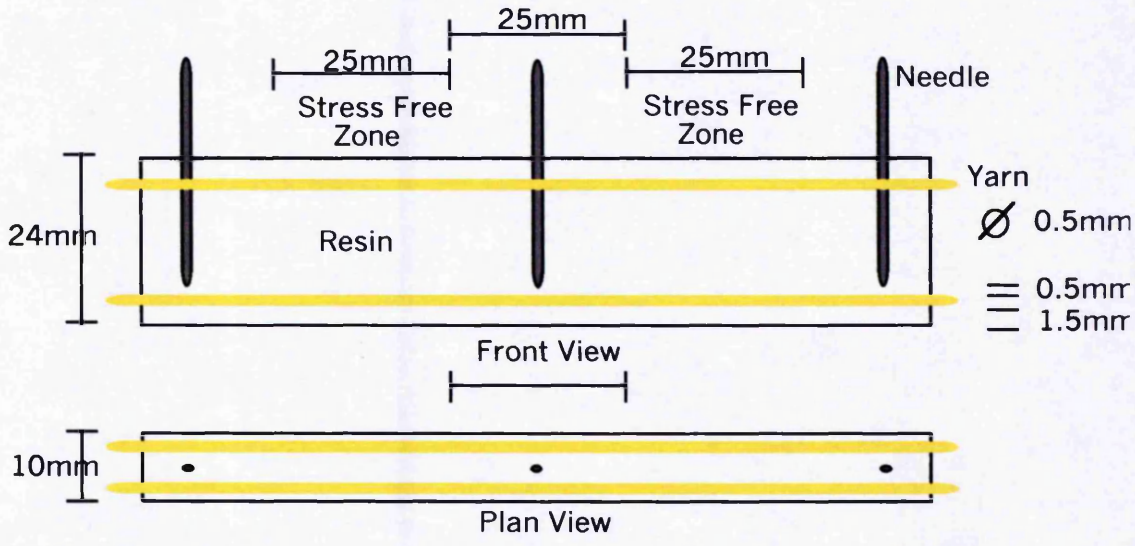

Figure (10.8) Pre-stressed Pin Sample Positioning Dimensions

Although the yarn holes are cast into the mould to allow the yarn to sit 2mm above the base of the sample, loading the quad samples causes the yarn to sit lower in the mould. In pre-tensioned samples the yarn diameter is 0.7mm, reducing to 0.5mm in the pre-stressed samples because of their higher loading. The pin distance is the same for both pre-tensioned and pre-stressed samples, the difference being in the spacing between pin to yarn and yarn to plane as shown in **Figure (10.9)** for a pre-tensioned sample.

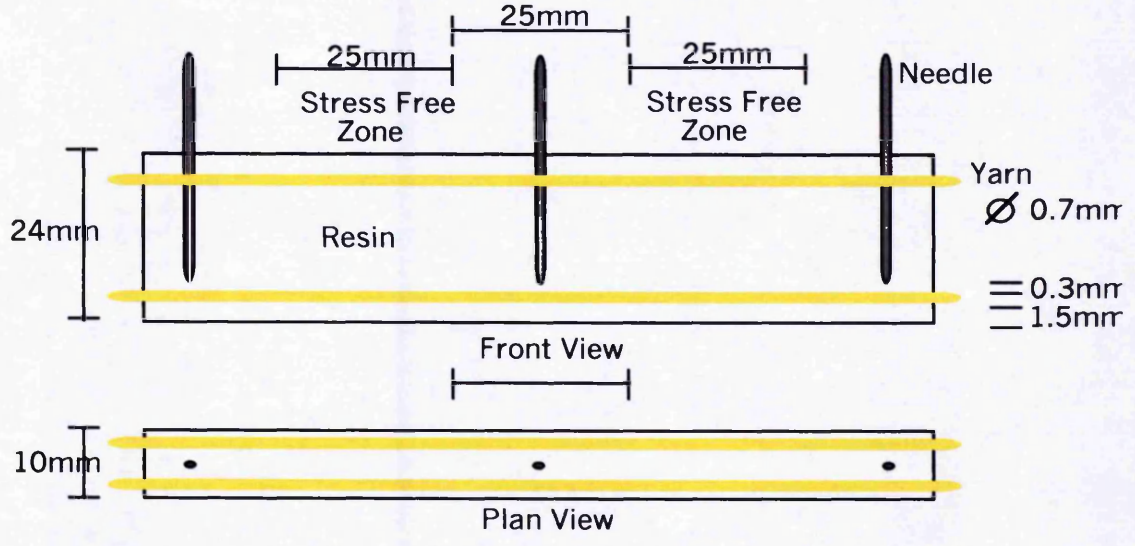

Figure (10.9) Pre-tensioned Pin Sample Positioning Dimensions

10.3.2 Depth & Central Alignment of Needles

The needle depth was controlled by mounting the needle gantry, complete with needles, into a gantry holder constructed from Meccano®, as shown in the photograph in **Figure (10.10)**. Each end of the gantry was held in place by pairs of parallel brackets fixed 1mm above the base plate. A ruler was then inserted between the gantry and the base plate. By standing over the holder and looking down onto the ruler under the pin tip, the needles could be set accurately to the required length depending on the type of sample being made. Once the needles were at the correct length the adjusters could be tightened to hold them in place. Again great care was taken not to touch the delicate pin tips. The central alignment of the needles in the respective samples was controlled by the use of needle gantry positioning frames as discussed in *Chapter 8, section 8.8.*

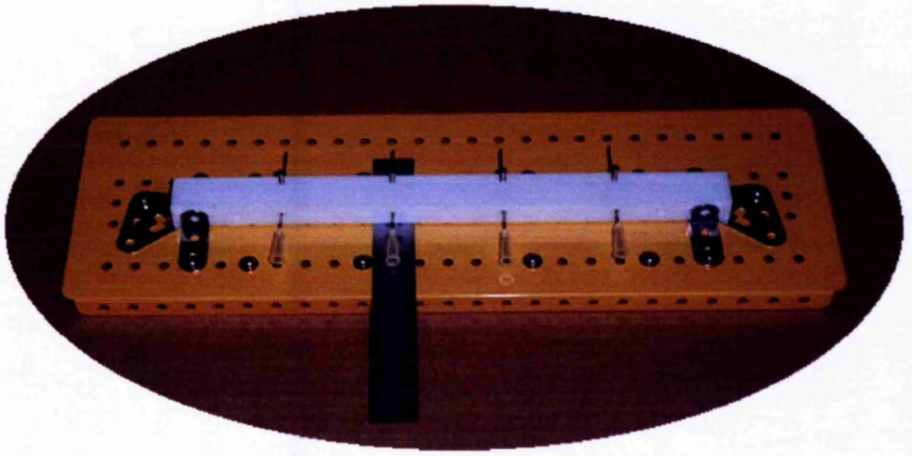

Figure (10.10) Needle Gantry Holder

10.4 Test Equipment

Electrical tree testing facilities are available in the department. These are housed in a separate room within the main high voltage laboratory. Two identically equipped high voltage cages were prepared for testing. Each cage consists of a 1.5kVA single phase step up transformer which has a range of 0-30kV_{rms} from its secondary winding. A mains supply of 240V_{rms} at a frequency of 50Hz is connected to the primary of the transformer via a variac and earth leakage trip switch circuit breaker. The switch is set to *'trip out'* at 30mA in approximately 30ms, this allows the failsafe operation of test equipment when the pin-plane samples break down. The switch is mounted on a panel above the cage next to the illuminated power switch. This switch also activates the timer for test duration monitoring and the large red warning lights outside the room and main laboratory to show tests in progress. A simplified circuit of the high voltage supply is illustrated in **Figure (10.11)**.

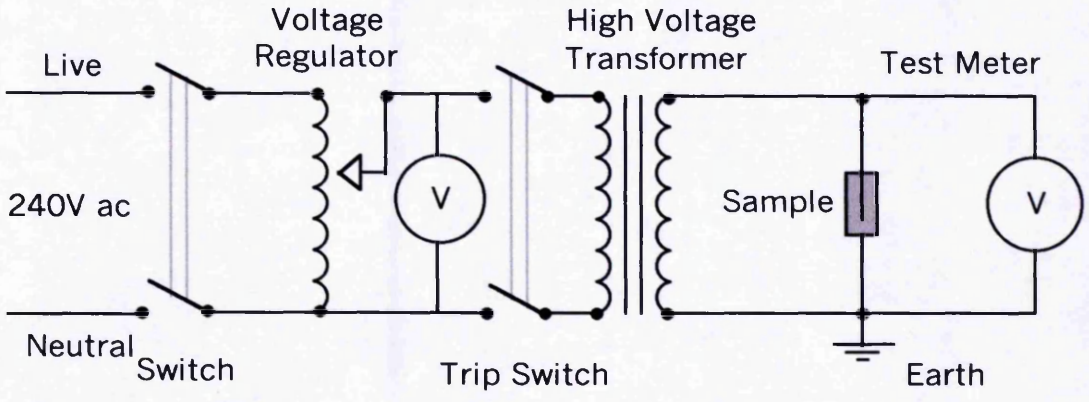

Figure (10.11) High Voltage Testing Circuit

In order to monitor tree growth, two free standing observation trolleys have been constructed by the department, one trolley can be seen in the photograph in **Figure (10.12)**. An x-y positioning device with an Olympus SZ-30 microscope (x30) with phototube attachment for the connecting of an Olympus OM-4Ti camera is fitted to each trolley. The camera has a Winder 2 motor drive which is controlled by an M. Quartz Remote Controller 1 with an electronic timer. This permits the unmanned observation of the samples. Options include single or sequential shooting and preset time lapse pictures. Data imprinting is possible using the Recordata Back 4 camera backs, allowing day, month and year or hour and minute imprinting. These are useful features when calculating initiation, propagation and breakdown times of the various samples.

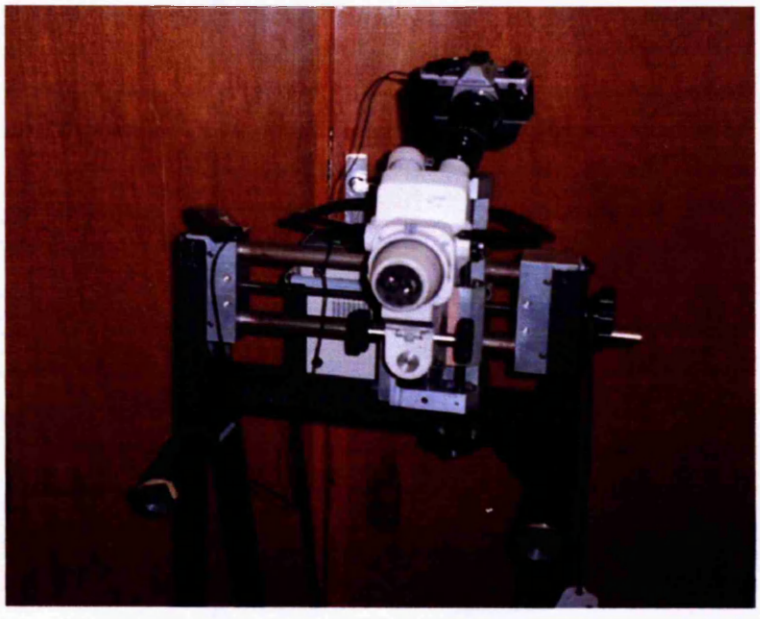

Figure (10.12) Observation Trolley

Representative sets of photographs can be seen in *Appendices 10 and 11*, see notes in section 10.9. Samples were illuminated using fibreoptic light boxes (Olympus Highlight 1000), it should be noted that one of these light boxes had a green filter.

10.5 Testing of Araldite 5052 Samples

The initial pin samples made using Araldite® Epoxy 5052 were embedded with Ogura needles. These were produced in the existing Silastic-S moulds and, although reasonably clear to the naked eye, were very grainy through the camera lens. It was possible to remove this grain effect by polishing the sample, but this would introduce alien stresses into the samples. It was therefore decided to polish the metal die in the former and produce new moulds. All of the Hypodermic and Tungsten needle samples were produced from the new moulds. The resulting pin samples were very clear and photographed well.

All of the samples were subjected to a voltage of $10kV_{rms}$ at a frequency of 50Hz, this was in keeping with previous work carried out in the department for example, Auckland *et al* [128]. Each cage was set using a high voltage meter and checked before each test, at which point the timer was reset. Samples were mounted onto stands for observation by the cameras. After connecting the high voltage leads the power was switched on and the cameras were activated using the remote control. This was programmed to take a single shot every 30 minutes (or 1 hour) until the film ran out. If, during the tests, the camera failed, and missed the initiation, it meant that only breakdown times were recorded and so the results were discarded. Overall results obtained from camera observations can be found in **Tables 10.1 to 10.3** and show the results of a specific sample type using different needles. Whereas the full results given in **Appendices 8 & 9** are presented showing the results of a specific type of needle embedded into the different sample types.

The full results shown in the *Appendices 8 & 9* are split into three colums. Column one records the sample number, the date of its postcure and the date the test started. Column two shows the times recorded from switching on the power supply to significant points in tree development. The first significant development in tree growth is its time to **initiate**. The next most significant stage is the time it takes to grow from the needle tip to the base of the sample, namely the time it takes to **propagate**. Finally, the third stage shows the **overall breakdown** time. Column three isolates the propagation and breakdown times by removing the initiation period, the initiation of

the tree becomes time zero, this highlights the benefits of mechanically pre-stressing electrical insulation.

Initially pin samples were left to age for 30 days after postcuring before testing commenced. For a period of two days before testing, the pin-plane samples were left to condition in the testing room atmosphere. Note that all of the results for Hypodermic needles shown in the following Tables and Appendices relate to needles with the silicone coating removed, as detailed in section 10.2.1.1.

10.5.1 Plain Samples – (Full Results in Appendix 8)

Table 10.1 Plain Samples

Type of Needle	Number Tested	Time to Propagate (hours)	Time to Breakdown (hours)
Hypodermic	**4**		
mean		**1**	**3.95**
median		*1*	*4.15*
Ogura	**8**		
mean		**1**	**2.48**
median		*1*	*2.2*
Tungsten	**8**		
mean		**1**	**4.86**
median		*1*	*5.15*

NB - Breakdown results (IN BRACKETS) in the tables that follow.

In some samples the breakdown time exceeded 100 hours, so a second set of breakdown results is given in brackets for comparison purposes. The 100 hour sample results have been removed from the mean and median breakdown results, for full results see the appropriate Appendix.

10.5.2 Pre-tensioned Samples 2.25kg – (Full Results in Appendix 8)

Table 10.2 Pre-tensioned Samples

Needle Type	Number Tested	Time to Propagate (hours)	Time to Breakdown (hours)	
Hypodermic	**4**			
mean		**1**	**20.9**	
median		*1*	*20.4*	
Ogura	**8**			
mean		**1**	**14.53**	
median		*1*	*14.45*	
Tungsten	**8**			**(NO 0.2.4)**
mean		**1**	**49.77**	**(31.84)**
median		*1*	*28*	*(26.2)*

10.5.3 Pre-stressed Samples 20kg – (Full Results in Appendix 8)

Table 10.3 Pre-stressed Samples

Type of Needle	Number Tested	Time to Propagate (hours)	Time to Breakdown (hours)	
Hypodermic	**4**			
mean		**2.5**	**48.8**	
median		*2.5*	*47.5*	
Ogura	**8**			
mean		**1.44**	**11.68**	
median		*1.25*	*11.5*	
Tungsten	**20**			**(NO 4.2.2)**
mean		**2.64**	**30.44**	**(23.17)**
median		*2.5*	*17.15*	*(16.3)*

10.6 Observations from 30 Day Samples

Removing the silicone coating from the surface of the hypodermic needles led to a more consistent set of results. This confirmed that the silicone was inhibiting

resin/electrode interfacial bonding. This suggests that the future use of hypodermic needles for preliminary testing is reliable provided that the silicone coating has been removed. Therefore, hypodermic needles provide a relatively inexpensive method of electrical tree testing for preliminary investigations. The photographs in **Appendix 10**, see section 10.9, show that, not only is the needle asymmetrical, but also that the trees growing from hypodermic needles are themselves asymmetrical.

10.6.1 Plain Vs Quad Samples

Visually there is a significant difference in the treeing area in Plain and Quad samples. The typical treeing area in a Plain sample is shown in **Figure (10.13)**. For comparison, **Figure (10.14)** shows a typical treeing area in a Quad sample, where it can be seen that the tree does not grow outside the boundary set by the yarn. The tree in a Quad sample is very fine and bushy in appearance. It is important to remember that the yarn does not form a physical barrier like those used by Auckland *et al* [41,43], where the needle tip was screened from the base of the sample. In the Quad samples the pin tip has an open path to the base. Nonetheless in the Pre-stressed samples the yarn does produce a mechanical barrier in the form of compressive stress.

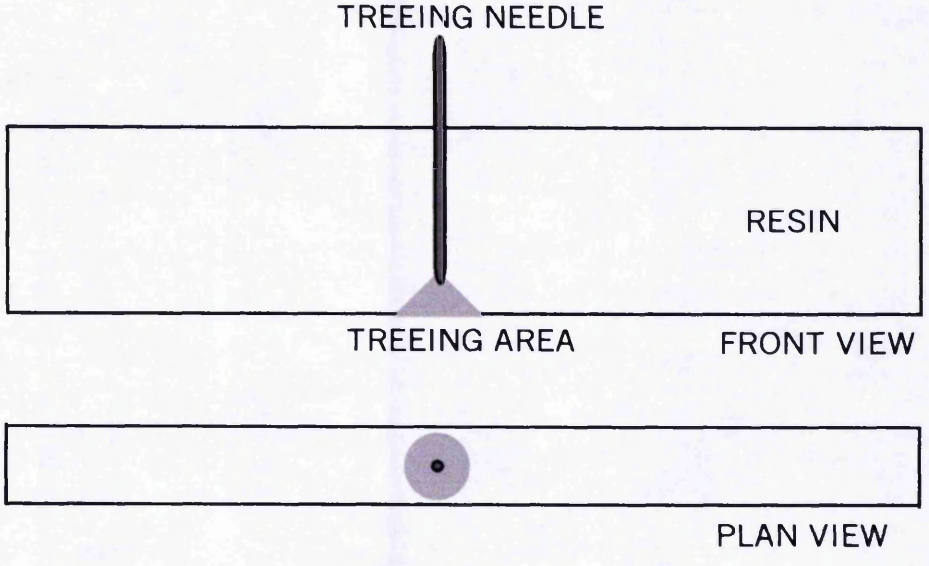

Figure (10.13) Typical Treeing Area in a Plain Sample

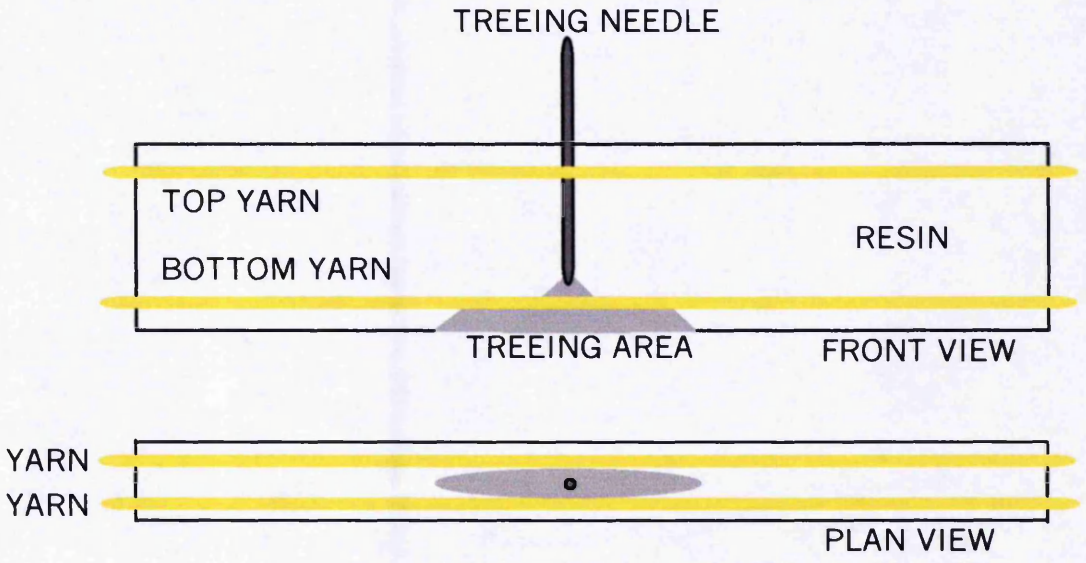

Figure (10.14) Typical Treeing Area in a Quad Sample

It is clear that Pre-stressing the Quad samples does prolong the time taken for the tree to grow from pin tip to the base of the sample, namely the propagation time, as shown in the graph in **Figure (10.15)**. Yarn inclusion also prolongs the time to breakdown (from initiation), see the graph in **Figure (10.16)**. This conclusion was reinforced as the trend is replicated for each needle type.

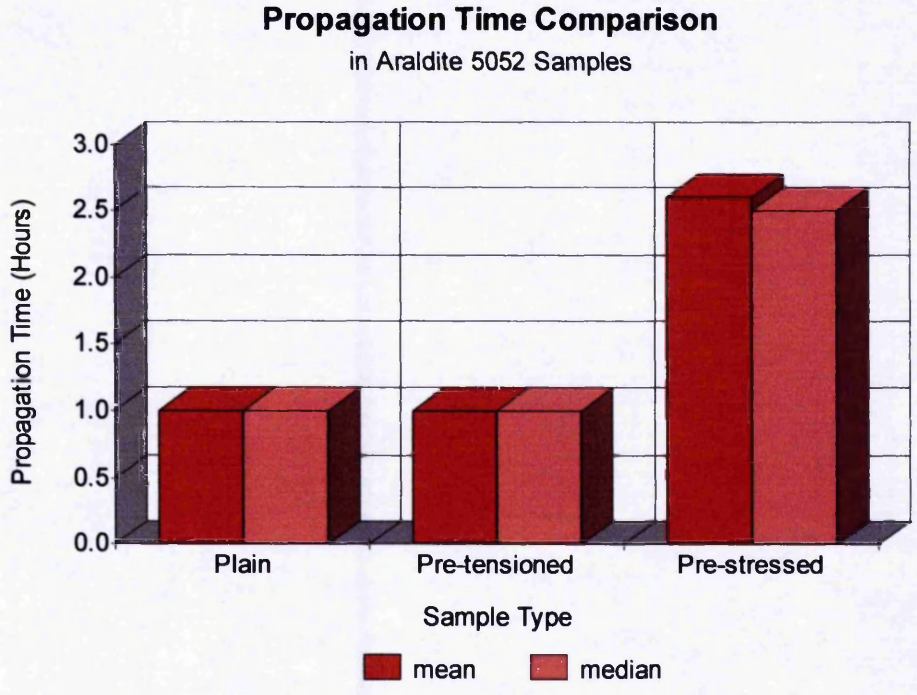

Figure (10.15) Propagation Time Comparison (Tungsten Needles)

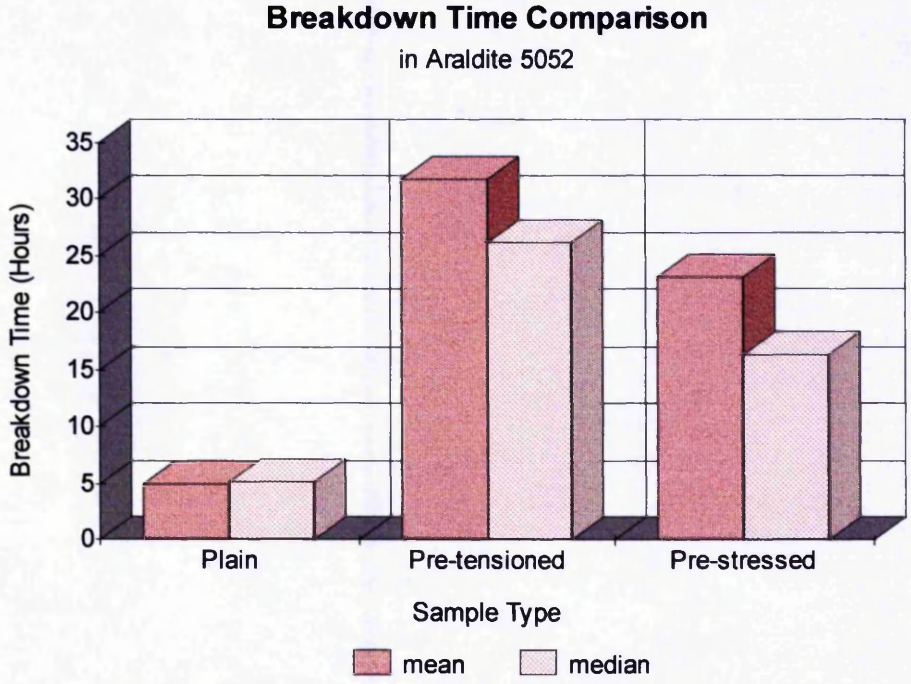

Figure (10.16) Breakdown Time Comparison (Tungsten Needles)

10.6.2 The Return-failure Process

It is widely accepted that a tree can fully bridge the electrode gap without breakdown occuring. This is because the diameter of the tree channels is too small to sustain a discharge, the air trapped in the channels has a higher breakdown strength than the surrounding resin. To sustain a discharge the channel needs to broaden out before the air will allow breakdown to take place. Usually breakdown follows within a few minutes or hours, as seen in the plain samples. Photographs show that branches thicken from the ground plane up. This is called the '*return-failure*' process and is considered to take place quite quickly, as observed by Cooper *et al* [129]. However in the Quad samples this return-failure process has slowed down quite significantly and the overall time to breakdown has increased by at least 5 times compared to plain samples. A typical 30 Day Quad sample return-failure is shown in the photographs in **Figure (10.17)**. Starting from the completion of the propagation stage in photograph (a) the branches start to thicken from the ground plane back up to the pin tip.

Figure (10.17) The Return-failure Process in a Quad Sample

(a) Propagation has been completed

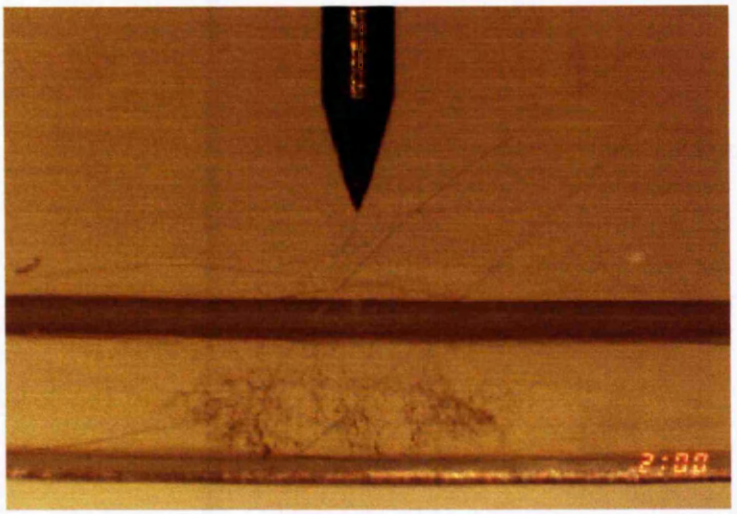

(b) 1 Hour after Propagation completed

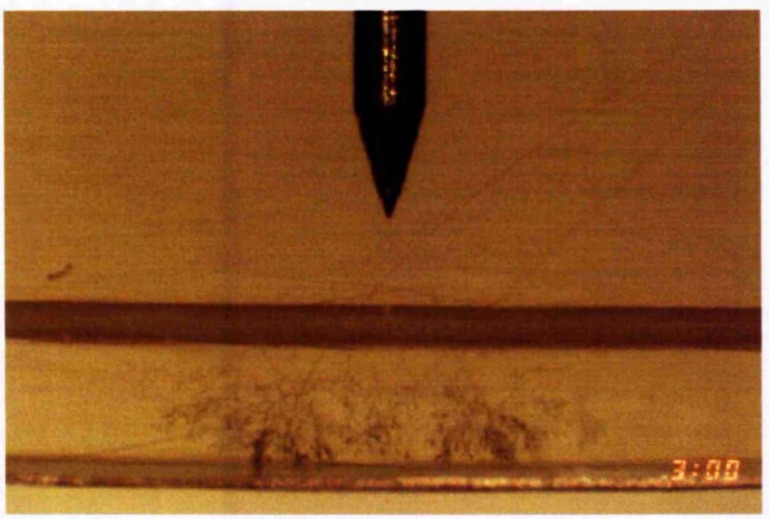

(c) 6 Hours after Propagation completed

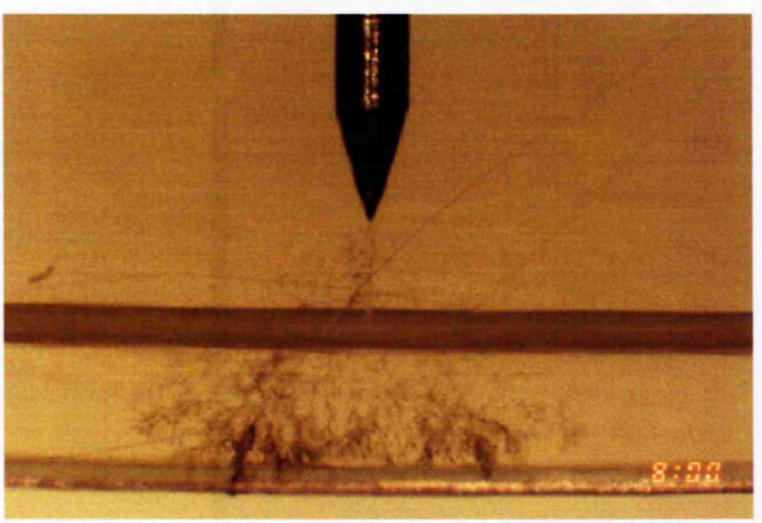

(d) 11 Hours after Propagation completed

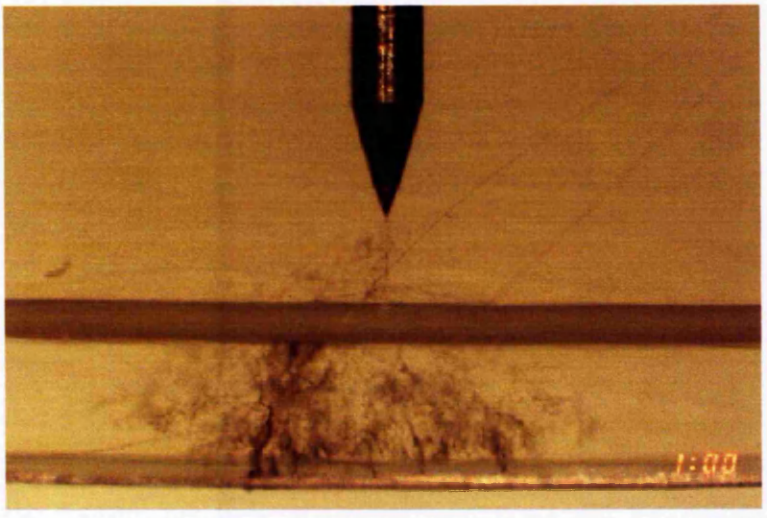

(e) 23 Hours after Propagation completed

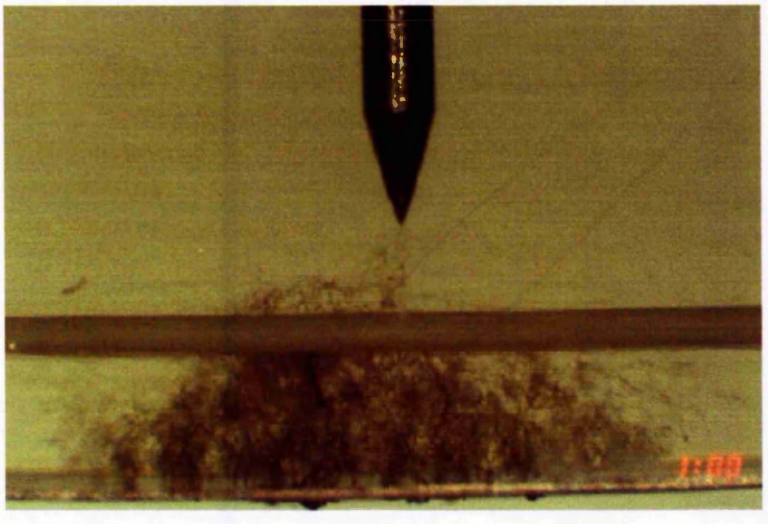

(f) 35 Hours after Propagation completed

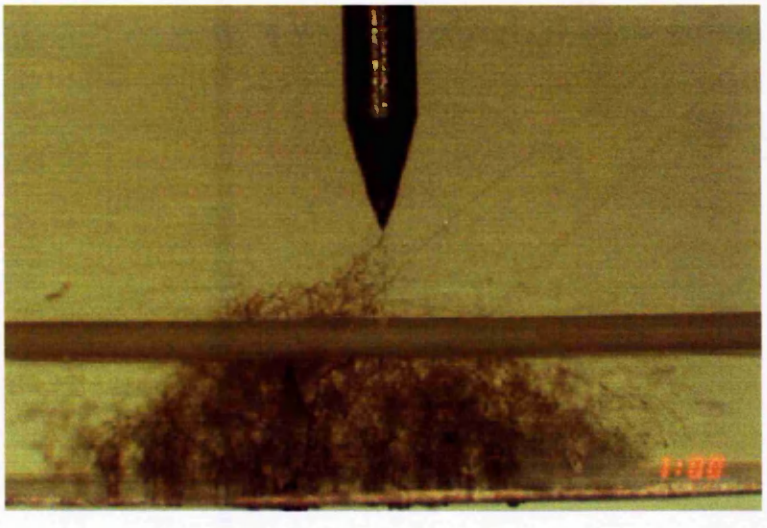

It should be noted that photographs (e) and (f) were taken from a second roll of film. Photographs (b), (c), (d), (e) and (f) show the progress of the return-failure process which eventually leds to breakdown 37.1 hours after propagation has been completed (40.1 hours after the start of initiation). Although the Quad sample in the photographs is pre-stressed, visually and in terms of time, there is little or no difference in the return-failure process shown here from that of a pre-tensioned sample. The difference in a pre-stressed and pre-tensioned sample shows up in the **propagation times**. The Quad sample shown in **Figure (10.17)** is Pre-Stressed with a Tungsten needle, batch number **1.1** Needle number **3** (Photo set **PST11N3**), see *Appendix 8*.

10.6.3 Pre-stressed Samples

A closer examination of the Pre-stressed Tungsten pin sample results revealed that there is a further comparison to be made. If the results are split into short initiation times (less than 50 hours) and long initiation times (more than 50 hours) there is a further improvement in the propagation time as seen in **Table 10.4** and **Figure (10.18)**.

Table 10.4 Pre-stressed Tungsten Samples – A Further Comparison

Type of Sample	Number Tested	Time to Propagate (hours)	Time to Breakdown (hours)	
Short Initiation Time (<50 hours)				
Tungsten	**7**			**(NO 4.2.2)**
mean		**2.14**	**37.1**	**(22.47)**
median		*2*	*18*	*(17.15)*
Long Initiation Time (>50 hours)				
Tungsten	**7**			
mean		**3.14**	**23.7**	
median		*3*	*16.2*	
Full Results				
Tungsten	**14**			**(NO 4.2.2)**
mean		**2.6**	**30.44**	**(23.17)**
median		*2.5*	*17.15*	*(16.3)*

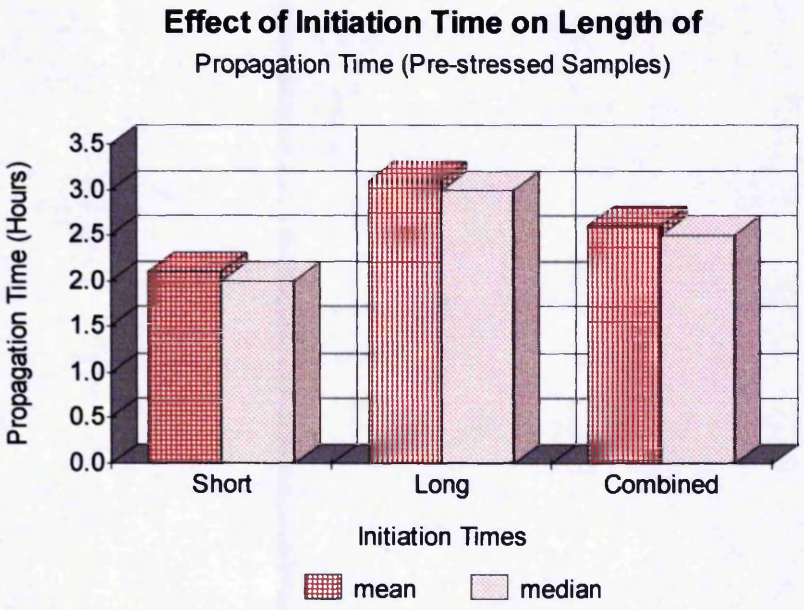

Figure (10.18) Propagation Time Comparison (Pre-stressed Samples)

This difference in initiation times is attributed to possible debonding of the needles during Raman analysis, needles could have been knocked when fitting the pin sample into the microscope stand, nevertheless the propagation time is still longer than for plain or pre-tensioned samples and overall the time to breakdown remains consistent for both types of pre-stressed samples. It is speculated that the increased propagation time seen in samples with long initiation times could be attributed to the continuous water absorption by the resin matrix. Raman analysis in *Chapter 6* has shown that water absorption increases the level of pre-stress in the sample, this increases the compressive stress within the resin matrix during testing. The water absorption evaluation carried out in *Chapter 7* confirmed that water absorption is a continuous process in Araldite® 5052 samples. This raised the question of whether or not older 5052 resin samples would exhibit slower treeing times.

10.7 Testing Older Samples

A selection of pin samples were left untested from the 30 Day Test Schedule and were approximately 9 Months Old. Raman analysis showed that the pre-tensioned samples were now lightly pre-stressed and that the pre-stressed samples had increased levels of pre-stress by nearly 50%, due to the resin matrix swelling. These pin samples were now tested in the same manner as the 30 Day samples for comparison.

10.7.1 Hypodermic Pin Sample Results – (Full Results in Appendix 9)

Table 10.5 Older Hypodermic Samples

Type of Sample	Number Tested	Time to Propagate (hours)	Time to Breakdown (hours)
PLAIN	**4**		
mean		**5.5**	**7.73**
median		*5.5*	*7.15*
PRE-TENSIONED	**4**		
mean		**7.78**	**66.28**
median		*7.25*	*47.85*
(NO 0.2.3)			
mean		**(6.83)**	**(45.73)**
median		***(7)***	***(44.70)***
PRE-STRESSED	**4**		
mean		**9.13**	**45**
median		*9*	*45.45*

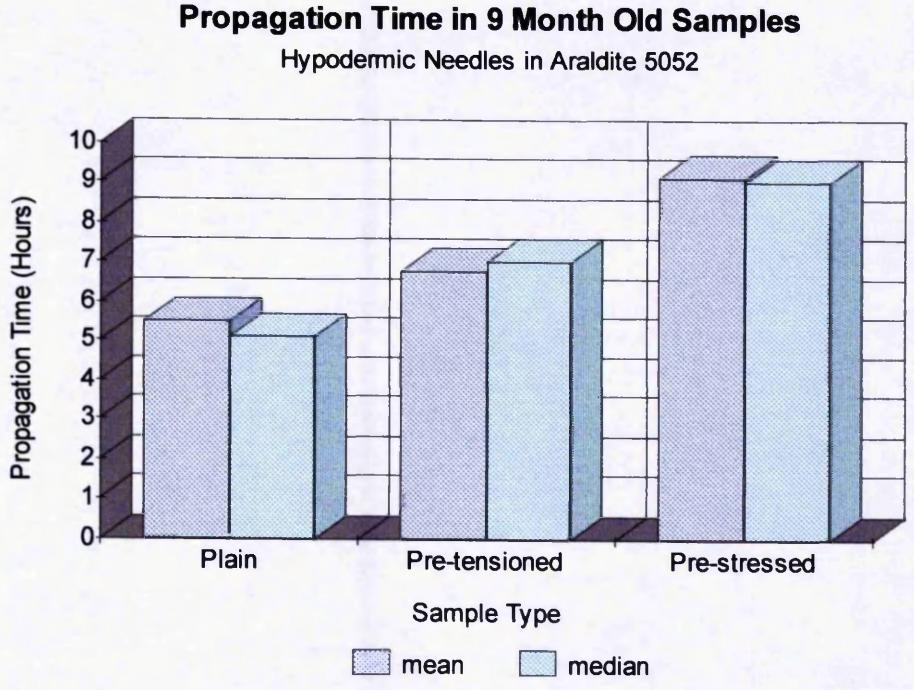

Figure (10.19) Propagation Time in 9 Month Old Hypodermic Samples

10.7.2 Tungsten Pin Sample Results – (Full Results in Appendix 9)

Table 10.6 OlderTungsten Samples

Type of Sample	Number Tested	Time to Propagate (hours)	Time to Breakdown (hours)
PLAIN	**4**		
mean		**4.9**	**6.28**
median		*4.3*	*6.1*
PRE-TENSIONED	**2**		
mean		**5**	**37.4**
median		5	37.4
PRE-STRESSED	**1**		
mean		**8.1**	**34.5**
median		8.1	34.5

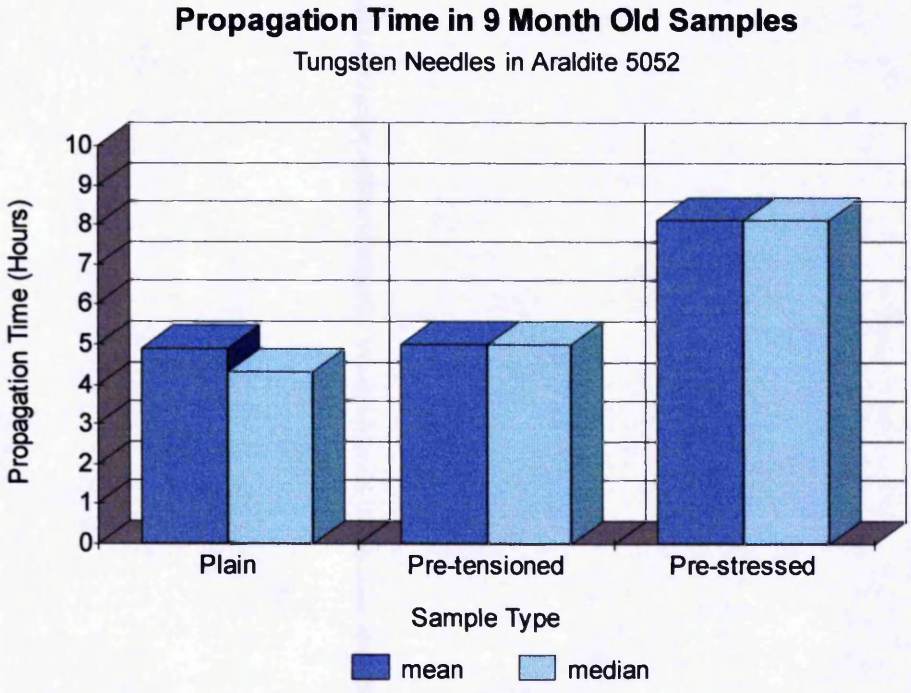

Figure (10.20) Propagation Time in 9 Month Old Tungsten Samples

10.8 Observations from 9 Month Samples

The effect of water absorption on the resin matrix has retarded the treeing process in all types of sample. This is supported by the findings of Champion *et al* [106] when producing plain samples using Araldite® CY1300. He reported that *'the ingress of moisture was acting as a barrier to tree growth'*, a phenomenon also seen by Cooper [130]. When this process occurs in the Quad samples, resin swelling increases the level of pre-stress and produces an even greater retardation in the propagation time. The development of the Heavy Duty Stress Bed will permit the manufacture of pre-stressed samples at higher loads thus the benefits of higher levels of pre-stress could be utilised from the time of manufacture and would be further enhanced by the aging process.

More recent work by Champion *et al* [131] has made a further assessment of the effects of externally applied mechanical stress and water absorption (sample-swelling) on electrical tree growth. The percentage mass uptake of water in CY1300 plain samples is shown to be similar to the percentage mass uptake seen by the author in 5052 plain samples immersed in water at ambient temperature. It was found that these resins have similar hydroxyl group concentrations, 0.35mol kg^{-1} and 0.18mol kg^{-1} [132] respectively uncured. This is in keeping with Champion's suggestion that hydroxyl group concentrations affect water absorption levels.. An increase in the propagation time of plain samples has also been observed by Champion although he applied **external** mechanical stresses to his samples **after postcure**.

All of the pre-stressed samples produced for this project have an integral mechanical stress by the end of the postcure cycle. This mechanical stress has been quantified and is compressive in nature, unlike previous work into the mechanical aspects of treeing where the evidence has been inconclusive, as pointed out by David *et al* [133]. Furthermore this compressive stress is uniform as no bending is evident in the samples. NO external mechanical stress has been applied to any of the electrical tree tested samples used in this project. Raman analysis has demonstrated that the internal stress levels (level of pre-stress) after postcure are identical for samples produced using the same level of pre-loading ie 20kg gives a consistent Raman bandshift of -2.0cm^{-1}.

The results show that although water absorption can have a significant effect on the plain sample propagation time, the breakdown time does not improve noticeably. It is clear from the results that pre-stressing does significantly improve both the propagation and the breakdown times; here water absorption only improves the propagation time. Pre-tensioned samples demonstrate that yarn inclusion greatly extends the time to breakdown. Water absorption then serves not only to improve the propagation time but also causes the yarn to become pre-stressed. This two fold effect would account for the enhanced propagation time when compared with plain samples. The intial tree tests after 30 Days give identical propagation times for plain and pre-tensioned samples, whereas after 9 Months the pre-tensioned samples exhibit longer propagation times. Nevertheless there is no significant improvement in the breakdown time. Futhermore the plain samples break down much more quickly than pre-tensioned samples even after water absorption has taken place. This demonstrates that the mechanical pre-stressing of the resin matrix makes a greater contribution to the tree retadation process than the effect of water absorption. This is not to say that water absorption has no part to play, moreover water absorption investigations must form part of any future work if the benefits of mechanically pre-stressing are to be validated.

10.9 Electrical Treeing Photographs

Appendices 10 and 11 contain representative sets of photographs of pin samples with hypodermic needles and tungsten needles respectively. These photographs show the treeing process from initiation through to breakdown. The times indicated in the bottom right hand corner record the actual time (am or pm) the photographs were taken, not the duration times. The duration times are given above each photograph, firstly the time elapsed after "power on" and, secondly, the time elapsed after tree initiation, with an indication of the treeing stage taking place.

Photographs of plain and pre-tensioned samples were taken from the 9 month schedule in order to show more detail. For a typical set of photographs for a 30 day plain sample see *Chapter 1* **Figure 1.1** in which the sample initiates, propagates and breaks down in a very short time period, providing very little detail. By contrast, the pre-stressed photographs were taken from the 30 day schedule, providing ample detail. The 30 day pre-tensioned samples have the same initiation to propagation

characteristics as the plain samples, but have the return-failure characteristics of the pre-stressed samples.

The photographs are typical of all the valid electrical treeing result photograph sets that show the start of tree initiation, propagation to the base of the sample and the return-failure stage leading to breakdown. It was found that, by leaving the camera remote control directly in front of the test cage, sample breakdown triggered the remote control to take a picture and switch off. As a consequence of this, the times recorded on the breakdown pictures are out of sequence with the other photographs. In some instances the flash of the breakdown discharge was actually captured on film, as can be seen in the photographs in **Figure (10.21).**

Figure (10.21) BREAKDOWN Triggers Camera

Timer set to 1 hour intervals

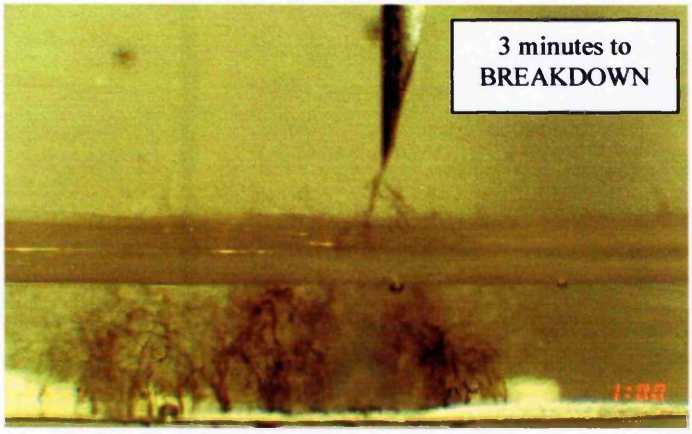

BREAKDOWN triggers camera

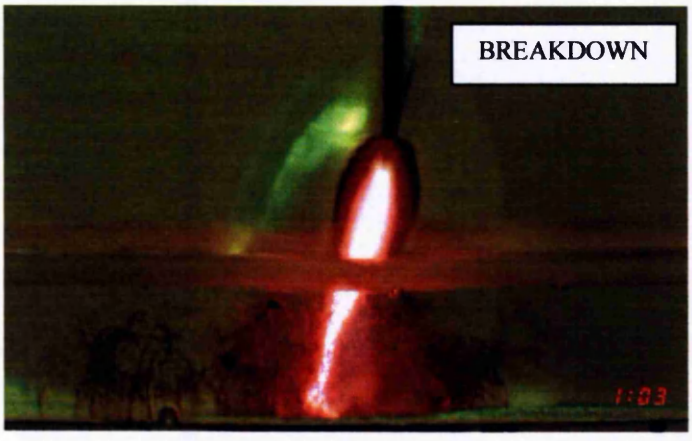

Pre-Tensioned Hypodermic, Batch No. 02, Needle No. 2 – Photo set **PTH02N2**
Taken from 9 Month Schedule – see full results in *Appendix 9.*

10.10 Summary

The work described in this Chapter is a key part of the research into the Mechanical Prestressing of Electrical Insulation. Electrical tree testing was performed to observe the breakdown process in plain and yarn embedded samples and to compare the effects of this on the lifetime of the samples. In order to show the full potential of mechanically pre-stressed electrical insulation it was essential to investigate the three distinct sample configurations namely Plain, Pre-tensioned and Pre-stressed.

The size of sample had already been determined in *Chapter 8,* giving the potential for inclusion of more than four needles. Nevertheless, it was decided that, because each needle creates its own stress field, that each sample would contain only four needles, thus creating a stress-free zone between each needle. The needle spacings were in keeping with previous work carried out by the Department. However, unlike previous specimens, they were ready to use with no machining or polishing to ensure that the samples were free of alien stresses.

Initially three types of needle were considered, two of which were used for the final statistical analysis. Mass produced Hypodermic needles were the least expensive but produced unreliable results. This was partly caused by the silicone coating on the needles and was to some extent overcome by the use of a silicone digestant that removed this coating, producing more consistent results. Secondly, high quality Tungsten needles were used. These were the most expensive, but gave reproducible results.

A needle gantry was designed to hold the needles in place and to control the height and position of the needles. This was used in conjunction with the needle gantry positioning frames discussed in *Chapter 8.* In order to set up the needle gantry it was placed in a specially constructed holder to ensure that needles were fixed accurately. The modular approach meant that each sample type had its own set of equipment.

The Electrical tree testing carried out in Chapter 10 was in keeping with previous work in the Department in respect of test equipment and test conditions. All samples were

subjected to a voltage of $10kV_{rms}$ at a frequency of 50Hz. All tests were monitored by use of a time lapse camera and critical time periods were noted. Test samples were left for two days prior to testing in order to condition them in testing room atmosphere. Statistical analysis results show mean and median values for comparison.

The comparison between plain and yarn embedded samples outlined in this Chapter shows that the treeing area is different for plain and quad samples. In plain samples the tree grows around the area of the needle whereas in the quad samples the tree grows within the boundary set by the yarn. It is important to remember that the yarn does not form a physical barrier, that is to say that the tree has an open path from the pin tip to the base. In pre-stressed samples the yarn produces a mechanical barrier in the form of compressive stress, which has been quantified by Raman analysis. Pre-stressing the yarn extends the propagation time and yarn inclusion prolongs the time to breakdown, as seen by the significant increase in the return-failure time. This conclusion is reinforced as the trend is replicated for each type of needle.

In general pre-stressed samples with long initiation times show a further improvement in the retardation of the propagation time. Raman analysis of older samples showed increased levels of pre-stress in all quad samples. Tree testing of these older samples showed an increased propagation time, in all types of sample. This increase in the propagation time is attributed to water absorption swelling the resin matrix. Nevertheless, the arguments presented in Chapter 10 have shown that the mechanical influence of pre-stressing has a greater impact on increasing the life of resin samples and this impact is in fact enhanced by the aging effects of water absorption.

Chapter 11

Discussion & Conclusion

11.0 Background

This research has focused on the mechanical aspects of treeing, although this is not to suggest that treeing is exclusively a mechanical phenomenon. Clearly treeing is an electrical phenomenon: no volts – no trees. Nonetheless this project has demonstrated the mechanical influence on tree propagation and the potential to retard tree growth by utilising the inherent mechanical properties of composite insulation.

The diverse and original nature of the work carried out in this project has meant that each stage of the research has had an impact upon other aspects of the work. For this reason, the findings of each chapter have been summarised and discussed at the end of that particular chapter. This final Chapter therefore discusses and presents the key findings from the investigation as a whole and draws conclusions about the implications of these findings for the *Mechanical Prestressing of Electrical Insulation*.

11.1 Introduction

The main objectives of this research project were defined in Chapter 1 section 1.1:

- To increase the lifetime of electrical insulation, by improving the resistance of composite insulation to the growth of electrical trees.
- To utilise the inherent mechanical properties of composite materials, by inducing compressive stresses into composite insulation.
- To cast high performance fibre yarns (HPFY) that have been tensioned (hence pre-stressed) within a resin matrix

The theoretical result of this tensioning operation would be the production of a self-balancing system of internal stresses, tensile stresses in the fibre yarn and compressive stresses in the resin matrix, similar to the mechanism employed in the pre-stressing of concrete, leading to improved treeing resistance in composite insulation.

In order to achieve these objectives it was essential to investigate three distinct sample configurations. These were as follows: plain resin samples to observe the characteristics of the resin matrix in isolation, which provided the baseline for comparisons with yarn embedded samples; pre-tensioned samples to observe the effects of embedding yarn in the resin matrix, which provided a baseline for comparison with mechanically pre-stressed samples and finally, pre-stressed samples to observe the effects of pre-stressing the fibres in yarn embedded samples.

11.2 Literature Review

The effects of internal mechanical stress appeared to play a pivotal role in the treeing process. Examination of previous work in Chapter 2, especially where the mechanical effects had been isolated, showed it was possible to produce increased treeing resistance in polymeric materials using a controlled region of compressive stress. The objectives proposed to cast a high performance fibre yarn into the resin matrix to produce this region of compressive stress. Furthermore the casting of a high modulus fibre into a low modulus resin matrix would in theory also result in enhanced mechanical strength.

11.3 Polymers and Yarns

The Department knew little about yarns prior to this project, so it was necessary to identify the fundamental properties of polymers and yarns. This enabled the author to determine a set of criteria for selection of suitable HPFYs. In addition to standard yarns, the commercial availability of enhanced adhesion yarns was also investigated. Samples of the most suitable HPFYs were then acquired and analysed.

11.4 Yarn Analysis

Analysis of the selected yarn samples was carried out to determine the actual working parameters for analysis against manufacturer's data. A methodical approach to the checking process of the yarns required mechanical testing, linear density tests and surface energy tests to be performed. The process narrowed down the choice of yarn for the project. It also identified yarn deficiencies in their susceptibility to filament damage, irregular shape of yarn filaments and patchy distribution of surface coatings. It became good practice to check newly acquired yarn to ensure compatibility of results. The process finally resulted in the selection of Sample No. 10 the Aramid fibre yarn Twaron® 1001 with its high strength and high surface energy value. It also highlighted the susceptibility of aramid fibres to UV degradation, potential failure caused by shock loading and tendency of yarn to exhibit creep.

11.5 Aramid Fibre

A detailed review of aramid fibres highlighted that these yarns have highly ordered crystalline structure, which explains why they are very strong under tensile stress. However under compressive stress kink banding occurs leading to premature failure and hence this must be avoided.

The importance of the bond angle is key. This is especially important under load when bond stretching produces changes in molecular vibration. This can be used to monitor and quantify the internal stress levels via Raman spectroscopy.

11.6 Raman Spectroscopy

The ability to monitor the internal stress levels within the yarn embedded samples without destroying them was of vital importance to validating the research. It had originally been envisaged that the internal state of the resin matrix would be analysed using the Department's circular polariscope. However the polariscope only indicates the presence of strain and cannot be used to measure or quantify it as being tensile or

compressive. The polariscope presents a two dimensional image of a three dimensional sample, ignoring the integration effects of the sample thickness, thereby making it inaccurate. Other traditional test methods were known to destroy the samples and hence were unsuitable.

Non-destructive Raman Spectroscopy was introduced by the author to measure the internal stress levels in samples. It is a reliable and accurate method of measuring axial fibre strain in HPFY embedded in a resin matrix. In particular the $1610cm^{-1}$ Raman waveband has a strain dependent shift in relation to aramid fibres. This bandshift phenomenon had a significant impact on the project and led directly to changes in sample design and choice of resin.

Consistent quality samples were produced and the results from one week old RT postcured samples demonstrated a linear relationship between applied load and the negative Raman bandshift (yarn in tension) in pre-stressed samples, as discussed in Varlow and Malkin [134,135]. Pre-tensioned samples of the same age showed no bandshift (yarn in equilibrium). On the other hand, pre-tensioned samples that had been postcured at elevated temperatures exhibited a positive Raman bandshift (yarn in compression) due to increased resin shrinkage.

A stress/strain calibration was carried out to evaluate the internal mechanical stress levels present, calculated using the force/balance equation for axial radial stress in a continuous fibre embedded in a resin matrix that shrinks. This mechanical stress has been quantified and is compressive in nature. The compressive stress must be uniform, as there was no evidence of bending in quad samples. This was in keeping with the initial theory, which proposed that the tensioning operation would produce a self-balancing system of internal stresses (as seen with prestressed concrete).

Aging, as indicated by increased levels of pre-stress, was initially attributed to the effect of water absorption swelling the resin matrix. This sample-swelling effect meant that pre-tensioned samples became pre-stressed, showing negative bandshifts.

At the end of the project the manufacture of elevated temperature postcured pre-stressed samples (20kg per level) showed that pre-stress was retained but at a reduced level (reduced by 33%).

The research identified several factors that adversely affect Raman readings when comparing a yarn sample in air (on a microscope slide) with yarn embedded in a resin matrix. Firstly, if the Raman laser is out of alignment it will distort the Raman reading. Secondly, the age of the yarn on the microscope slide, due to the effects of; **a.)** UV light on the exposed yarn and; **b.)** water absorption by the epoxy coating, both of which will alter the differential reading. Finally the age of the yarn embedded sample, due to water absorption swelling the resin matrix, will increase the differential reading. It was found that, using a fresh RT postcured 20kg pre-stressed sample (less than 8 weeks old) as a benchmark, in conjunction with yarn taken from the same section of yarn (therefore comparing like with like), resulted in a consistent Raman bandshift reading of $-2cm^{-1}$ ($\pm 0.2cm^{-1}$). This eliminates these adverse effects and ensures reliable results for comparison with the older samples.

11.7 Resin

The selection of resins was initially in keeping with previous work in the Department. However Raman analysis identified problems relating to sample design and resin shrinkage. The introduction of symmetrical yarn samples eliminated the effect of sample bending yet the effects of resin shrinkage remained. This led the author to develop *'the criteria for pre-stress'*, which proposed that in order to obtain pre-stress, the strain in the yarn must exceed strain in the resin (shrinkage). This highlighted the two critical factors, firstly the coefficients of linear expansion and secondly the temperature fall following cure/postcure cycles. The temperature fall had the most significant impact on shrinkage. The selection of the cold cure epoxy resin Araldite® 5052 eliminated the temperature fall (giving very little resin shrinkage) and led to the successful manufacture of the first pre-stressed sample at RT.

Unfortunately RT postcured samples, with a Tg of 65°C, have a safe operating temperature of only 40°C. The safe operating temperature of the resin matrix was limited by the Tg value, therefore the Tg needed to be raised. Preliminary experiments with heat-cycling RT postcured samples were unsuccessful. Fortunately it is possible to postcure 5052 at elevated temperatures, which increases the Tg.

A re-examination of initial resin choices showed Resin C to have maximum obtainable Tg of only 53.4°C ±1°C, as shown by Cooper [95], therefore making it unsuitable for production of high-temperature test insulation samples. On the other hand CT1200 has a maximum obtainable Tg of 130°C, as stated by Ciba Polymers [136], hence could be considered suitable for manufacture of samples for testing at high-temperatures.

A selection of plain samples was manufactured and postcured at different temperatures. Some of these samples were used to investigate the effects of the postcure temperature on the Tg. This confirmed that increasing the postcure temperature increases the Tg within limits, although the results from these Tg tests were below the manufacturer's data. Subsequent consultations with the manufacturer revealed that the overall percentage postcure was in line with the manufacturer's estimates for a given postcure cycle. The remaining samples were used to observe the effects of aging. This evaluation confirmed that there was a continuous uptake of moisture in the samples, thereby confirming the results of the Raman analysis, which showed a steady increase in pre-stress levels. This phenomenon has also been observed in other research, which has showed that water absorption continues until the relative humidity of the sample reaches equilibrium with its surrounding environment.

In order to manufacture pre-stressed samples at elevated temperatures it was necessary to design and build a heavy duty stress bed. This finally led to the successful production of a pre-stressed sample with a realistic working temperature of around 100°C (Tg 113°C).

11.8 Sample Design

A systematic modular approach was adopted from the start, which gave maximum flexibility to the development of the project. The sample configuration was a compromise between the requirements of Raman analysis, tensile testing, electrical tree testing and the size of the production apparatus itself. From the outset of the project it had always been the intention to produce identical samples for all of the tests, thus comparing like with like.

The author initiated the use of Meccano® as a prototyping tool. An initial model of a stress bed that would fit into the oven was built and this determined the size of mould, hence the standard sample size. The new moulding materials were chosen as they would yield reproducible quality samples that required no machining, polishing or mould release agents. Moulds were cast from a former designed in a modular and flexible style allowing for the production of plain, single yarn and multiple yarn samples from the same former.

The manufacture of single yarn samples was abandoned due to findings of the Raman analysis. Instead symmetrical yarn samples were produced, which eliminated sample bending. The quad sample configuration allowed production of pin samples. Central alignment of treeing needles was achieved by using the bolt on needle gantry positioning frames.

Quad sample production split into two distinct sample types: pre-tensioned and pre-stressed. The two developments took place concurrently and were mutually beneficial. The author's earlier development of the criteria for pre-stress had highlighted the need for higher loads. This necessitated the development of apparatus with free-standing moulds and also identified the requirement for a heavy duty stress bed. Production of pre-stressed samples began using weights hanging from samples on a Pre-stress Rig. The later development of a heavy duty stress bed gave the potential for greater control over the pre-stressing process, making it possible to manufacture samples at higher loads.

Procedures were established for the manufacture of samples at RT and elevated temperatures. The production of reproducible high quality samples was achieved for all sample types.

11.9 Mechanical Testing

Mechanical testing of the three distinct sample types was carried out in order to establish the effects and potential benefits of yarn inclusion in resin matrix. These tests were based on BSI Standards applicable to the testing of fibre reinforced materials. The sample configuration required the fitting of end-pieces with cold setting epoxide adhesive as the bonding agent. The author established a suitable geometry of 30° inverted tapered end pieces, which gave reliable and consistent results with samples failing in the gauge length of test pieces. This was in keeping with ASTM D3039 in respect of sample configuration and bond lines in order to reduce stress concentrations at the test piece/machine grip interface. It incorporates a failure mode code, a characterisation system for comparison of tested samples. Samples were tested at a rate of 1mm/min and statistical analysis was shown giving the mean and median values.

Inclusion of yarn in the resin matrix increased the strength of samples, showing a linear relationship between the increase in tensile strength and number of yarns embedded in the resin matrix, as outlined in Varlow and Malkin [137]. In theory this makes it possible to reduce the thickness of electrical insulation systems potentially giving rise to important benefits, namely lighter structures and improved heat dissipation, enabling equipment to operate at higher loads. Both of these benefits could lead to reduced costs and improved efficiency.

11.10 Electrical Tree Testing

Electrical tree testing was performed to observe the breakdown process in plain and yarn embedded samples. Again, the identically prepared three distinct sample types were used with the addition of embedded needles. Although the sample size gave the potential for the inclusion of more than four needles, it was decided that, because each needle creates its own stress field, each sample would contain only four needles. Thus a stress free zone was left between each needle and, in addition, pin samples were used with no machining or polishing to ensure that the samples were free of alien stresses.

Initially three types of needle were considered although statistical analysis was carried out using only hypodermic and tungsten needles. Hypodermic needles were used after their silicone coating had been removed giving a good needle/resin bond thus leading to more consistent results. The tungsten needles were more expensive but gave reproducible results. A needle gantry was designed to hold needles in place and to control height and position of needles in conjunction with the needle gantry positioning frames.

Electrical tree testing was in keeping with previous work using the existing equipment and applying the same test conditions namely $10kV_{rms}$ at a frequency of 50Hz. Samples were monitored using a time lapse camera to note the critical time periods. All pin samples were conditioned in the testing room atmosphere prior to testing. Statistical analysis was carried out using the mean and median values for comparison.

Visually the treeing area is different for plain and quad samples. In plain samples the tree grows around the area of the needle, whereas in quad samples the tree grows within the boundary set by the yarn. Nonetheless the yarn does not form a physical barrier, with an open path from pin tip to base. Instead the yarn produces a mechanical barrier in the form of compressive stress, which has been quantified by Raman analysis.

It has been demonstrated that pre-stressing extends propagation time, as presented in Varlow and Malkin [138]. It has also been shown that yarn inclusion prolongs time to breakdown as seen by the significant increase in return-failure time when compared to plain samples. This trend was replicated in each type of needle. Furthermore pre-stressed samples with long initiation times showed further improvement in the retardation of the propagation time.

Raman analysis of older samples showed steadily increasing levels of pre-stress in yarn embedded samples. An increased propagation time was seen in all samples, this was due to water absorption swelling the resin matrix, although the mechanical influence of pre-stressing was shown to have greater impact on increasing the life of resin samples. This was demonstrated in aged pre-tensioned samples, which with age became pre-stressed. Here the propagation time was longer than aged plain samples, whereas one week old pre-tensioned samples had the same propagation time as one week old plain samples.

If the water absorption was the more significant retardation factor surely the water absorption effect would overwhelm the mechanical pre-stressing effect and ALL the aged samples would have the same propagation and breakdown times. Clearly this is not the case, and the impact of the mechanical effect was enhanced by the aging of the samples due to water absorption swelling the resin matrix. Moreover it was shown that not only did pre-stressed samples have a uniform integral mechanical stress by the end of the postcure cycle, but that this was also retained even if the sample was sectioned. This integral mechanical stress improved the treeing resistance of the insulation member even as it aged. Thus fulfilling the first of the original objectives to increase the lifetime of electrical insulation, by improving the resistance of composite insulation to the growth of electrical trees.

11.11 Final Conclusions

The main objectives of this research project as defined in *Chapter 1, section 1.1* have been achieved. It has been demonstrated that it is possible to increase the lifetime of electrical insulation by producing composite insulation with an in-built resistance to

electrical treeing. This has been accomplished by establishing a controlled region of compressive stress within the insulation thereby utilising the inherent mechanical properties of composite materials. The above has been achieved by the inclusion of high performance fibre yarns under tension during the curing process of the composite material. The results of this tensioning operation has produced a self balancing system of internal stresses, in a manner not dissimilar to that used in the prestressing of concrete.

During the course of this investigation numerous unforeseen challenges have presented themselves. Successfully overcoming these has added new dimensions to the research at almost every stage and has highlighted yet more areas for future work. Recommendations for this future work are outlined in *Chapter 12.*

CHAPTER 12

Future Work

12.0 Background

The development of mechanically pre-stressed electrical insulation, during the course of the EPSRC contract, has been taken from a theoretical concept to a reproducible quality small-scale sample. The construction of the heavy duty stress bed has produced the first pre-stressed sample with a realistically workable Tg. The heavy duty stress bed now provides a starting point for the future work. This enables the production of pre-stressed samples postcured at 100°C while the yarn is under tension. Plain and yarn embedded samples postcured at 100°C will also need to be produced in the future in order to observe the following:

1. The characteristics of the resin matrix in isolation (Plain samples).
2. The effects of embedding yarn into the resin matrix (Pre-tensioned samples).
3. The effects of pre-stressing the fibres in the yarn embedded samples (Pre-stressed samples).

Again it will be important to isolate the contribution made by pre-stressing to the retardation of tree growth. Therefore, if these benefits are to be highlighted, the production of pre-tensioned samples will be essential. If a state of equilibrium (ie. no stress) is to exist in the pre-tensioned samples, the level of pre-loading will have to be increased in order to compensate for the increase in resin shrinkage due to the elevated postcure. As well as determining the load level to obtain equilibrium in the Twaron® yarn embedded samples (pre-tensioned), it will also be necessary to determine at what load a reasonable level of pre-stress exists, for example a $-0.5cm^{-1}$ Raman waveband shift.

12.1 Pre-stressed Samples

Producing pre-stressed samples using the heavy duty stress beds not only allows for production at elevated temperatures, but will also enable the manufacture of samples at higher loadings. In this way the problems associated with weight hanging ie. shock loading are eliminated and the full load bearing potential of the yarns can be achieved. Tensile testing of the yarns indicated at least 26kg and stress bed calibration tests, see *Chapter 8 section 8.12.3*, indicated it may be possible to apply in excess of 30kg. Higher loaded room temperature cured samples could also be produced in the stress beds and tree tested to compare with the results obtained during this research. Higher levels of pre-stress obtained so far have been due to water absorption, therefore it would be useful to examine how this higher loading might contribute to retarding tree growth, if achieved during manufacture.

The portable nature of the heavy duty stress bed will permit Raman analysis of the yarn under tension prior to resin encapsulation. It is recommended that future work includes this examination in order to observe the effects of the curing process on the initial level of pre-stress attained in the yarn. It is anticipated that the level of pre-stress in the yarn will reduce, even for samples postcured at room temperature. This effect has already been shown when comparing samples postcured at room temperature with those postcured at elevated temperatures, eg 100°C.

It must be noted that the heavy duty stress bed is not yet fully developed and only limited modifications have so far been made to the initial design. It is anticipated that future work will need to involve further modifications to eliminate the problems encountered during sample manufacture. Production of the first pre-stressed sample in the heavy duty stress bed exposed a number of areas for improvement. These are examined in the following two paragraphs.

12.1.1 Stress Relaxation

It was found during this project, that the dead weight hanging procedure, used for pre-stressed sample manufacture, served to eliminate the effects of stress relaxation in the yarn. This occurred due to the constant dead weight (a steady load) acting vertically on the yarn (by the force of gravity), which provided a compensatory effect by

allowing the yarn to creep. Using the heavy duty stress bed, on the other hand, provides no such inherent compensating effect. In the heavy duty stress bed, the load is applied in the horizontal direction and the length of the yarn is fixed. Therefore, once the load has been applied and the yarn is under a constant strain, stress relaxation begins in the yarn. This is evident from the load cell monitor reading which falls over time. Consequently, if no further load is applied, by the end of the gel off period the level of pre-stress achieved is less than required. The random nature of the stress relaxation process also means that the load will vary from sample to sample therefore having an impact on reproducibility. To compensate for the effects of stress relaxation, it will be necessary to adjust the yarn loading during the gel off period or, alternatively, to apply additional load at the start of the process, for example a further 10%.

12.1.2 Securing the Yarn

Raman analysis highlighted the potential for uneven loading of the yarns, as shown in *Chapter 6, section 6.10.* This may be due to friction at the pulley, but is more likely to be caused by the tie off method of securing the yarn. Currently this tie off process is controlled by the individual operator, a factor that clearly brings an element of human error into the procedure. Further design work may therefore be required to ensure that the yarn ends are secured tightly and uniformly. This may also be a contributing factor in the stress relaxation process, since, in securing the yarn, the operator is tensioning the backbone of the yarn in an arbitrary way.

12.2 Reproducible Samples

It is essential that the production process produces consistent quality samples if valid comparisons are to be made. Once reproducibility has been demonstrated, future work will need to determine the performance of the elevated postcured samples during tensile tests and tree tests at room temperature. It will be essential to show the increase in the tensile strength of samples that have been postcured at 100°C and the effect this has on the treeing process. Furthermore, it will be important to monitor the effects of water absorption which swells the resin matrix and the impact this swelling will have on Raman bandshift levels and treeing times in aged samples.

12.3 Elevated Temperature Tests

Work carried out so far using DSC analysis on room temperature cured samples has determined the safe operating temperature for pre-stressed samples. It will now be necessary to ascertain the safe operating temperature of elevated postcured samples and the effects of long-term heat cycling on pre-stressing. The work to date has already determined the Tg of 5052 samples postcured over a range of temperatures. For example, samples postcured at room temperature have a Tg of 65°C, whereas samples postcured at 100°C have a Tg of 113°C, see *Chapter 7 section 7.6.*

The time available for this project did not permit elevated temperature tests to be carried out on the tensile and treeing samples produced at room temperature. It will therefore be essential for the next stage of the work to involve elevated temperature tests on the elevated postcured samples in order to determine the practical working boundaries of the pre-stressed electrical insulation. It has already been demonstrated by Auckland *et al* [139] that elevated temperature testing produces a decrease in tensile strength and accelerates the treeing process.

12.4 Multiple Parallel Fibres

The next logical step in this work would be to increase the number of bundles of yarn in the standard sample, see *Chapter 8 section 8.2.* This has the potential to increase the extent of compressive stress in the resin matrix, see *Chapter 6 section 6.8.* It has already been demonstrated in *Chapter 9 section 9.6* that increasing the number of yarn bundles increases tensile strength and it follows that this should further retard the treeing process, however this still remains to be shown above four yarns. The continued use of a symmetrical sample design is essential if bending is to be avoided.

12.5 Filled Samples

As already indicated in *Chapter 7* the use of fillers should reduce resin shrinkage, see Ciba [98]. This has the potential to increase the level of pre-stress in the samples,

thus further retarding the treeing process. For a number of years at the University of Manchester considerable work has been carried out using Aluminium Oxide Al_2O_2 and Zinc Oxide ZnO as both filler, Auckland *et al* [140] and barrier materials, Auckland *et al* [41]. Future work with these fillers would have to look at filler concentrations and their effect on both pre-tensioned and pre-stressed samples. The samples produced in this way would be opaque, therefore tree tests would have to be monitored using the base of the sample to indicate when the tree had propagated and the initiation time eliminated by debonding the needles. This would only allow data comparison with treeing times after initiation. Again, the effects of water absorption would have to be monitored with the additional use of soaked samples and desiccated samples.

12.6 Orthogonal Samples

The future work described above uses samples constructed with bundles of yarn running the length of the samples, further work could involve running yarn bundles both down the length and width of the samples, at 90° to each other (Orthogonal). This would have the effect of creating a yarn or stress matrix within the resin matrix.

The initial design work could be carried out by modifying one of the pre-stress rigs to accommodate the orthogonal yarn bundles. It has already been demonstrated that results obtained using the weight hangers are repeatable and reliable. For instance consideration would need to be given to the question of whether the extra pairs of yarn would go over or under the existing yarns, or whether they would interweave with them. Modifications to the former box could be made before attempting to redesign the heavy duty stress bed. This would break down the design process and highlight potential problems with orthogonal samples. The cost of redesigning the heavy duty stress bed would be reduced and the expense of buying more load cells delayed until such time as necessary. All of the proposals put forward for future work in *sections 12.0 to 12.5* could then be applied to orthogonal samples and comparisons made.

12.7 Summary

The volume of future work indicated would be too great for one researcher to carry out, therefore several separate investigations would be required in order to develop the project as described in this chapter. However to give focus to future work it will be necessary to investigate the potential end uses of this insulation system. The collaboration of an insulation manufacturer or insulated component builder would focus the research to investigate the areas applicable to commercial exploitation of the process. This step would be in keeping with the spirit of the EPSRC initiative of providing Universities with future sources of revenue whether in the form of financial support for research work or royalties for designs and processes.

Appendix 1

High Performance Fibre Yarn Sample Details

SAMPLE 1. :-	**NYLON 6.6**	**Type 728**
Manufactured by :-	Du Pont	
Received :-	04-09-96	1kg
dtex :-	1400	
Number of filaments :-	210	
Density :-	1.14 g/cm^3	
Fibre diameter :-	27μm ± 5% (27.29μm)	
Shape :-	Off-round not constant	
Condition :-	Natural colour spin finish	
Surface Energy :-	40.7 mJ/m^2	
SAMPLE 2. :-	**DYNEEMA SK65**	**(Ref: 3638)**
Manufactured by :-	DSM	
Received :-	18-09-96	1.5kg
dtex :-	1760	
Number of filaments :-	1560	
Density :-	0.97 g/cm^3	
Type :-	SK65 1760 DTEX 430	
Spool No. :-	1760-1560-430 (ID No.206993)	
Fibre diameter :-	12μm ± 5% (12.18μm)	
Shape :-	Bean not constant.	
Conditon :-	Natural colour spin finish	
Surface Energy :-	32 mJ/m^2	
SAMPLE 3. :-	**DYNEEMA SK66**	**(Ref : 3638)**
Manufactured by :-	DSM	
Received :-	18-09-96	1kg
dtex :-	440	
Number of filaments :-	390	
Density :-	0.97 g/cm^3	
Type :-	SKX8 220 DTEX 430	
Spool No. :-	440-390-430 (1135045) (ID No. 115914)	
Fibre diameter :-	12μm ± 5% (12.18μm)	
Shape :-	Bean not constant.	
Condition :-	Natural colour spin finish	
Surface Energy :-	32 mJ/m^2	
SAMPLE 4. :-	**KEVLAR 29**	
Manufactured by :-	Du Pont	
Received :-	18-09-96	100g
dtex :-	1670	
Number of filaments :-	1000	
Density :-	1.44 g/cm^3	
Fibre diameter :-	12μm ± 5% (12.15μm)	
Shape :-	Off-round not constant.	
Condition :-	Natural colour spin finish	
Surface Energy :-	33 mJ/m^2	

Appendix 1

High Performance Fibre Yarn Sample Details

SAMPLE 5. :-	**KEVLAR 119 (He)**	
Manufactured by :-	Du Pont	
Received :-	18-09-96	100g
dtex :-	1670	
Number of filaments :-	1000	
Density :-	1.44 g/cm^3	
Fibre diameter :-	12μm ± 5% (12.15μm)	
Shape :-	Off-round not constant.	
Condition :-	Natural colour spin finish	
Surface Energy :-	33 mJ/m^2	
SAMPLE 6. :-	**KEVLAR 129 (Ht)**	
Manufactured by :-	Du Pont	
Received :-	18-09-96	100g
dtex :-	1670	
Number of filaments :-	1000	
Density :-	1.44 g/cm^3	
Fibre diameter :-	12μm ± 5% (12.15μm)	
Shape :-	Off-round not constant.	
Condition :-	Natural colour spin finish	
Surface Energy :-	33 mJ/m^2	
SAMPLE 7. :-	**KEVLAR 29**	
Manufactured by :-	Du Pont	
Received :-	14-10-96 (approx. 10 years old)	0.5kg
dtex :-	1670	
Number of filaments :-	1000	
Density :-	1.44 g/cm^3	
Type :-	1500-1000-R80-904	
Fibre diameter :-	12μm ± 5% (12.15μm)	
Shape :-	Off-round not constant.	
Condition :-	Natural colour spin finish	
Surface Energy :-	33 mJ/m^2	
SAMPLE 8. :-	**KEVLAR K49**	
Manufactured by :-	Du Pont	
Received :-	14-10-96 (approx. 8 years old)	0.5kg
dtex :-	1580	
Number of filaments :-	1000	
Density :-	1.45 g/cm^3	
Type :-	1420-1000-0-965	
Fibre diameter :-	12μm ± 5% (11.78μm)	
Shape :-	Off-round not constant.	
Condition :-	Natural colour spin finish	
Surface Energy :-	33 mJ/m^2	

Appendix 1

High Performance Fibre Yarn Sample Details

SAMPLE 9. :-	**TWARON 1000**	
Manufactured by :-	Akzo Nobel	
Received :-	20-01-97	100g
dtex :-	1680	
Number of filaments :-	1000	
Density :-	1.44 g/cm^3	
Fibre diameter :-	12μm ± 5% (12.19 μm)	
Shape :-	Off-round not constant.	
Condition :-	Natural colour spin finish.	
Surface Energy :-	33 mJ/m^2	
SAMPLE 10. :-	**TWARON 1001**	
Manufactured by :-	Akzo Nobel	
Received :-	20-01-97	100g
dtex :-	1680	
Number of filaments :-	1000	
Density :-	1.44 g/cm^3	
Fibre diameter :-	12μm ± 5% (12.19 μm)	
Shape :-	Off round not constant.	
Condition :-	Natural colour spin finish with **Epoxy Component.**	
Surface Energy :-	45 mJ/m^2	
SAMPLE 11. :-	**DYNEEMA SK65C**	**(Ref: 970043)**
Manufactured by :-	DSM	
Received :-	07-02-97	1.5kg
dtex :-	1760	
Number 0f filaments :-	1560	
Density :-	0.97 g/cm^3	
Fibre diameter :-	12μm ± 5% (12.18μm)	
Shape :-	Bean not constant.	
Conditon :-	Natural colour spin finish with **Corona Treatment.**	
Surface Energy :-	49 mJ/m^2	

N.B.

Additional large bobbins of TWARON 1000 & 1001 were obtained for the production of Quad yarn samples.

Additional Sample Identification Numbers eg. **Sample 9.2.1. - Twaron 1000**

9. Origional sample reference number.
2. The batch number.
1. The package number.

Appendix 1

High Performance Fibre Yarn Sample Details

SAMPLE 9.2. / 9.2.1. :-	**TWARON 1000**	/ After transfer
Manufactured by :-	Akzo Nobel	
Received :-	29-04-97	2kg/1.5kg
dtex :-	1680	
Number of filaments :-	1000	
Density :-	1.44 g/cm^3	
Fibre diameter :-	12μm ± 5% (12.19 μm)	
Shape :-	Off-round not constant.	
Condition :-	Natural colour spin finish.	
Surface Energy :-	35 mJ/m^2	
SAMPLE 9.2.2. :-	**TWARON 1000**	new cone
Manufactured by :-	Akzo Nobel	
Received / Transfered :-	29-04-97 / 09-10-97	0.5kg
dtex :-	1680	
Number of filaments :-	1000	
Density :-	1.44 g/cm^3	
Fibre diameter :-	12μm ± 5% (12.19 μm)	
Shape :-	Off-round not constant.	
Condition :-	Natural colour spin finish.	
Surface Energy :-	35 mJ/m^2	
SAMPLE 10.2. / 10.2.1. :-	**TWARON 1001**	/ After transfer
Manufactured by :-	Akzo Nobel	
Received :-	29-04-97	1.5kg
dtex :-	1680	
Number of filaments :-	1000	
Density :-	1.44 g/cm^3	
Fibre diameter :-	12μm ± 5% (12.19 μm)	
Shape :-	Off round not constant.	
Condition :-	Natural colour spin finish with **Epoxy Component.**	
Surface Energy :-	45 mJ/m^2	
SAMPLE 10.2.2. :-	**TWARON 1001**	new cone
Manufactured by :-	Akzo Nobel	
Received / Transfered:-	29-04-97 / 09-10-97	0.5kg
dtex :-	1680	
Number of filaments :-	1000	
Density :-	1.44 g/cm^3	
Fibre diameter :-	12μm ± 5% (12.19 μm)	
Shape :-	Off round not constant.	
Condition :-	Natural colour spin finish with **Epoxy Component.**	
Surface Energy :-	45 mJ/m^2	

Appendix 2

Plain Resin Samples

Plain resin samples produced using the initial choices of resin starting with a list of the samples manufactured during the first year, numbered with their testing status allocation.

Polyester Resin C

Postcured 25-04-97 Repostcured 14-11-97

Sample no.	Testing Status
1	Library
2	Library
3	Library
4	Library
odd nos. 5-43	For Mechanical Testing at Ambient Temperatures
even nos. 6-44	For Mechanical Testing at Elevated Temperatures
45	Library

Epoxy CT1200

Postcured 10-03-97

Sample no.	Testing Status
1	Library
2	Library
3	Library
4	Library
odd nos. 5-43	For Mechanical Testing at Ambient Temperatures
even nos. 6-44	For Mechanical Testing at Elevated Temperatures
45	Library

The status of **Library** sample is for mechanical testing at a later stage to observe the effects of physical aging on the samples.

Appendix 2

Plain Resin Samples

Below is a list of the plain resin samples manufactured during the second year. Tensile test results are given for those preliminary test samples that were tested.

Epoxy CT1200

Sample no.	Date of Postcure	Testing Status
0.001-0.010 0.011-0.012	25-10-97	For Mechanical Testing at Ambient Library
0.013-0.022 0.023-0.024	13-11-97	For Mechanical Testing at Ambient Library

Preliminary Test Samples

Sample	Taper	Date of Postcure	Date of Test	Code	Results
0.1	**30°**	**28-11-97**	**03-12-97**	**AWV**	**13420 N**
0.2	30°			LGT-RT	7660 N
0.3	30°inv			LGB-RT	10560 N
0.4	**30°inv**			**AMV**	**19880 N**
0.5	**30°inv**			**AWT**	**14980 N**
mean				**72.63MPa**	**17430 N**
median				*72.63MPa*	*17430 N*
SD				14.44MPa	3465 N
0.6	30°inv		04-12-97	LAB-RT	9020 N
0.7	30°inv			LAB-RT	10560 N
0.8		28-11-97	Library		
0.9			Library		
0.10			Library		
0.11			Library		
0.12			Library		
0.13			Library		
0.14			Library		
0.15			Library		
0.16			Library		

Appendix 2

Plain Resin Samples

List of Plain Pin Samples in Polyester Resin C - Unused

Batch No.	Sample No	Number of Needles in Sample Hypodermic	Tungsten	Postcured
1.0				**23-09-97**
	1.1	4		
	1.2		4	
	1.3	4		
	1.4		4	
2.0				
	2.1	4		
	2.2		4	
	2.3	4		
	2.4		4	
3.0				
	3.1	4		
	3.2		4	
	3.3	4		
	3.4		4	
4.0				**21-10-97**
	4.1	4		
	4.2		4	
	4.3	4		
	4.4		4	
5.0				
	5.1	4		
	5.2		4	
	5.3	4		
	5.4		4	
6.0				
	6.1	4		
	6.2		4	
	6.3	4		
	6.4		4	
Total Number of Needles		**48**	**48**	

Appendix 3

Samples Used For Taper Tests

Polyester RESIN C – PLAIN SAMPLES
1 Day Cure followed by 3 hour Postcure @ 80°C.

Valid Sample Failure Results Shown in **BOLD**

Sample	Taper	Date of Postcure	Date of Test	Code	Results
		(Glue used on end-pieces - Loctite® 4210)			
0.1	90°	31-05-97	30-06-97	GIV-RB	0000 N
0.2	90°	31-05-97	23-06-97	GIV-RB	1900 N
0.3	90°			GIV-RB	7000 N
0.4	90°			GIV-RB	4600 N
0.5	90°			GIB-RB	2500 N
0.6	90°			GIB-RB	2300 N
0.7	90°			GIV-RB	0000 N
0.8	90°	31-05-97	30-06-97	GIV-RB	0000 N
		(Glue used on end-pieces - ECCOBOND® 286)			
0.9	60°	12-08-97	09-09-97	GAT-RB	1418 N
0.10	60°			GAB-RB	1810 N
0.11	**30°**			**AGB**	**4066 N**
0.12	**30°**			**AWB**	**2926 N**
0.13	**30°**	**13-08-98**	**09-09-97**	**AWB**	**3004 N**
0.14	45°			GIB-RB	1840 N
0.15	45°			GIB-RB	1586 N
0.16	45°			GIB-RB	1644 N
0.17	25°	12-09-97	06-10-97	GIB-RB	2274 N
0.18	20°			GIB-RB	2452 N
0.19	15°			GIB-RB	1994 N
0.20	25°			GIB-RB	4774 N
0.21	15°			GIB-RB	3056 N
0.22	35°	12-09-97	13-10-97	GIB-RB	1526 N
0.23	35°			GIB-RB	2760 N
0,24	30°			GIB-RB	1798 N
0.25	30°			GIB-RB	1628 N
0.26	30°			GIB-RB	1646 N
0.27	**30° inv**	**20-10-97**	**27-10-97**	**AWV**	**5708 N**
0.28	**30° inv**			**AWV**	**6148 N**
0.29	**30°**			**AWB**	**2428 N**
0.30	**30°**			**AWT**	**2210 N**
0.31	30° lug			GIV-RB	2440 N

Appendix 3

Samples Used For Taper Tests

Sample	Taper	Date of Postcure	Date of Test	Code	Results
0.32	**30°**	**20-10-97**	**30-10-98**	**AWV**	**4488 N**
0.33	30° lug			GIV-RB	3280 N
0.34	30° lug			GIT-RB	3932 N
0.35	90°	20-10-97	05-11-97	GIV-RB	4570 N
0.36	90°			GIV-RB	5300 N
0.37	30° inv	10-11-97	12-11-97	GIB-RB	1318 N
0.38	30° inv			AWB-RT	2254 N
0.39	30° inv			AWV-RT	3332 N
0.40	30° inv			AWT-RT	3128 N
0.41	**30° inv**			**AWV**	**5066 N**
0.42	90°			GIV-RB	3058 N
0.43	90°			GIT-RB	3360 N
0.44	90°			GIT-RB	1880 N
0.45	Library				
0.46	Library				
30° taper (6 samples)					
mean				**13.28MPa**	**3187 N**
median				*12.35MPa*	*2965 N*
SD				3.77MPa	905 N
30° taper inverted (3 samples)					
mean				**23.5MPa**	**5641 N**
median				*23.78MPa*	*5708 N*
SD				2.27MPa	544 N

lug: **Lug type end-pieces**
inv: **Inverted end-pieces**

Appendix 4

Preliminary Quad Samples

Epoxy ARALDITE 5052
Embedded with TWARON 1001

Sample	Yarn Load	Cure Cycle	Postcure Cycle	Date of Postcure	Date of Testing
A	2kg	24 hrs - RT	+ 6 days - RT	17-11-97	
B	2kg		10 hrs - 50°C	11-11-97	
C	2kg		08 hrs - 80°C	13-11-97	
D	2kg	24 hrs - RT	+ 8 hrs - 80°C	19-11-97	05-01-98 TT 9460 N
E	2kg	24 hrs - RT	+ 8 hrs - 80°C	19-11-97	05-01-98 TT 11100 N
F (Twin)	5kg	24 hrs - RT	+ 2 hrs - 80°C	26-11-97	
G	**5kg**	**24 hrs - RT**	**+ 6 days - RT**	**08-12-97**	
H	*11kg*	*24 hrs - RT*	*+ 6 days - RT*	*15-12-97*	
I	**20kg**	**24 hrs - RT**	**+ 6 days - RT**	**20-01-98**	
J (PIN)	2kg	24 hrs - RT	+ 6 days - RT	02-02-98	23-02-98
K failed TB	25kg	24 hrs - RT	+ 6 days - RT	02-02-98	
L failed TB	22kg	24 hrs - RT	+ 6 days - RT	04-02-98	
M	**20kg**	**24 hrs - RT**	**+ 6 days - RT**	**05-02-98**	10-03-98 TT 7554 N
N (PIN)	2kg	24 hrs - RT	+ 6 days - RT	09-02-98	02-03-98
O failed TB	20kg	24 hrs - RT	+ 6 days - RT	23-02-98	10-03-98 TT 5860 N
P	**15kg**	**24 hrs - RT**	**+ 6 days - RT**	**24-02-98**	
Q failed -B	20kg	24 hrs - RT	+ 6 days - RT	02-03-98	10-03-98 TT 5546 N
R (PIN) failed	20kg	24 hrs - RT	+ 6 days - RT	03-03-98	04-03-98
S (PIN)	**20 kg**	**24 hrs - RT**	**+ 6 days - RT**	**03-03-98**	04-03-98
T (PIN)	**20kg**	**24 hrs - RT**	**+ 6 days - RT**	**14-03-98**	01-04-98
U failed T-	20kg	24 hrs - RT	+ 6 days - RT	14-03-98	
V	**20kg**	**24 hrs - RT**	**+ 6 days - RT**	**13-04-98**	12-05-98 **TT 9700 N**

Appendix 4

Preliminary Quad Samples

Sample	Yarn Load	Cure Cycle	Postcure Cycle	Date of Postcure	Date of Testing
W	**10kg**	**24 hrs - RT**	**+ 6 days - RT**	**26-04-98**	
X	**15kg**	**24 hrs - RT**	**+ 6 days - RT**	**12-05-98**	
Y	**20kg**	**24 hrs – RT**	**+ 4 hrs - 100°C**	**03-06-99**	
Z	2.25kg	24 hrs – RT	+ 4 hrs - 100°C	06-06-99	

Raman Analysis was carried out on the following samples, made from same batch of resin, when they were one week old.

5	**5kg**	**24 hrs – RT**	**+ 6 days – RT**	**01-06-99**	**08-06-99**
10	**10kg**	**24 hrs – RT**	**+ 6 days – RT**	**01-06-99**	**08-06-99**
15	**15kg**	**24 hrs – RT**	**+ 6 days – RT**	**01-06-99**	**08-06-99**
20	**20kg**	**24 hrs – RT**	**+ 6 days – RT**	**01-06-99**	**08-06-99**

BOLD	**Samples successfully Pre-stressed**
italics	*Sample embedded with Dyneema SK65C*
TT	Samples tensile tested, load in Newtons

Appendix 5

Raman Analysis – Twaron® 1001 embedded in Araldite® 5052

Cure Cycle (Number Tested)	Applied Load per layer kg	RAMAN 1 Week Old cm^{-1}	BANDSHIFT 39 Weeks Old cm^{-1}	READINGS 60 Weeks Old cm^{-1}
1d @ RT+ 6d @ RT				
(3)	2 kg	0.0	-0.2	-0.3
(22)	2.25 kg	0.0	-0.7	
(2)	5 kg	-0.5	-1.0	-1.3
(2)	10 kg	-1.0	-1.3	-1.4
(3)	15 kg	-1.5	-2.0	-2.1
(22)	20 kg	-2.0	-2.3	-2.7
1d @ RT+ 2hrs @ 80°C				
(2)	2 kg	+0.2		
1d @ RT + 8hrs @ 80°C				
(3)	2.25 kg	+0.3		
(1)	4.5 kg	+0.2		
10hrs @ 50°C				
(1)	2kg	+0.5		
8hrs @ 80°C				
(1)	2 kg	+0.6		
1d @ RT + 4hrs @ 100°C				
(1)	2.25 kg	+0.5		
(1)	20 kg/layer (total 40kg)	-1.2 & -1.6 front-back		

Note: Raman Bandshift Readings shown are the mean values.

Appendix 6

30 Day Schedule Valid Tensile Test Results

Epoxy ARALDITE 5052
1 Day Cure followed by 6 Day Postcure @ Room Temperature

Sample No.	Total No. Tested	Results		
PLAIN	**(24)**	**Load**		**Elongation**
0.12		8880 N		3.6%
0.13		6980 N		3.1%
0.15		9160 N		3.9%
0.18		6980 N		3.4%
0.19		7900 N		3.6%
1.2		7980 N		3.8%
2.3		8280 N		3.6%
2.5		9500 N		4.2%
3.2		8100 N		3.2%
3.4		8780 N		4.5%
mean		**8254 N**	**34.4MPa**	**3.7%**
median		***8190 N***	***34.1MPa***	***3.6%***
SD		851 N	3.5MPa	0.4%
PRE-TENSIONED	**(18)**			
0.2		11780 N		6.0%
0.3		9700 N		4.5%
0.4		11980 N		6.9%
0.6		7650 N		3.1%
0.8		6720 N		3.1%
0.10		9940 N		4.1%
1.1		9140 N		3.9%
1.2		8380 N		4.2%
1.3		8880 N		4.8%
2.3		10860 N		4.7%
3.1		8860 N		4.5%
mean		**9445 N**	**39.4MPa**	**4.5%**
median		***9140 N***	***38.1MPa***	***4.5%***
SD		1635 N	6.8MPa	1.1%
PRE-STRESSED	**(14)**			
V		9700 N		4.2%
0.2		8180 N		3.2%
0.3		9380 N		5.0%
1.2		10260 N		7.4%
2.1		8360 N		3.5%
4.1		9800 N		4.5%
4.3		9280 N		4.4%
4.4		9480 N		4.5%
5.1		9380 N		3.8%
mean		**9315 N**	**38.8MPa**	**4.5%**
median		***9380 N***	***39.1MPa***	***4.4%***
SD		663 N	2.8MPa	1.2%

Appendix 6

30 Day Schedule Valid Tensile Test Results

Epoxy ARALDITE 5052
1 Day Cure followed by 6 Day Postcure @ Room Temperature

Sample No.	**Total No. Tested**	**Results**		
DOUBLE PRE-TENSIONED	**(8)**	**Load**		**Elongation**
0.4		8580 N	35.8MPa	3.2%
0.7		9380 N	39.1MPa	5.2%
mean		**8980 N**	**37.4MPa**	**4.2%**
median		***8980 N***	***37.4MPa***	***4.2%***
SD		566 N	2.4MPa	1.4%
FAILED PRE-STRESSED	**(8)**	**Load**		**Elongation**
0.1T-		8580 N		3.3%
0.2TB		8620 N		3.7%
1.1-B		10060 N		4.2%
mean		**9090 N**	**37.9MPa**	**3.7%**
median		***8620 N***	***35.9MPa***	***3.7%***
SD		843 N	3.5MPa	0.5%

Epoxy ARALDITE 5052
1 Day Cure followed by 8 hour Postcure @ 80°C

Sample No.	**Total No. Tested**	**Results**		
PLAIN	**(10)**	**Load**		**Elongation**
80 0.1		**12900 N**		**5.1%**
80 0.2		**14300 N**		**6.2%**
80 0.3		**13500 N**		**6.1%**
80 0.4		**14520 N**		**6.5%**
80 0.5		**17460 N**		**7.8%**
80 0.6		**14420 N**		**7.0%**
80 0.9		**15580 N**		**7.8%**
80 0.10		**13780 N**		**6.2%**
mean		**14500 N**	**60.7MPa**	**6.6%**
median		***14360 N***	***59.8MPa***	***6.3%***
SD		1416 N	5.9MPa	0.9%

Appendix 7

15 Week Schedule Valid Tensile Test Results

Epoxy ARALDITE 5052
1 Day Cure followed by 6 Day Postcure @ Room Temperature

Sample No.	Total No. Tested	Results		
PLAIN	**(34)**	**Load**		**Elongation**
2.2		7960 N		3.5%
2.3		8720 N		4.2%
2.4		8860 N		4.0%
2.8		7460 N		3.1%
2.9		8560 N		3.1%
2.10		10720 N		4.2%
3.1		8100 N		2.8%
3.2		9680 N		3.8%
3.4		8580 N		3.5%
3.7		8660 N		3.7%
3.9		10060 N		3.8%
3.10		8280 N		3.8%
RT 3.1		9500 N		3.8%
mean		**8860 N**	**36.9MPa**	**3.6%**
median		***8660 N***	***36.1MPa***	***3.8%***
SD		908 N	3.8MPa	0.4%
PRE-TENSIONED	**(10)**			
RT 1.5		9280 N		3.9%
RT 1.7		11620 N		4.8%
RT 1.8		8580 N		5.4%
RT 1.9		7820 N		3.0%
RT 1.10		9220 N		3.6%
mean		**9300 N**	**38.8MPa**	**4.2%**
median		***9220 N***	***38.4MPa***	***3.9%***
SD		1423 N	5.9MPa	1.0%
PRE-STRESSED	**(11)**			
PS 1.1		10260 N		4.3%
PS 2.2		13060 N		6.0%
PS 2.4		9060 N		4.4%
PS 3.1		9840 N		4.1%
PS 3.2		10360 N		4.5%
mean		**10500 N**	**43.8MPa**	**4.7%**
median		***10260 N***	***42.8MPa***	***4.4%***
SD		1512 N	6.3MPa	0.8%

Appendix 7

15 Week Schedule Valid Tensile Test Results

Epoxy ARALDITE 5052
1 Day Cure followed by 8 hour Postcure @ 80°C

Sample No.	**Total No. Tested**	**Results**		
PLAIN	**(24)**	**Load**		**Elongation**
80 1.1		15440 N		8.1%
80 1.10		14240 N		6.4%
80 2.4		13260 N		7.4%
80 2.6		14340 N		7.3%
80 2.10		15300 N		8.2%
80 3.1		13320 N		5.9%
80 3.2		13300 N		5.8%
mean		**14170 N**	**59.0MPa**	**7.0%**
median		***14240 N***	***59.3MPa***	***7.3%***
SD		934 N	3.9MPa	1.0%
PRE-TENSIONED	**(6)**			
80 1.4		15760 N		6.8%
80 45 0.1		15560 N		7.8%
mean		**15660 N**	**65.3MPa**	**7.3%**
median		***15660 N***	***65.3MPa***	***7.3%***
SD		141 N	0.6MPa	0.7%

Appendix 8

30 Day Schedule Valid Tree Test Results

Epoxy ARALDITE 5052 – 1 Day Cure + 6 Day Postcure @ Room Temperature

Key to Sample Identification Number - Resin Batch No.01, Needle No.1 = **0.1.1**

HYPODERMIC PIN SAMPLES – Treeing time in **hours**

ID No.	Date of Postcure	Date of Test	Time from Initiate	POWER Propagate	ON to: Overall Breakdown	Time from to: Propagate	Initiation Breakdown
Plain							
0.1.1	29-04-98	29-05-98	44.00	45.00	48.00	1.00	4.00
0.1.2		06-07-98	10.00	11.00	14.30	1.00	4.30
0.1.3		07-07-98	39.00	40.00	42.00	1.00	3.00
0.1.4		09-07-98	25.70	26.70	30.20	1.00	4.50
mean			**29.68**	**30.68**	**33.63**	**1.00**	**3.95**
median			32.35	33.35	36.10	1.00	4.15
SD			15.22	15.22	14.85	0.00	0.67
Pre-tensioned							
4.3.1	23-04-99	24-05-99	11.00	12.00	30.90	1.00	19.90
4.3.2		26-05-99	12.00	13.00	24.30	1.00	12.30
4.3.3		11-06-99	51.30	52.30	72.20	1.00	20.90
4.3.4		14-06-99	29.50	30.50	59.70	1.00	30.50
mean			**25.95**	**26.95**	**46.78**	**1.00**	**20.90**
median			20.75	21.75	45.30	1.00	20.40
SD			18.91	18.91	22.88	0.00	7.46
Pre-stressed							
0.1.1	29-04-98	29-05-98	36.00	38.00	114.20	2.00	78.20
0.1.2		06-07-98	14.00	16.00	36.00	2.00	22.00
0.1.3		08-07-98	17.00	20.00	69.20	3.00	52.20
0.1.4		14-07-98	2.00	5.00	44.80	3.00	42.80
mean			**17.25**	**19.75**	**66.05**	**2.50**	**48.80**
median			15.50	18.00	57.00	2.50	47.50
SD			14.08	13.72	35.04	0.58	23.31

Appendix 8

30 Day Schedule Valid Tree Test Results

Epoxy ARALDITE 5052 – 1 Day Cure + 6 Day Postcure @ Room Temperature

OGURA PIN SAMPLES – Treeing Time in **hours**

ID No.	Date of Postcure	Date of Test	Time from Initiate	POWER Propagate	ON to: Overall Breakdown	Time from to: Propagate	Initiation Breakdown
Plain							
0.2.1	09-02-98	02-03-98	9.00	10.00	11.30	1.00	2.30
0.2.2		03-03-98	11.00	12.00	13.10	1.00	2.10
0.2.3		06-05-98	1.00	2.00	2.40	1.00	1.40
0.2.4		06-05-98	2.00	3.00	6.10	1.00	4.10
mean			**5.75**	**6.75**	**8.23**	**1.00**	**2.48**
median			5.50	6.50	8.70	1.00	2.20
SD			4.99	4.99	4.89	0.00	1.15
Pre-tensioned							
(J) 0.1.2	02-02-98	23-02-98	7.00	8.00	23.40	1.00	16.40
(J) 0.1.3		24-02-98	20.00	21.00	40.50	1.00	20.50
(N) 0.1.1	09-02-98	02-03-98	10.00	11.00	8.70	1.00	8.70
(N) 0.1.3		06-05-98	5.10	6.10	17.60	1.00	12.50
mean			**10.53**	**11.53**	**22.55**	**1.00**	**14.53**
median			8.50	9.50	20.50	1.00	14.45
SD			6.63	6.63	13.41	0.00	5.07
Pre-stressed							
(S) 0.1.1	03-03-98	12-03-98	14.00	15.00	20.20	1.00	6.20
(S) 0.1.2		04-03-98	34.00	35.00	40.70	1.00	6.70
(S) 0.1.3		06-03-98	60.00	61.00	77.60	1.00	17.60
(S) 0.1.4		09-03-98	46.00	48.00	62.20	2.00	16.20
(T) 0.2.1	14-03-98	01-04-98	13.00	15.00	31.70	1.50	17.70
(T) 0.2.2		21-04-98	29.00	31.00	35.00	2.00	6.00
(T) 0.2.3		23-04-98	14.00	16.00	26.50	2.00	12.50
(T) 0.2.4		27-04-98	1.00	2.00	11.50	1.00	10.50
mean			**26.38**	**27.88**	**38.18**	**1.44**	**11.68**
median			21.50	23.50	33.35	1.25	11.50
SD			19.68	19.66	21.91	0.50	5.08

Appendix 8

30 Day Schedule Valid Tree Test Results

Epoxy ARALDITE 5052 – 1 Day Cure + 6 Day Postcure @ Room Temperature

TUNGSTEN PIN SAMPLES – Treeing in **hours**

ID No.	Date of Postcure	Date of Test	Time from Initiate	POWER Propagate	ON to: Overall Breakdown	Time from Initiation to: Propagate	Time from Initiation to: Breakdown
Plain							
0.1.1	29-04-98	01-06-98	43.00	44.00	44.10	1.00	2.10
0.1.2		03-06-98	24.50	25.50	29.50	1.00	5.00
0.1.3		05-06-98	81.00	82.00	86.30	1.00	5.30
0.1.4		09-06-98	150.40	151.40	151.70	1.00	1.30
4.3.1	23-04-99	27-05-99	32.50	33.50	40.90	1.00	8.40
4.3.2		29-05-99	13.00	14.00	22.90	1.00	9.90
4.3.3		01-06-99	15.00	16.00	16.30	1.00	1.30
4.3.4		17-06-99	110.50	111.50	116.10	1.00	5.60
mean			**58.74**	**59.74**	**63.48**	**1.00**	**4.86**
median			37.75	38.75	42.50	1.00	5.15
SD			50.27	50.27	49.26	0.00	3.20
(NO 0.1.4	**& 4.3.4)**						
0.1.1	29-04-98	01-06-98	43.00	44.00	44.10	1.00	2.10
0.1.2		03-06-98	24.50	25.50	29.50	1.00	5.00
0.1.3		05-06-98	81.00	82.00	86.30	1.00	5.30
4.3.1	23-04-99	27-05-99	32.50	33.50	40.90	1.00	8.40
4.3.2		29-05-99	13.00	14.00	22.90	1.00	9.90
4.3.3		01-06-99	15.00	16.00	16.30	1.00	1.30
mean			**34.83**	**35.83**	**40.00**	**1.00**	**5.33**
median			28.50	29.50	35.20	1.00	5.15
SD			25.22	25.22	25.00	0.00	3.38

Appendix 8

30 Day Schedule Valid Tree Test Results

Epoxy ARALDITE 5052 – 1 Day Cure + 6 Day Postcure @ Room Temperature

TUNGSTEN PIN SAMPLES – Treeing in **hours**

ID No. Pre-tensioned	Date of Postcure	Date of Test	Time from Initiate	POWER Propagate	ON to: Overall Breakdown	Time from to: Propagate	Initiation Breakdown
0.2.1	22-05-98	22-06-98	2.00	3.00	26.50	1.00	24.50
0.2.2		22-06-98	25.00	26.00	42.00	1.00	17.00
0.2.3		22-06-98	22.00	23.00	48.20	1.00	26.20
0.2.4		22-06-98	120.50	121.50	259.90	1.00	139.40
1.1.1	14-07-98	13-08-98	298.70	299.70	360.40	1.00	61.70
1.1.2		08-09-98	497.60	498.60	526.40	1.00	29.80
mean			**160.97**	**161.97**	**210.57**	**1.00**	**49.77**
median			120.50	73.75	154.05	1.00	28.00
SD			198.49	198.49	206.54	0.00	46.57
(NO 0.2.4)							
0.2.1	22-05-98	22-06-98	2.00	3.00	26.50	1.00	24.50
0.2.2		22-06-98	25.00	26.00	42.00	1.00	17.00
0.2.3		22-06-98	22.00	23.00	48.20	1.00	26.20
1.1.1	14-07-98	13-08-98	298.70	299.70	360.40	1.00	61.70
1.1.2		08-09-98	497.60	498.60	526.40	1.00	29.80
mean			**169.06**	**170.06**	**200.70**	**1.00**	**31.84**
median			25.00	26.00	48.20	1.00	26.20
SD			220.81	220.81	229.33	0.00	17.33

Appendix 8

30 Day Schedule Valid Tree Test Results

Epoxy ARALDITE 5052 – 1 Day Cure + 6 Day Postcure @ Room Temperature

TUNGSTEN PIN SAMPLES – Treeing in **hours**

ID No. Pre-stressed	Date of Postcure	Date of Test	Time from Initiate	POWER Propagate	ON to: Overall Breakdown	Time from Initiation to: Propagate	Breakdown
0.1.1	29-04-98	01-06-98	1.00	3.00	12.10	2.00	11.10
1.1.3		12-06-98	31.00	34.00	71.10	3.00	40.10
3.1.2	18-02-99	14-05-99	1.00	3.00	10.25	2.00	9.50
4.2.1	29-03-99	14-05-99	1.00	3.00	19.00	2.00	18.00
4.2.2		16-05-99	1.00	3.00	125.90	2.00	124.90
4.2.3		22-06-99	1.00	3.00	40.80	2.00	39.80
4.2.4		26-06-99	3.00	5.00	19.30	2.00	16.30
0.1.3	29-04-98	12-06-99	95.00	98.00	132.10	3.00	37.10
0.2.2	22-05-98	22-06-98	244.20	246.20	258.10	2.00	11.90
1.1.1	14-07-98	13-08-98	111.00	115.00	154.00	4.00	43.00
1.1.4		12-10-98	416.00	420.00	425.80	4.00	9.80
3.1.1	18-02-99	13-04-99	342.50	345.50	376.30	3.00	33.80
3.1.3		16-05-99	429.00	432.00	445.20	3.00	16.20
3.1.4		06-06-99	464.00	467.00	478.60	3.00	14.60
mean			**152.91**	**155.55**	**183.47**	**2.64**	**30.44**
median			63.00	66.00	129.00	2.50	17.15
SD			184.88	185.31	177.65	0.74	30.01
(NO 4.2.2)							
0.1.1	29-04-98	01-06-98	1.00	3.00	12.10	2.00	11.10
1.1.3		12-06-98	31.00	34.00	71.10	3.00	40.10
3.1.2	18-02-99	14-05-99	1.00	3.00	10.25	2.00	9.50
4.2.1	29-03-99	14-05-99	1.00	3.00	19.00	2.00	18.00
4.2.3		22-06-99	1.00	3.00	40.80	2.00	39.80
4.2.4		26-06-99	3.00	5.00	19.30	2.00	16.30
0.1.3	29-04-98	12-06-99	95.00	98.00	132.10	3.00	37.10
0.2.2	22-05-98	22-06-98	244.20	246.20	258.10	2.00	11.90
1.1.1	14-07-98	13-08-98	111.00	115.00	154.00	4.00	43.00
1.1.4		12-10-98	416.00	420.00	425.80	4.00	9.80
3.1.1	18-02-99	13-04-99	342.50	345.50	376.30	3.00	33.80
3.1.3		16-05-99	429.00	432.00	445.20	3.00	16.20
3.1.4		06-06-99	464.00	467.00	478.60	3.00	14.60
mean			**164.59**	**167.28**	**187.90**	**2.69**	**23.17**
median			95.00	98.00	132.10	3.00	16.30
SD			186.97	187.38	184.09	0.75	13.22

Appendix 8

30 Day Schedule Valid Tree Test Results

Epoxy ARALDITE 5052 – 1 Day Cure + 6 Day Postcure @ Room Temperature

TUNGSTEN PIN SAMPLES – Treeing in **hours**

ID No.	Date of Postcure	Date of Test	Time from Initiate	POWER Propagate	ON to: Overall Breakdown	Time from to: Propagate	Initiation Breakdown
Pre-stressed							
LONG	**Initiation**	**Period**					
0.1.3	29-04-98	12-06-99	95.00	98.00	132.10	3.00	37.10
0.2.2	22-05-98	22-06-98	244.20	246.20	258.10	2.00	11.90
1.1.1	14-07-98	13-08-98	111.00	115.00	154.00	4.00	43.00
1.1.4		12-10-98	416.00	420.00	425.80	4.00	9.80
3.1.1	18-02-99	13-04-99	342.50	345.50	376.30	3.00	33.80
3.1.3		16-05-99	429.00	432.00	445.20	3.00	16.20
3.1.4		06-06-99	464.00	467.00	478.60	3.00	14.60
mean			**300.24**	**303.39**	**324.30**	**3.14**	**23.77**
median			342.50	345.50	376.30	3.00	16.20
SD			152.57	152.55	142.45	0.69	13.70
SHORT	**Initiation**	**Period**					
0.1.1	29-04-98	01-06-98	1.00	3.00	12.10	2.00	11.10
1.1.3		12-06-98	31.00	34.00	71.10	3.00	40.10
3.1.2	18-02-99	14-05-99	1.00	3.00	10.25	2.00	9.50
4.2.1	29-03-99	14-05-99	1.00	3.00	19.00	2.00	18.00
4.2.2		16-05-99	1.00	3.00	125.90	2.00	124.90
4.2.3		22-06-99	1.00	3.00	40.80	2.00	39.80
4.2.4		26-06-99	3.00	5.00	19.30	2.00	16.30
mean			**5.57**	**7.71**	**42.64**	**2.14**	**37.10**
median			1.00	3.00	19.30	2.00	18.00
SD			11.24	11.61	42.49	0.38	40.74
(NO 4.2.2)							
0.1.1	29-04-98	01-06-98	1.00	3.00	12.10	2.00	11.10
1.1.3		12-06-98	31.00	34.00	71.10	3.00	40.10
3.1.2	18-02-99	14-05-99	1.00	3.00	10.25	2.00	9.50
4.2.1	29-03-99	14-05-99	1.00	3.00	19.00	2.00	18.00
4.2.3		22-06-99	1.00	3.00	40.80	2.00	39.80
4.2.4		26-06-99	3.00	5.00	19.30	2.00	16.30
mean			**6.33**	**8.50**	**28.76**	**2.17**	**22.47**
median			1.00	3.00	19.15	2.00	17.15
SD			12.11	12.52	23.42	0.41	13.90

Appendix 9

9 Month Schedule Valid Tree Test Results

Epoxy ARALDITE 5052 – 1 Day Cure + 6 Day Postcure @ Room Temperature

Key to Sample Identification Number - Resin Batch No.02, Needle No.1 = **0.2.1**

HYPODERMIC PIN SAMPLES – Treeing time in **hours.**

ID No.	Date of Postcure	Date of Test	Time from Initiate	POWER Propagate	ON to: Overall Breakdown	Time from to: Propagate	Initiation Breakdown
Plain							
0.2.1	12-05-98	19-02-99	0.00	7.00	9.00	7.00	9.00
0.2.2		22-02-99	0.70	4.70	6.00	4.00	5.30
0.2.3		24-02-99	2.30	8.10	13.60	5.80	11.30
0.2.4		25-02-99	0.30	5.50	5.60	5.20	5.30
mean			**0.83**	**6.33**	**8.55**	**5.50**	**7.73**
median			0.50	6.25	7.50	5.50	7.15
SD			1.02	1.52	3.69	1.25	2.95
Pre-tensioned							
0.2.1	22-05-98	13-01-99	1.00	7.00	45.70	6.00	44.70
0.2.2		15-01-99	5.00	12.00	46.50	7.00	41.50
0.2.3		16-02-99	37.50	48.10	165.40	10.60	127.90
0.2.4		24-02-99	20.00	27.50	71.00	7.50	51.00
mean			**15.88**	**23.65**	**82.15**	**7.78**	**66.28**
median			12.50	19.75	58.75	7.25	47.85
SD			16.57	18.49	56.73	1.98	41.27
(NO 0.2.3)							
0.2.1	22-05-98	13-01-99	1.00	7.00	45.70	6.00	44.70
0.2.2		15-01-99	5.00	12.00	46.50	7.00	41.50
0.2.4		24-02-99	20.00	27.50	71.00	7.50	51.00
mean			**8.67**	**15.50**	**54.40**	**6.83**	**45.73**
median			5.00	12.00	46.50	7.00	44.70
SD			10.02	10.69	14.38	0.76	4.83
Pre-stressed							
0.2.1	22-05-98	03-02-99	1.00	8.00	43.50	7.00	42.50
0.2.2		05-02-99	1.00	13.00	35.70	12.00	34.70
0.2.3		08-02-99	0.50	7.00	48.90	6.50	48.40
0.2.4		16-02-99	2.00	13.00	56.40	11.00	54.40
mean			**1.13**	**10.25**	**46.13**	**9.13**	**45.00**
median			1.00	10.50	46.20	9.00	45.45
SD			0.63	3.20	8.73	2.78	8.41

Appendix 9

9 Month Schedule Valid Tree Test Results

Epoxy ARALDITE 5052 – 1 Day Cure + 6 Day Postcure @ Room Temperature

TUNGSTEN PIN SAMPLES – Treeing time in **hours**.

ID No.	Date of Postcure	Date of Test	Time from Initiate	POWER Propagate	ON to: Overall Breakdown	Time from to: Propagate	Initiation Breakdown
Plain							
0.2.1	12-05-98	20-01-99	8.00	12.00	14.70	4.00	6.70
0.2.2		21-01-99	139.70	144.30	145.20	4.60	5.50
0.2.3		02-02-99	113.50	120.50	121.10	7.00	7.60
0.2.4		08-02-99	62.00	66.00	67.30	4.00	5.30
mean			**80.80**	**85.70**	**87.08**	**4.90**	**6.28**
median			87.75	93.25	94.20	4.30	6.10
SD			58.29	59.06	58.21	1.43	1.08
Pre-tensioned							
1.1.3	14-07-98	20-01-99	8.00	13.00	44.30	5.00	36.30
1.1.4		04-01-99	385.40	390.40	423.90	5.00	38.50
mean			**196.70**	**201.70**	**234.10**	**5.00**	**37.40**
median			196.70	201.70	234.10	5.00	37.40
SD			266.86	266.86	268.42	0.00	1.56
Pre-stressed							
0.1.2	29-04-98	04-06-99	0.10	8.20	34.60	8.10	34.50
mean			**0.10**	**8.20**	**34.60**	**8.10**	**34.50**
median			0.10	8.20	34.60	8.10	34.50

Appendix 10

Photographs of Hypodermic Needle Samples

This Appendix contains sets of photographs of pin samples containing hypodermic needles showing the treeing process from initiation through to breakdown.

Time indicated in bottom right-hand corner is actual time (am or pm) the photograph was taken (not a duration time). Duration times are given above each photograph.

List of Photographs in Appendix 10

PLAIN

Plain **H**ypodermic, Batch No. **02**, **N**eedle No. **4** – Photo Set **PH02N4**

Taken from 9 Month Schedule – see full results in *Appendix 9*

PRE-TENSIONED

Pre-**T**ensioned **H**ypodermic, Batch No. **02**, **N**eedle No. **1** – Photo Set **PTH02N1**

Taken from 9 Month Schedule – see full results in *Appendix 9*

PRE-STRESSED

Pre-Stressed **H**ypodermic, Batch No. **01**, **N**eedle No. **2** – Photo Set **PSH01N2**

Taken from 30 Day Schedule – see full results in *Appendix 8*

Appendix 10

PLAIN

10 minutes – No Tree

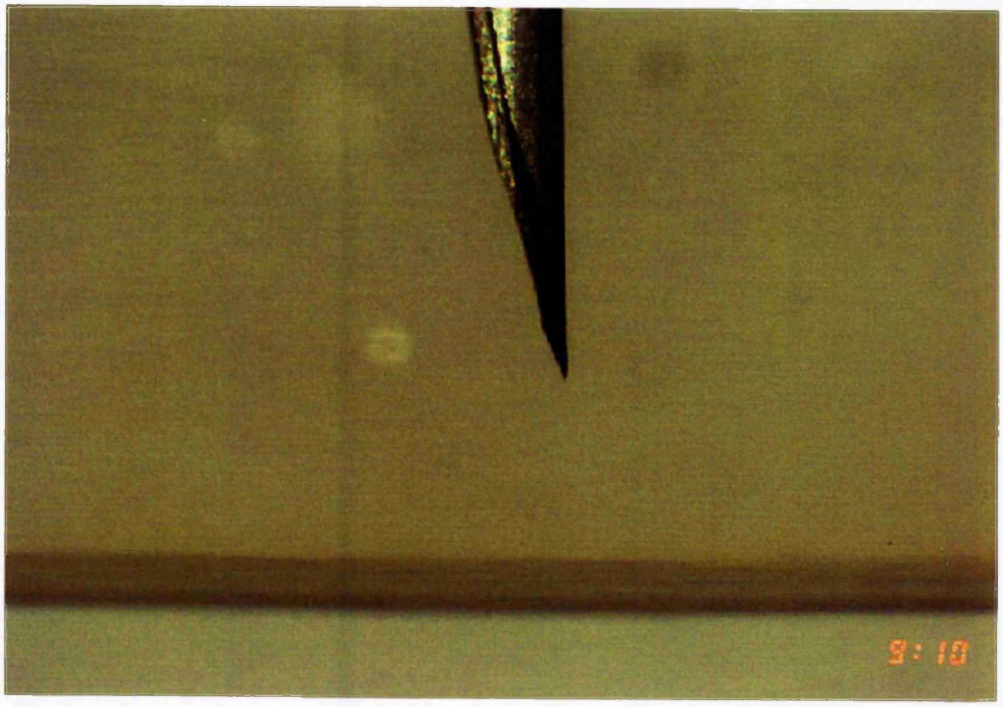

20 minutes – Tree Initiates

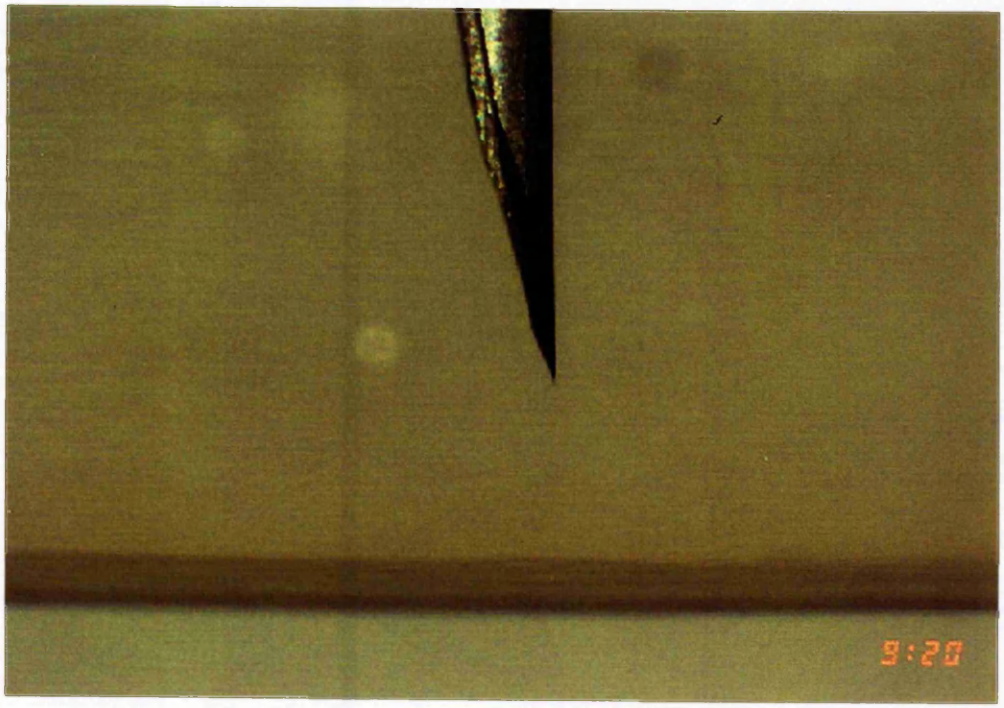

PLAIN

30 minutes – Propagation Time 10 minutes

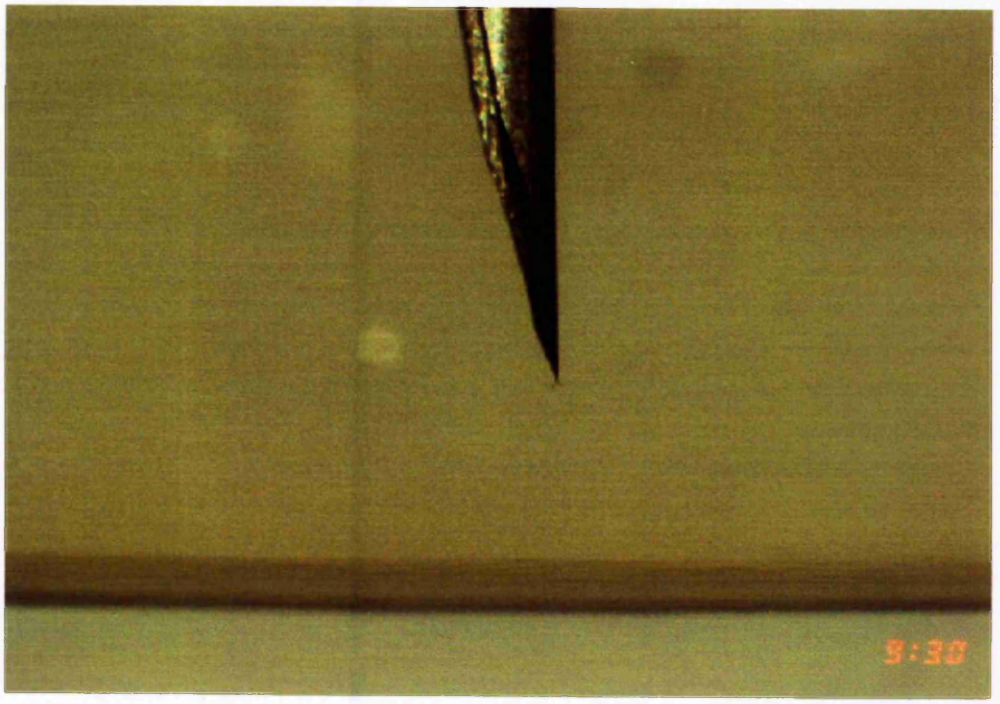

1 hour 30 minutes – Propagation Time 1 hour 10 minutes

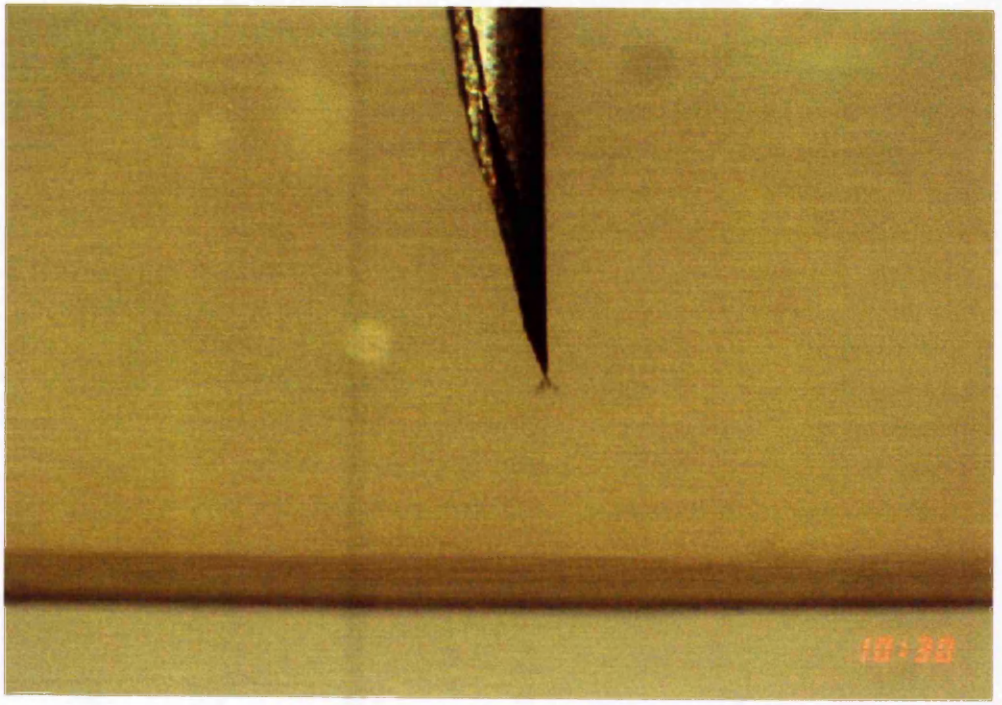

PLAIN

2 hours 30 minutes – Propagation Time 2 hours 10 minutes

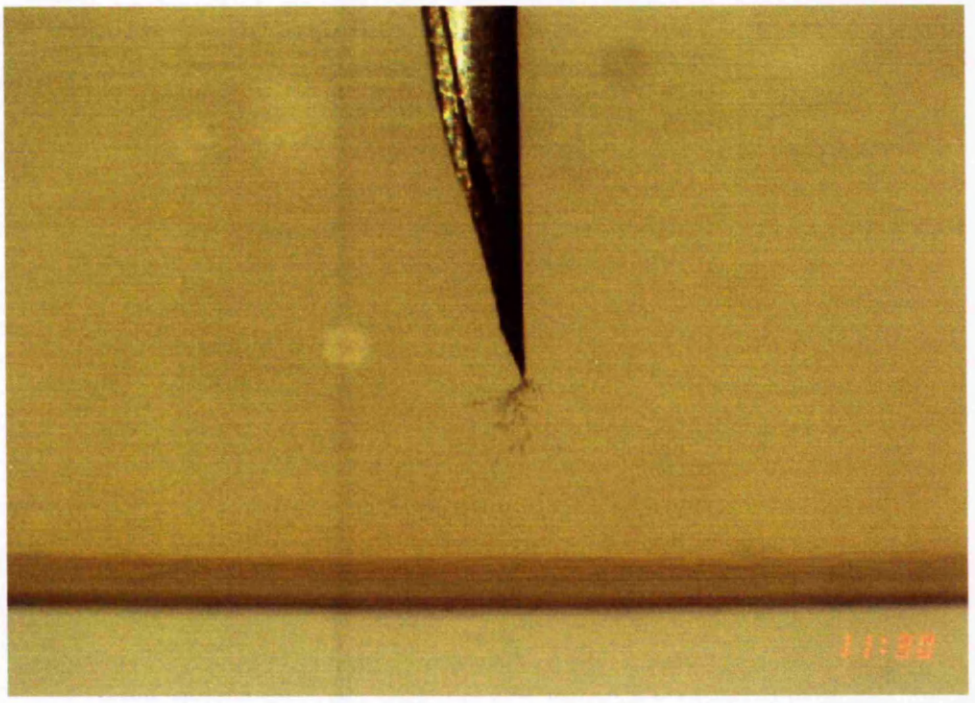

3 hours 30 minutes – Propagation Time 3 hours 10 minutes

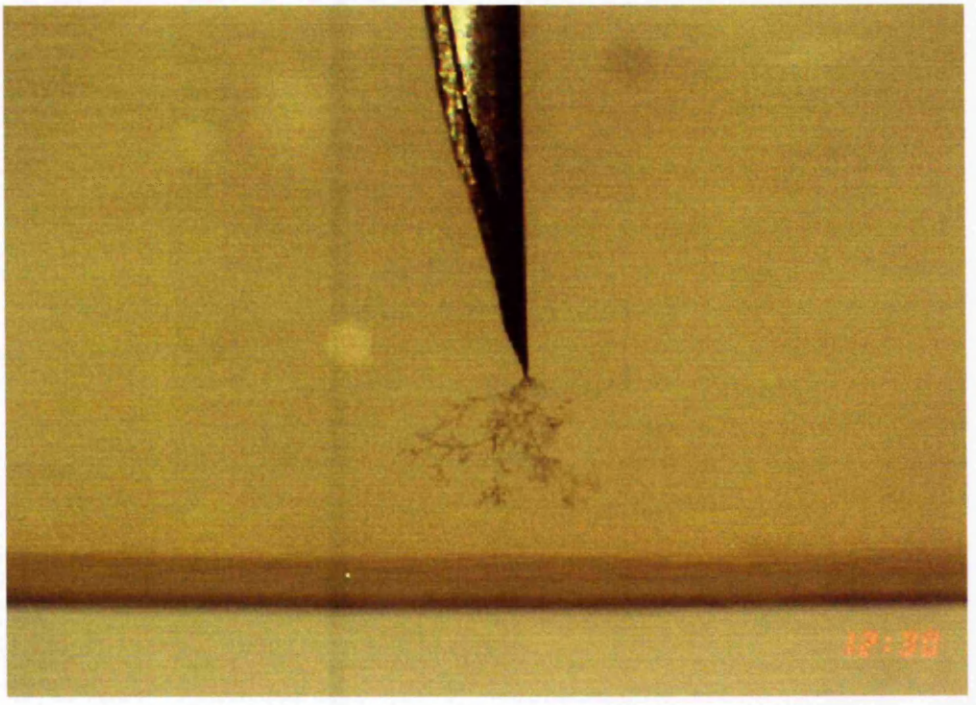

PLAIN

4 hours 30 minutes – Propagation Time 4 hours 10 minutes

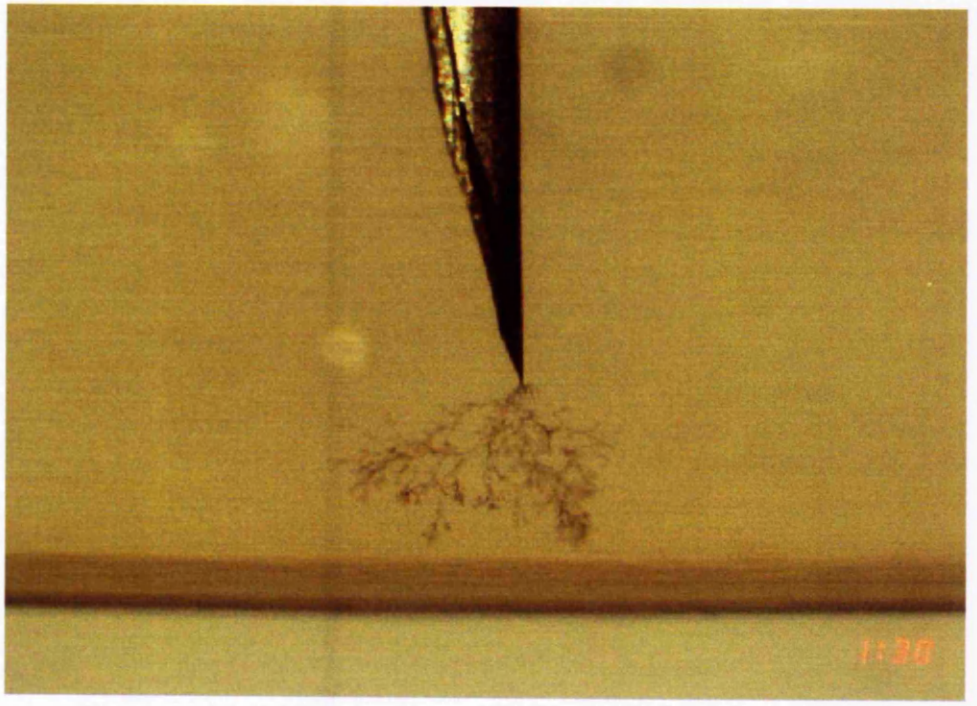

5 hours 20 minutes – Propagation Time 5 hours

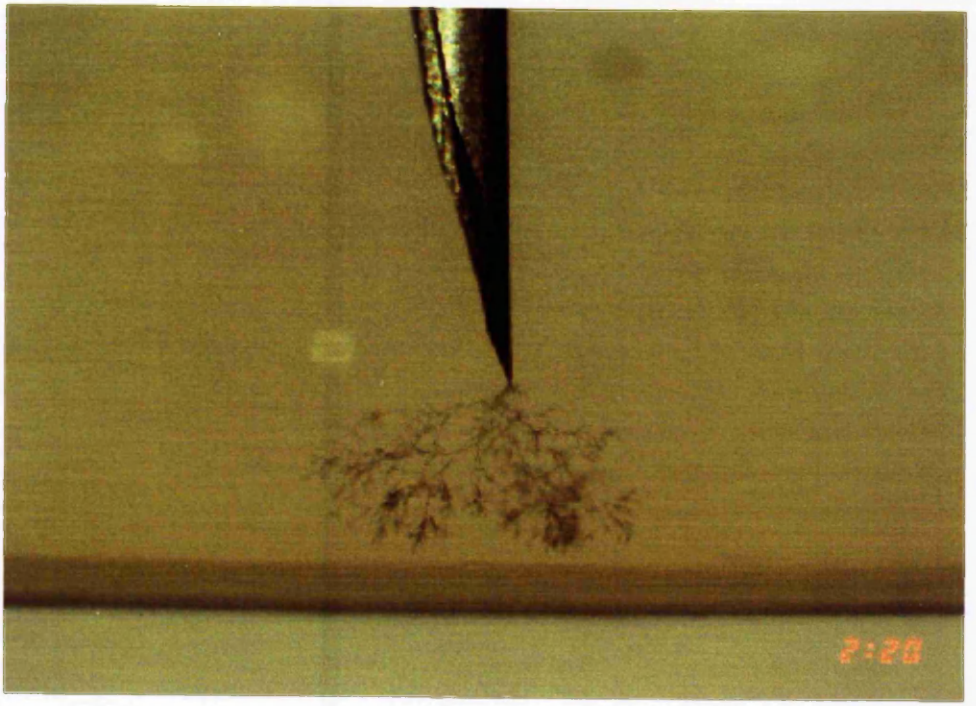

PLAIN

5 hours 30 minutes – Propagation Finished 5 hours 10 minutes

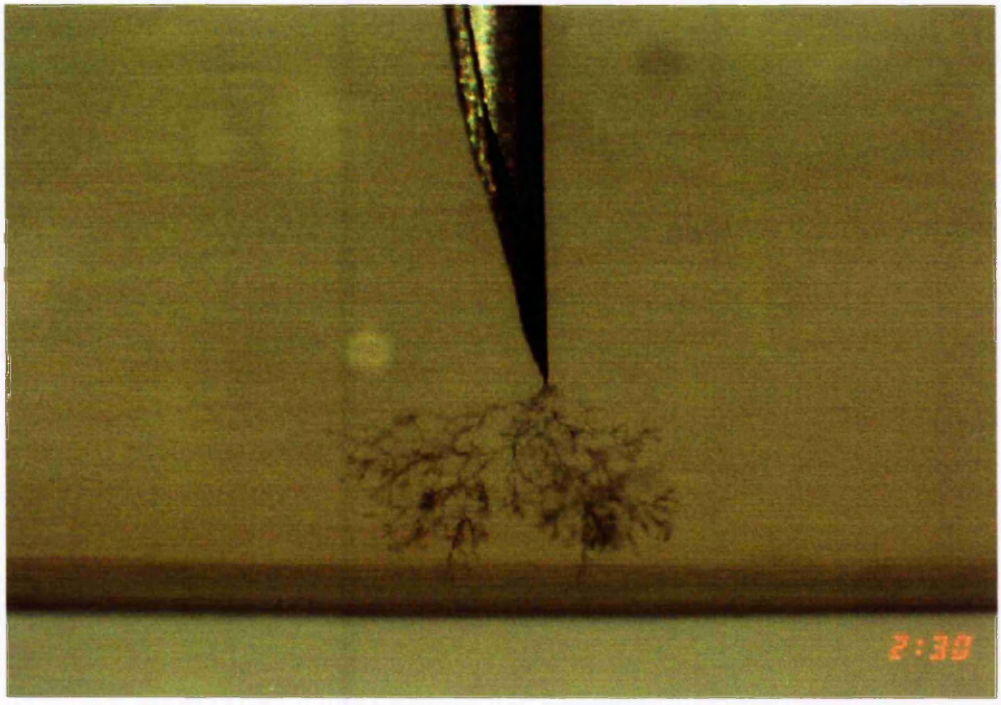

5 hours 36 minutes – BREAKDOWN (5 hours 16 minutes)

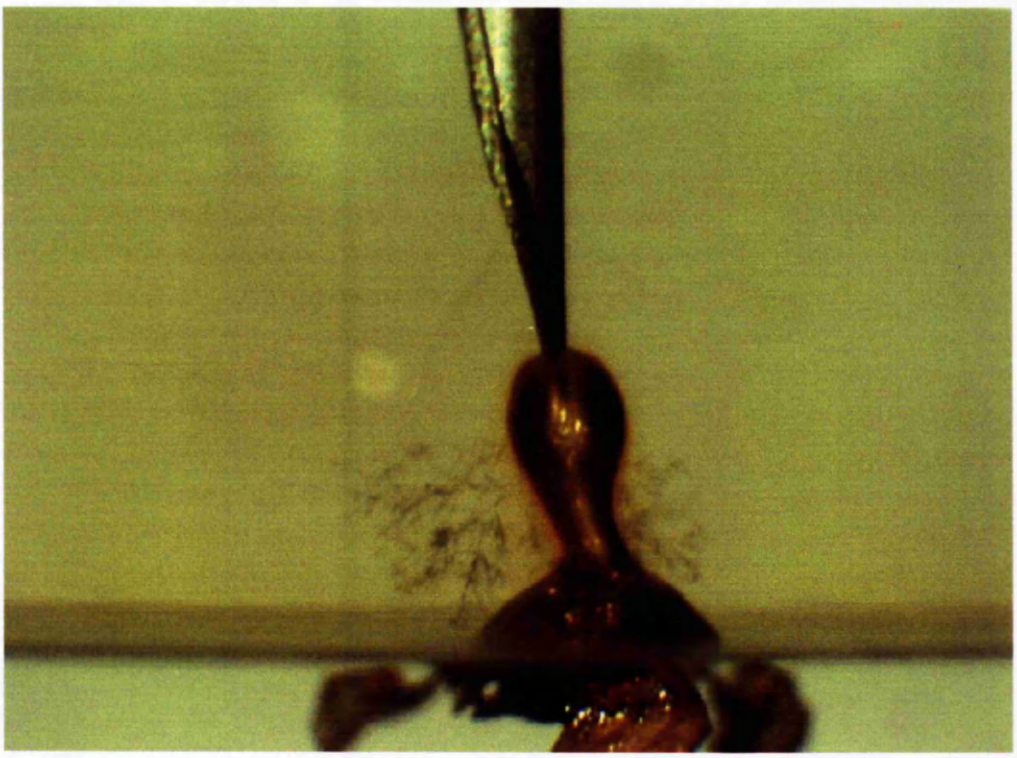

PRE-TENSIONED

Power ON at 4.00pm

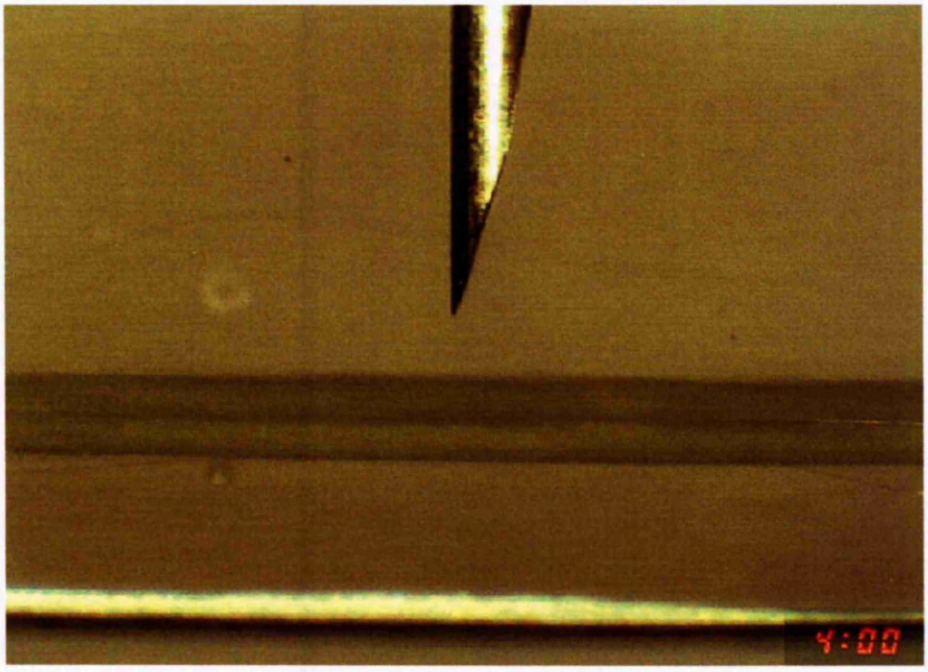

1 hour – Tree Initiates

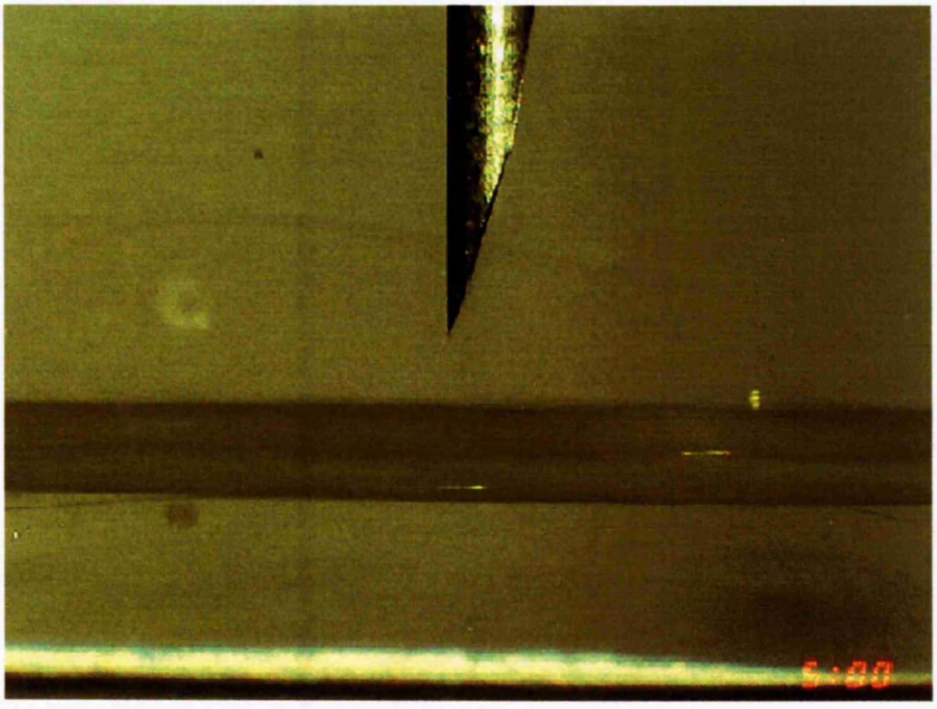

PRE-TENSIONED

2 hours – Propagation Time 1 hour

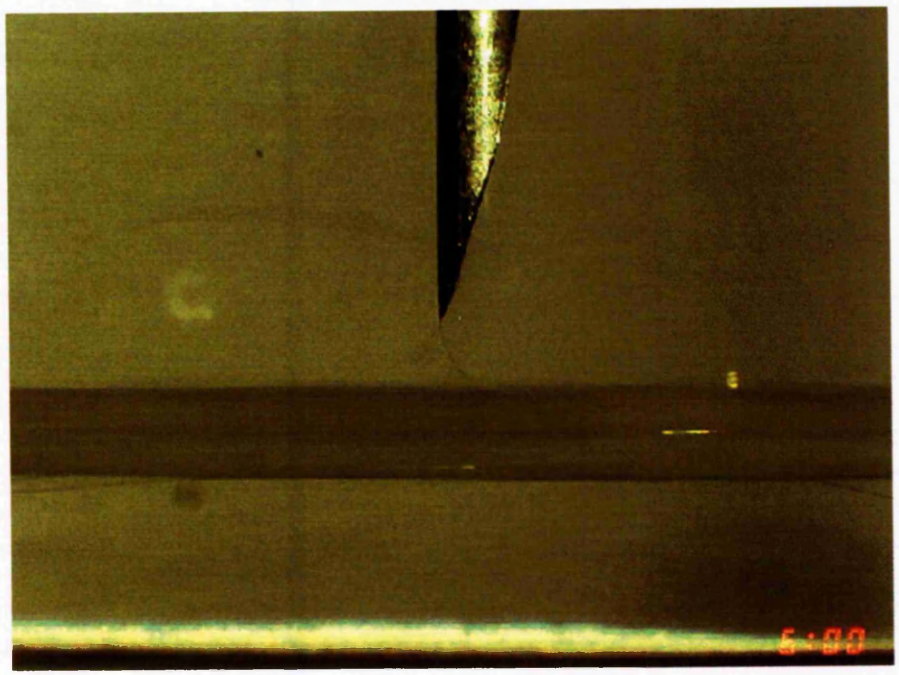

3 hours – Propagation Time 2 hours

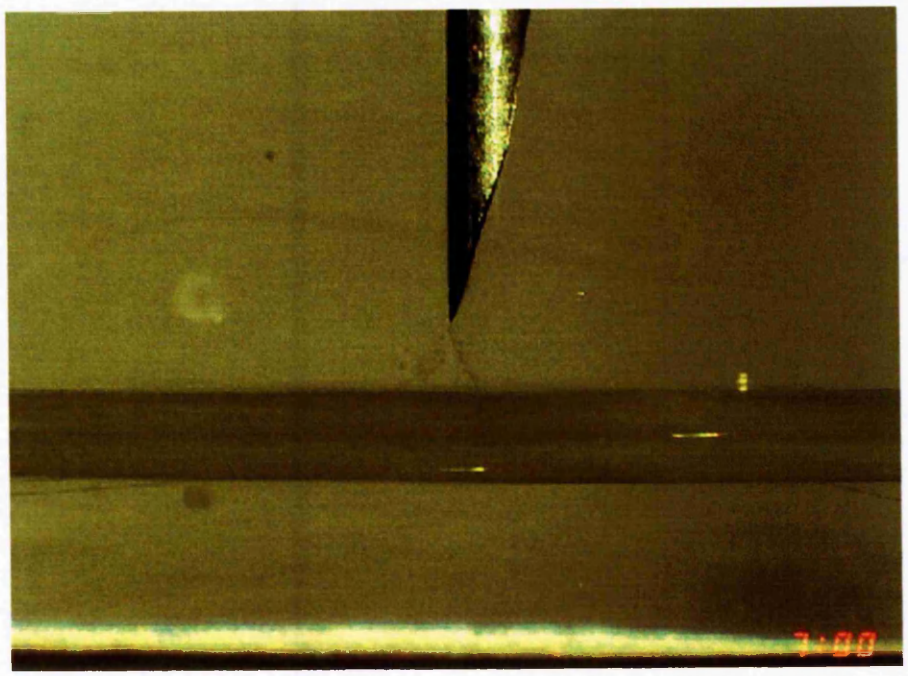

PRE-TENSIONED

4 hours – Propagation Time 3 hours

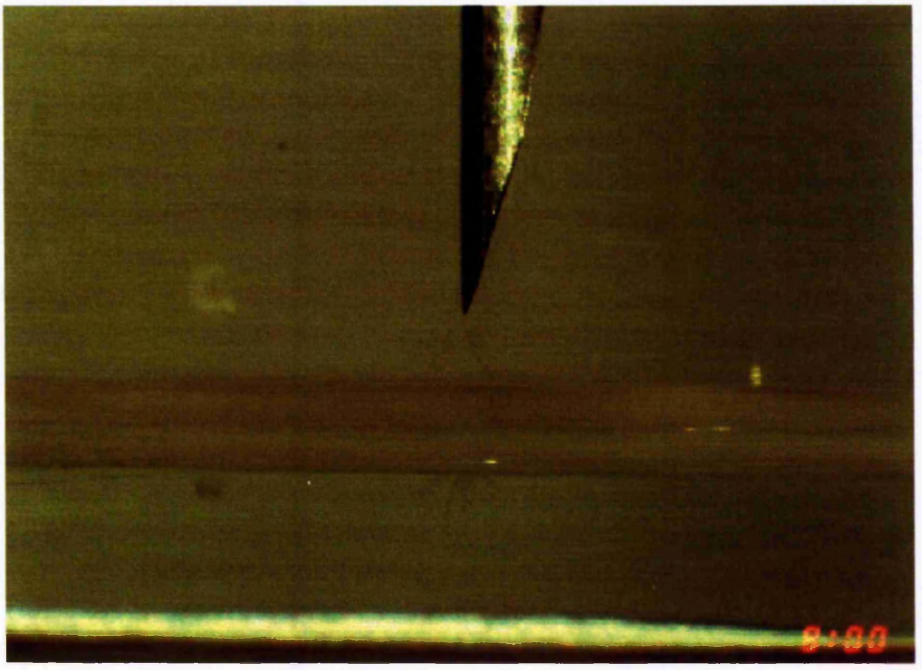

5 hours – Propagation Time 4 hours

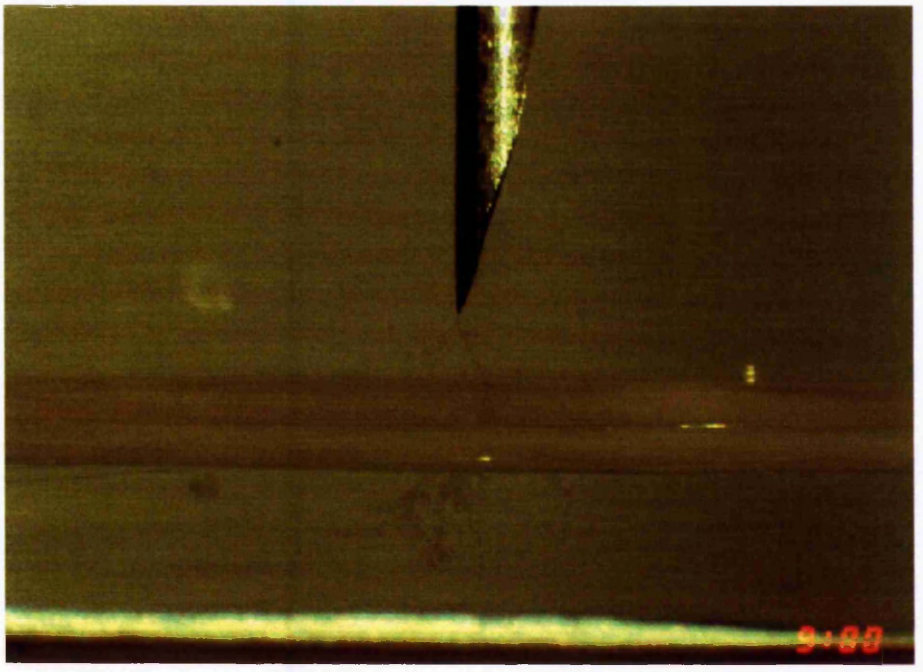

PRE-TENSIONED

6 hours – Propagation Time 5 hours

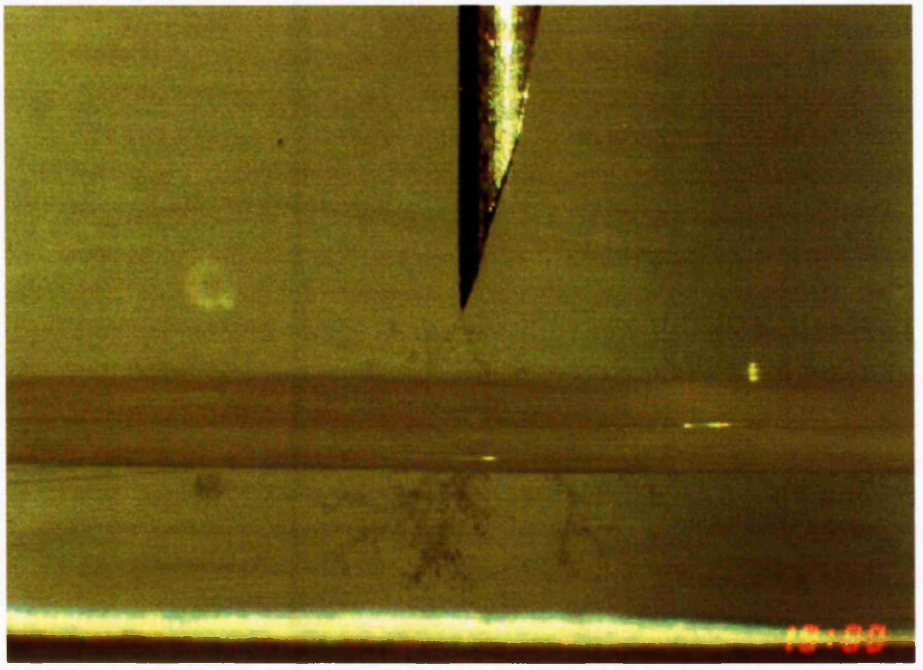

7 hours – Propagation Finished 6 hours

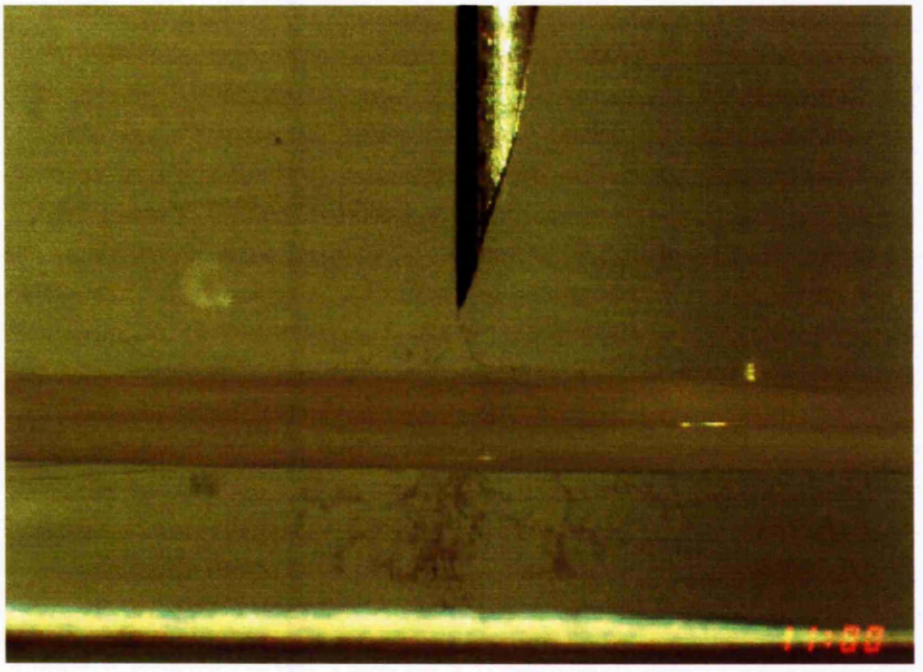

PRE-TENSIONED

8 hours – Return-failure Stage (Initiation + 7 hours)

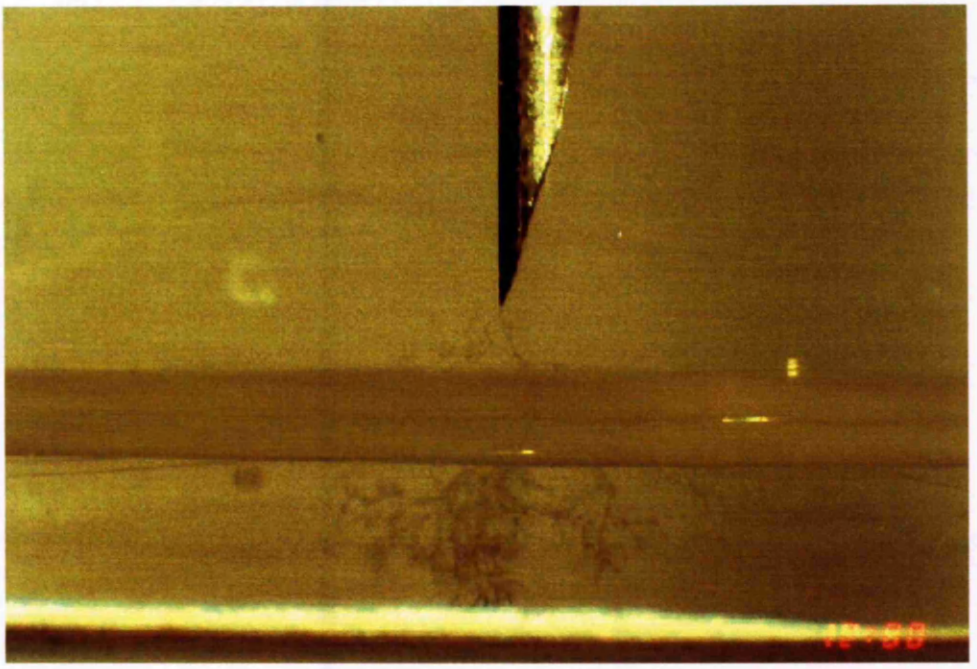

20 hours – Return-failure Stage (Initiation + 19 hours)

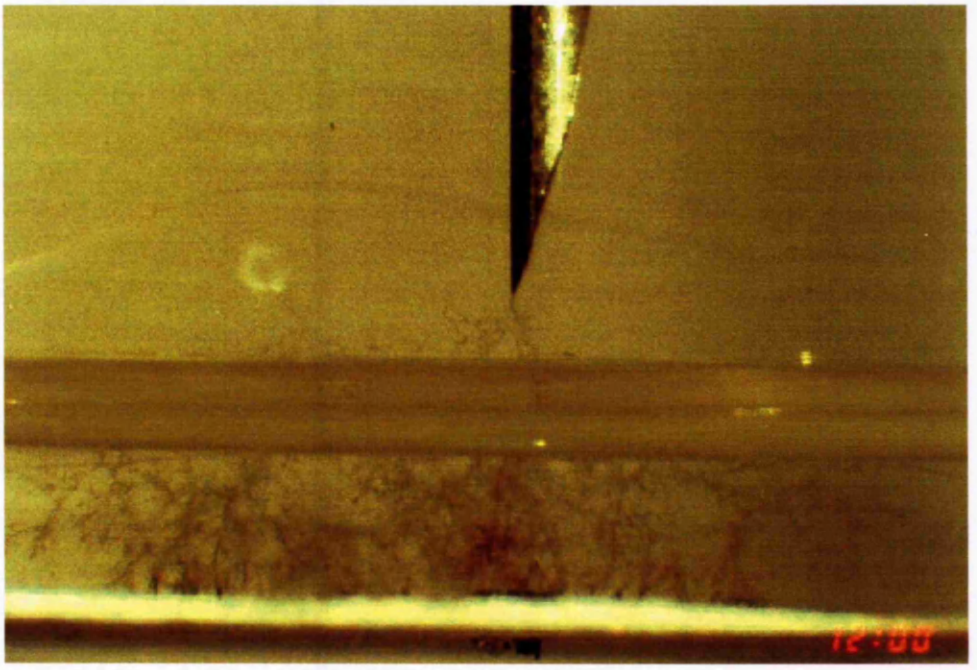

PRE-TENSIONED

45 hours – 45 minutes before Breakdown

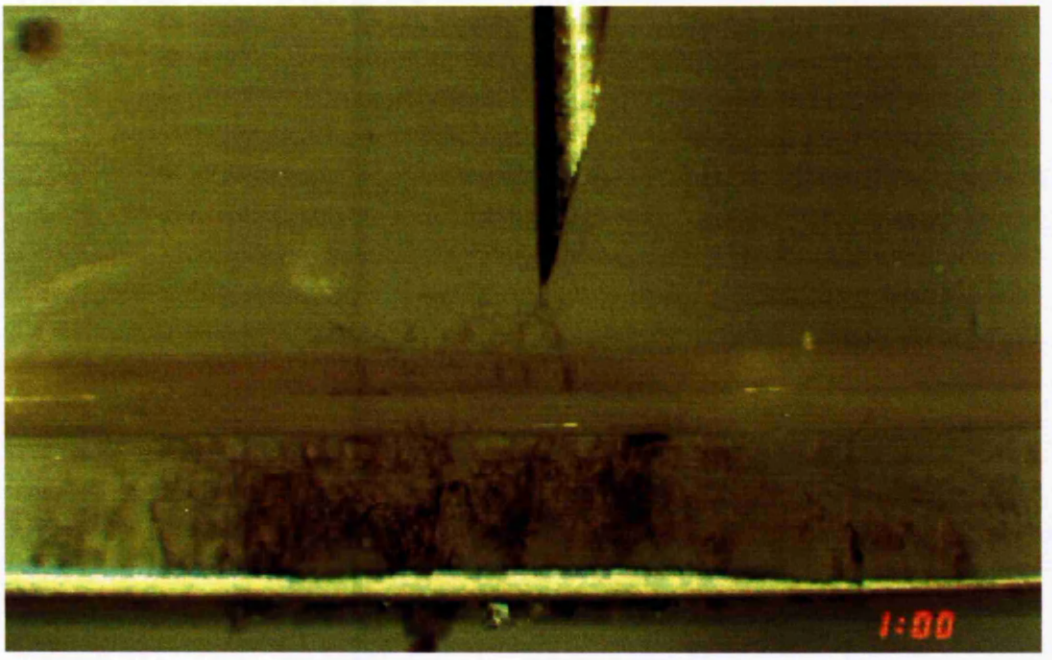

45 hours 45 minutes – BREAKDOWN (Initiation + 44 hours 45 minutes)

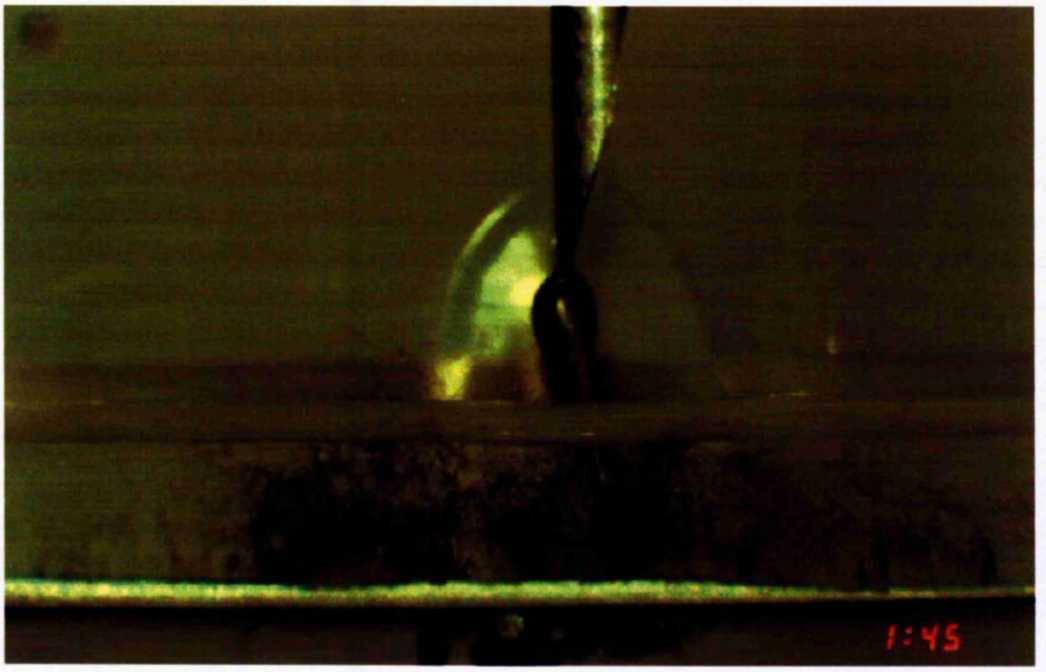

Appendix 10

PRE-STRESSED

10 hours – No Tree

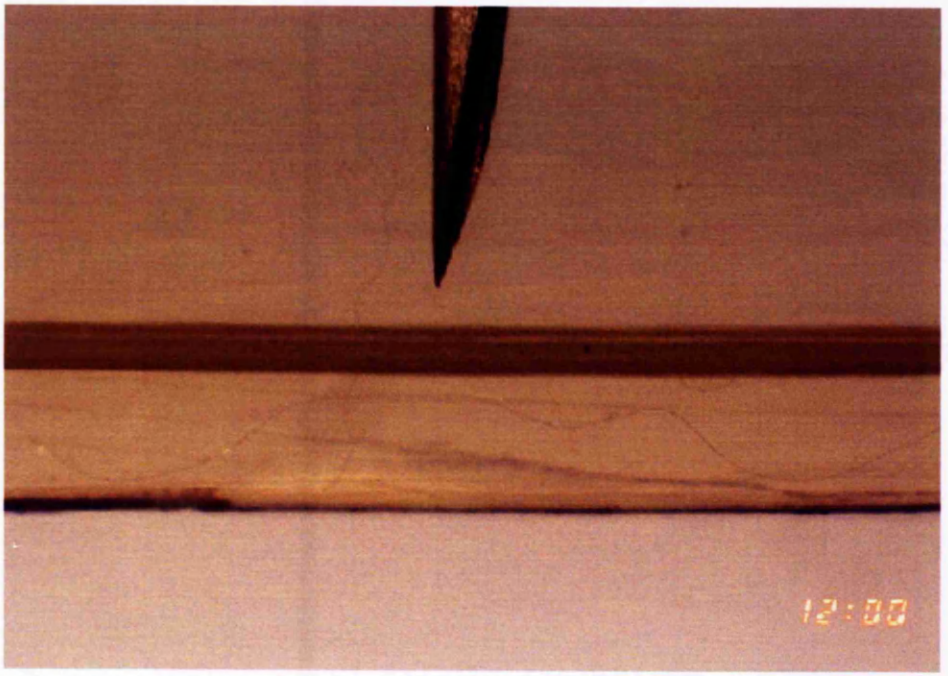

12 hours – No Tree

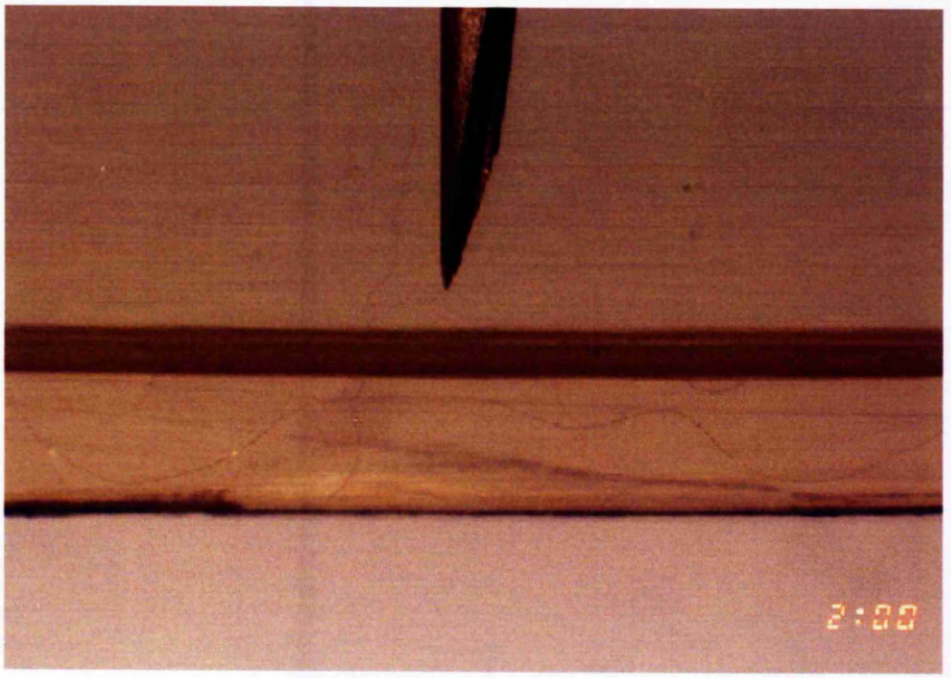

PER-STRESSED

14 hours - Tree Initiated

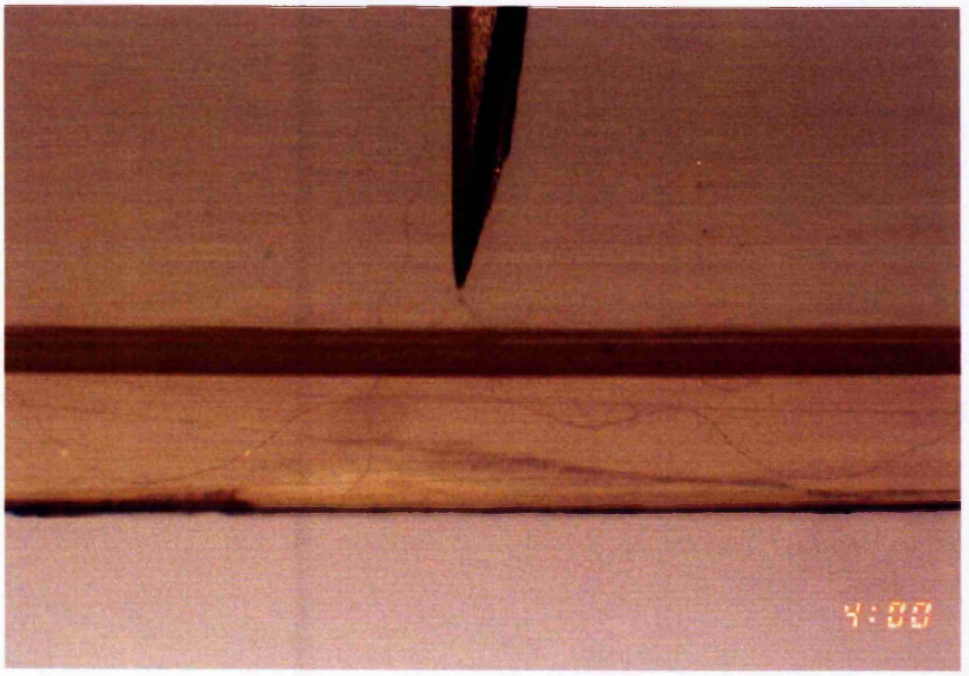

16 hours – Propagation Finished 2 hours

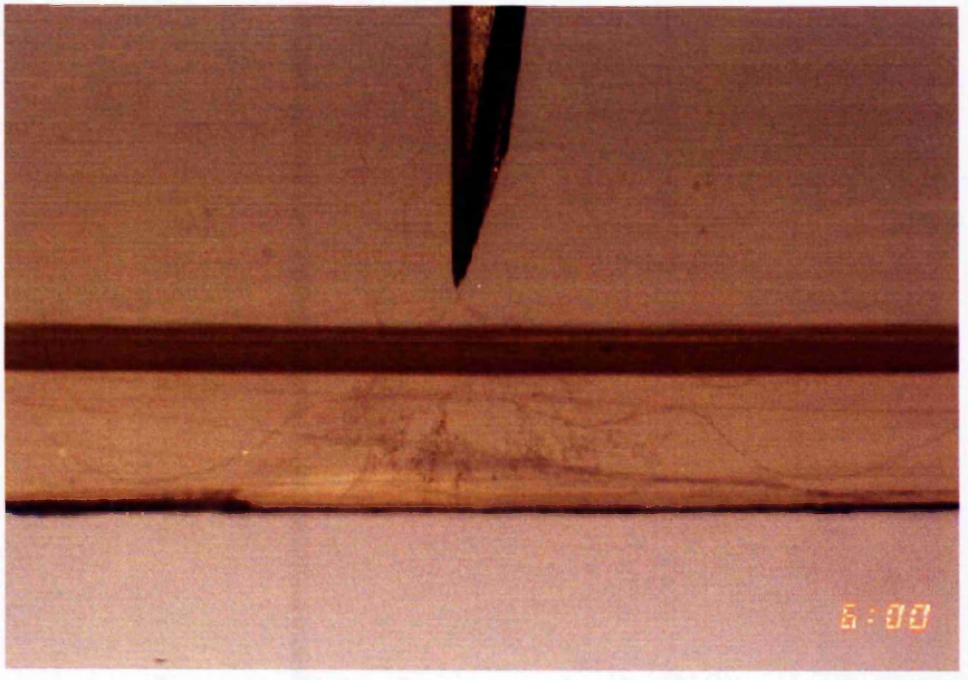

PRE-STRESSED

18 hours - Return-failure Stage (Initiation + 4 hours)

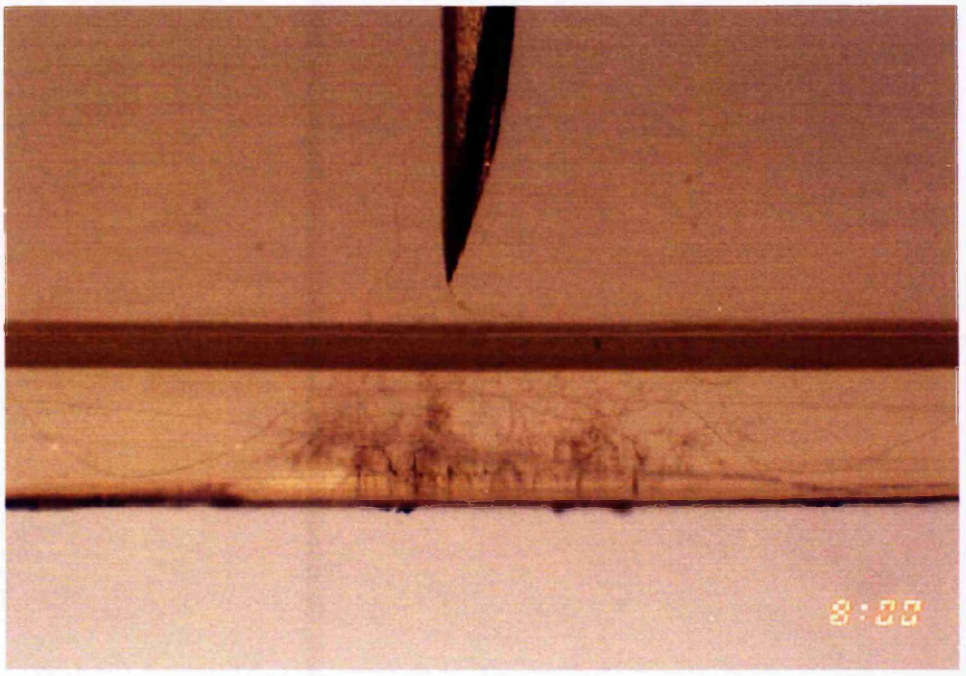

30 hours - Return-failure Stage (Initiation + 16 hours)

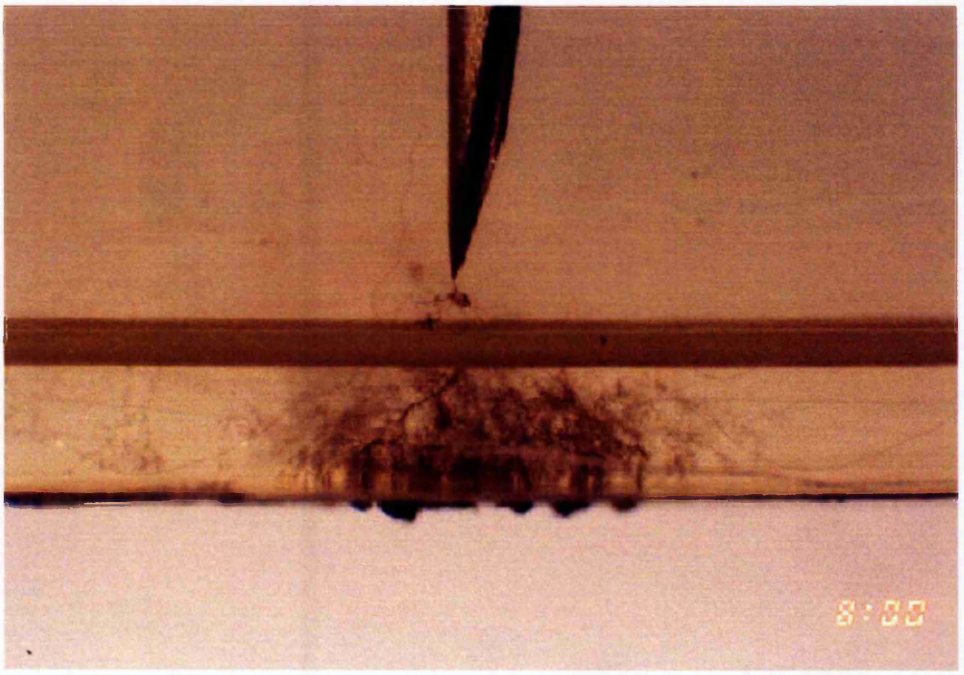

PRE-STRESSED

36 hours – 1 minute before Breakdown

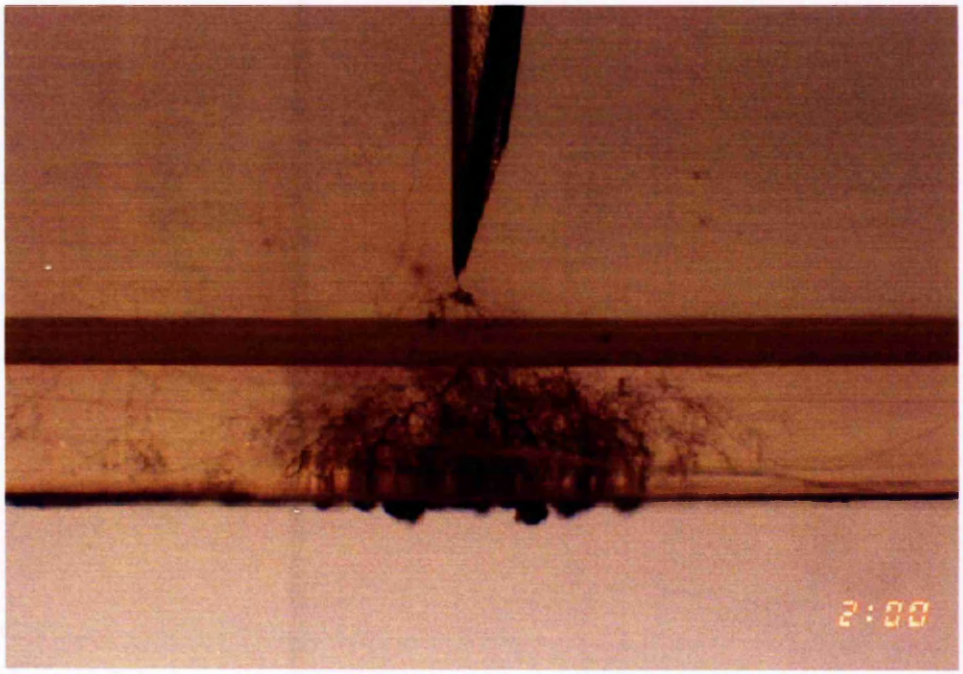

36 hours 1 minute – BREAKDOWN (Initiation + 22 hours 1 minute)

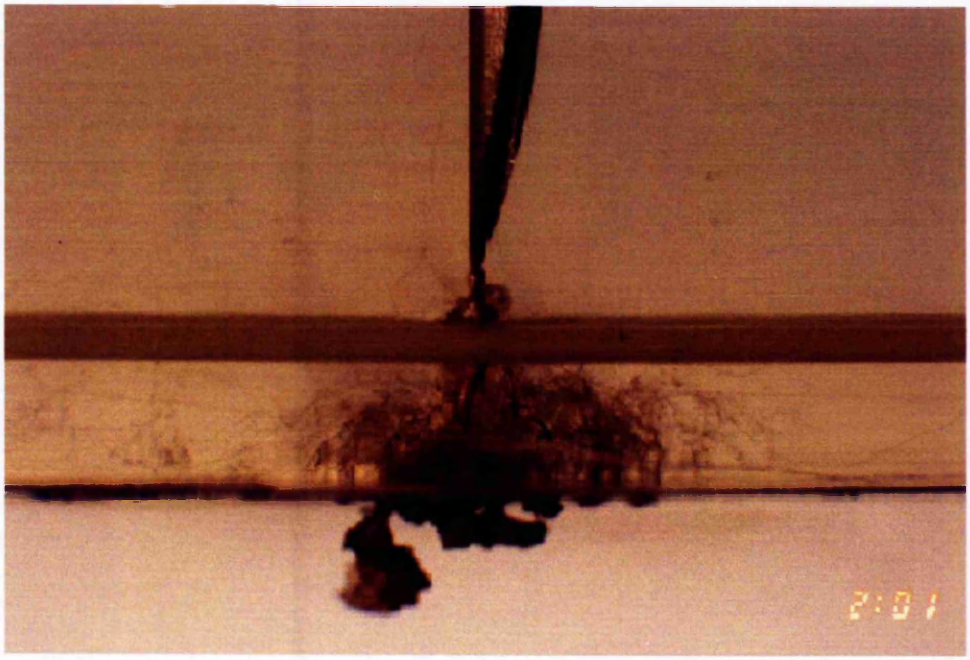

Appendix 11

Photographs of Tungsten Needle Samples

This Appendix contains sets of photographs of pin samples containing tungsten needles showing the treeing process from initiation through to breakdown.

Time indicated in bottom right-hand corner is actual time (am or pm) the photograph was taken (not a duration time). Duration times are given above each photograph.

List of Photographs in Appendix 11

PLAIN

Plain Tungsten, Batch No. 02, Needle No. 1 – Photo Set **PT02N2**

Taken from 9 Month Schedule – see full results in *Appendix 9*

PRE-TENSIONED

Pre-Tensioned Tungsten, Batch No. 1.1, Needle No. 4 – Photo Set **PTT11N4**

Taken from 9 Month Schedule – see full results in *Appendix 9*

PRE-STRESSED

Pre-Stressed Tungsten, Batch No. 3.1, Needle No. 3 – Photo Set **PST31N3**

Taken from 30 Day Schedule – see full results in *Appendix 8*

PLAIN

139 hours 15 minutes – No Tree

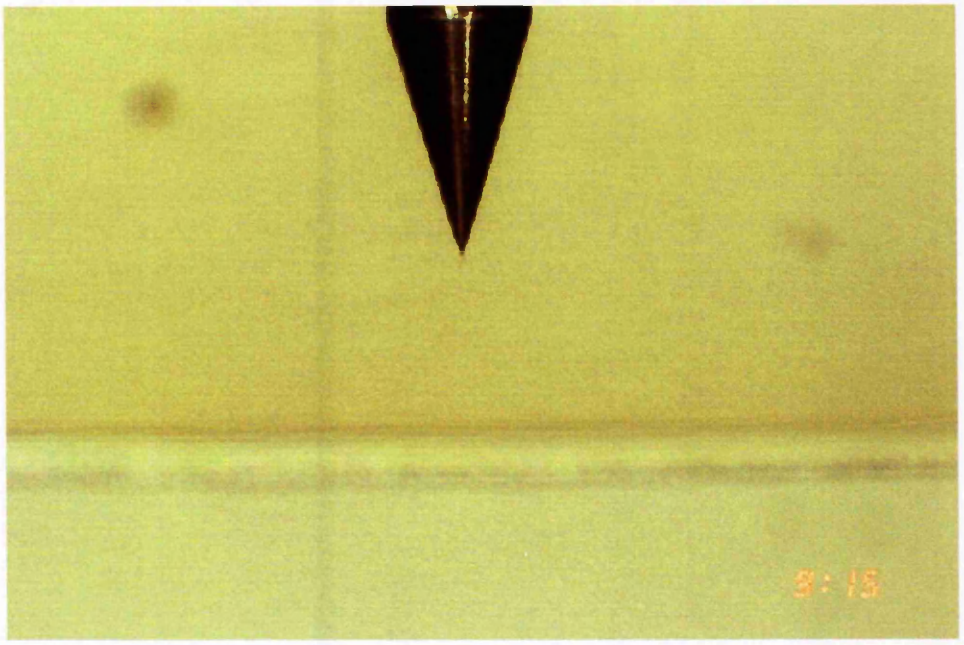

139 hours 45 minutes – Tree Initiates

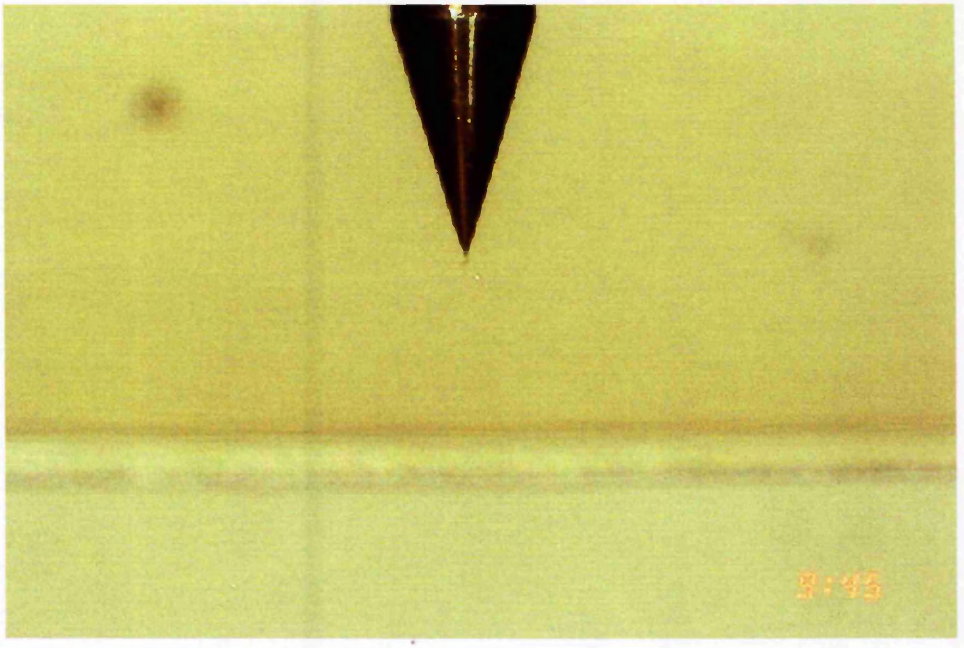

PLAIN

140 hours 45 minutes – Propagation Time 1 hour

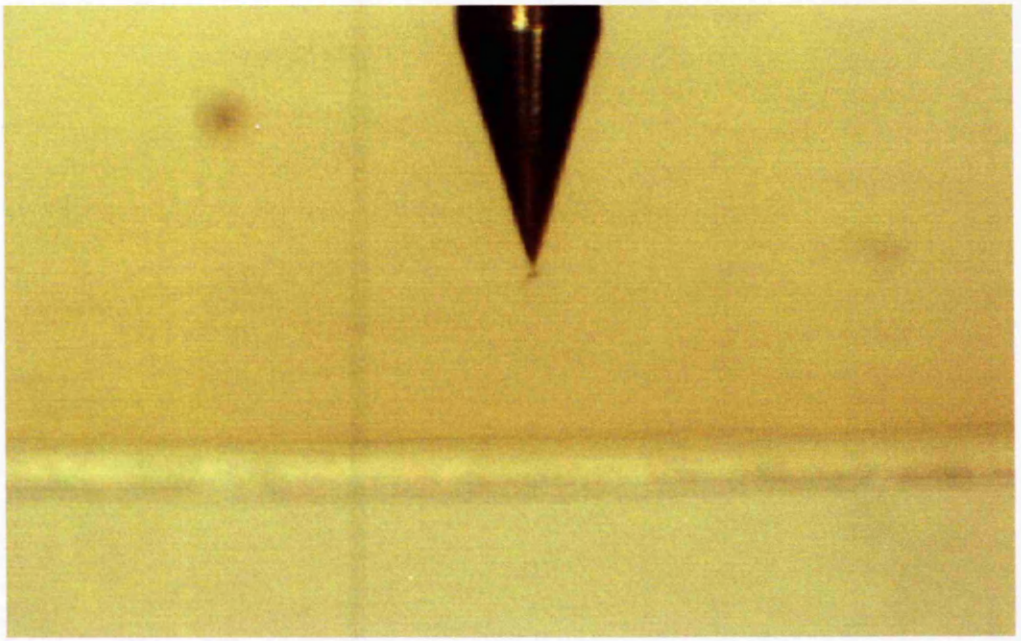

141 hours 45 minutes – Propagation Time 2 hours

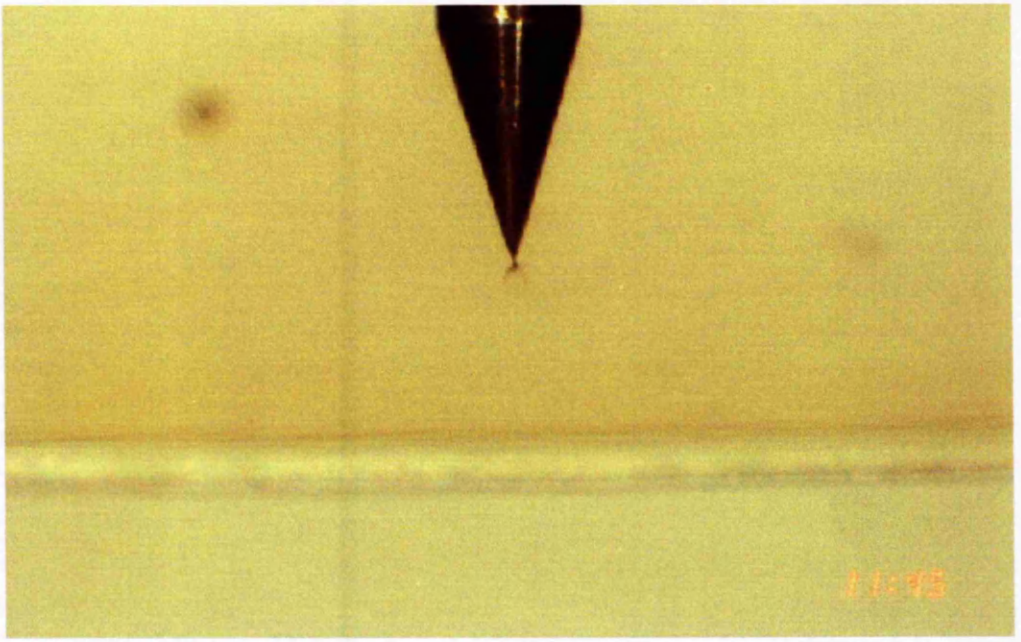

PLAIN

142 hours 45 minutes – Propagation Time 3 hours

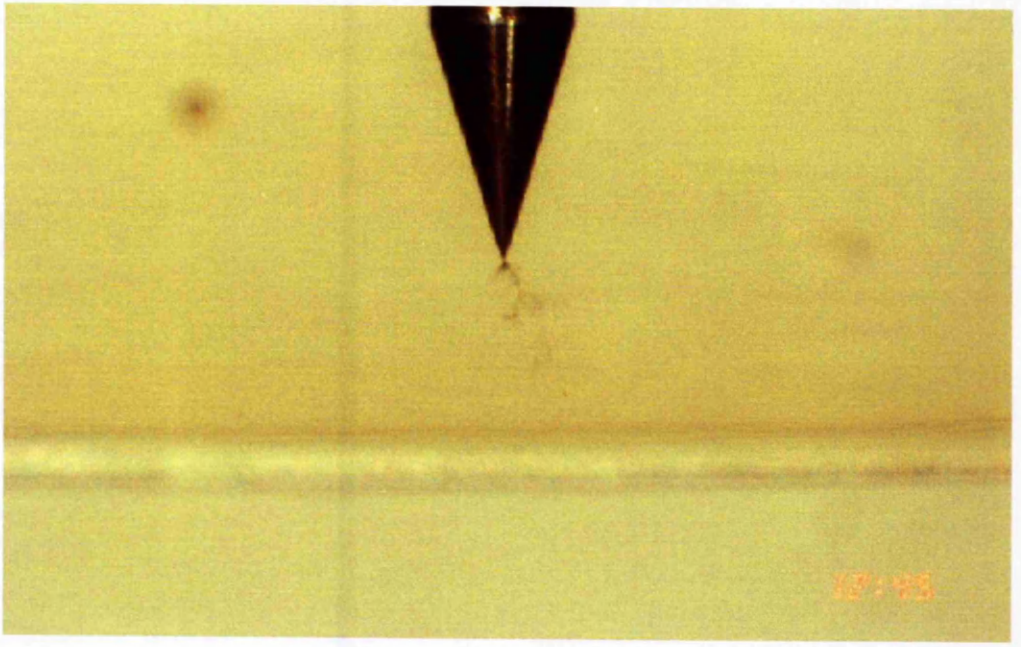

143 hours 45 minutes – Propagation Time 4 hours

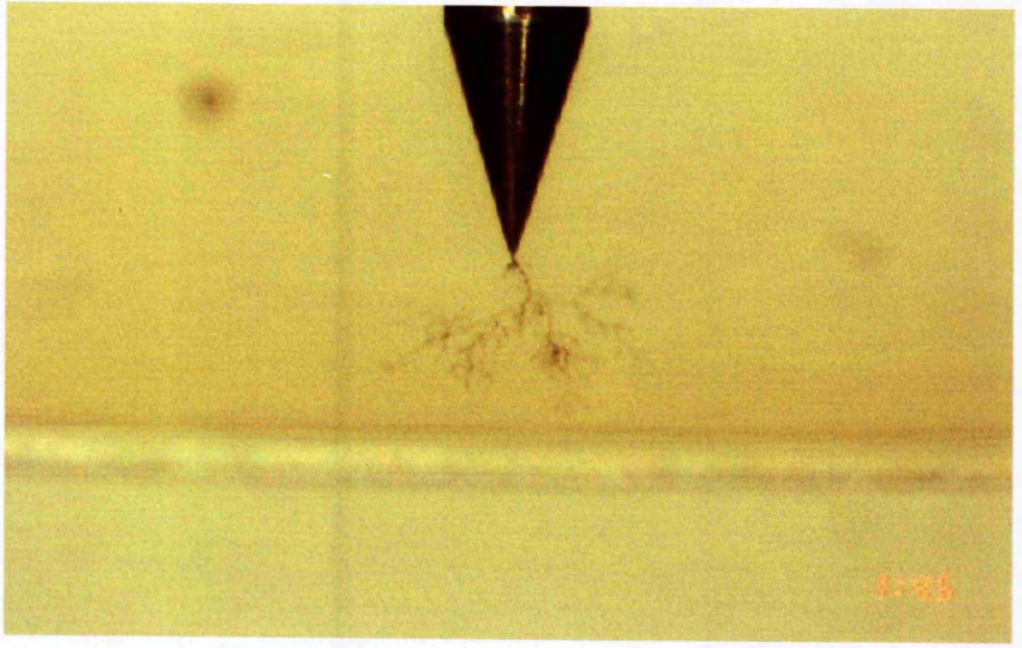

PLAIN

144 hours 15 minutes – Propagation Time 4 hours 30 minutes

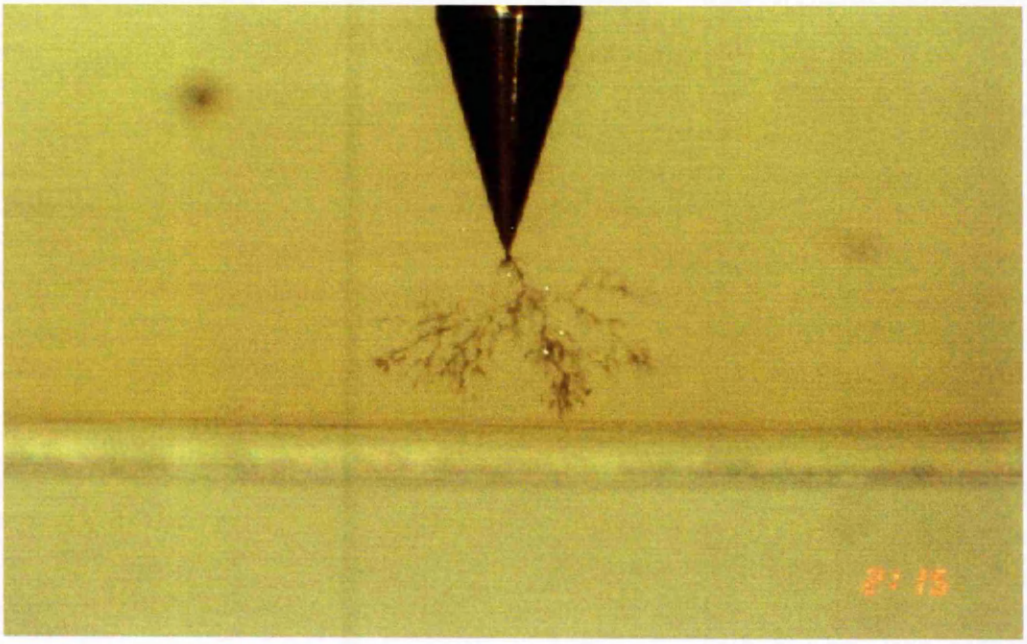

144 hours 20 minutes – Propagation Finished 4 hours 35 minutes

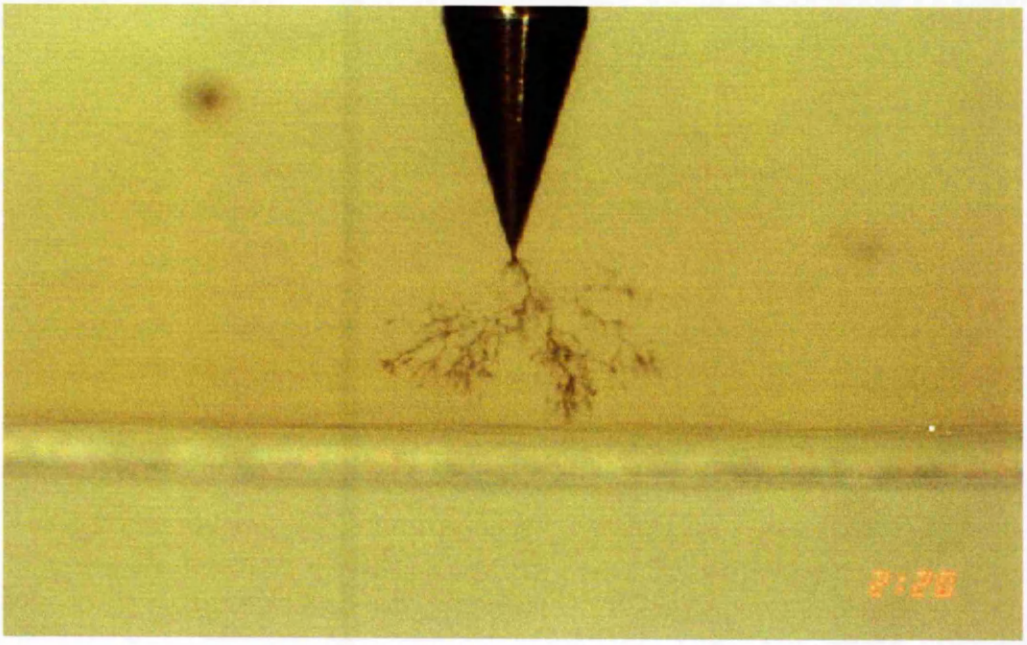

PLAIN

144 hours 45 minutes – Return-failure Stage (Initiation + 5 hours)

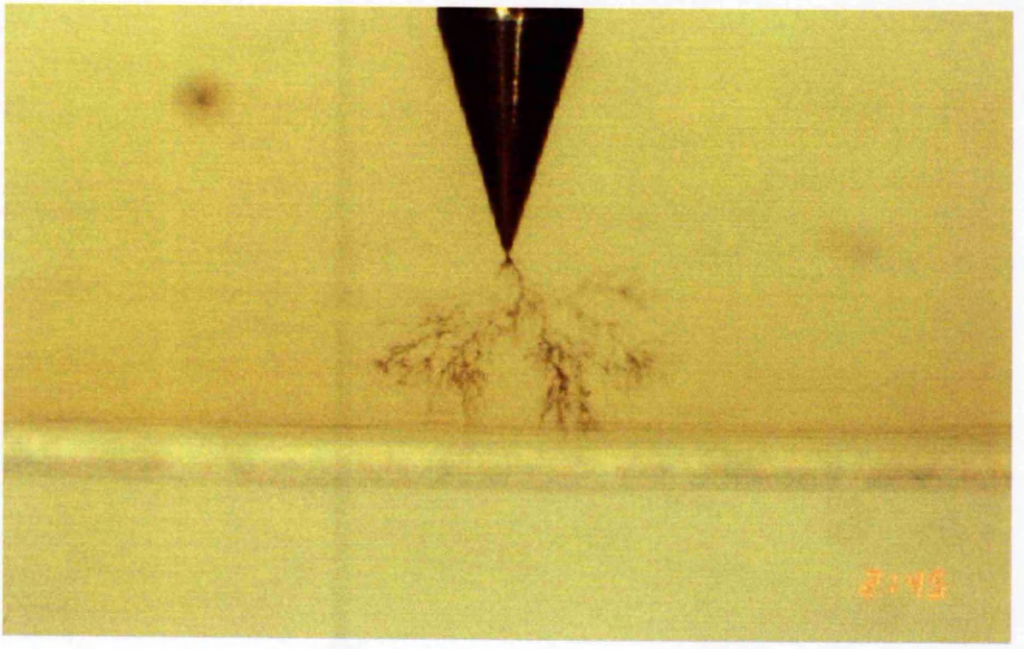

145 hours 15 minutes – BREAKDOWN (Initiation + 5 hours 30 minutes)

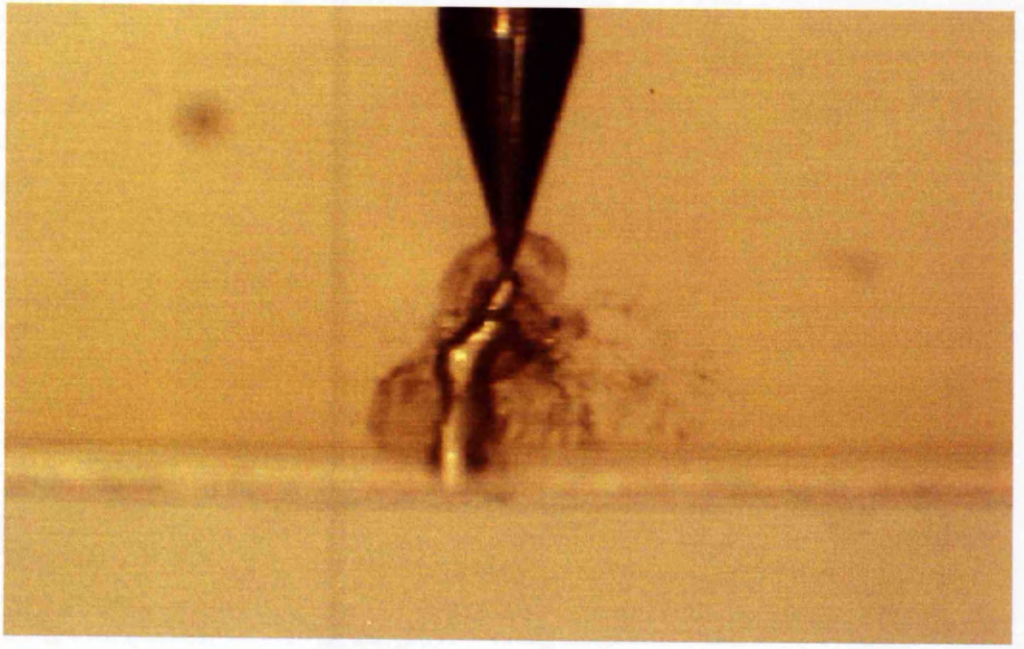

PRE-TENSIONED

384 hours 24 minutes – No Tree

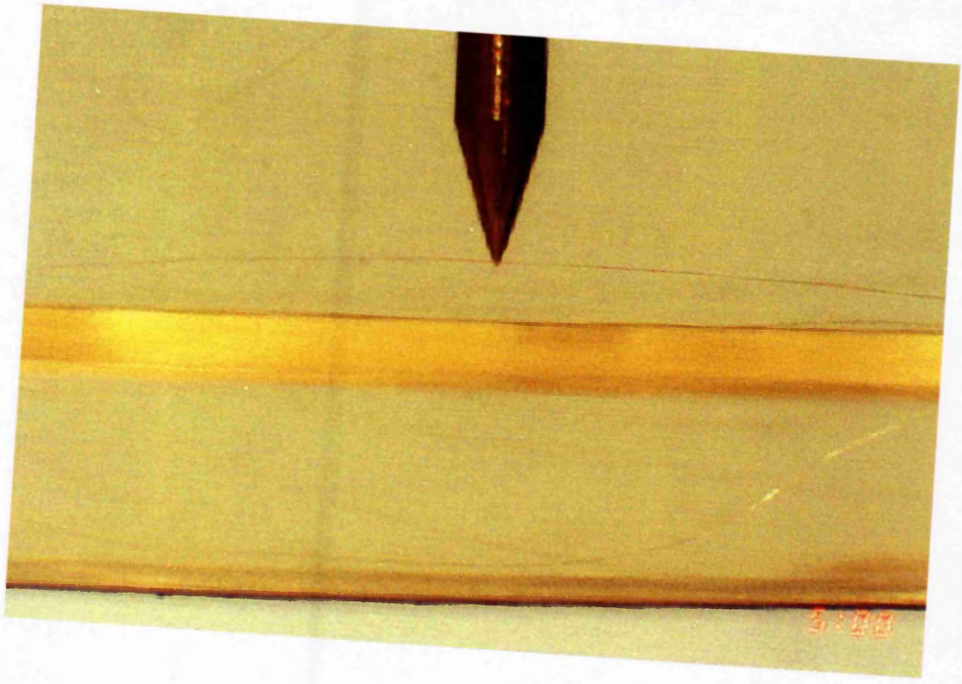

385 hours 24 minutes – Tree Initiates

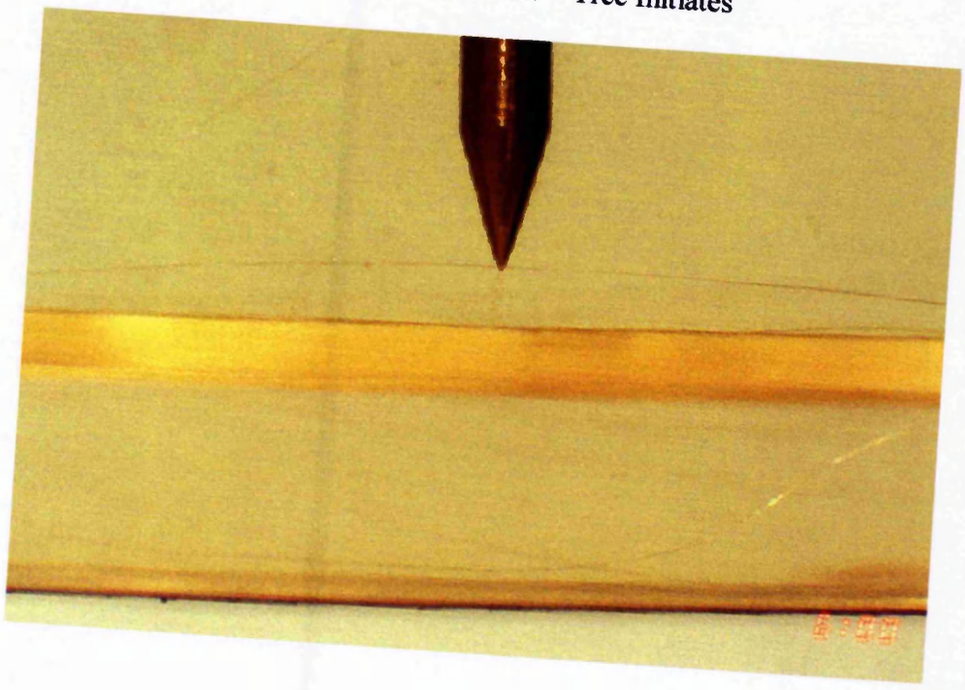

PRE-TENSIONED

386 hours 24 minutes – Propagation Time 1 hour

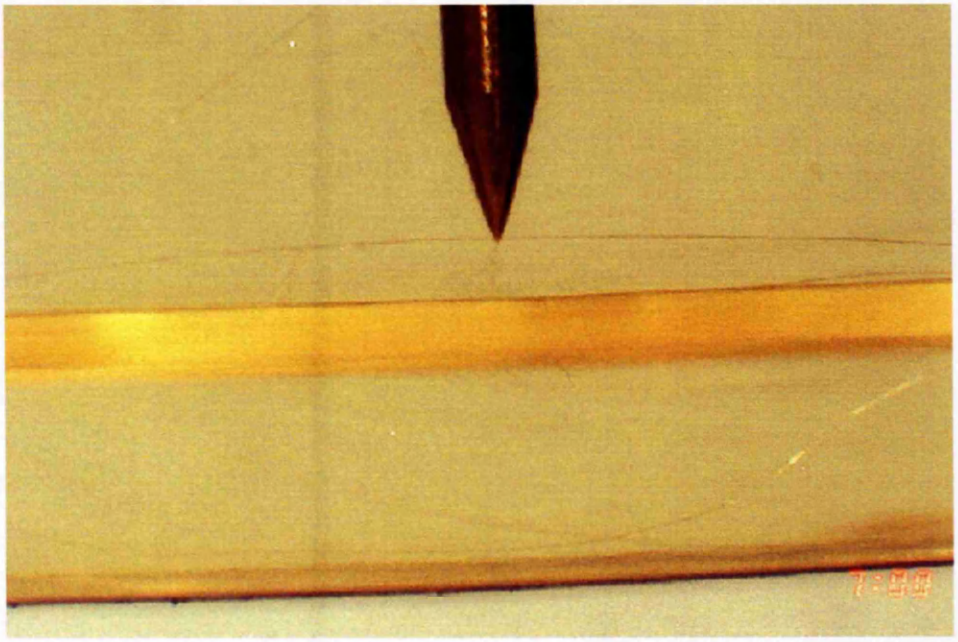

387 hours 24 minutes – Propagation Time 2 hours

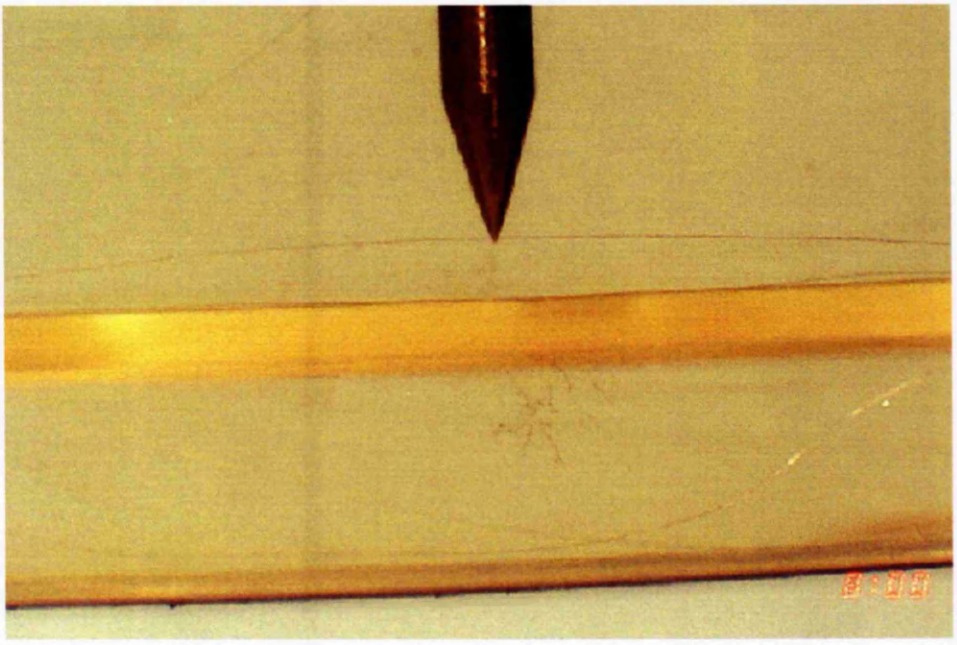

PRE-TENSIONED

388 hours 24 minutes – Propagation Time 3 hours

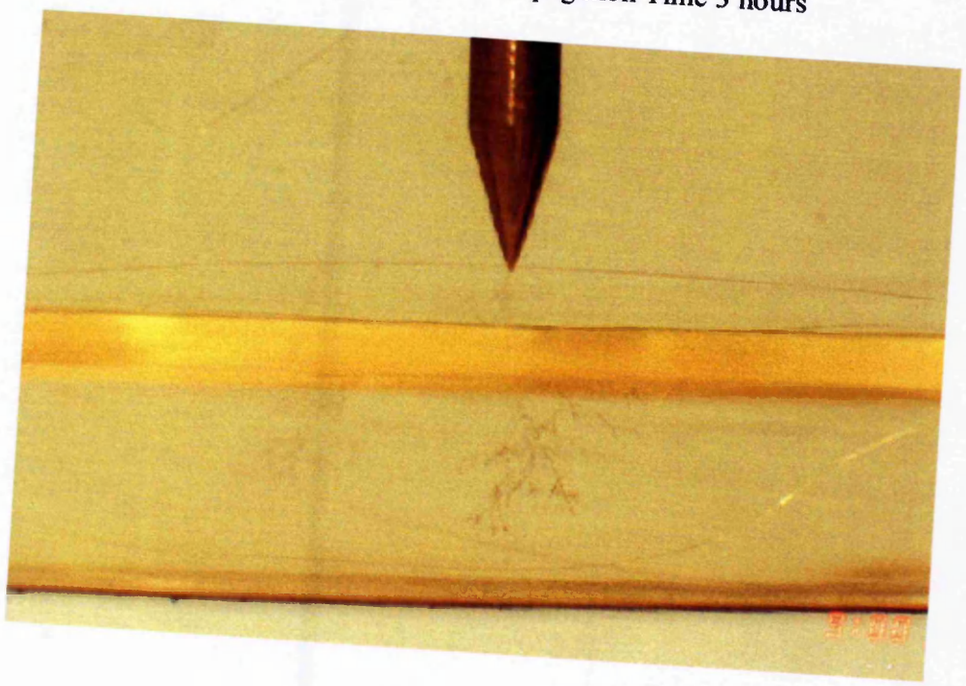

389 hours 24 minutes – Propagation Time 4 hours

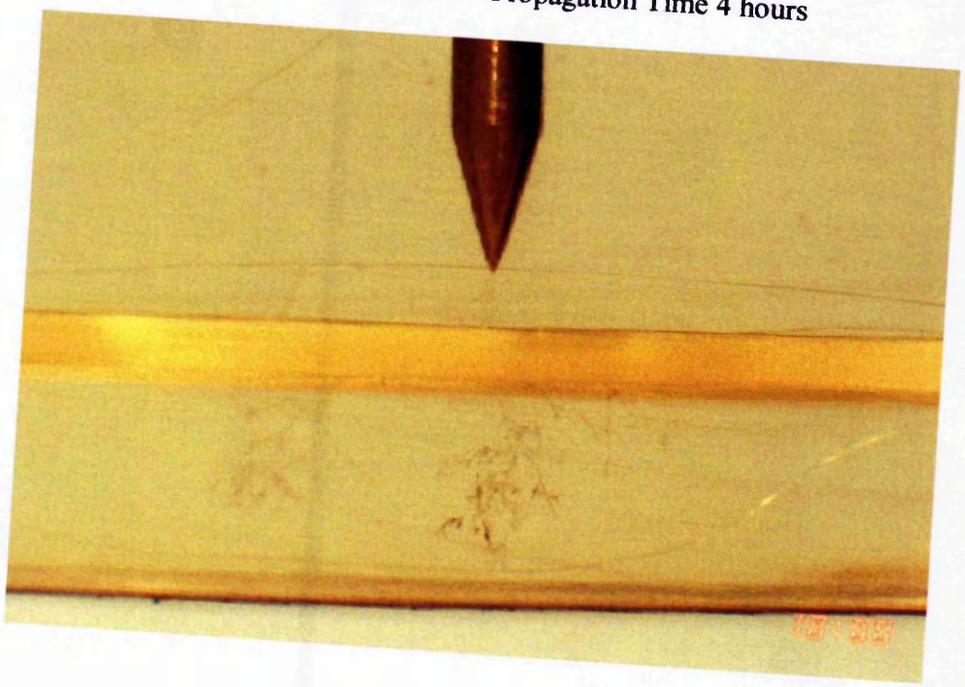

PRE-TENSIONED

390 hours 24 minutes – Propagation Finished 5 hours

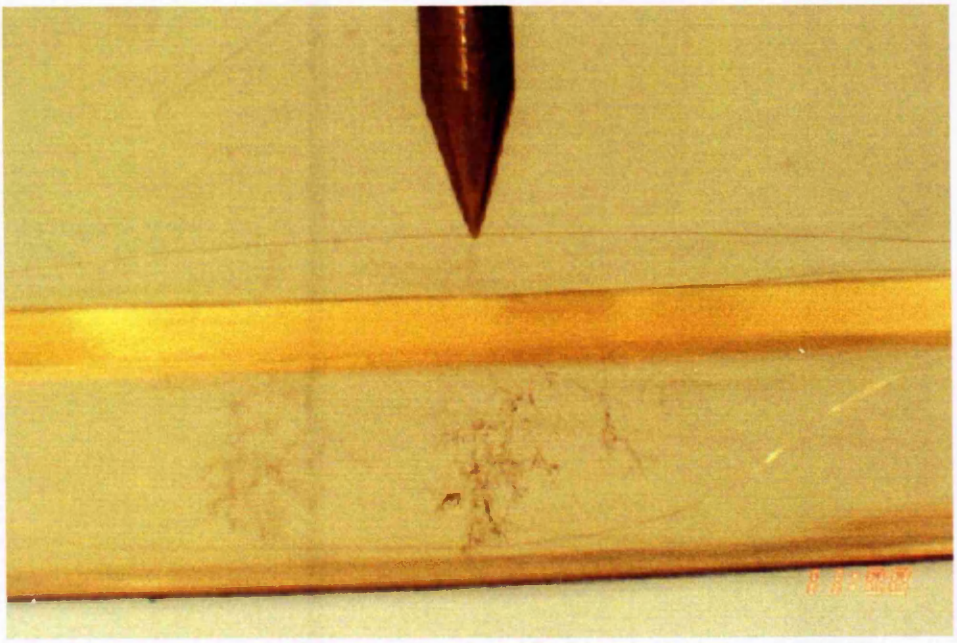

391 hours 24 minutes – Return-failure Stage (Initiation + 6 hours)

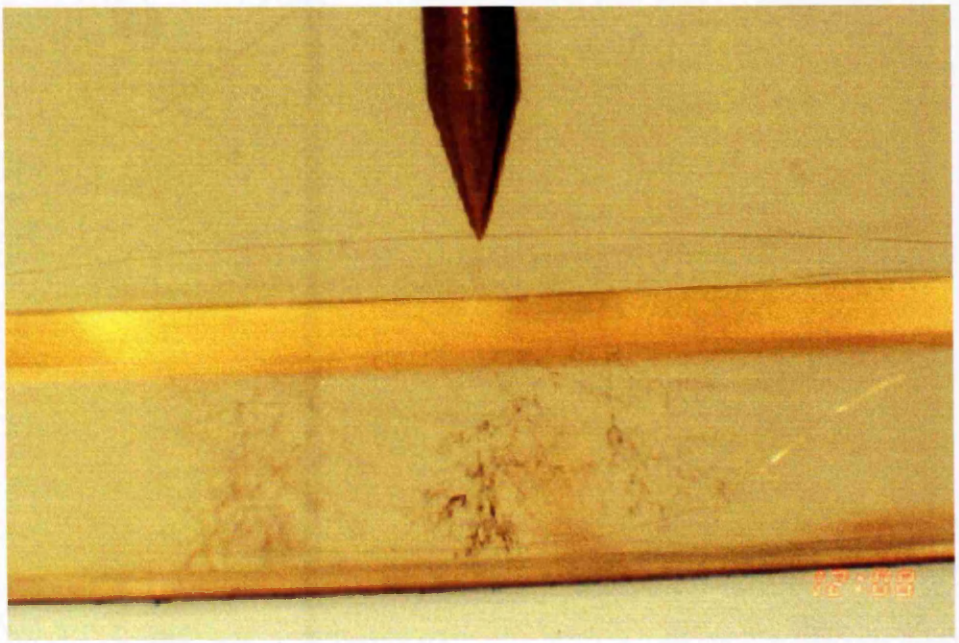

PRE-TENSIONED

403 hours 24 minutes – Return-failure Stage (Initiation + 18 hours)

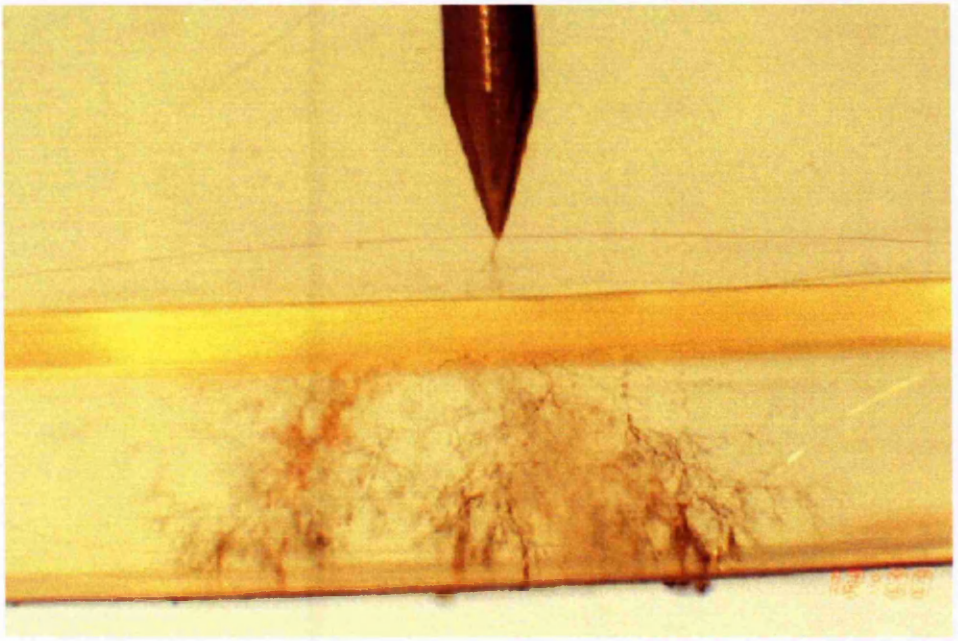

423 hours 54 minutes – BREAKDOWN (Initiation + 38 hours 30 minutes)

PRE-STRESSED

428 hours – No Tree

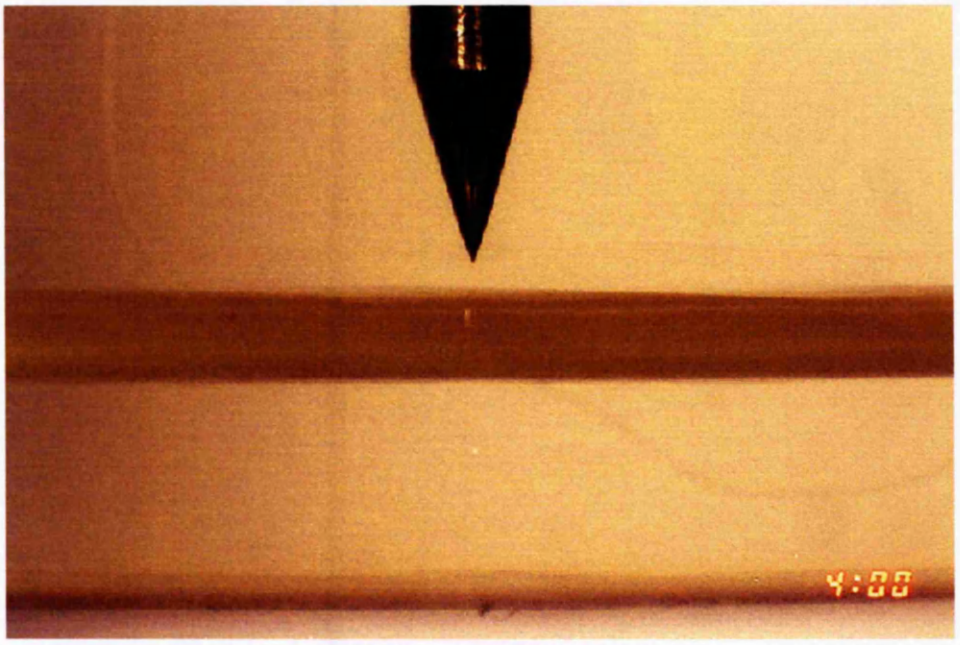

429 hours – Tree Initiates

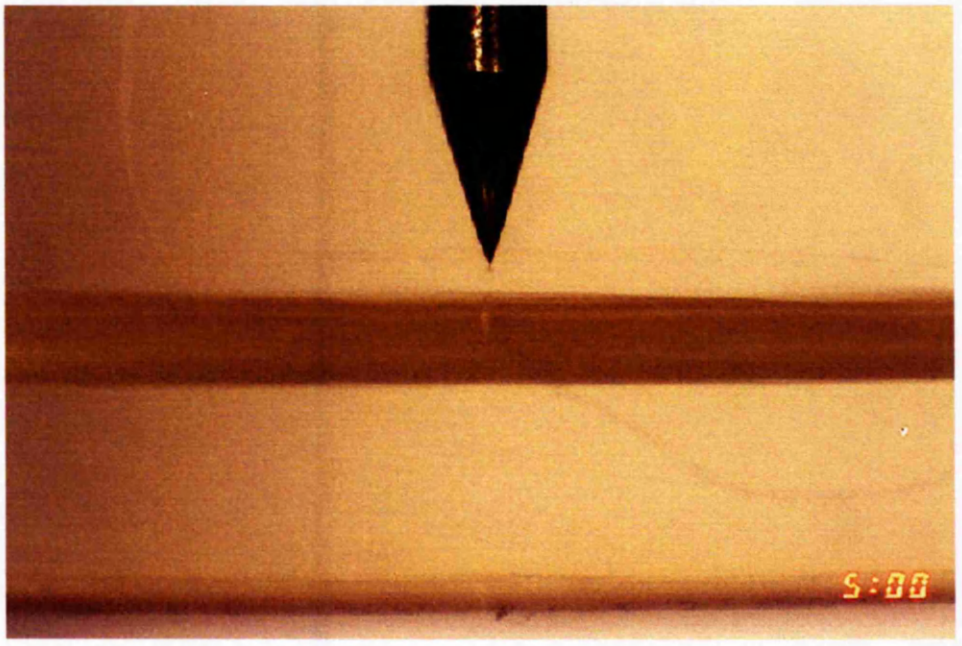

PRE-STRESSED

430 hours – Propagation Time 1 hour

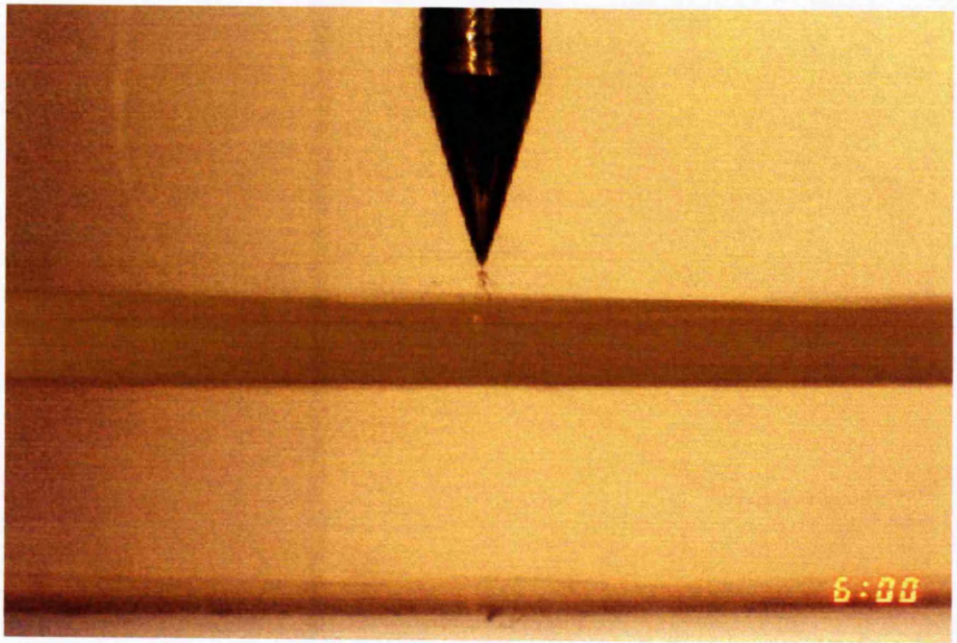

431 hours – Propagation Time 2 hours

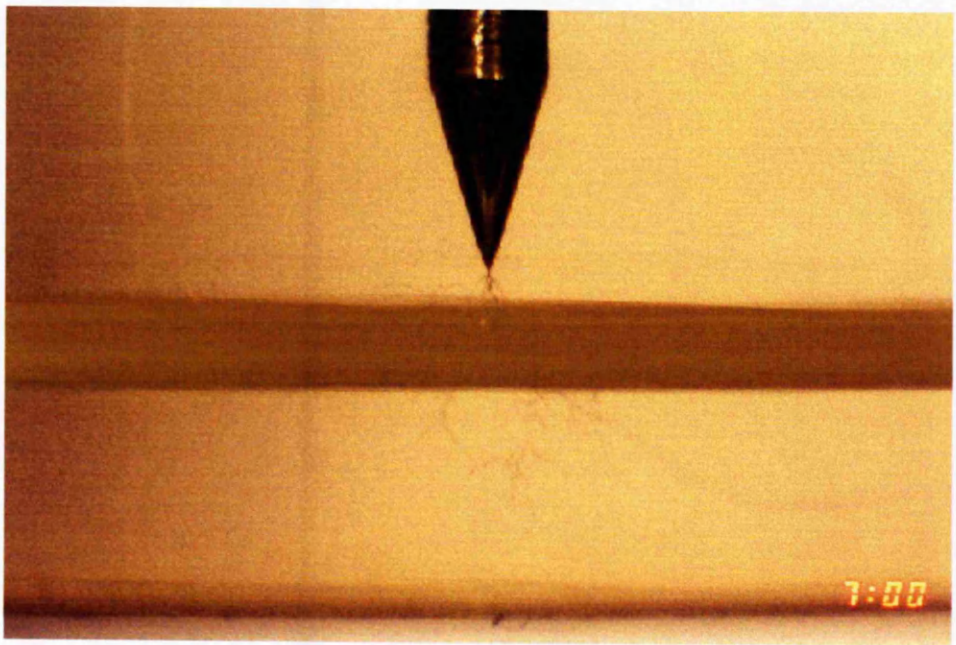

PRE-STRESSED

432 hours – Propagation Finished 3 hours

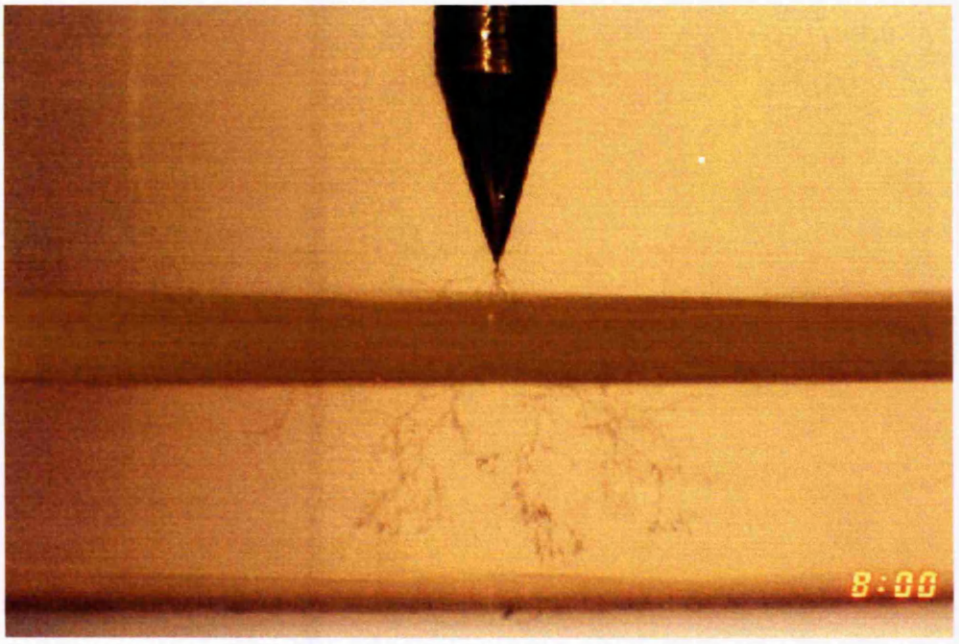

433 hours – Return-failure Stage (Initiation + 4 hours)

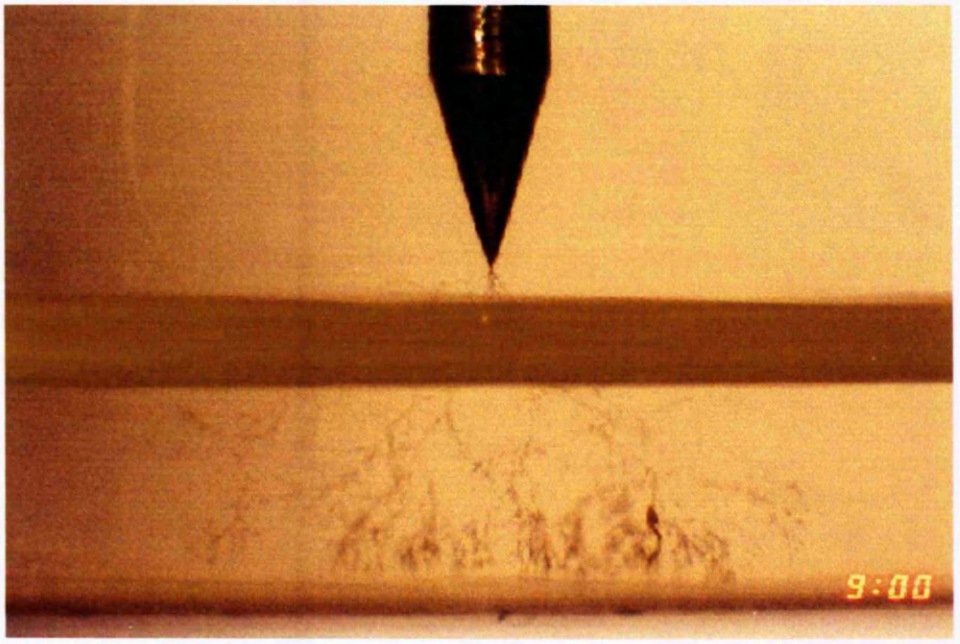

PRE-STRESSED

434 hours – Return-failure Stage (Initiation + 5 hours)

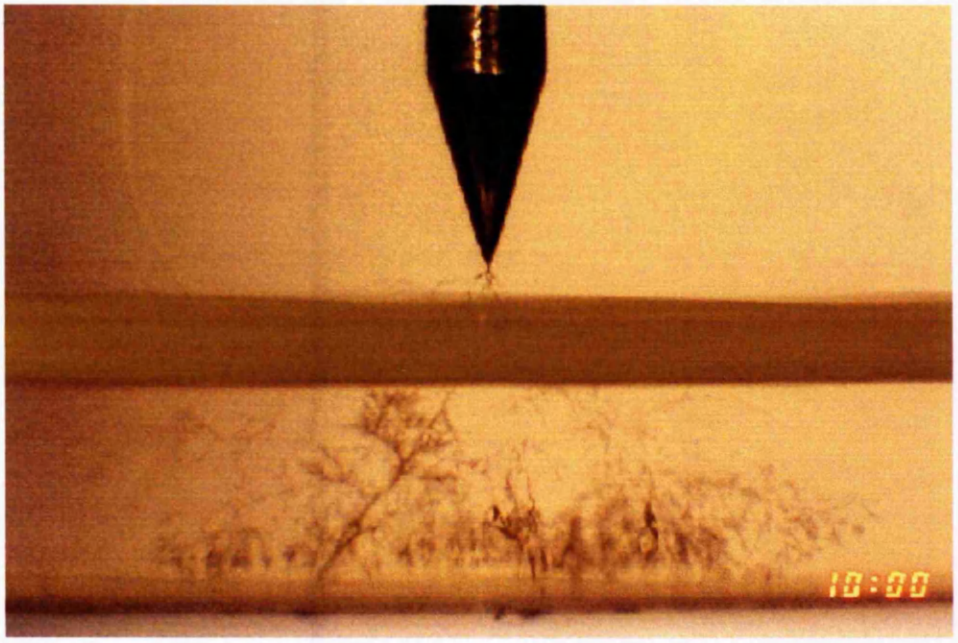

434 hours 30 minutes – Return-failure Stage (Initiation + 5 hours 30 minutes)

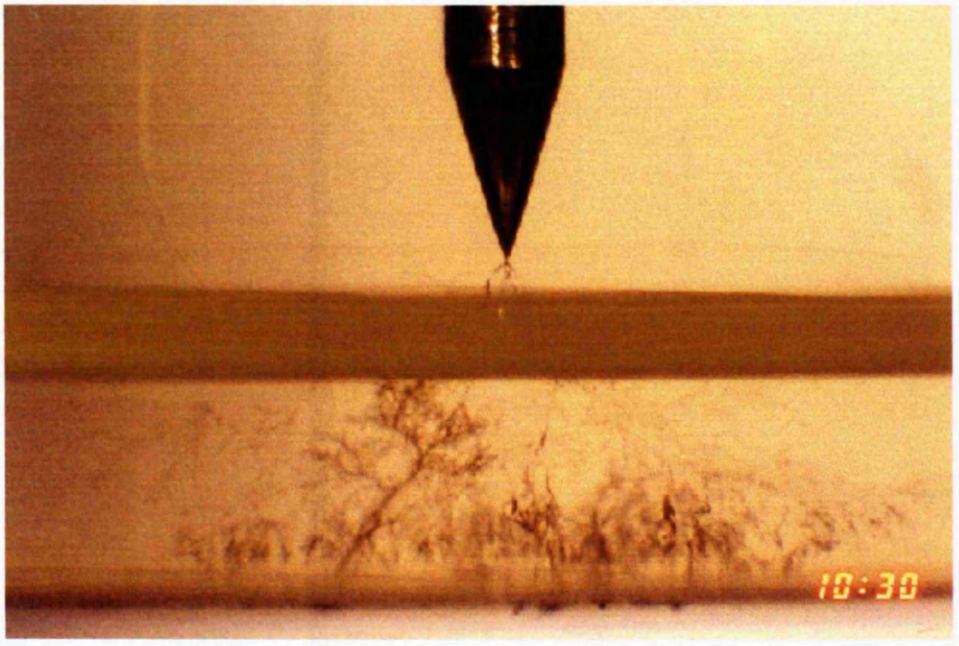

PRE-STRESSED

434 hours 35 minutes – Audible Discharge but sample does not fail (Author Present)

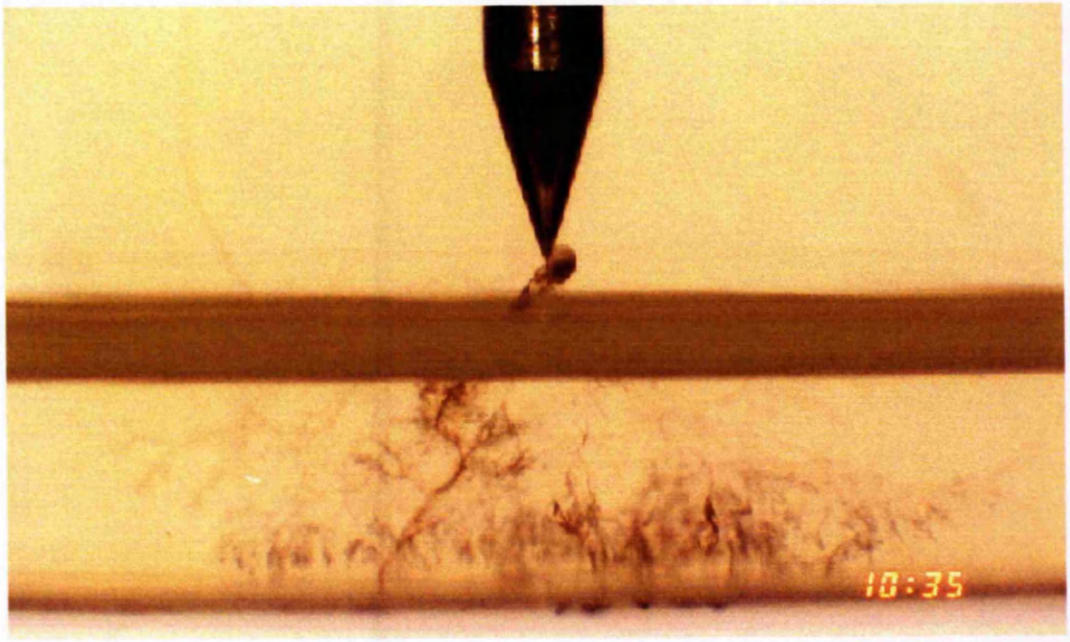

435 hours 30 minutes – Return-failure Stage (Initiation + 6 hours 30 minutes)

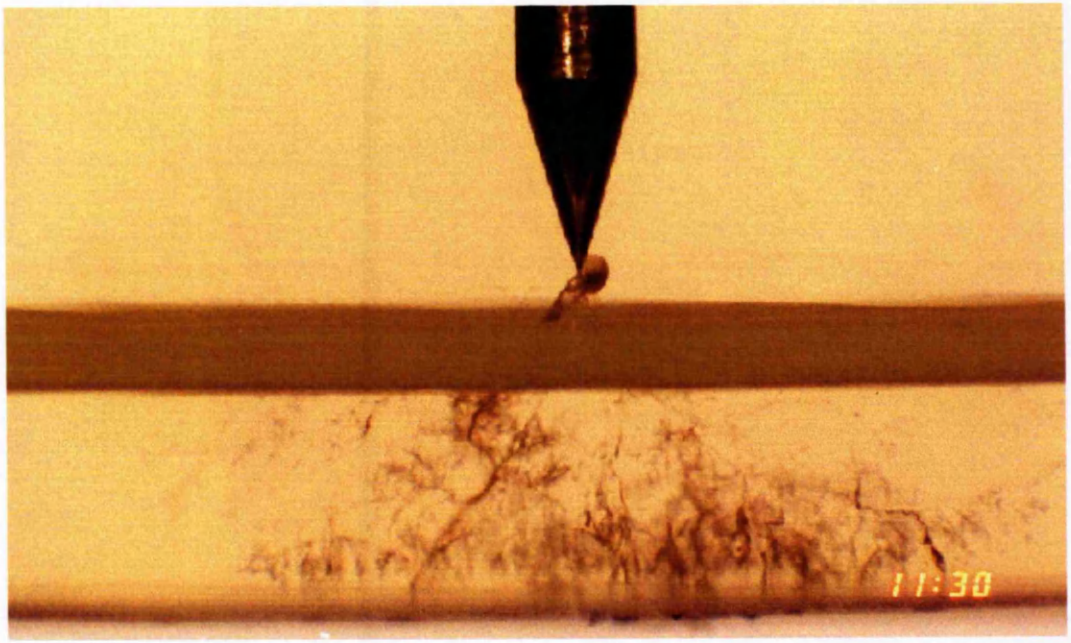

PRE-STRESSED

436 hours 30 minutes – Return-failure Stage (Initiation + 7 hours 30 minutes)

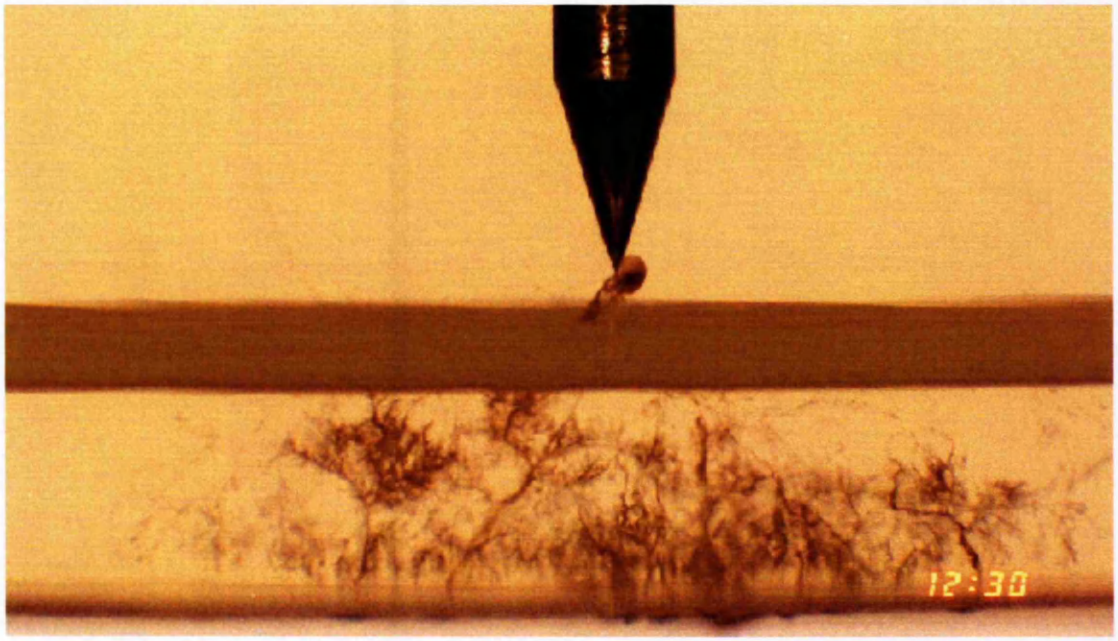

442 hours 30 minutes – Return-failure Stage (Initiation + 13 hours 30 minutes)

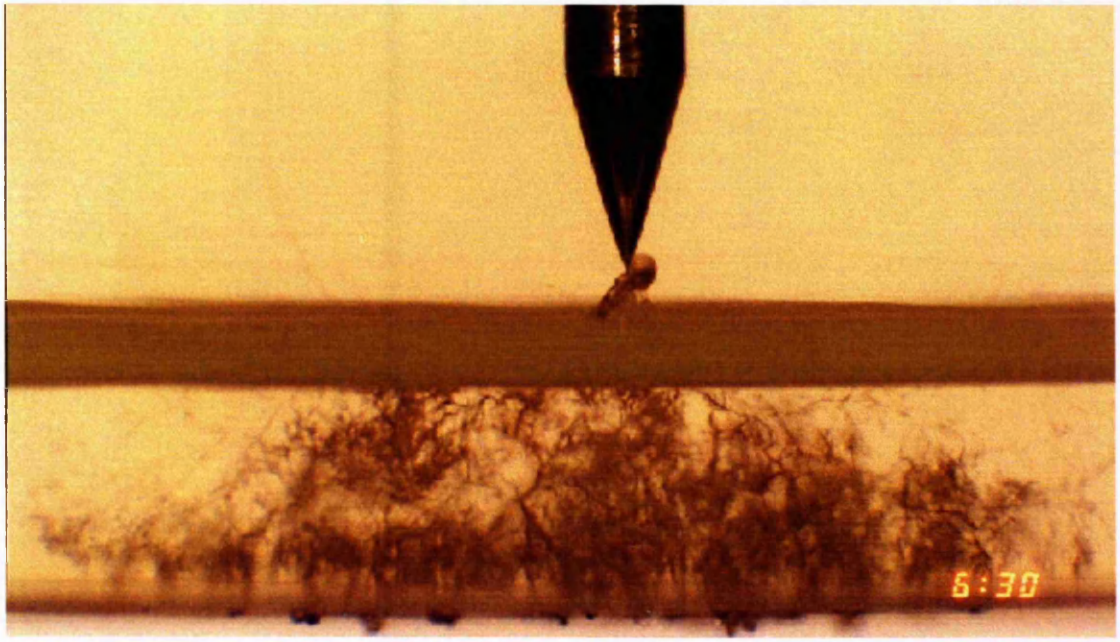

PRE-STRESSED

445 hours 13 minutes – BREAKDOWN (Initiation + 16 hours 13 minutes)

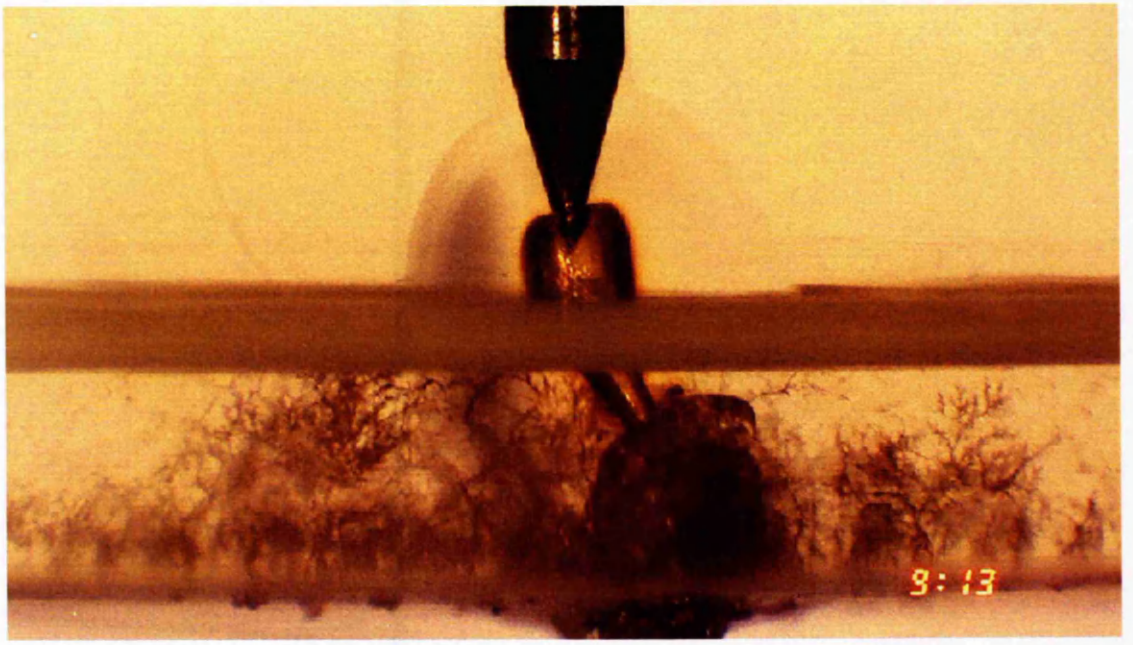

REFERENCES

[1] Shimizu N. and Laurent C.
'Electrical Tree Initiation.'
IEEE Transactions on Dielectrics and Electrical Insulation (DEI),
Vol. 5, No.5, Oct. 1998, pp. 651-659

[2] Auckland D.W. and Varlow B.R.
'Dependence of electrical tree inception and growth on mechanical properties.'
IEE Proc. Part A, Vol. 138, No.1, Jan 1991, pp. 51-54

[3] Varlow B.R. and Auckland D.W.
'Mechanical aspects of electrical treeing in solid insulation.'
IEEE Electrical Insulation Magazine, Vol. 12, No.2, Mar/Apr 1996, pp. 21-26

[4] Varlow B.R. and Auckland D.W.
'The influence of the mechanical factors on electrical treeing.'
IEEE Trans. DEI, Vol. 5, No.5, Oct. 1998, pp. 761-766

[5] Billing J.W. and Groves D.J.
'Treeing in mechanically strained h.v.-cable polymers using conducting polymer electrodes.'
IEE Proc., Vol. 121, No. 11, Nov 1974, pp. 1451-1456

[6] Arbab M.N. and Auckland D.W.
'Growth of electrical trees in electrical insulation.'
IEE Proc. Part A, Vol. 136, No. 2, March 1989, pp. 73-78

[7] Champion J.V., Dodd S.J., and Stevens G.C.
'An examination of the effect of mechanical stress on electrical breakdown in synthetic resin insulators.'
J. Phys. D., Appl. Phys. Vol. 27, 1994, pp.142-147

[8] Varlow B.R.
'Electrical treeing as a mechanically driven phenomenon.'
Proc. of the Int. Symp. on Elec. Ins. Mat., Japan, Sept. 1998, pp. 403-408

[9] Collins M.P. and Mitchell D.
'Prestressed Concrete Basics.'
Canadian Prestressed Concrete Institute, 1987

[10] BTG plc
'Keeping a Laboratory Notebook.'
BTG plc, Guidelines, 1996

[11] Dissado L.A. and Fothergill J.C.
'Electrical Degradation and Breakdown in Polymers.'
IEE Materials and Devices, series 9, 1992

REFERENCES

[12] Bahder G., Dakin T.W., and Lawson J.H.
'Analysis of treeing type breakdown.'
CIGRE Report, 1973, Paper 15-05, pp. 1-16

[13] Eichorn R.M.
'Treeing in solid extruded insulation.'
IEEE Transactions on Electrical Insulation, EI-12, 1977, pp.2-18

[14] Ieda M.
'Dielectric breakdown process of polymers.'
IEEE Trans., EI-15, 1980, pp. 206-224

[15] McMahon E.J.
'A tutorial on treeing.'
IEEE Trans., EI-13, 1978, pp. 277-288

[16] Bolton B., Cooper R., and Gupta K.G.
'Impulse breakdown of perspex by treeing.'
IEE Proc., Vol. 112, No. 6, June 1965, pp. 1215-1220

[17] Mason J.H.
'The deterioration and breakdown of dielectrics resulting from internal discharges.'
IEE Proc., Vol. 98, Part 1, Jan 1951, pp.44-59

[18] Mason J.H.
'Breakdown of solid dielectrics in divergent fields.'
IEE Proc., Vol. 102C, April 1955, pp. 254-263

[19] Shibuya Y., Zoledziowski S., and Calderwood J.H.
'Void formation and electrical breakdown in epoxy resin.'
IEEE Transactions on Power Apparatus and Systems, PAS 96, 1977, pp.198-206

[20] Shibuya Y., Zoledziowski S., and Calderwood J.H.
'Light emission and deterioration in epoxy resin subject to power frequency electric fields.'
IEE Proc., Vol. 125, No. 4, April 1978, pp. 455-459

[21] Zeller H.R. and Schneider W.R.
'Electrofracture mechanics of dielectric aging.'
J. Appl. Phys. 56 (2), July 1984, pp. 455-459

[22] O'Dwyer J.J.
'The Theory of Electrical Conduction and Breakdown in Solid Dielectrics.'
Clarendon Press, Oxford, 1973

REFERENCES

[23] Stark K.H. and Garton C.G.
'Electrical strength of irradiated polythene.'
Nature, Vol. 176, Dec 1955, pp.1225-1226

[24] Yamada Y.
'Treeing Phenomena.'
Sumitomo Electric Review, 101, 1969, pp.24-36

[25] Ieda M. and Nawata M.
'A consideration of treeing in polymers.'
Conference on Electrical Insulation and Dielectric Phenomena, CEIDP 1972, pp. 143-150

[26] Noto F. and Yashimura N.
'Voltage and frequency dependence of tree growth in polyethylene.'
CEIDP 1974, pp. 207-217

[27] Densley R.J.
'An investigation into the growth of electrical trees in XLPE cable insulation.'
IEEE Trans., EI-14 No.3, June 1979, pp. 148-158

[28] Ildstad E. and Hagen S.T.
'Electrical treeing and breakdown of mechanically strained XLPE cable insulation.'
IEEE Int. Sympos. On Electrical Insulation, 1992, pp.135-139

[29] Auckland D.W., Cooper R., and Sanghera J.
'Photographic investigations of formative stage of electric breakdown in diverging fields.'
IEE Proc. Part A, Vol. 128, No. 3, April 1981, pp. 209-214

[30] Arbab M.N. and Auckland D.W.
'The influence of vibration on the initiation of trees in dielectrics.'
IEE Proc. Part A, Vol. 133, No. 9, Dec 1986, pp. 618-622

[31] Arbab M.N., Auckland D.W., and Varlow B.R.
'Mechanical processes in the long term degradation of solid insulation.'
IEE Conf. Pub. No. 289, Dielectric Materials, Measurements and Applications (DMMA) 1988, pp. 231-233

[32] Auckland D.W., McNicol A.A., and Varlow B.R.
'Development of strain in solid dielectric due to vibrational electrostatic forces.'
J. Phys. D: Appl. Phys. Vol. 23, 1990, pp. 1606-1613

[33] Champion J.V., Dodd S.J., and Stevens G.C.
'Quantitative determination of the residual mechanical stress and its relaxation in synthetic resin with an embedded electrode.'
J. Phys. D: Appl. Phys. Vol. 25, 1992, pp. 1821-1824

REFERENCES

[34] Champion J.V., Dodd S.J., and Stevens G.C.
'Quantitative measurement of mechanical stress in resins and its effect on electrical treeing.'
IEE Conf. Pub. No. 363, DMMA 1992, pp.193-196

[35] David E., Parpal J.L., and Crine J.P.
'In-situ photoelastic monitoring of electrical treeing in polyethylene.'
CEIDP 1993, pp. 769-774

[36] David E., Parpal J.L., and Crine J.P.
'Influence of internal stress and strain on electrical treeing in XPLE.'
CEIDP 1994, pp. 575-581

[37] David E., Parpal J.L., and Crine J.P.
'Aging of XLPE cable insulation under combined electrical and mechanical stresses.'
IEEE Int. Sympos. on Electrical Insulation, 1996, Vol. 2, pp 716-719

[38] Zeller H.R., Hibma T., and Pfluger P.
'Electrofracture Mechanics of Dielectric Ageing.'
CEIDP 1984, pp.85-88

[39] Hitika M., Tajima S., Kanno I., Ishino I., Sawa G., and Ieda M.
'High-field conduction and electrical breakdown of polyethylene at high temperatures.'
Jap. J. Appl. Phys. Vol. 24, No. 8, Aug 1985, pp. 988-996

[40] Fothergill J.C.
'Filamentary Electromechanical Breakdown.'
IEEE Trans., EI-26, No. 6, Dec 1991, pp.1124-1129

[41] Auckland D.W., Kabir S.M.F., and Varlow B.R.
'Effect of barriers on the growth of trees in solid insulation.'
IEE Proc. Part A, Vol. 139, No. 1, Jan 1992, pp. 14-20

[42] Williams P.I. and Dissado L.A.
'Aspects of breakdown inhibition in filled composites.'
IEEE 5th Int. Conf. on Cond. and Breakdown in Solid Dielectrics, 1995, pp.533-537

[43] Auckland D.W., Rashid A., and Varlow B.R.
'Effect of barriers on tree growth in solid insulation.'
IEE Proc., Sci. Meas. Technol., Vol. 142, No. 4, July 1995, pp.283-287

[44] Auckland D.W., Varlow B.R., and Syamsuar M.
'Mechanical aspects of water treeing.'
IEEE Trans., EI-26, 1991, pp. 790-796

REFERENCES

[45] Auckland D.W., Taha A., and Varlow B.R.
'Mechanical interaction of electrical trees and barriers in insulating resins.'
IEE Proc., Sci. Meas. Technol., Vol. 143, No.5, Sept. 1996, pp.265-269

[46] Stevens M.P.
'Polymer Chemistry an Introduction.' 2nd Edition
Oxford University Press, 1990

[47] Chambers
'Materials Science and Technology Dictionary.'
Chambers Harrap Publishers Limited, 1993

[48] Brydson J.A.
'Plastics Materials.', 6th Edition
Butterworth-Heinemann, 1995

[49] Young R.J. and Lovell P.A.
'Introduction to Polymers.', 2nd Edition
Chapman and Hall, 1991

[50] BS EN 20139 : 1992
Textiles
'Standard Atmospheres for Conditioning and Testing'.

[51] BS EN ISO 2062 : 1995
Textiles - Yarns from packages.
'Determination of Single-end Breaking Force and Elongation at Break'.

[52] BS EN 20139 : 1992
Textiles
'Standard Atmospheres for Conditioning and Testing'.

[53] BS 2010 : 1963 (replaced by BS EN ISO 2060 : 1995)
'Method for Determination of the Linear Density of Yarns from Packages'.

[54] BS EN ISO 2060 : 1995
Textiles - Yarn from packages
'Determination of linear density (mass per unit length) by the skein method'.

[55] Kabir S.M.F.
'The influence of Charge and Barriers on Treeing in Solid Insulation.'
Ph.D thesis, The University of Manchester, May 1992

[56] Shaw D.J.
'Colloid & Surface Chemistry.' 4th Edition,
Butterworth Heinemann, 1992

REFERENCES

[57] Kaelble D.H.
'Dispersion-Polar surface tension properties of organic solids.'
Journal of Adhesion, Vol. 2, 1970, pp 66-81

[58] Girifalco l..A. and Good R.J.
'A theory for the estimation of surface and interfacial energies.'
Journal of Physical Chemistry, Vol. 61, 1957, pp 904-909

[59] Fowkes F.M.
'Determination of interfacial tensions, contact angles, and dispersion forces in surfaces by assuming additivity of intermolecular interactions in surfaces.'
Journal of Physical Chemistry, Vol. 66, 1962, p 382

[60] Domingue J.
'Solid Surface Energy Analysis Yesterday and Today.'
Cahn Instruments, Inc. Product Note, August 1991, pp 1-4

[61] Wu S.
'Calculation of interfacial tension by polymer systems.'
Journal of Polymer Science, Part C, No. 34, 1971, pp 19-30

[62] Dalal E.N.
'Calculation of solid surface tensions.'
Langmuir, Vol. 3, 1987, pp 1009-1015

[63] Mahy J., Jenneskens L.W. and Grabandt O.
'The fibre/matrix interphase and the adhesive mechanism of surface treated Twaron® aramide fibre.'
Composites, Vol. 25, No. 7, 1994, pp. 653-660

[64] De Lange P.J. and Mahy J.
'ToF-SIMS and XPS investigations of fibres, coatings and biomedical materials.'
The Fresenius Journal of Analytical Chemistry, Vol. 353, 1995, pp 487-493

[65] Goodfellow
'Goodfellow Catalogue 1998/99.'
Goodfellow Cambridge Limited

[66] Yang H.H.
'Kevlar Aramid Fibre'
John Wiley & Sons, U.S.A., 1993

[67] Northolt M.G. and van Aarsten J.J
'On the crystal and molecular structure of poly(*p*-phenylene terephthalamide)'
Journal of Polymer Science, Polymer Letters Edition 11, 1973, pp 333-337

REFERENCES

[68] Panar M., Avakian P., Blume R.C., Gardner K.H., Glerke T.D. and Yang H.H
'Morphology of poly(*p*-phenylene terephthalamide) fibres'
Journal of Polymer Science, Part-B Polymer Physics, Vol. 21, 1983, pp 1955-1969

[69] Bunsell A.R.
'The tensile and fatigue behaviour of Kevlar-49 (PRD-49) fibre'
Journal of Materials Science, Vol. 10, 1975, pp 1300-1308

[70] Konopasek L., Hearle J.W.S.
'The tensile fatigue behaviour of para-oriented aramid fibres and their fracture morphology'
Journal of Applied Polymer Science, Vol. 21, 1977, pp 2791-2815

[71] Dobb M.G., Johnson D.J., and Saville B.P.
'Supramolecular structure of a high-modulus polyaromtic fibre (Kevlar 49)'
Journal of Polymer Science, Polymer Physics Edition 15, 1977, pp 2201-2211

[72] Northolt M.G. and van Aartsen J.J
'Chain orientation distribution and elastic properties of poly(*p*-phenylene terephthalamide), a "rigid-rod" polymer'
Journal of Polymer Science, Polymer Symp., No. 58, 1977, pp 283-296

[73] Northolt M.G.
'The structure and mechanical properties of poly(p-phenylene terephthalamide) fibre'
British Polymer Journal, Vol. 13, 1981, pp 64-65

[74] van der Zwaag S., Northolt M.G., Young R.J., Robinson I.M., Galiotis C., and Batchelder D.N.
'Chain stretching in aramid fibres'
Polymer Communications, Vol. 28, 1987, pp 276-277

[75] Morgan R.J., Pruneda C.O., and Steele W.J.
'The relationship between the physical structure and the microscopic deformation and failure processes of poly(p-phenylene terephthalamide)'
Journal of Polymer Science, Polymer Physics Edition 21, 1983, pp1757-1783

[76] Young R.J
'Monitoring deformation processes in high-performance fibres using Raman Spectroscopy.'
Journal of the Textile Institute, Vol. 86, No. 2, 1995, pp361-381

[77] Prasad K. and Grubb D.T.
'Deformation behaviour of Kevlar fibres studied by Raman Spectroscopy'
Journal of Applied Polymer Science, Vol. 41, 1990, pp 2189-2198

REFERENCES

[78] Herrera-Franco P.J. and Drzal L.T.
'Comparison of methods for the measurement of fibre/matrix adhesion in composites.'
Composites, Vol. 23, No. 1, Jan 1992, pp 2-27

[79] Young R.J.
Chapter 6 - 'Characterization of interfaces in Polymers and Composites Using Raman Spectroscopy.', pp 131-159
Feast W.J., Munro H.S. and Richards R.W.,
Polymer Surfaces and Interfaces II, Wiley, 1993.

[80] Young R.J.
'Evaluation of Composite Interfaces Using Raman Spectroscopy.'
Key Engineering Materials, Vols. 116-117, 1996, pp 173-192

[81] Hendra P., Jones C. and Warnes G.
'Fourier Transformation Raman Spectroscopy - Instrumentation and Chemical Applications'
Ellis Horwood, England, 1991

[82] Bower D.I. and Maddams W.F.
'The Vibrational Spectroscopy of Polymers'
Cambridge University Press, Cambridge, 1989

[83] Ferraro J.R. and Nakamoto K.
'Introductory Raman Spectroscopy'
Academic Press, Boston, 1994

[84] Spiegal M.R.
'Mathematical Handbook of Formulas and Tables'
Schaum's Outline Series, McGraw-Hill, 1993

[85] Young R.J., Lu D., Day R.J., Knoff W.F., and Davis H.A.
'Relationship between structure and mechanical properties for aramid fibres.'
J. of Materials Science, Vol. 27. 1992, pp 5431-5440

[86] van der Zwaag S., Northolt M.G., Young R.J., Robinson I.M., and Galiotis C. and Batchelder D.N.
'Chain stretching in aramid fibres.'
Polymer Communications, Vol. 28, Oct 1987, pp 276-277

[87] Andrews M.C., Lu D. and Young R.J.
'Compressive properties of aramid fibres.'
Polymer Vol. 38, No. 10, 1997, pp 2379-2388

[88] Young R.J. and Andrews M.C.
'Deformation micromechanics in high-performance polymer fibres and composites'
Materials Science and Engineering, A184, 1994, pp 197-205

REFERENCES

[89] Andrews M.C., Bannister D.J. and Young R.J.
'Review – The interfacial properties of aramid/epoxy model composites'
Journal of Materials Science, Vol. 31, 1996, pp 3893-3913

[90] Safety in Universities: Notes of Guidance, Revised 1992
Part 2:1 Lasers
CVCP

[91] Hull D. and Clyne T.W.
'An Introduction to Composite Materials.' 2nd. Edition,
Cambridge University Press, 1996.
(Chapter 10, section 10.1.2 'Thermal expansivities' pp 240-244)

[92] Cervenka A.J., Bannister D.J. and Young R.J.
'Moisture absorption and interfacial failure in aramid/epoxy composites.'
Composites, Part A, Vol. 29A, 1998, pp 1137-1144

[93] Bannister D.J.
'Micromechanical and Hydrothermal Behaviour of Single-fibre Epoxy Resin Composites.'
Ph.D Thesis, UMIST/University of Manchester, October 1996

[94] Taha A.J.
'The Effect of Temperature on the Treeing Characteristics of Composite Resin Insulation.'
Ph.D Thesis, The University of Manchester, October 1994

[95] Cooper J.M.
'Factors Affecting the Assessment of Electrical Treeing in Synthetic Resins.'
Ph.D Thesis, The University of Manchester, March 1993

[96] Scott Bader
'Crystic Polyester Handbook.'
Scott Bader Company Limited, 1994

[97] Scott Bader
'Strand Craft Guide.'
Scott Bader Company Limited, 1991

[98] Ciba-Geigy
'Araldite® CT200 with Hardener HT901.'
Ciba-Geigy, Instruction Sheet No. C.1d, March 1981

[99] Ciba Polymers
'Araldite® CT1200-1 – Solid Epoxy Casting Resin.'
Ciba Polymers, March 1993

REFERENCES

[100] Champion J.V. and Dodd S.J.
'The effect of voltage and material age on the electrical tree growth and breakdown characteristics of epoxy resins.'
J. Phys. D: Appl. Phys. Vol. 28, 1995, pp. 398-407

[101] BS 2782 : Part 3 : 1976 (Confirmed 1986)
Part 3. Mechanical properties.
'Methods 320A to 320F. Tensile strength, elongation and elastic modulus.'

[102] Breithaupt J.
'Understanding Physics for Advanced Level.' 2nd Edition,
Stanley Thornes (Publishers) Ltd., 1990

[103] Ciba-Geigy Polymers
'Araldite LY5052 / Hardner HY5052.'
Ciba-Geigy, March 1988

[104] Ciba Polymers
'Araldite LY5052 / Hardner HY5052, Cold-curing epoxy laminating system.'
Ciba Polymers, March 1996

[105] Auckland D.W., Taha A. and Varlow B.R.
'Correlation of mechanical properties with electrical treeing behaviour at elevated temperatures.'
CEIDP 1993, pp 636-641

[106] Champion J.V. and S.J. Dodd
'The effect of absorbed water on electrical treeing in epoxy resins.'
IEE Conf. Pub. No. 430, DMMA 1996, pp. 206-210

[107] Pahl G and Beitz W
'Engineering Design a Systematic Approach.'
The Design Council, London, Edited by K Wallace, 1988

[108] Cross N
'Engineering Design Methods.'
The Open University, John Wiley & Sons, 1989

[109] Dow Corning
'Product Information for Silastic® 3120 RTV Silicone Rubber.'
Dow Corning, 1989

[110] Dow Corning
'Product Information – Silastic® T-1 Base/Curing Agent.'
Dow Corning, 1996

[111] Dow Corning
'Product Information – Silastic® S – Base/Curing Agent.'
Dow Corning, 1996

REFERENCES

[112] Hepburn DM, Kemp IJ, Shields AJ and Cooper JM
'Effect of mould release agent on epoxy resin surface degredation.'
IEE Proc. Sci. Meas. Technol., Vol. 146, No.6, Nov. 1999, pp 277-284

[113] McNicol A.A.
'The Electrical Degradation of Polymeric Insulation.'
Ph.D Thesis, The University of Manchester, September 1991

[114] BS 2782 : Part 0 : 1995
'Methods of Testing Plastics.'
Part 0. Introduction.

[115] BS 2782 : Part 3 : 1976 (Confirmed 1986)
Part 3. Mechanical properties.
'Methods 320A to 320F. Tensile strength, elongation and elastic modulus.'

[116] GRACE Specialty Polymers
'Selector Guide Adhesives.'
GRACE Specialty Polymers, 1994

[117] ASTM D 3039/D 3039M - 95a
Standard Test Method for
Tensile Properties of Polymer Matrix Composite Materials.

[118] Naik N.K.
'Woven Fabric Composites.'
Technomic Publishing, Lancaster, USA, 1994

[119] Clarke G.M. and Cooke D.
'A Basic Course in Statistics.' 2nd Edition,
Edward Arnold, 1983

[120] Cassell D., Hardwick I., Rouncefield M., and Burghes D.
'Statistics.'
Heinemann, 1994

[121] Jotun Polymer Technical Infromation Sheet
'Norpol 34-50.' Sold by Scott Bader as Resin C
Jotun Polymer (UK) Ltd, 1995

[122] Abderrazzeq M.H.
'High Voltage Composite Insulation Under the Influence of Water Absorption.'
Ph.D Thesis, The University of Manchester, May 1997

[123] Anderson J.C., Leaver K.D., Rawlings R.D., and Alexander J.M.
'Materials Science.' 4th Edition
Chapman & Hall, 1990, Chapter 11, section 11-12
'Mechanical properties of continuous fibre composites.' pp.329-334

REFERENCES

[124] **BS DD ENV 61072** : 1995
'Methods of test for evaluating the resistance of insulating materials against the initiation of electrical trees.'

[125] RS 186-3593
'Silver Conductive Paint.'
RS Product Information Sheet

[126] Penn-White Limited
'Silstrip NHLO "Low-odour solvent/remover for silicones".'
Penn-White Limited, February 1996

[127] Material Safety Data Sheet
'SILSTRIP NHLO LIQUID'
Penn-White Limited, 28/4/97

[128] Auckland D.W., Cooper J.M. and Varlow B.R.
'Factors affecting electrical tree testing.'
IEE Proc. Part A, Vol. 139, No. 1, Jan 1992, pp. 9-13

[129] Cooper J.M. and Stevens G.C.
'The influence of physical properties on electrical treeing in a cross-linked synthetic resin.'
J. Phys. D: Appl. Phys., Vol. 23, 1990, pp 1528-1535

[130] Cooper J.M.
'Lifetime reductions in epoxy resin systems.'
8th BEAMA Int. Elec. Insul. Conf., May 1998, pp351-358

[131] Champion J.V. and Dodd S.J.
'An assessment of the effect of enternally applied mechanical stress and water absorption on the electrical tree growth behaviour in glassy epoxy resins.'
J. Phys. D:Appl. Phys. Vol. 32, 1999, pp 305-316

[132] Vantico Limited (Formerly Ciba Polymers)
Private Communication
June 2000

[133] David E., Perpal J-L. and Crine J-P.
'Influence of internal mechanical stress and strain on electrical performance of polyethylene electrical treeing resistance.'
IEEE Trans. DEI, Vol. 3 No. 2, April 1996, pp. 248-257

[134] Varlow B.R. and Malkin G.J.
'Electrical treeing in mechanically pre-stressed insulation.'
CEIDP 1999, pp 593-596

REFERENCES

[135] Varlow B.R. and Malkin G.J.
'Electrical treeing in mechanically pre-stressed insulation.'
IEEE Trans. DEI, Vol.7, No.6, Dec. 2000, pp 721-724

[136] Ciba Polymers
'Heavy Electrical - ®Araldite Casting Resin System (B_{41} or B_{46}).'
Ciba Speciality Chemicals, Performance Polymers, Edition Jan. 1998

[137] Varlow B.R. and Malkin G.J.
'Improvements in electrical and mechanical strength of pre-stressed insulation.'
IEE, Pub. No.473, 8th DMMA, Edinburgh 2000, pp 470-473

[138] Varlow B.R. and Malkin G.J.
'Enhanced resistance to electrical treeing in mechanically pre-stressed insulation.'
2nd International Conference on Dielectrics and Insulation (ICDI), Kosice, Slovakia, June 2000, pp 40-45

[139] Auckland DW, Taha A and Varlow BR
'Mechanical interaction of electrical trees and barriers in insulating resins.'
IEE Proc. Sci. Meas. Technol., Vol.143, No.5, Sept. 1996, pp 265-269

[140] Auckland DW, Su W and Varlow BR
'Nonlinear fillers in electrical insulation.'
IEE Proc., Sci. Meas. Technol., Vol. 144, No.3, May 1997, pp 127-133